UCLouvain

AGRO LOUVAIN

Faculté des bioingénieurs

What are the environmental factors determining the secondary forest diversity in mountain ecosystems?

A case study in the Gran Paradiso National Park, Italy

Auteur : Louis Léonard
Promoteurs : Matteo Garbarino & Quentin Ponette
Lecteurs : Thierry Hance & Julien Radoux
Année académique : 2025-2026
Mémoire de fin d'étude présenté en vue de l'obtention du diplôme de Bioingénieur : gestion des forêts et des espaces naturels

Acknowledgments

I would like to thank everyone who, in one way or another, has contributed to the successful completion of this thesis. The advice and support of all these people have been of great importance to me throughout this project.

First and foremost, I would like to express my deepest gratitude to my two supervisors, Matteo Garbarino and Quentin Ponette. It goes without saying that without them, this project would never have come to fruition. I would like to thank Matteo Garbarino for designing the project, supervising it and providing support throughout this thesis. I would like to thank Quentin Ponette for listening to me, supervising my work and offering valuable advice. Thank you for the time you have given me. Thanks to you, I have learnt a great deal during this project; your advice and comments have enabled me to take my thinking further and improve my work.

I would also like to express my sincere gratitude to Nicolò Anselmetto and Simona Cavallo for their assistance with this thesis. Their constant supervision throughout the process, as well as their invaluable advice, were essential to the successful completion of my thesis. I would also like to thank them, along with Matteo Garbarino, for their warm welcome during my various stays in Turin. I look forward to working with you next year.

I would also like to thank Federico Olimpi and Viola Ghislandi for their invaluable help during the fieldwork carried out in the summer of 2025. It would have been much more difficult without them. I will cherish the memories of the time we spent together during that long month. I would also like to thank the various researchers, park rangers and staff at the Gran Paradiso National Park who provided their support during the data collection.

Of course, I am incredibly grateful to my family for their constant support. I thank them for believing in me over the past five years, and for supporting and encouraging me during the toughest times. I doubt I would have made it this far without them. Whether it's my parents, my sisters, my grandparents, my cousins, my uncles or my aunts, I thank them all for being there this year, but also in the past, which has enabled me to get to where I am today.

And finally, I would like to thank all my friends who have also helped me get to where I am today. I would like to mention the whole team on the third floor, with whom I have shared so many emotions over the course of this year. All the moments I've shared with them will remain fond memories.

Thank you all.

CRediT

CRediT	Louis Léonard	Contributors*	AI
Conceptualisation	V	M.G.	
Méthodologie	V	M.G., N.A., S.C.	
Investigation	V	F.O., V.G.	Claude, NotebookLM
Analyse formelle	V	M.G., N.A.	Claude
Validation	V	M.G., N.A., Q.P.	Claude, Perplexity
Rédaction – version originale	V		Claude
Rédaction – révision et édition	V	M.G., N.A., Q.P.	Claude
Visualisation	V	M.G., N.A., Q.P.	Claude
Supervision		M.G., Q.P.	

*NA: Nicolò Anselmetto, SC: Simona Cavallo, MG: Matteo Garbarino, VG: Viola Ghislandi F.O: Federico Olimpi, QP: Quentin Ponette.

This thesis is the result of collaborative work between the author and his supervisors. Certain stages were carried out with the aid of various tools, including artificial intelligence models.

The conceptualisation and the initial research idea were discussed with the supervisor, Matteo Garbarino.

The methodology was developed within Matteo Garbarino's team, with the support of Nicolò Anselmetto and Simona Cavallo.

The research and data collection carried out during the summer of 2025 were conducted with the support of the two interns, Viola Ghislandi and Federico Olimpi. Some artificial intelligence tools (Claude and NotebookLM) were used to assist in the search for scientific articles.

The analysis was carried out by the author. An artificial intelligence tool (Claude) was used to help explore avenues of analysis and verify some interpretations. These resources have always been used as supplements, once the author has completed the initial work.

The validation and interpretation of the results were carried out by the author, drawing on scientific literature and the Claude tool, under the supervision of both supervisors and Nicolò Anselmetto.

The text was drafted by the author, with the help of the Claude text-generation tool. This tool was also used to improve the quality of the graphs.

The entire project was supervised by Nicolò Anselmetto, Matteo Garbarino and Quentin Ponette.

Table of contents

List of Figures

List of Tables

List of abbreviations

BA: Basal Area
BLF: abundance of broadleaves, in terms of basal area
Cov litter: litter cover
Cov regen: regeneration cover
DBH: Diameter at Breast Height
Mean DBH: DBH - average
DBH sd: DBH - standard deviation
DTM: Digital Terrain Model
GSL: Growing Season Length
GPNP: Gran Paradiso National Park
HB sa: Brillouin index for saplings
HB se: Brillouin index for seedlings
HLI: Heat Load Index
LTI: Light Tolerance Index
LULCC: Land-Use/ Land-Cover Change
PCA: Principal Component Analysis
PDPs: Partial Dependence Plots
RF: Random Forest
RFE: Recursive Feature Elimination
SCD: Snow Cover Days
TPH: Trees Per Hectare (density of trees)
TPH sa: density of saplings
TPH se: density of seedlings
TPH t: density of trees
TPI: Topographic Position Index
TRI: Topographic Ruggedness Index
TWI: Topographic Wetness Index

1.Introduction

For millennia, European mountain landscapes have been highly shaped by the exploitation of forests, grazing, mining and maintenance of agricultural land, resulting in a loss of forest cover (Mietkiewicz et al., 2017). Since the Industrial Revolution, a major rural exodus has led to the decline of the traditional sylvo-pastoral systems (MacDonald et al., 2000; Tasser and Tappeiner, 2002). The European Alps (hereafter, the Alps) have been particularly affected by this transition. Due to those centuries of intensive use followed by pervasive land abandonment, land-use change has emerged as one of the most important drivers of landscape change in the Alps alongside climate change (Gehrig-Fasel et al., 2007). Understanding the history of land-use change is therefore essential for predicting future landscape changes.

After the abandonment of agricultural and pastoral lands, vegetation succession has occurred leading to a natural reforestation of those lands (Tasser and Tappeiner, 2002). A major expansion of the forest cover has started in the Alps. It has shifted from 6 million ha in 1936 to 11 million ha in 2015 in Italy, with an increase of 20% in the last 30 years (Ferretti et al., 2018). At the Alpine scale, forest cover has been estimated to increase by approximately 4% per decade since the mid-20th century (Bebi et al., 2017). This natural forest expansion has occurred through two processes bringing new forests to abandoned land: gap-filling of former open areas at lower elevation and treeline upshift at higher elevation (Tasser et al., 2005).

Those new forests are called secondary forests and can be defined as “a forest regenerated largely through natural processes after significant human or natural disturbance of the original forest vegetation” (FAO, 2000). Those forests differ from primary forests not only because of their age but also because of their composition and structure (Hermy et al., 1999). They are strongly dependent on the historical context of the establishment site and the land-use legacies (Chazdon et al., 2020).

This natural forest expansion has a significant positive impact on the environment, e.g. higher carbon sequestration (Tasser et al., 2007), more stable soils (Tasser and Tappeiner, 2002), clean water (Hunsaker and Levine, 1995), therefore offering passive restoration opportunities (Plieninger et al., 2016). However, canopy closure can lead to a loss of the landscape mosaic and moreover a loss of open habitats formerly maintained by grazing (Otero et al., 2015; Ridding et al., 2020). It may therefore lead to a major loss of biodiversity. Abandoned lands can also be more vulnerable to invasive species (Munroe et al., 2013). Beyond biodiversity, microclimatic conditions are strongly modified by the establishment of secondary forests (De Frenne et al., 2019). The susceptibility of mountain ecosystems to natural disturbances (e.g. drought, wildfires, and pest outbreaks) is also altered with the natural forest expansion (Seidl et al., 2017).

The natural process of reforestation is strongly influenced by several natural and anthropogenic factors. The main drivers of the process are the altitudinal gradient (Rochefort and Peterson, 1996), biotic legacies (Flinn and Marks, 2007), snow cover and avalanches (Garbarino et al., 2013) and seed dispersal strategies (Pedersen et al., 2023). Among anthropogenic variables, type and intensity of previous land use are the most informative ones (Wickham et al., 1999). In the Alps, the most common previous land-use types were pastures and mowed grasslands (Tasser and Tappeiner, 2002). These persistent effects of past land use, conceptualised as land-use legacies, can affect forest establishment for decades or even centuries after abandonment (Foster et al., 2003; Hermy and Verheyen, 2007). The importance of each factor remains however strongly debated depending on regional and landscape contexts.

This diversity of factors creates a large range of establishment conditions for those secondary forests. It creates a series of different succession trajectories dependent on these starting conditions. Secondary forests can evolve toward a mature community dominated by shade-tolerant tree species, but they can also remain at a pioneer stage with light-demanding species (Poorter et al., 2023; Schulze et al., 2007). This diversity of successional trajectories results in a complex mosaic of structurally and compositionally different forests (Garbarino et al., 2020). This is increasingly recognised as a defining feature of post-abandonment landscapes in the Alps.

The Gran Paradiso National Park (GPNP), located in the western Italian Alps on the border between the Aosta Valley and the Piedmont regions, offers a wide variety of secondary forests. The large amount of data on land-use changes within the GPNP makes it an ideal place to study the determinants of secondary forest diversity and structure. The Park covers a large variety of environmental conditions, from 800 to 4,061 m a.s.l., spanning wide climatic and biogeographical gradients, and has been subject to land-use/land-cover changes over the past seventy years (Richiardi et al., 2025). The thesis of Gontier (2026) has provided a first characterisation of the secondary forests in the Aosta Valley sector of the GPNP. Ten distinct forest groups were identified along an altitudinal-thermal gradient.

However, this analysis remains geographically restricted to the Aosta valley sector and does not include the secondary forest types of the Piedmont sector, which presents different climatic conditions and land-use legacies. Moreover, this study does not provide a quantitative ranking of the different factors structuring the forest diversity. The literature therefore presents a significant gap in the identification of different secondary forest types and environmental factors explaining the diversity.

This study aims to fill this gap by characterising the secondary forest diversity across the entire GPNP and identifying the environmental factors that best explain this diversity. Based on 283 sampling plots distributed across both Aosta Valley and Piedmont sectors, three complementary sub-objectives are pursued in this work: (i) identify the different secondary forest types in the GPNP through a hierarchical cluster analysis; (ii) link these forest types to environmental factors and identify which factors explain the variation between the secondary forest types through a principal component analysis; and (iii) quantify the relative importance of those factors through a Random Forest classifier. Together, these three sub-objectives are expected to provide a more complete and quantitatively grounded picture of the factors determining secondary forest diversity in the western Italian Alps.

2. State of the art

2.1. Land-use change

2.1.1. Land-use change history

Alongside climate change, the modification of land use is one of the most important drivers of landscape transformation in the Alps (Tasser et al., 2017). Indeed, human actions have been one of the major forces shaping the Alpine region for thousands of years and generating the semi-natural and cultural landscapes still visible (Ellis et al., 2013).

The anthropogenic pressure has significantly shaped the dynamics of the evolution of the land-use/land-cover change (LULCC). Since the Neolithic, humans started to modify the landscape by slash-and-burn farming (Kutschera et al., 2014), which generated first pasturelands and made hunting easier by removing thick vegetation layers from the landscape (Gilck and Poschlod, 2021). This practice intensified during the Bronze Age with a large-scale deforestation for both agro-pastoralism and metallurgical activities (von Scheffer et al., 2019) and continued throughout Antiquity, peaking in the Middle Ages (Muigg et al., 2025; von Scheffer et al., 2019). Population growth in the Alps at higher altitudes since the 14th century has accelerated the process of deforestation using slash-and-burn farming, creating new pastureland and allowing people to settle (Gilck and Poschlod, 2021). The start of the industrialization (late 18th century) caused a new wave of deforestation (Bebi et al., 2017). This exploitation for energy, construction and intense grazing has led to the lowest level of forest cover on record in the middle of the 19th century (Mather et al., 1999). Several studies applying vegetation reconstructions through pollen data identified climate as the main driver of alpine vegetation changes before 6500 BC (Dziomber et al., 2024; Roberts et al., 2018). Afterwards, however, human impact had become increasingly important and eventually dominant (Figure 1).

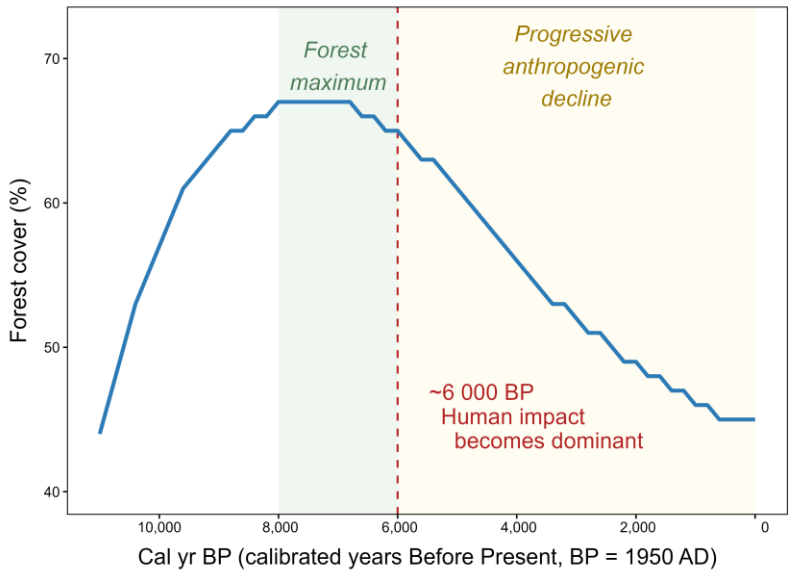

Figure 1: Decline of forest cover in mid-latitude and northern Europe over the last 11,000 years, reconstructed from pollen data. The blue curve shows the PBMsc (Pseudo-Biomization Method, closed sum), which transforms pollen proportions into a forest cover score by summing scores assigned to needle-leaf and broad-leaf closed forest land cover classes. The green shaded area highlights the Holocene forest maximum. The dashed red line marks the onset of progressive anthropogenic deforestation linked to Neolithic agriculture across mid-latitude Europe. Source: Roberts et al. (2018), adapted.

2.1.2. Land-use patterns

The history of land use in the Alps has produced landscapes shaped by humans. Those landscapes are a complex mosaic of forests, pastures and croplands shaped over thousands of years by the combined action of nature and humans (Tappeiner et al., 2008). Today, two main drivers explain the type of land use in the Alpine region: the altitudinal gradient and the topography (Garbarino et al., 2013).

The Alpine landscape is strongly influenced by the altitudinal gradient. The distribution of the land uses follows this gradient due to the productive capacities of ecosystems and results in distinct landscape zones/belts in the region (Egarter Vigl et al., 2017). Five main bioclimatic zones can be identified in the Alps: nival, alpine, subalpine, montane, and hilly (Tasser et al., 2009). At the same time, those five zones can be grouped in four major functional areas based on their land use: the agricultural areas, the forest belt, the alpine pastures and high-altitude grasslands, and the mineral zone (Lavorel et al., 2019).

The agricultural areas are located at low altitudes, usually below 600 m a.s.l., and constitute the area with the highest concentration of human activity (Tappeiner et al., 2008). The vegetation is generally composed of broadleaves, with a high share of croplands and settlements, taking advantage of areas with gentle slopes, often less than 5% (Monteiro et al., 2011).

The forest belt is part of the montane and subalpine bioclimatic zones and constitutes the heart of the traditional agro-forestry-pastoral system (Egarter Vigl et al., 2017). Lying between 600 m a.s.l. and the treeline (1500 – 2200 m a.s.l.), this belt is composed of a mosaic of forests and permanent hay meadows (Tasser et al., 2009). These are the areas where the traditional silvo-pastoral activities occurred historically (Motta and Lingua, 2005). This long-lasting human action left landscapes where dense and sparse forests coexist together with open areas and wood pastures, the so-called semi-natural or cultural landscapes (Garbarino et al., 2011).

The alpine pastures and high-altitude grasslands, located above the treeline and also known as the subalpine zone, are characterised by open landscapes (Egarter Vigl et al., 2017). Generally composed of natural grasslands and dwarf shrub heaths, the alpine grasslands are ecosystems rich in biodiversity, making them target areas for conservation (Bita-Nicolae et al., 2023). The land use in this belt is extensive and seasonal, associated with summer grazing for cattle and sheep (Lavorel et al., 2019).

The mineral zone is the area with the highest summits, where the extreme natural conditions limit the development of life (Praeg et al., 2025). Those landscapes are dominated by steep slopes covered by rock outcrops, scree slopes, perpetual snow, and glaciers (Tasser et al., 2009). Human influence is almost non-existent and natural ecosystems and rare pioneer species occupy the few suitable sites (Tappeiner et al., 2008).

Those four functional areas respond to an overall altitudinal gradient creating a land use gradient in turn. Figure 2 confirms the organisation into landscape belts. It quantifies the distribution of land use by ten different ecoregions and their changes since 1865 (Tasser et al., 2009). Each ecoregion has its own signature of land use. This altitudinal zonation is however not uniform as other topographical features act as a second spatial filter modulating land-use intensity within each zone.

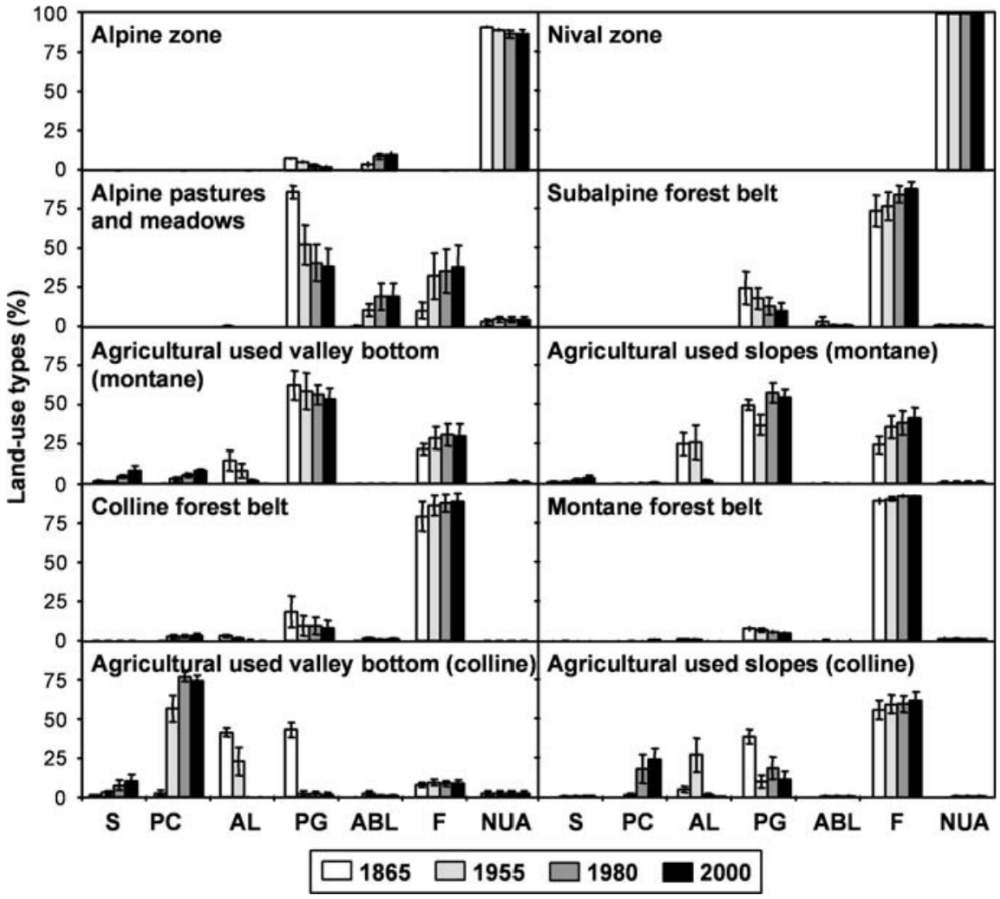

Figure 2: Historical land-use changes from 1865 to 2000 in the different ecoregions. Results from an analysis of several case studies all over the mountain region. ***S*** *= settlements;* ***PC*** *= permanent crops;* ***AL*** *= arable land;* ***PG*** *= permanent grassland;* ***ABL*** *= abandoned land;* ***F*** *= forest;* ***NUA*** *= non agriculturally usable area. Source: Tasser et al., 2009.*

The topography in the Alpine region creates a spatial heterogeneity due both to physical characteristics of the terrain (i.e., slope and aspect) and to technical accessibility (Kulakowski et al., 2010), acting as a selective filter for the intensity and shape of anthropogenic use of the landscape (Marzini et al., 2025). The rugged terrain characteristics of the Alps restrict the mechanisation, thus limiting the human agricultural activities to the accessible areas to exploit (Lavorel et al., 2019). Those are the areas with gentle slopes often located in the floodplains and valley floors, which has historically been home to the most intensive farming and permanent settlements (Monteiro et al., 2011). The steep slopes, which do not allow for intensive farming and heavy mechanisation, therefore called for manual management (Tappeiner et al., 2008). This topographic filter results in a highly fragmented landscape, characterised by a mosaic of small traditional plots. This structural heterogeneity stems from a precise adaptation to meso- and micro-variations in the terrain and results in a complex socio-ecological pattern given by the interaction between the biophysical mountain template and economic paradigms (Tasser et al., 2009). The land use in the Alps is also affected by the distance from the infrastructures (Theissen et al., 2022). The intensity of use by humans is directly dependent on time and efforts of moving around the land, with decreasing anthropogenic pressure and intensity of use as the distance from villages or roads (Lavorel et al., 2019).

It is precisely those areas that are topographically constrained, difficult to access and historically marginalised that were the first to be affected by agricultural decline and land

abandonment (Tasser et al., 2007). While spatial heterogeneity in Alpine landscapes arose until the 19th century because of traditional activities, a homogenisation followed in the last 200 years due to land abandonment and agricultural decline (Lavorel et al., 2017).

2.2. Land abandonment and forest expansion

The phenomenon of land abandonment has followed the Industrial Revolution and major socio-economic changes in the middle of the 19th century around most of the European mountain ranges, and the Alps were no exception (Bebi et al., 2017). Land abandonment is defined as a process 'whereby human control over land (e.g. agriculture, forestry) is given up, and the land is left to nature' (FAO, 2006). While some parts of the world are marked by an ephemeral abandonment, that may be rapidly followed by an agricultural use (Crawford et al., 2022), this process marked the end of the traditional agro-sylvo-pastoral system, based on the complementary use of cultivation, grazing and forests, in the Alps (Decocq et al., 2018). Several interrelated factors have driven this transition.

2.2.1. Land-abandonment drivers

With the Industrial Revolution, a rural exodus has started in the marginal valleys (Gelabert et al., 2022). This exodus has amplified across generations. Young farmers have been drawn to better-paid jobs, enabling them to leave the rural areas where their ancestors lived in favour of nearby towns or cities (Dax et al., 2021). These valleys were left in the hands of an ageing population with no one to inherit the land, leading to land abandonment (MacDonald et al., 2000).

The collapse of the traditional agro-sylvo-pastoral system was caused by shifts in production paradigms linked to the specialisation of production systems and globalisation (Taillefumier and Piégay, 2003). Improvements in transport and technology have left Alpine agriculture unable to compete with the monocultures of the lowland valleys, leading to a decline in local self-sufficiency (Mather, 1992). Globalisation and the opening of markets have also contributed to a decline in the competitiveness of subsistence farming (Mietkiewicz et al., 2017).

Land abandonment is not random but is strongly influenced by topography, as already discussed. Lands situated on steep slopes with shallow or infertile soils were the first to be abandoned (Schweizer and Matlack, 2014). These conditions made it impossible to mechanise farming, thereby reducing its productivity (MacDonald et al., 2000). Adverse weather conditions such as frost, drought and short growing seasons, combined with the terrain, make mountainous areas far less suitable for agriculture than the valley bottoms (Perpiña Castillo et al., 2021).

The Common Agricultural Policy (CAP) and other European policies have had a mixed impact on land abandonment in the Alps (MacDonald et al., 2000). By encouraging intensification and specialisation in the valleys, they have exacerbated disparities in competitiveness with mountain farms, which are often small and subject to greater constraints (Ustaoglu, 2018). Direct aid and market measures have concentrated production in the most profitable areas, whilst compensation for less-favoured areas and compensatory allowances have proved insufficient to maintain traditional extensive farming systems (Dax et al., 2021).

All those drivers have therefore synergistically led to a land abandonment that is now identified as the most important local-scale cause of landscape change in European mountain ranges (Plieninger et al., 2016). This phenomenon halted forest exploitation and, in some regions,

resulted in an expansion of the forest cover (Motta et al., 2006). This marked a genuine turning point for the forest, reversing centuries of deforestation to usher in a phase often called natural forest expansion that continues to this day (Anselmetto et al., 2024). This process of a natural forest expansion after land abandonment is coherent with the "forest transition theory" formulated by Mather (1992), that states that forest naturally expands as the result of secondary successions as economies move away from pre-industrial and industrial phases. After reaching its lowest historical extent in the mid-19th century, the Alpine forest has been expanding almost continuously ever since (Bebi et al., 2017).

2.2.2. Natural forest expansion

Following the land abandonment in the Alps, secondary succession has led to a natural forest expansion of the areas that had been used as croplands and pastures for millennia (Anselmetto et al., 2024). This process of natural forest expansion is now one of the most important changes in land use in Europe (Meli et al., 2017). Figure 3 shows an example of the forest cover gains across the Italian Alps in the last 20 years. This forest expansion is clearly visible almost everywhere in this part of the Alps. But this expansion is not limited to the Italian Alps, the forest cover has increased across the entire Alps with an average +4% per decade over the past 25–115 years (Bebi et al., 2017). The natural forest expansion is the main land-use transition in almost all landscapes and watersheds of the Alps (Anselmetto et al., 2024; Garbarino et al., 2020; Marengo et al., 2025).

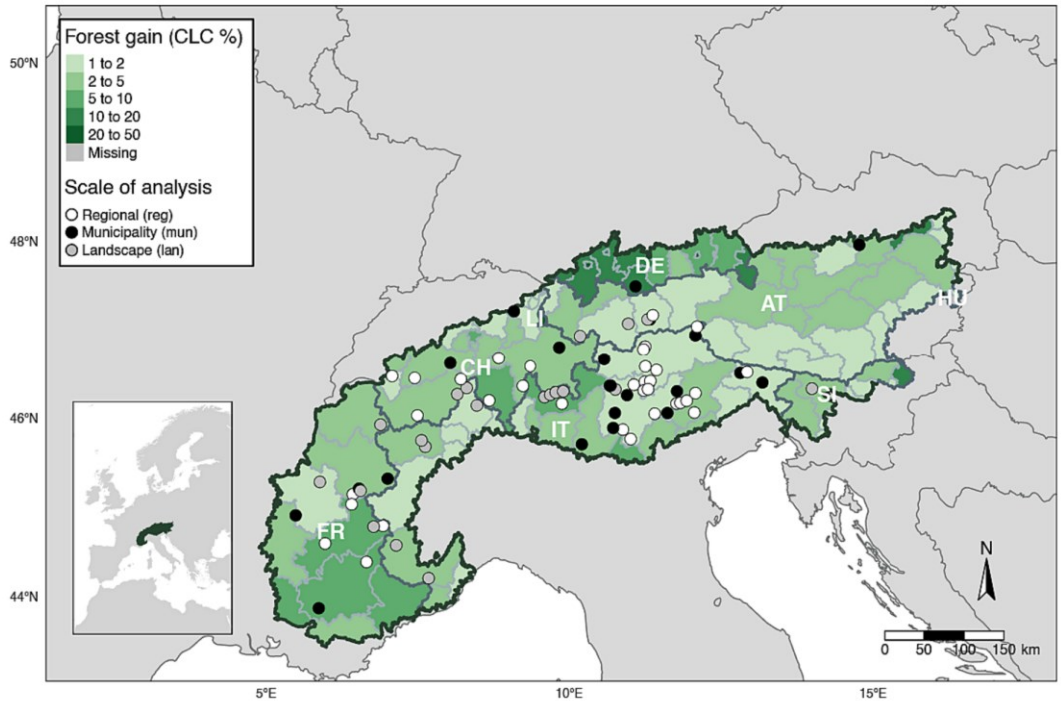

Figure 3:Forest gains across the Alps, including the Italian Alps. Green polygons shading show the forest gain at NUTS lv3 derived from Corine Land Cover dataset (CLC, a pan-European land-cover mapping programme based on satellite imagery) for the period 2000–2018. Three scales of analysis are represented by distinct point symbols: the regional scale (reg, open circles, n = 80) covers spatially defined case studies without quantitative forest gain data; the municipality scale (mun, filled circles, n = 108) includes studies reporting observed annual forest gain; and the landscape scale (lan, grey-rimmed circles, n = 21) corresponds to studies with precise spatial attributes. The inset map shows the location of the European Alps within Europe. ***AT*** *= Austria,* ***CH*** *= Switzerland,* ***DE*** *= Germany,* ***FR*** *= France,* ***IT*** *= Italy. Source: Anselmetto et al., 2024.*

But this natural forest expansion is not homogenous across time and space, as its intensity and scale are dictated by numerous drivers such as the topography, climate, and distance from

human infrastructures (Anselmetto et al., 2024). Two main patterns of natural forest expansion can be described: the treeline upshift and the gap filling (Tasser et al., 2005).

The treeline upshift is a phenomenon globally occurring at high altitudes in the transition zones between the upper limit of the forests (i.e., forestline or timberline) and the alpine grasslands (Anselmetto et al., 2022; Chan et al., 2024; Harsch et al., 2009). The main mechanism of this process is an encroachment of trees and brushes - a process also referred to as shrubification - that invade alpine meadows traditionally kept open through grazing (Kulakowski et al., 2010). In European mountains such as the Alps, the abandonment of pastoral activities is the main reason for this shift. Indeed, a lower pressure of grazing results in improved conditions for trees to survive in these environments (Gehrig-Fasel et al., 2007). On top of this, climate change results in warmer temperatures and the relaxation of thermal constraints, with more favourable conditions for the tree growth (Snell et al., 2022).

The gap filling process is occurring, on the contrary, at low and middle altitude, within the forest matrix (Anselmetto et al., 2022; Garbarino et al., 2020). This process consists of the colonisation by forests of isolated non-forested areas within an existing forest matrix (Malandra et al., 2019). The gap filling is strongly correlated with the process of land abandonment (Marengo et al., 2025). After the abandonment, the small, enclosed grassland areas that were historically used for grazing or mowing are invaded by woody vegetation. The spatial patterns of gap filling are therefore not random. The areas where reforestation proceeds faster are precisely those that were first abandoned: steep, south-facing slopes in remote and sparsely populated municipalities, where agricultural mechanisation was impossible (Anselmetto et al., 2024). At middle elevations, where abandonment began earlier, this process is now gradually decelerating as available space becomes saturated, while at higher elevations the treeline continues to advance. After the abandonment, vegetation succession begins first with a dense shrub cover followed by reforestation (Tasser et al., 2005). The rate of the succession depends heavily on two main factors: the proximity of seed sources and the past land use (Marengo et al., 2025). The closer an abandoned area is to a forested area, the higher the reforestation rate (Tasser et al., 2007). In the article of Tasser et al. (2007), the authors report that reforestation rates decrease sharply with distance from established trees, with the most vigorous regrowth occurring within the first 10 metres and declining significantly beyond 200 metres. The intensity of the past land use creates the conditions of soil and vegetation more or less favourable to forest colonisation (Rebele, 2013). Forests that have developed from abandoned grasslands still exhibit conditions similar to those prior to abandonment, whereas those that have developed from formerly forested areas follow trajectories closer to a natural state (Marengo et al., 2025). Figure 4 illustrates the drivers discussed earlier, as well as other factors that act as barriers or catalysts to forest expansion. Many of them are linked to the land abandonment characteristics.

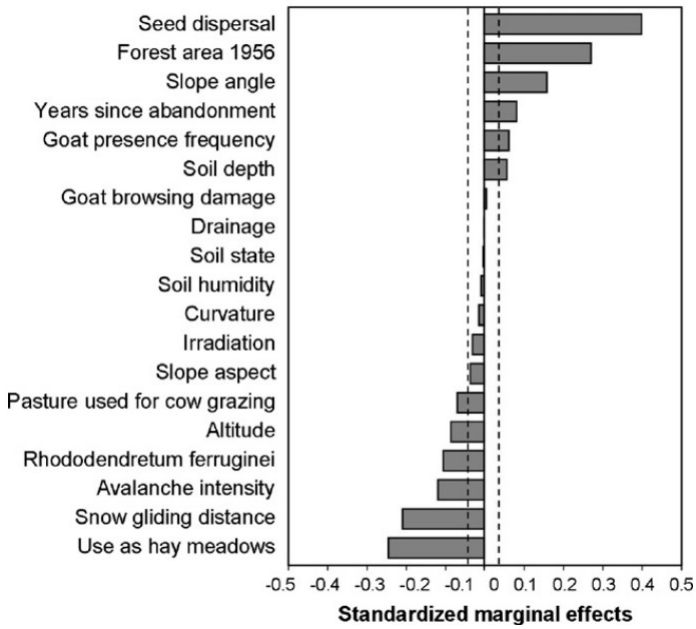

Figure 4: Standardised marginal effects of biotic, abiotic and land-use variables on natural reforestation rates in the Eastern Central Alps. Positive values indicate factors favouring tree colonisation; negative values indicate inhibiting factors. Variables are defined as follows: Seed dispersal = modelled probability (%) of seed reaching a site, based on the seeding distances of Picea abies; Forest area 1956 = binary variable indicating whether the site was already forested in 1956; Slope aspect = continuous variable (0–360°), significant for determining tree density rather than tree presence/absence; Soil humidity = ordinal variable ranging from 0 (moderately dry) to 2 (wet soil); Soil state = ordinal variable ranging from 0 (undisturbed) to 2 (eroded); Rhododendretum ferruginei = binary variable indicating presence of Rhododendron ferrugineum shrub cover; Snow gliding distance = modelled downslope displacement of the snowpack (mm); Avalanche intensity = ordinal variable ranging from 0 (no avalanches) to 2 (regular dismounts); Use as hay meadows = intensity of mowing use (0–3), where higher values indicate more frequent cutting; Goat presence frequency = ordinal variable ranging from 0 (rare) to 2 (frequent presence). Source: Tasser et al. (2007).

The natural forest expansion is not only a biophysical phenomenon, but it also generates measurable and documented ecosystem services. In fact, natural forest expansion in the Alps has brought significant ecological services. The increase of the forest cover contributes to better water regulation, reduces surface runoff and improves the soil stability on steep slopes from an hydrological point of view (Gafur et al., 2003). The forest expansion leads to a significant increase in forest biomass, which serves as a major carbon sink contributing to the climate change mitigation (Bebi et al., 2017). As mentioned earlier, this phenomenon occurs primarily on slopes steeper than 30%. These slopes correspond to avalanche starting zones (Bebi et al., 2009) and therefore, expansion of forest cover in these starting zones has led to a significant reduction in avalanche occurrence (Vacchiano et al., 2015).

However, natural forest expansion comes with more complex effects, which may result in negative consequences for some parts of the ecosystems. The most significant is the loss of diversity in the landscape (MacDonald et al., 2000). The forest expansion reduces the open areas, leading to lower levels of landscape heterogeneity (Sitzia et al., 2010). Figure 5 shows the transition of land cover from 1954-1962 to 2012 across several mountain landscapes of the Italian Alps. It clearly shows that natural forest expansion takes place mainly in areas previously occupied by grasslands. The semi-natural mosaic created by thousands of years of land use is disappearing, replaced by large, uniform forests. This leads to the loss of open areas such as alpine grasslands, hay meadows and wood-pastures which are among the most biodiverse ecosystems in Europe and listed as priority habitats under the EU Habitats Directive (92/43/EEC) (Gavrichkova et al., 2022). This loss of the mosaic leads to an important loss of

biodiversity for some ecological traits associated with ecotones and open habitats (Verhulst et al., 2004). At the stand level, secondary forests that establish on formerly open land are often structurally simpler and less biodiverse than both old-growth forests and the semi-natural habitats they replace (Gerhardt and Foster, 2002; Lindborg and Eriksson, 2004).

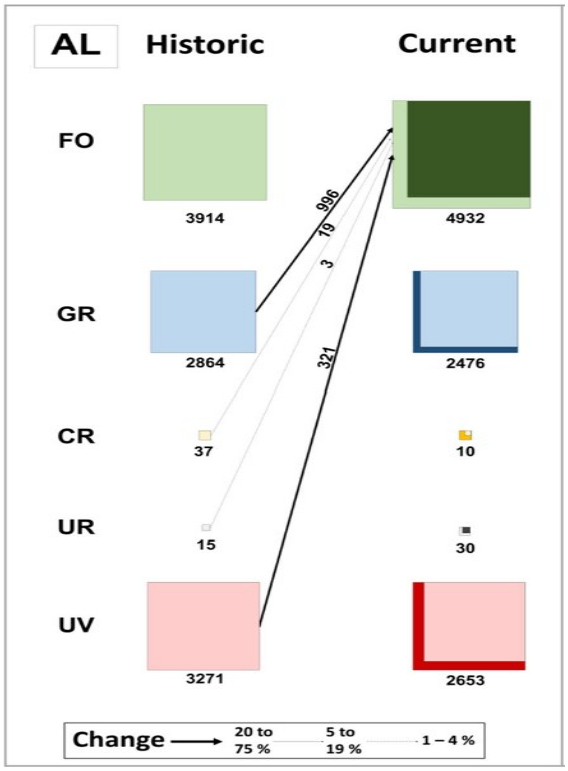

Figure 5: Area of land-cover classes (ha) and land-cover transitions from historic (1954–1962) to present time (2012) in the Alps. The width of the arrows is proportional to the percentage of converted area. ***FO*** *= forests,* ***GR*** *= grasslands,* ***CR*** *= croplands,* ***UR*** *= urban areas,* ***UV*** *= unvegetated areas. Source: Garbarino et al. (2020), adapted.*

These post-abandonment forests, commonly referred to as secondary forests, are therefore not ecologically equivalent to the ecosystems they replace. Their specific composition, structure and dynamics, shaped by centuries of prior land use, constitute the central focus of the following chapter.

2.3. Secondary mountain forests

A secondary forest is defined as "a forest regenerated largely through natural processes after significant human or natural disturbance of the original forest vegetation" (FAO, 2000). In the Alpine context, this definition is part of a transition from agricultural land use to forest cover, via a period of land abandonment (De Frenne et al., 2011). Unlike plantations, secondary forests result from spontaneous regrowth, which often makes them more resilient to climate-related disturbances such as droughts, storms, diseases or heavy rainfall (Jactel et al., 2017).

Secondary forests are different from primary forests, which are those that have maintained an uninterrupted forest cover as they did not undergo significant human disturbance (Hermy and Verheyen, 2007). The main difference between secondary and primary forests is the continuity of the forest cover in time. It is also important to distinguish between the terms ancient and recent forests, which refer respectively to forests present continuously since a specific date (often middle of 19th century) and the secondary forests established after the specific date

(Hermy and Verheyen, 2007). Vegetation structure can be very different between both forests. The term "vegetation structure" refers to the physical arrangement of the trees in a stand including both vertical and horizontal attributes of the forest as well as size-related attributes (McElhinny et al., 2005). Secondary forests establishing on abandoned lands are particularly prone to develop a different vegetation structure because their establishment trajectory is shaped by multiple legacies inherited from the pre-abandonment period. Land-use legacies such as past grazing intensity, terracing, or soil compaction modify soil properties, seed banks, and microsite availability, and can persist for decades to centuries after abandonment (Foster et al., 2003) while biotic legacies such as surviving trees, advance regeneration, seed banks, and root systems directly determine the species and the densities that initiate secondary succession (Franklin et al., 2000). The combination of these legacies with biotic processes during succession generates a wide range of structural configurations which could create different succession trajectories (section 2.3.2). Those structural variations can have major consequences for the ecological functioning of the resulting forests by influencing microclimates, determining the susceptibility to disturbances and affecting biodiversity (De Frenne et al., 2019; McElhinny et al., 2006; Seidl et al., 2017). For these reasons, the characterisation of structural diversity is essential not only to describe the current state of post-abandonment secondary forests, but also to anticipate their future trajectories and their contribution to ecosystem services in mountain landscapes.

2.3.1. Establishment of secondary forests

While section 2.2.2. has described the spatial patterns of the forest expansion at the landscape scale, this section focuses on the biological and ecological mechanisms at the stand level that determine whether and how individual trees establish on abandoned land. The process of establishment of secondary forest can be divided into two parts: the colonisation and the growth.

Colonisation phase

The first part of the establishment is the arrival of seeds. There are two spatial patterns of colonisation, mainly depending on land-use legacies (Alberti et al., 2009). The first type occurs from the edges of existing forests, advancing inwards, and is known as frontal colonisation (Hermy and Verheyen, 2007) (Figure 6). This process occurs fast enough for gaps to be closed, advancing at a rate of around 20 to 100 metres per century for a large number of forest species (Honnay et al., 1999). The second type is the nuclear colonisation around heritage trees also known as the centrifugal colonisation (Hermy and Verheyen, 2007). The condition for this pattern is the presence of isolated trees retained in the site by the past land use (Alberti et al., 2009). The process begins around these isolated trees, which serve as direct sources of seeds, enabling the forest to spread out in all directions from the centre of the site (Harper, 1977). This pattern is illustrated in Figure 6.

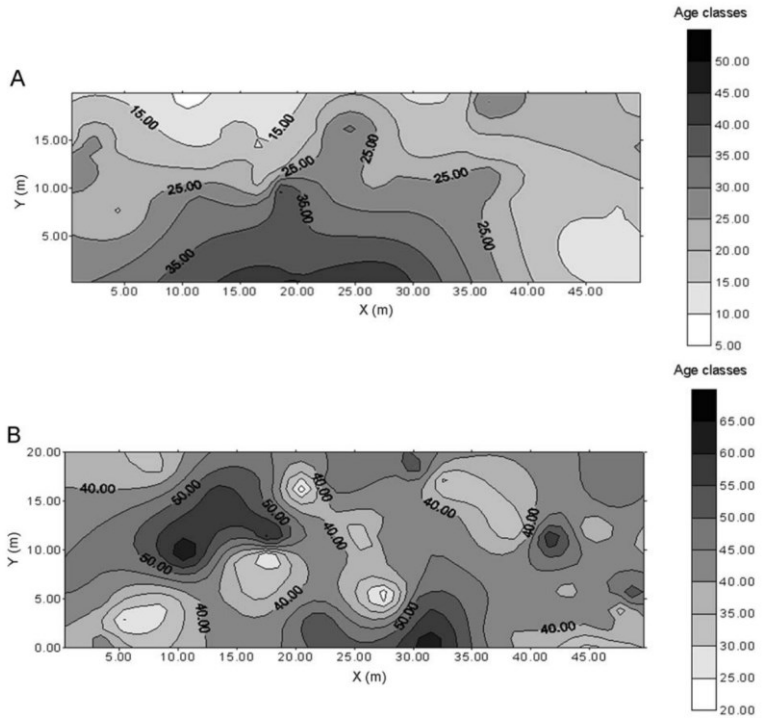

Figure 6: (A) Example of frontal pattern of colonisation. (B) Example of a nucleated pattern of colonisation. Source: Alberti et al. (2009)

The successful establishment of tree seedlings depends on specific microhabitats where they are protected from past or present disturbances (Chazdon et al., 2020). Those specific microhabitats can be anthropogenic, zoogenic and vegetal (Tasser and Tappeiner, 2002). For example, stone walls and piles resulting from the historical clearing of fields provide key habitats for the establishment of secondary forests (Venturi et al., 2022). As these structures are inaccessible to the scythe of the reapers and protected from grazing livestock, they allow trees to survive there and act as seed trees where the colonisation starts once human disturbance has partly or totally ceased (Marengo et al., 2025). Whilst the presence of herds is generally detrimental to the establishment of secondary forests, the trampling caused by these herds paradoxically creates areas of bare ground that are conducive to the germination of certain heliophilous species such as European larch (*Larix decidua*) (Tasser et al., 2007). Deadwood and litter on the ground may also generate favourable conditions for seedling establishment like lower soil temperatures and higher soil moisture (Facelli and Pickett, 1991). The deadwood on the floor represents a good physical protection against browsing from wild animals but also from herds (Botero et al., 2014). The presence of deadwood and litter can also accelerate nutrient cycles, providing higher amount of nutrient in the ground (Marzano et al., 2013; Tilman and Downing, 1994).

However, these excess nutrients often benefit competitive grasses more than pioneer trees (Bohner et al., 2019). This can increase the competition from grasses and create a biophysical barrier for the germination of the pioneer trees in abandoned lands (Tasser and Tappeiner, 2002). A very dense layer of vegetation or a massive accumulation of dead plant matter can physically prevent tree seeds from reaching the ground or germinating (Bohner et al., 2012). Even more, the high density of grasses and the accumulated dead plant matter alters microclimatic gradients by intercepting the majority of the available light at ground level with tree seedlings experiencing severe light deficit (De Frenne et al., 2011). In extreme cases, this competitive filter leads to a state of arrested succession where the vegetation remains locked in a shrubby or herbaceous stage for decades without tree growth (Bebi et al., 2017). The Alpine regions are places where those extreme cases are particularly documented because of the short

growing season, the absence of nearby seed sources and the physical resistance of ericaceous shrubs such as alpenrose (*Rhododendron ferrugineum*) or other trees such as green alder (*Alnus viridis*) (Pornaro et al., 2013).

The phenomenon of arrested succession is an illustration of the fact that land abandonment does not in all the cases lead to natural forest expansion. The colonisation phase of the tree establishment depends on numerous factors such as seed availability, microsite conditions, and the competition dynamics with the existing vegetation.

Land abandonment in mountain regions does not only initiate native secondary succession but also creates favourable conditions for the establishment of invasive alien species. The combination of disturbed sites, high light availability, low initial competition and proximity to dispersal corridors (roads, watercourses, settlements) makes abandoned lands particularly vulnerable to colonisation by non-native pioneer species (Lazzaro et al., 2018). In the Alps, five tree species are of particular concern in protected forest habitats: black locust (*Robinia pseudoacacia* L.), tree of heaven (*Ailanthus altissima* (Mill.) Swingle), box elder (*Acer negundo* L.), black cherry (*Prunus serotina* Ehrh.) and northern red oak (*Quercus rubra* L.) (Campagnaro et al., 2018). Among them, the tree of heaven has been increasingly documented in the southern Alps, where its allelopathic compounds suppress native regeneration and durably alter community composition (Knüsel et al., 2015). Climate warming is expected to further facilitate the upward migration of these species, expanding their potential range into montane or subalpine forest belts (Petitpierre et al., 2016), which makes the management of secondary forests on abandoned lands a key issue for the conservation of native alpine plant communities.

Growing phase

Once the seedlings are established and have overcome the challenges of competition, the focus shifts from the colonisation phase to the growth phase. During this phase, the question is no longer whether establishment has taken place, but how is establishment proceeding.

The growing phase of secondary forest is strongly dependent on the abiotic conditions of the site. The environmental variables explain the differences between two secondary forests of the same age with completely different structures. One of the dominant climatic variables is the mean annual temperature, which acts like a speed regulator for the secondary succession (Pornaro et al., 2013). The elevation lags of temperature generate strong gradients with significantly faster reforestation at lower altitudes (Moser et al., 2005). On the other hand, at the treeline, the harsher climate conditions drastically constrain tree growth (Bani et al., 2019). The aspect of the slope directly affects the amount of light energy received by plants, thereby affecting their growth rate (Garbarino et al., 2013). South-facing slopes are warmer and sunnier, which favours light-demanding species and accelerates initial growth while north-facing slopes tend to favour shade-tolerant species, which often grow more slowly but are more persistent (Anselmetto et al., 2024; Garbarino et al., 2013). Another important abiotic factor influencing tree growth is soil heritage. Soil quality, shaped by past land use, is a key determinant of productivity (Alberti et al., 2009). Soils derived from former hay meadows often retain significant residual fertility, which accelerates tree growth compared to more acidic natural forest soils (Koerner et al., 1999). Conversely, soils that have undergone prolonged overgrazing can become heavily compacted, which slows down root development and overall tree growth (Pedersen et al., 2023).

Those factors affect tree growth and the establishment of secondary forests in different ways, depending on their stage of development (Alberti et al., 2009). Three main phases can be identified: slow establishment, canopy closure, and exclusion of stems (Pornaro et al., 2013). The slow establishment sees the first trees establishing sparsely across the site, whilst the herbaceous layer still largely dominates the site (Van Uytvanck et al., 2008). This period, which lasts for approximately the first 10 years following abandonment, is characterised by low stem density and slow growth rates due to significant competition from herbaceous and shrubby vegetation for light and nutrients (Finegan, 1984). The second phase, the canopy closure, occurs between 10 and 20 years after abandonment, with stable woody vegetation spreading across the entire site (Finegan, 1984). During this period, the canopy closes in, thereby eliminating most grassland species due to the shade it casts (Alberti et al., 2009). The third phase of the establishment of trees is the exclusion of stems when the intraspecific competition becomes dominant, beginning approximately 30-45 years after land is abandoned (Smit and Olff, 1998). The number of stems decreases significantly, with dominant trees growing in both height and diameter (Alberti et al., 2009; Scridel et al., 2022).

These three developmental phases describe the structural assembly of a secondary forest stand during its first decades. However, beyond this initial establishment window, the long-term trajectory of the forest is strongly shaped by the land-use history of the site

2.3.2. Succession dynamics in secondary forest

Once the establishment phase is complete, secondary forests then enter a long-term succession process guided by a series of different dynamics. In the past, classical succession theory described a final state, known as a *climax* community, as the result of a deterministic and directional process directed by the climate (Clements, 1916; Connell and Slatyer, 1977). According to this perspective introduced by Clements (1916), all forests at a given site would inevitably converge towards the same final state, regardless of the initial conditions. However, recent research carried out in the Alps has begun to provide empirical evidence against this simplistic model. This research shows that succession pathways are far more complex, non-linear and heavily dependent on initial conditions (Poorter et al., 2023). Figure 7 shows the two different conceptions of the succession dynamics. Figure 7(A) illustrates the concept of climax, the fact that species succession is driven by a series of consecutive processes (Clements, 1916) while Figure 7(B) illustrates the importance of the starting conditions, especially the human activities in this case (Jakovac et al., 2021). This idea of different successional pathways is particularly relevant in the Alpine region (Marengo et al., 2025). Understanding why this diversity of successional states exists is a central question in mountain forest ecology.

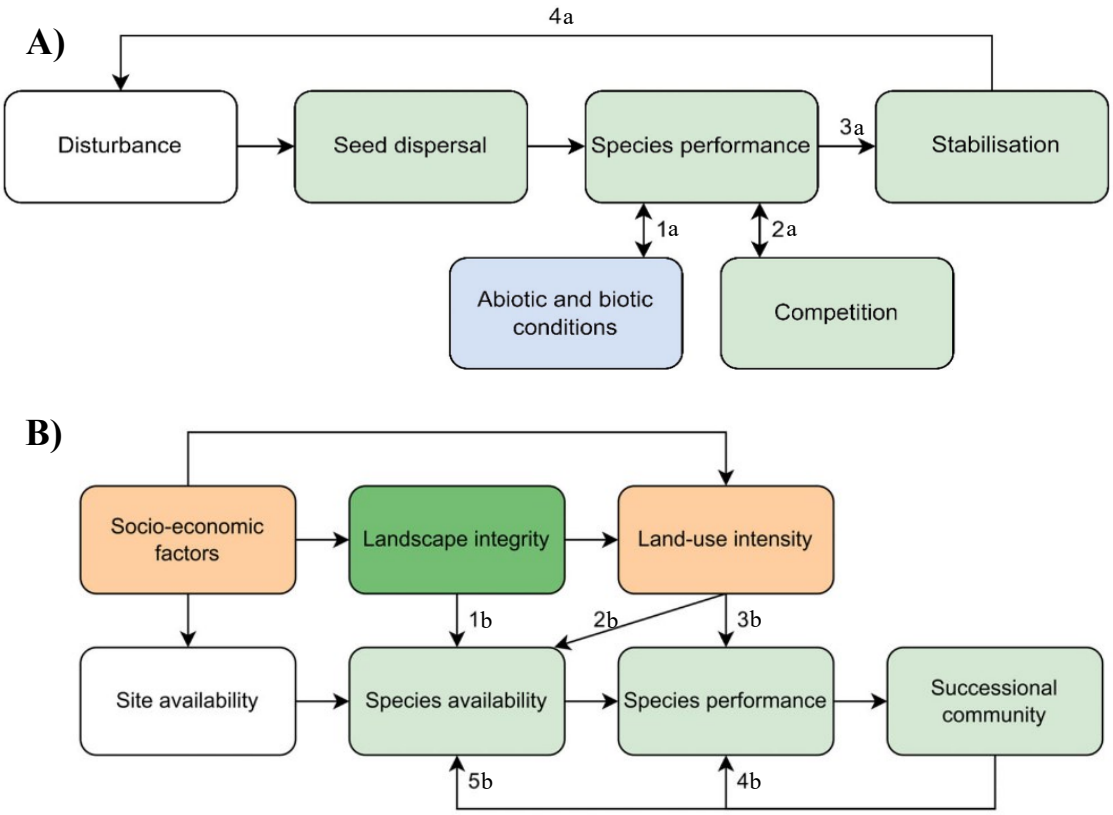

Figure 7: Comparison between the two conceptions of the succession dynamics. A) Relay floristics (Clements, 1916). Seed dispersal to the new site leads to differential species performance (germination, establishment, growth), which is modified by changes in abiotic and biotic conditions (1a) and competition (2a). Over time, the rate of successional change will decline (3a), leading to stabilisation of the community into a climax vegetation, until a new disturbance creates an open site (4a), resetting succession to an earlier successional stage. B) Land-use intensity (Jakovac et al., 2021). Humans transform the landscape and directly or indirectly determine succession. Socio-economic factors determine landscape integrity land-use intensity, and site availability. Site availability initiates succession. Landscape integrity affects species availability through propagule production and dispersal (1b). Past land-use intensity varies in duration, extent, frequency, intensity, and length, which all leave different environmental legacies that affect species availability (2b) and performance (3b). The developing successional community has successional feedback loops and modifies the environment thus affecting species performance (4b) and contains reproductive trees that affect local seed availability (5b). Source: Poorter et al. (2023), adapted.

Contemporary research in forest ecology embraces the theory that, rather than following a single possible path, succession is a network of possible paths depending on initial conditions and the legacy of land use (Poorter et al., 2023). A key example is the study of Marengo et al. (2025), which shows that forests originating from former woodland exhibit ecological conditions closer to natural trajectories, whereas those that have developed from abandoned grassland still show pre-forest conditions after several decades of abandonment. Various mechanisms may explain why succession trajectories tend to diverge rather than converge. The first species to colonise an abandoned site may monopolise the resources, preventing subsequent species from arriving for years and decades to come (Connell and Slatyer, 1977). This process is called the priority effects. This often happens in the Alps, where green alder (*Alnus viridis*), alpenrose (*Rhododendron ferrugineum*), and *Rubus* spp. can hinder tree growth for decades, thereby causing the trajectory to deviate from the expected climax stage (Alberti et al., 2009). The initial conditions, especially the land-use legacies (soil properties, seed bank, biological legacies), create divergences that may persist for a long time (Garbarino et al., 2013). The random arrival of seeds creates an irreducible variability between sites that are otherwise similar in terms of climate and topography (Clark et al., 2019). This random arrival is completed

by the dispersal limitation mechanism: a lot of specialist species from the classic climax state have low colonisation ability and depend on slow-dispersing vector (Flinn and Marks, 2007). As a result, even if a site offers favourable conditions for these species to establish themselves, they can only do so if they are in the immediate vicinity of that site (Hermy et al., 1999). Pioneer species alter the microbial composition of the soil to favour or hinder the arrival of other species, thereby influencing the course of succession (Jakovac et al., 2021). In the alpine context, examples include larch and dwarf mountain pine (*Pinus mugo*), which promote their own regeneration whilst delaying the establishment of species of more advanced stages (Bebi et al., 2017; De Giuli et al., 2024). And as already said before, fine-scale variations in topography and soil create filters that affect all species, leading to small-scale variations (Pornaro et al., 2013).

Another important idea developed by the contemporary research is the fact that the divergence among secondary forests is not a temporary phase but also a persistent state (Poorter et al., 2023). Research conducted across the Alps has shown that forests originating from different land-use types remain floristically and structurally distinct long after abandonment (Marengo et al., 2025). This persistence of land-use legacies has been documented over periods exceeding half a century, suggesting that the memory of past land use is not erased by succession but rather actively shapes its long-term trajectory (Hermy and Verheyen, 2007). Some empirical experiments have proven that key forest soil properties remain measurably reduced in post-agricultural forests 85 to 100 years after abandonment compared to primary forest (Flinn and Marks, 2007). In the Austrian Alps, it has been proven that land-use legacies continue to affect forest carbon dynamics for at least one century after the abandonment (Thom et al., 2018). The floristic recovery of post-agricultural forests is an extremely slow process where the transition to a close forest may require a major anthropogenic or natural disturbance (Chazdon et al., 2020; De Frenne et al., 2011). An example in the Alps are grasslands rich in shrubs or competitive grasses such as *Brachypodium pinnatum*, which prevent the establishment of woody species, thereby maintaining the system in an alternative stable state that prevents progression towards more advanced succession stages (Bohner et al., 2019). Another example is the shrub states maintained by mountain pine which represent also alternative stable states where the transition to a close forest requires a significant disturbance or a human intervention (De Giuli et al., 2024). Those examples show that the transitions between states are not gradual but often require a threshold-crossing event, like a stand-replacing natural disturbance or human intervention, to shift the system from one stable state to another (Poorter et al., 2024). The idea of alternative stable states is directly linked to the notion of divergent trajectories, the idea that under same environmental conditions, an ecosystem can exist in multiple distinct configurations (Pornaro et al., 2013).

This evolution theory of the successional dynamics shows that, as successional trajectories are shaped by identifiable and measurable factors, the type of secondary forest present in a precise location should be predictable from both its biophysical environmental template and the historical context of the landscape (Poorter et al., 2023). This predictability is based on the idea that, although certain random processes such as the arrival of seeds may introduce some variability, the structure and composition of a secondary forest are largely determined by deterministic factors (Anselmetto et al., 2024). If the successional trajectories were purely stochastic, the structure and the composition of secondary forests would be unpredictable and completely random. But the evidence reviewed above shows that an important part of the variability of those forests can be attributed to deterministic factors such as climate and topographic conditions and land-use history of the site, and the pre-existing seed pool available (Marengo et al., 2025). As mentioned previously, one of the most important differences among the secondary forest types is the successional stage. Some abandoned places remain covered by

shrubby species such as alpenrose, green alder, mountain pine or *Rubus* spp. for decades (Alberti et al., 2009; De Giuli et al., 2024). Some remain in early pioneer phase, characterised by open stands of light-demanding species as white birch (*Betula pendula*), European ash (*Fraxinus excelsior*), larch, etc with thick and persistent herbaceous understory (Marengo et al., 2025). Others have reached an intermediate state with a closure of the canopy and an increasingly complex structure (Alberti et al., 2009). The intraspecific competition becomes important, leading to the stage of stem exclusion, where density is high but with a low vertical diversity (Pornaro et al., 2013). A small proportion, often those that have benefited from natural legacies or situated in pre-existing wooded areas, approaches the late successional state, close to the potential natural vegetation (Marengo et al., 2025). This continuum of successional state is a product of the main factors identified earlier in this paragraph (Tasser and Tappeiner, 2002).

Despite significant advances in understanding these factors individually, their combined and relative influence on secondary forest type at the local scale remains insufficiently documented. Most studies have focused on the spatial patterns of natural forest expansion at the landscape scale or on the successional dynamics of a specific species such as larch forests. A multi-driver approach to predict secondary forest types at the site scale remains a significant gap in the literature. A first step towards filling this gap was recently made by Gontier (2026), who tried to characterise the secondary forest types in the Aosta Valley sector of the Gran Paradiso National Park (Italy). He has surveyed 182 plots and identified ten distinct forest groups structured along an altitudinal-thermal gradient. However, this study was limited to a single climatic sector of the park and did not provide a quantitative ranking of the relative importance of the environmental drivers structuring forest diversity.

3. Objectives

The evolution of the mountain landscapes in the Alps beginning with widespread deforestation over thousands of years and ending with natural forest expansion has led to the current landscape structure. Land abandonment started in the 19th century with the industrial revolution and the rural exodus has created a heterogeneous mosaic of secondary forests in the Alps. The different patterns of successional dynamics are strongly influenced by multiple climatic, topographic and anthropogenic factors (hereafter, environmental factors). Due to the wide variety of conditions, the trajectories of those secondary forests do not converge towards a single natural state but remain strongly influenced by their initial conditions at the time of establishment. These differences in secondary forest types based on variations in factors have so far received relatively little attention. The scientific literature lacks information on the ability to predict secondary forest types based on different factors.

This thesis therefore fits into this context. Its overall aim is to answer the following question:

"What are the environmental factors determining the secondary forest diversity in mountain ecosystems?"

To answer this question, three specific sub-objectives have been identified. The first is to try to identify the different types of secondary forests based on forest variables relating to the structure, composition and regeneration of stands. This classification will help to describe these different types of secondary forest in detail based on forest-related variables. More specifically, this sub-objective aims to identify several ecological gradients that distinguish the different types from one another. The second sub-objective is to link the environmental factors with the different forest types described previously and identify which factors explain the variation between the secondary forest types. Finally, the third sub-objective is to quantify and rank the relative importance of climatic, topographic and anthropogenic variables. This study also aims to compare the results obtained with those of Gontier (2026) in the Aosta Valley sector. This comparison aims to assess the robustness of the forest types and ecological gradients identified across different spatial extents and methodological frameworks, and to explicitly identify the contribution of the Piedmont sector to the overall diversity of secondary forests in the Gran Paradiso National Park.

4. Materials and methods

4.1. Study site

4.1.1. Location of the GPNP

The study area corresponds to the Gran Paradiso National Park (GPNP), the oldest Italian National Park that is located in the Western Italian Alps and encompasses more than 70,000 ha in the Aosta Valley and Piedmont regions (Richiardi et al., 2025) (Figure 8). The Aosta Valley sector of the GPNP has been the focus of recent ecological investigations on post-abandonment forest dynamics (Gontier, 2026).

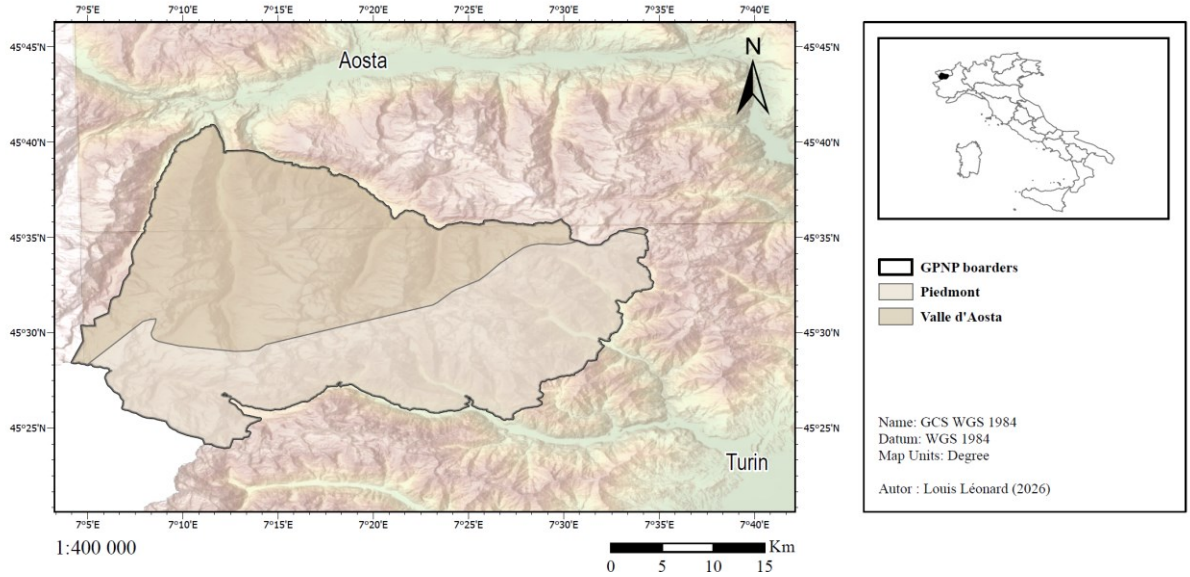

Figure 8: Location of the GPNP, within two Italian regions: Piedmont in the South and Aosta Valley, in the North. The South-Western portion of the Park borders the Vanoise National Park, in France.

A portion of the GPNP was designated as a hunting zone in 1836 and became in 1856 the Royal Hunting Reserve of the Gran Paradiso ("Gran Paradiso National Park | Alps, Wildlife, Nature | Britannica," n.d.). With this new classification, the creation of multiple trails has been launched by King Vittorio Emanuele II, to protect the fauna, especially the Alpine ibex (*Capra ibex*). In 1922, the hunting reserve was transferred to the Italian state and the GPNP was inaugurated ("Histoire," n.d.). In the decades after the Second World War, the scientific research within the Park was given more attention and funds. In 2007, the GPNP received the European Diploma for Protected Areas thanks to its outstanding natural heritage, the good conservation level of its ecosystems, the integration of tourism and agricultural activities, and its role as a cross-border protected Alpine area. GPNP is also the only Italian national park to be on the IUCN Green List since 2014, an award that highlights its very important role in the conservation and the management of protected areas.

The GPNP, like all the Alpine region, is affected by the significant decline of the human population. To give an example, the population in the municipality of Noasca, located in the Orco valley (Piedmont region) has decreased by 47.5% between 2001 and 2021. Furthermore, 43.4% of the population is above 65 years old (Sella et al., 2025). The main consequence of the ageing and population decline is the loss of the traditional farming and pastoral activities.

Across the valley, indeed, secondary post-abandonment forests quickly replace the grasslands, pastures and productive forests like coppice stands.

4.1.2. Physical context

The park has a very specific topography. Its lowest point rises to approximately 800 m a.s.l. and the highest point is 4,061 m a.s.l., corresponding to the Gran Paradiso summit. Around 75% of the Park's surface is higher than 2,000 m a.s.l. and 58% higher than 3,000 m a.s.l. (Poussin et al., 2019). The variety of elevations, slopes and aspects within the GPNP creates a large range of diverse meso- and micro-environments.

The climate within the GPNP is extremely variable as a result of this complex topography. According to the Köppen–Geiger classification, the climate in the GPNP is classified as *ET-Dfb* which means cold winters, cold-to-warm summers and no dry seasons (Peel et al., 2007). The mean temperatures depend on the altitude, with values higher than 0.4°C below 1,800 m a.s.l. and lower than 2°C above 1,800 m (Morgese et al., 2024). The coldest months are December to March, while the warmest are July and August. The historical trend in temperatures shows an average increase of 1.5°C across the Italian Alps over the last 150 years (Brunetti et al., 2009).

The GPNP's high elevation creates barriers for moist air masses coming from the Mediterranean and Atlantic regions, leading to significant spatial disparities among the valleys. The central zone has an arid climate with a mean annual rainfall around 500 mm while at the edges of the Park and valley heads, rainfall can exceed 1,400 mm per year (Morgese et al., 2024). The rainfall pattern is seasonal, with a bimodal seasonal precipitation pattern showing peaks in spring and autumn.

Figure 9 (Poussin et al., 2019) shows the climatological annual mean cycle of temperature and precipitation in the GPNP based on dataset developed for the Greater Alpine Region, HISTALP (Auer et al., 2007).

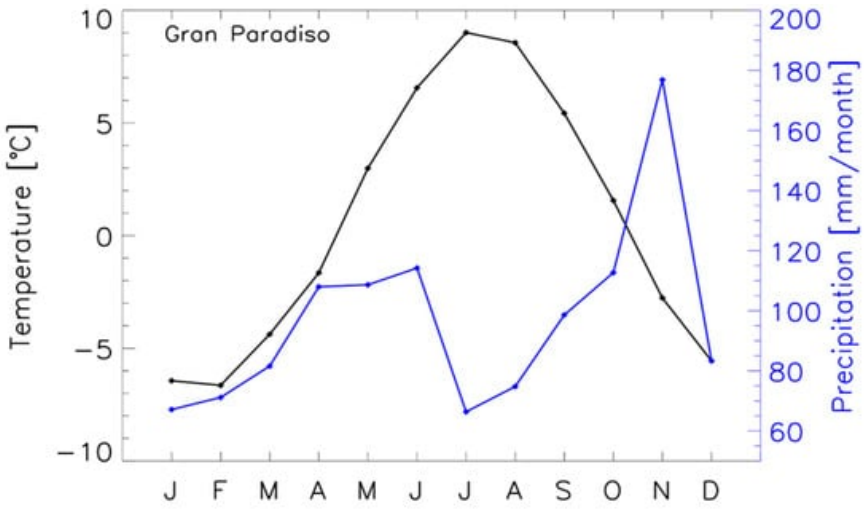

Figure 9: Climatological annual cycle of temperature and total precipitation spatially averaged over the GPNP for the period 1950-2014 (Poussin et al., 2019).

The hydrography of the park is characterised by two main catchment areas with the Orco and Dora Baltea rivers, respectively in the South (Piedmont region) and the North (Aosta Valley region) of GPNP. These rivers are fed by a large series of smaller rivers and streams. The GPNP is also characterised by a seasonal supply of water at the start of the summer. This intake can

be explained by the melting of the snowpack and glaciers (Tiberti et al., 2010). Many lakes can be found inside the park. They are present up to almost 3,000 m and vary greatly in terms of a range of characteristics such as size, depth, frost period, etc.

Geologically speaking, the massif in which the Gran Paradiso National Park is located is formed of rocks dating from several different geological periods. The main rock component of the massif, a fragment of the European continental margin, is gneiss. Overlying the continental massif is the Piedmont zone, composed mainly of calc-schists (metamorphosed sedimentary rocks rich in carbonates) and serpentinites from the oceanic plate (Caso et al., 2021). The significant presence of iron ore veins in the massif had a major influence on the lives of the GPNP's inhabitants in the past ("Parco Nazionale Gran Paradiso: L'Espace Protégé," n.d.).

The soils in the GPNP are linked to the contrasting geology and the glacial processes affecting the landscape. In areas dominated by gneiss, soils are generally more acidic, whereas they are carbonate soils where calcareous schists parent material dominates (Parisi et al., 2024; Tiberti et al., 2010). Some recent research shows that the weathering of soils recently released by glaciers is surprisingly rapid and can be explained by significant biological weathering (D'Amico et al., 2020). The dynamics of the soils within the GPNP are also strongly influenced by significant seasonal variations in temperature and water regime and the snow cover (Parisi et al., 2024).

4.1.3. Biological context

The GPNP presents a wide variety of environments with glaciers, high summits, alpine grasslands and a wide variety of forest types. Forest stands in the bottom of the valley are composed mainly of a mix of deciduous trees such as maples (*Acer* spp.), white birch (*Betula pendula*), sweet chestnut (*Castanea sativa*), common hazel (*Corylus avellana*), European beech (*Fagus sylvatica*), European ash (*Fraxinus excelsior*), oaks (*Quercus* spp.). At higher altitudes up to the treeline, the forests are dominated by conifers, mainly silver fir (*Abies alba*), European larch (*Larix decidua*), Norway spruce (*Picea abies*), and Swiss stone pine (*Pinus cembra*) (Richiardi et al., 2025).

The GPNP is also renowned for its remarkable biodiversity in terms of flora. More than 247 species of plants have been found in the alpine grasslands of the GPNP (Hoffmann et al., 2019). Overall, the species richness is higher at intermediate altitudes before declining towards the nival belt (Baumann et al., 2016).

The GPNP is a sanctuary for alpine fauna, especially for wild ungulates. More than 2600 Alpine ibex (*Capra ibex*) and 6300 chamois (*Rupicapra rupicapra*) were counted in the year 2022 (Parisi et al., 2024).

Within the park, about 60% of the surface area is covered by habitats with scarce or no vegetation, 20% is covered by woodlands and shrublands, 17% by meadows and pasture and 1% by croplands and settlements (Poussin et al., 2019). As in most of the Alpine environment, the GPNP is also affected by widespread land-cover change in the last decades. The main change inside the GPNP is a decline of the grasslands, with a rate of 10.09 ha $year^{-1}$, and an increase of the shrublands, with a rate of 10.01 ha $year^{-1}$ between 1985 and 2023 (Richiardi et al., 2025). Overall, a greening trend has been observed across the area. Over a longer time scale (1954–2022), Gontier (2026) documented in the Aosta Valley sector of the GPNP a +11.17% increase in grassland and a +2.29% increase in dense forests, mainly at the expense of

unvegetated areas (−17.51%), illustrating a multi-decadal greening dynamic that combines glacier retreat at high elevations and post-pastoral succession at lower elevations.

4.2. Forest structure data

4.2.1. Sampling design and data collection

Forest structure was collected within plots representing secondary forests. The sampling design was based on a diachronic analysis based on both historical aerial photographs (HAPs) for the years 1954, 1975, 1991, and 2006, and a recent satellite image for the year 2024. Polygons of secondary forests were selected from the comparison of land-cover maps derived from the aerial images. Secondary forests are here defined as polygons that nowadays are covered by dense forests (i.e., canopy cover > 80%). Only polygons bigger than 1 ha were considered, and smaller polygons were filtered out. A second step was dedicated to select polygons guaranteeing a good balance between different land-use legacies, succession stages (i.e., the age of secondary forests based on the comparison of land-cover maps) and accessibility (i.e., polygons close to trails on moderate slopes, lower than 30°). The plot position within the selected polygons was randomly decided in the field. Overall, the sampling strategy resulted in 283 sampling plots (Figure 10). Of those, 182 plots (64.3%) are in the northern part of the GPNP, within the Aosta Valley section. These plots were surveyed in 2024 within the framework of the thesis of Gontier (2026). These shared plots were collected following an identical protocol and provided the structural and compositional dataset used in the present analysis. The remaining 101 plots (35.7%) were inventoried in the Piedmont sector using the same methodology, in order to ensure the comparability of the two datasets.

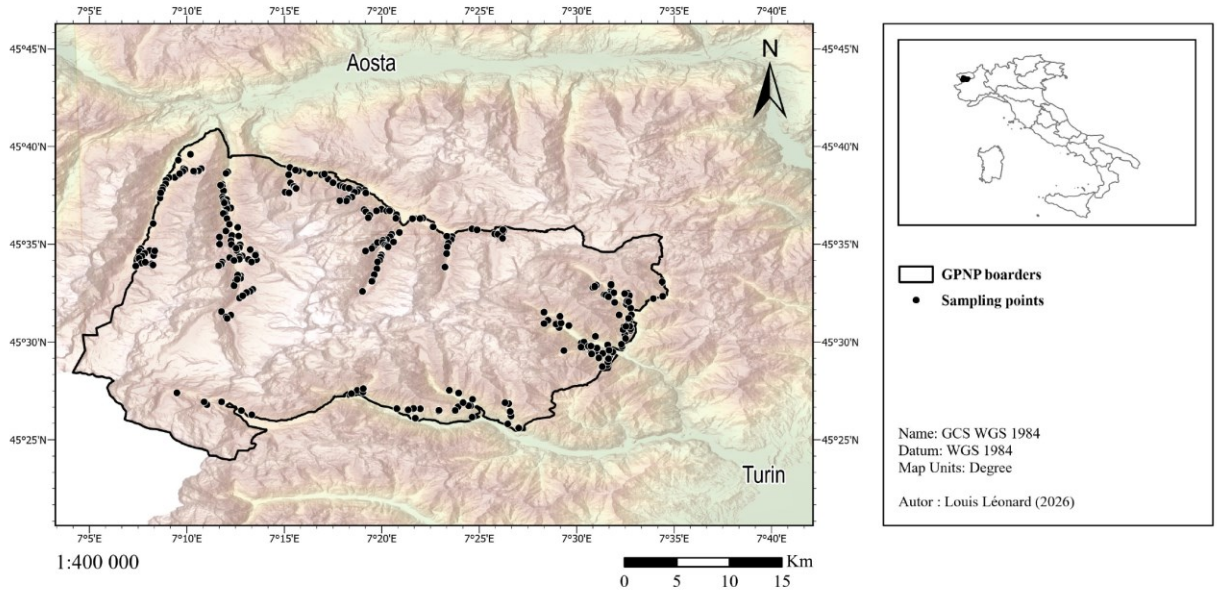

Figure 10: Location of the 283 sampling points across the GPNP.

4.2.2. Forest structure metrics

On each plot, two concentric subplots were placed to collect data on the forest structure. On the external one (diameter = 20m, measured parallel to the ground in the field), we performed a complete inventory of trees. A diameter at breast height (DBH) of 7.5 cm is chosen for the inventory threshold; for each tree with a DBH higher than this threshold, we determined the species and recorded the DBH. This larger subplot was also used to determine the surface cover in percentage. The following categories of surface were adopted: rocks, bare soil, deadwood,

litter, grass, shrub and forest regeneration. For each plot, the sum of the individual percentages is always equal to 100%.

The second inner subplot (diameter = 6 m) was established to collect information about the forest regeneration. Inside this one, all the trees with a DBH lower than 7.5 cm were counted for each species. Individuals were classified as seedlings or saplings; the former correspond to trees with a height of less than 1.5 m while the latter correspond to trees with a height of more than 1.5 m but with a DBH of less than 7.5 cm.

The coordinates of the centre of the two plots are saved by using the phone's GPS in the WGS84 system.

4.2.3. Data processing

A set of summary statistics was derived for each plot to characterise the forest structure.

The mean, maximum, minimum and standard deviation of the DBH were derived for each plot.

The DBH of each tree was used to determine the basal area (BA) in $m^2\ ha^{-1}$. First the DBH of each tree was converted into the surface area occupied by the trunk, calculated as follows (Equation 4.1):

$$s_i = \frac{(\pi.(\frac{DBH_i}{2})^2)}{10{,}000} \tag{4.1.}$$

With S_i being the surface occupied by the tree *i* (m^2) and DBH being the diameter measured for the tree *i* (cm).

The basal area for the plot was then obtained through the following equation (Equation 4.2.):

$$BA = \left(\frac{\sum S_i}{\pi.10^2}\right).10{,}000 \tag{4.2.}$$

With BA being the basal area of the plot ($m^2\ ha^{-1}$) and $\sum S_i$ being the sum of all the surface occupied by the trees in the plot (m^2).

The BA of each species in the plot was also calculated to determine the dominant species at the plot's scale.

As those formulas (Equations 4.1. and 4.2.) are based on the hypothesis that the plot is located on a flat area, they were then divided by the cosine of the slope angle to take the slope into account through Equation 4.3.:

$$BA_s = \frac{BA}{\cos(SLOPE)} \tag{4.3.}$$

With BA_s being the basal area considering the slope ($m^2\ ha^{-1}$) and SLOPE being the average slope of the plot, derived from the DTM in QGIS (°).

The third variable calculated was the tree per hectare (TPH) corresponding to the density of trees (trees ha^{-1}). This variable was calculated based on the number of trees counted on the external subplot through the following equation (Equation 4.4.):

$$TPH = \frac{n}{\pi . 10^2} . 10{,}000 \quad (4.4.)$$

With n being the number of trees counted on the plot and TPH being the density (number of trees ha^{-1}).

The same correction used for the BA was made to take the slope into account (Equation 4.3.).

The density was calculated for the seedlings and saplings as well with the data obtained on the inner subplot. The TPH was therefore calculated at three levels: per species for trees (TPH t), per species for seedlings (TPH se), per species for saplings (TPH sa), and as a total across all species for the tree layer (TPH).

To determine the diversity of the plot in terms of species composition, we used the Brillouin's index. This index is defined by the following equation (Equation 4.5.):

$$HB = \frac{\ln(N!) - \sum_{i=1}^{S} \ln(n_i!)}{N} \quad (4.5.)$$

With HB being the Brillouin diversity index, N being the total number of individuals recorded, S being the total number of species recorded and n_i being the number of individuals for the species i.

This index was preferred over the Shannon's one because, within the plot, the entire community is known as every stem was recorded. Indeed, the Brillouin index calculates the exact diversity, without statistical interference, of a collection where every individual is known, whereas the Shannon index assumes that the individuals measured represent a random subset of a community whose overall composition is unknown (Pielou, 1975). The Brillouin index was computed for each plot individually using a custom R function (R Core Team, 2023), retaining only species with positive counts within each plot. Absent species were excluded prior to calculation, ensuring that the index reflects the local species composition of each sampling unit rather than the regional species pool. Four indices are calculated: one for the trees (HB t), one for the saplings (HB sa), one for the seedlings (HB se), and one for the saplings and seedlings together (HB sesa).

A light tolerance index (LTI) was calculated for each plot. For that, we used an ecological indicator created by Landolt (2010). The indicator assigns a score from 1 to 5 for each species, with 1 referring to the lowest tolerant to light and 5 to the highest. So, species with a score of 1 or 2 can be considered as shade-tolerant while species with a score of 3 to 5 can be considered as light-demanding. A value was therefore assigned to each tree species within the plot, and a weighted average based on BA was then calculated to obtain the final value for the plot.

The abundance of broadleaves (BLF) was calculated as the ratio of the sum of the basal areas of all broadleaved species to the total basal area of the plot, expressed as a percentage.

All those variables were grouped in one matrix to characterise the forest for each data collection point. Inside this dataset, the information about the surface cover (Section 4.2.2) and the

abandonment stage were also included. This one was calculated based on the historical image data of the GPNP. Those data help to estimate the date of the establishment of the new forests. The abandonment stage variable ranges from 1 for newer forests established after 2006 to 5 for the forest stands established before 1954.

4.3. Environmental dataset

A secondary matrix containing information on the environmental conditions of each plot was created (Appendix 1). This environmental dataset groups factors that are known to drive the successional dynamics of the secondary forests. These variables are grouped in five main categories: topographic/terrain context, anthropogenic variables, land-cover legacies, climate and landscape metrics. All the environmental data are determined for a buffer zone with a diameter of 10 metres, except for the landscape metrics which are calculated within a buffer zone with a diameter of 100 metres. Once all the data have been determined for each plot, they are gathered in a second matrix, the first being with the forest data (section 4.2).

4.3.1. Topographic/terrain context

This category contains all the data linked with the topographic/terrain context of the plot. The region and the valley are determined by using the administrative boundaries. We used the R package *terra* (Hijmans et al., 2020) to develop the slope, elevation, topographic ruggedness index (TRI) and topographic position index (TPI). The TRI measures the surface roughness, a quantification of topographic heterogeneity and local spatial variability of the slope (Trevisani et al., 2023). The TPI measures the relative topographical position of a central point (e.g. ridge, slope, bottoms, etc.) by calculating the difference between the elevation of that point and the average elevation within a predetermined neighbourhood (De Reu et al., 2013).

The aspect of the plot position is characterised by determining the relative exposition of the plot to the South and directions through two complementary indices. The first one (i.e., southness) characterises the South exposition with the following equation (Equation 4.6.):

$$Southn = -\cos\theta \tag{4.6.}$$

With Southn being the South exposition (-) and θ being the aspect (rad).

The index Southn is equal to 1 when the plot position is oriented directly to the South and -1 with an orientation to the North.

The second one (i.e., eastness) characterises the East exposition with the following equation (Equation 4.7.):

$$Eastn = \sin\theta \tag{4.7.}$$

With Eastn being the East exposition (-) and θ being the aspect (rad).

The index Eastn is equal to 1 when the plot position is oriented directly to the East and -1 with an orientation to the West.

Other variables are the topographic wetness index (TWI) and the heat load index (HLI). The TWI is an indicator of soil moisture. It quantifies the variation in soil water content induced by

the shape of the terrain (Kopecký et al., 2021) . TWI was computed from a custom function (Equation 4.8.):

$$TWI = \ln \frac{\alpha}{\tan(\beta)} \quad (4.8.)$$

With TWI being the topographic wetness index (-), α being the specific catchment area ($m^2\ m^{-1}$) and β being the slope (rad) (Larson et al., 2022). The specific catchment area is obtained using the function *flowAccumulation* from the R package *terra*.

The HLI corresponds to a topographical index used to estimate the potential annual direct incident radiation received at a given location (Maxwell and Shobe, 2022). It was calculated with the function *hli* from the R package *spatialEco*.

4.3.2. Anthropogenic variables

Another type of location data calculated are the distances of each plot from the 1954 forest and today's human structures. For the former variable, three distances were calculated using the land-cover map of the GPNP from 1954 (Appendix 2) and the software ArcGIS. In this land-cover map, two types of forest were identified: the dense forest (canopy cover > 80%) and sparse forest (canopy cover between 20 and 80%). The three distances were: (i) the distance from the nearest dense forest, (ii) from the nearest sparse forest, and (iii) the nearest forest regardless of the type. To define remoteness, two types of human structures were used: roads and buildings.

4.3.3. Land-cover legacies

The land cover was determined by using the land cover raster of the GPNP from 1954 (Appendix 2). Five types of land cover are identified: (i) dense forest, (ii) sparse forest, (iii) grassland, (iv) unvegetated areas and (v) anthropogenic areas. The abandonment stage described in section 4.2.3 was also included in this part of the matrix. The year 1954 was chosen because it corresponds to the earliest systematic aerial photography available for the GPNP (Statuto et al., 2017). Moreover, this date corresponds to the major wave of land abandonment in the Italian Alps during the 1950s and 1960s (MacDonald et al., 2000; Tasser and Tappeiner, 2002).

4.3.4. Climate data

Climate conditions were characterised through CHELSA (Climatologies at high resolution for the Earth's land surface areas) dataset (Karger et al., 2017a) from the digital terrain model (DTM) of the GPNP (Appendix 3).

CHELSA is a global, kilometre resolution climate dataset generated through a downscaling model (Brun et al., 2022; Karger et al., 2017b). For this study, a series of climate variables was extracted for each plot position from the whole dataset: BIO1 (mean annual air temperature, °C), BIO2 (mean diurnal air temperature range, °C), BIO5 (mean daily maximum air temperature of the warmest month, °C), BIO6 (mean daily minimum air temperature of the coldest month, °C), BIO12 (annual precipitation amount, kg m^{-2} y^{-1}, equivalent to mm y^{-1}), gdd0 (heat sum of all days above the 0°C temperature accumulated over 1 year, °C), GSL (growing season length, number of days, defined as the period between the first and last occurrence of at least 6 consecutive days with mean daily temperature above 5°C), and SCD (number of days with snow cover, number of days).

4.3.5. Landscape metrics

To measure and analyse the spatial structure of the 1954 landscape context of each plot, a set of landscape metrics was derived at the class level, where the class was one of the five land cover types described in section 4.3.3. To calculate them, we used the R package *landscapemetrics* (Hesselbarth et al., 2019). This package allows the determination of metrics at the landscape, class, and patch level by reproducing the FRAGSTATS metrics approach directly in R language (Hesselbarth et al., 2019). The landscape metrics were calculated within a buffer of 100 m around the plot. In this study, five landscape metrics were chosen to describe the landscape: the land cover (C), the Simpson index (SIDI), the aggregation index (AI), the patch density (PD), and the edge density (ED). Each metric was calculated at the landscape scale and at the class scale except for SIDI and C, which were calculated only at the landscape scale and class scale, respectively.

The land cover (C) measures the surface area of each class within the 100 m buffer. It is expressed in hectares.

The Simpson index (SIDI) expresses the diversity of classes within the buffer. It has values between 0 and 1; 0 when the landscape contains only one patch (no diversity) and approaches 1 as the number of different patches increases and the proportional distribution of area among patch types becomes more equitable. The following equation has been used to calculate it (Equation 4.9.):

$$SIDI = 1 - \sum_{i=1}^{m} {P_i}^2 \tag{4.9.}$$

With P_i being the proportion of the landscape occupied by the class *i*.

The aggregation index (AI) represents the frequency with which different pairs of patch types appear side-by-side on the landscape. This index is calculated with the Equation 4.10. It ranges between 0 and 100, 0 when the focal patch type is fully disaggregated and 100 when the patch type is maximally aggregated into a single, compact patch:

$$AI = \left(\frac{g_{ii}}{max \rightarrow g_{ii}}\right) * 100 \tag{4.10.}$$

With g_{ii} being the number of like adjacencies (joins) between pixels of patch type the class *i* based on the single-count method and $\max \rightarrow g_{ii}$ being the maximum number of like adjacencies (joins) between pixels of patch type (class) i based on the single-count method.

The patch density (PD) indicates the number of patches of a certain class within the landscape surface and represents the fragmentation inside the landscape. The higher is the PD, the higher is the class fragmentation within the landscape. PD was calculated with the following equation (Equation 4.11.):

$$PD = \frac{N}{A} \tag{4.11.}$$

With PD being the patch density (number ha^{-1}), N being the number of patches in the landscape (-) and A being the area of the landscape (ha).

The edge density (ED) was obtained with the following equation (Equation 4.12.):

$$ED_i = \frac{E_i}{A} \quad (4.12.)$$

With ED_i being the edge density for the class i, E_i being the length of the borders of the class i (m) and A being the area of the landscape (m^2). This indicator also serves to indicate to fragmentation but at the class scale. So, this indicator is calculated for the five classes of land cover identified in the park.

4.4. Statistical analysis

Three main statistical analyses were carried out to statistically respond to the study objective. To identify common groups of secondary forests, a cluster analysis among the 283 plots was performed. After the creation of the cluster, we applied a principal component analysis (PCA) with the two matrices to characterise the forest and environmental structure of the clusters. This step helps to identify which environmental factors explain the variation between the forest types. With the same purpose, we trained a random forest (RF) classifier on the clusters to quantify the importance and effects of each driver.

4.4.1. Cluster analysis

Before starting the cluster analysis, a selection of variables among 105 variables was done. So many variables can cause problems when the analysis is carried out. Too many variables can be redundant causing multicollinearity issues and inflating the weight of ecological dimensions captured by multiple correlated variables. Furthermore, a large number of variables relative to the number of plots increases the risk of correlations and decreases the stability of the resulting clusters. A two-step selection was applied to flush out less informative variables and avoid redundancy. First, 13 ecologically meaningful variables were chosen as they were considered as key variables structuring secondary forest types based on theoretical considerations and literature. Those 13 variables were: BA, TPH, the average (mean DBH) and standard deviation (DBH sd) of the DBH, saplings (TPH sa) and seedlings (TPH se) density, regeneration cover (Cov regen), abundance of broadleaves (BLF), light tolerance index (LTI), Brillouin index for trees (HB t), saplings (HB sa), seedlings (HB se), and the Brillouin index for saplings and seedlings together (HB sesa). This choice was made in order to avoid the problem of dimensionality, to reduce redundancy between correlated variables, and to ensure that the Euclidean distances used in Ward's clustering retain ecological meaning (Legendre and Legendre, 2012). Secondly, a PCA was performed on the whole forest structure matrix to identify other variables with strong and independent contribution to the main axes of variation. Based on a visual inspection of the variable loadings on the first two principal components of the ordination, four other variables were included: beech BA, larch BA, spruce BA, and litter cover (Cov litter). The clustering was therefore performed using 17 forest structure variables (Appendix 4). Before performing the clustering, variable normalisation was carried out. As they are expressed in different units, a lack of standardisation will result in inflating the importance of those variables having the highest variance (Legendre and Legendre, 2012). After standardisation, each variable contributes equally to the total Euclidean distance, regardless of its original unit. The following equation was used to standardise the variables (Equation 4.13.):

$$z_{ij} = \frac{x_{ij} - \bar{x_j}}{s_j} \quad (4.13.)$$

With z_{ij} being the standardised score for observation *i* for the variable *j*, x_{ij} being the value of the observation *i* for the variable *j*, $\overline{x_j}$ being the mean of the variable *j* and s_j being the standard deviation of the variable *j*.

The method used for the cluster analysis was the Ward method, based on an agglomerative clustering algorithm. It begins, by way of comparison, with the detection of single leaves and gradually works its way up towards the trunk. It looks for groups of leaves that form branches, then branches that form twigs, eventually reaching the trunk. Ward's method starts with *n* clusters of size 1 and continues until all observations are grouped into a single cluster (Legendre and Legendre, 2012). The key factor that distinguishes this method from other clustering methods is the merging criterion, as it seeks, above all, to minimise the loss of information when merging two clusters (Murtagh and Legendre, 2014; Ward, 1963). To this end, it identifies the two clusters whose merge results in the smallest increase in the error sum of square (ESS) defined for a cluster C (Equation 4.14.):

$$ESS_C = \sum_{i \in C} \sum_{j=1}^{p} \left(x_{ij} - \overline{x_j}\right)^2 \qquad (4.14.)$$

With x_{ij} being the value for the variable *j* with the observation *i*, $\overline{x_j}$ being the mean of the variable *j* inside cluster C and p being the number of variables (Legendre and Legendre, 2012).

The ESS measures the dispersion of the observations around the centroid of their cluster (intra-cluster variability). Ward's method minimises the increase of ESS when merging two clusters. This clustering procedure was performed using Ward's minimum variance method (Ward.D2) implemented within the *hclust* function with Euclidean distances - computed using *vegdist* function – of the R package *vegan* (Borcard et al., 2018). This method is widely used in vegetation ecology because, by minimising at each step the within-cluster variance, it produces clusters of relatively homogeneous size and compact shape in the multivariate space, which facilitates the identification of well-differentiated vegetation types (Borcard et al., 2018; Murtagh and Legendre, 2014).

We assessed the optimal number of clusters by evaluating outcomes ranging from 5 to 8 groups using a visual inspection of the dendrogram to identify the most meaningful partition based on cophenetic distance (i.e., the fusion height). Each of the 283 sampling plots was assigned to one of the determined clusters and the number of the cluster was added to each sampling point in the principal data matrix.

Each cluster was then given a name based on the peculiar characteristics that separate it from the other clusters. For that purpose, the mean and the standard deviation of the 17 forest structure variables were derived for each cluster. In addition to these variables, the three dominant species of the clusters were used to describe them. If necessary, further variables were used to describe the different clusters.

4.4.2. Principal component analysis

To explore the correlation structure between the forest types (the clusters created with the clustering analysis) and the environmental factors, a principal components analysis (PCA) was used as an unconstrained multivariate ordination. The environmental factors were therefore projected passively on the PCA axes to assess their correlation with the main structural gradients. The PCA is a dimensionality reduction technique that transforms correlated variables

into a smaller set of uncorrelated and orthogonal components (i.e. the principal components), retaining the most important information while reducing redundancy and improving computational efficiency. It is commonly used to simplify large datasets into smaller sets while maintaining significant trends and patterns. The principal components are linear combinations of the initial variables. The first principal component (PC1) is the axis in the multidimensional space that accounts for the largest proportion of the total variance in the initial dataset. The second component (PC2) is orthogonal to the first, and therefore uncorrelated with it, and captures the largest proportion of the variance remaining after PC1. This process continues in the same way with the subsequent principal components. The value of the method lies precisely in the fact that the majority of the information is concentrated in the first few axes, allowing for a simplified representation of the original dataset in a low-dimensional space (Legendre and Legendre, 2012).

The PCA was performed in PC-ORD version 7.11 (McCune and Mefford, 2016) to identify the environmental factors that best explain the variation in the different secondary forest types identified during the cluster analysis. The PCA was conducted on forest structure descriptors from the principal matrix (Appendix 4). Three variables were removed, i.e., HB sa, HB se and DBH sd as their information was largely captured by other ecologically meaningful retained variables, i.e., HB sesa, mean DBH, and TPH, respectively. The hazel BA is added to the variables selected because it represents a structurally and functionally distinct component in certain forest clusters of the study area, providing information not captured by the other abundance variables related to broadleaves. Before starting the analysis, all the variables selected for the analysis were standardised according to Equation 4.13. The correlation-based PCA, by standardising all variables to unit variance, ensures that each variable contributes equally to the ordination independently of its measurement unit, which is the standard approach in vegetation ecology when variables are expressed in heterogeneous units (Legendre and Legendre, 2012).

To assign the significance of each ordination axis, two complementary methods were used. First, a broken-stick criterion that aims to compare the observed eigenvalue of each axis to the expected eigenvalue under a null model of randomly partitioned variance (Jackson, 1993). The observed eigenvalues are the quantity of variance explained by the axis in the dataset while the expected eigenvalues are the one expected under the null model. With the broken-stick criterion, the axes selected are the ones with an observed eigenvalue higher than the expected eigenvalue. The second method is a randomisation test performed with 9,999 permutations, comparing the observed eigenvalue of each axis to the distribution of eigenvalues obtained by randomly permuting the data matrix (Peres-Neto et al., 2005). Instead of using an analytical formula such as the broken-stick criterion, this method randomly mixes the data and recalculates a PCA every iteration. This gives an empirical distribution of the eigenvalues, and it is after compared to the observed eigenvalues. By combining those two methods, the number of significant axes was determined.

Once the PCA with the variables from the principal matrix was performed and the significant axes were chosen, the environmental factors from the secondary matrix were projected into the ordination as passive supplementary variables, without directly influencing the construction of the axes. Their relationship with each ordination axis was quantified using both Pearson correlation coefficients (r) and Kendall rank correlations (τ), computed between the environmental variable values and the plot scores along each axis, as provided by the PC-ORD output. The two coefficients were used jointly because they capture complementary aspects of the relationship: r assumes a linear relationship and is sensitive to outliers, while τ is a rank-based, non-parametric measure that detects any monotonic relationship and is robust to non-

normal distributions and extreme values. The consistency of r and τ for a given variable thus provides a diagnostic of the robustness of the identified relationship (Legendre and Legendre, 2012). The variables from this matrix that showed the strongest correlation with the axes selected were identified as the main factors structuring the diversity of secondary forest types.

4.4.3. Random forest model

To assess the main factors correlated with the different forest clusters, we created a Random Forest (RF) classification model using the *mlr3* universe in R (Lang et al., 2019) to explore the relative importance and the marginal effects of the environmental factors on secondary forest types. The target response of the model was the secondary forest cluster assigned to the 283 sampling plots through the cluster analysis (section 4.4.1).

RF is an ensemble method that constructs a large number of decision trees from bootstrap samples drawn from the training data, each using a random subset of predictor variables at each split, and then aggregates their predictions using majority voting (Breiman, 2001). Thanks to this double randomisation, the correlation between individual trees is reduced and it produces a model that is more robust and less prone to overfitting than a single decision tree. The classifier produced can handle non-linear relationships and multicollinearity among predictors, which is particularly useful in vegetation ecology (Cutler et al., 2007).

Before starting to create the classifier, a selection among the full dataset of environmental factors must be done. This selection was performed over two steps. First, a Recursive Feature Elimination (RFE) was done using the *mlr3fselect* R package (Becker et al., 2025). At each iteration, a Random Forest was trained on a subset of variables, and the least important variable was eliminated. This process was repeated until 15 variables remained. To account for the spatial autocorrelation inherent in ecological plot data, the predictive performance at each RFE iteration was evaluated through a spatial block cross-validation (*spcv_block* resampling, 5 folds, block radius = 1 km; Roberts et al., 2017). This spatial resampling strategy ensures that training and test plots are geographically separated, preventing spatial leakage. In the second step, pairwise Pearson correlations were computed among the variables retained by the RFE, and variables with a correlation coefficient above 0.7 were iteratively removed using the *findCorrelation* function from the caret R package (Kuhn, 2008), retaining the variable with the highest average correlation with the remaining ones.

The performance of a RF model depends on a set of hyperparameters (i.e., external configuration parameters that control how a model learns from data) such as the number of decision trees, the number of variables sampled at each node and the minimum node size. We applied an automatic hyperparameter tuning approach by using the Bayesian optimisation in the Model-Based Optimisation (MBO) framework implemented in the *mlr3tuning* and *mlr3mbo* R packages (Becker et al., 2025).

The first rule of geography formulated by Tobler states that "everything is related to everything else, but near things are more related than distant things." This phenomenon, also referred to as spatial autocorrelation, needs to be properly addressed in vegetation ecology modelling. Indeed, applying a standard random cross-validation procedure to a spatially explicit task would inflate the model performance as this model will memorize local spatial patterns instead of learning important relationships (Valavi et al., 2019). Therefore, a spatial cross-validation was performed using the R package *mlr3spatiotempcv* (Schratz et al., 2021). Within that method, we create two resampling strategies: an inner loop for the hyperparameter tuning and an outer one for the performance evaluation using spatial block resampling with 5 folds and a search

radius of 5 km. This block size ensured spatial separation between the training and test folds, which prevents the model from exploiting local spatial structures and enables an unbiased estimate of generalisation. Figure 11 shows an example of the spatial cross-validation. The performance of the model was then expressed using the overall classification accuracy (OA).

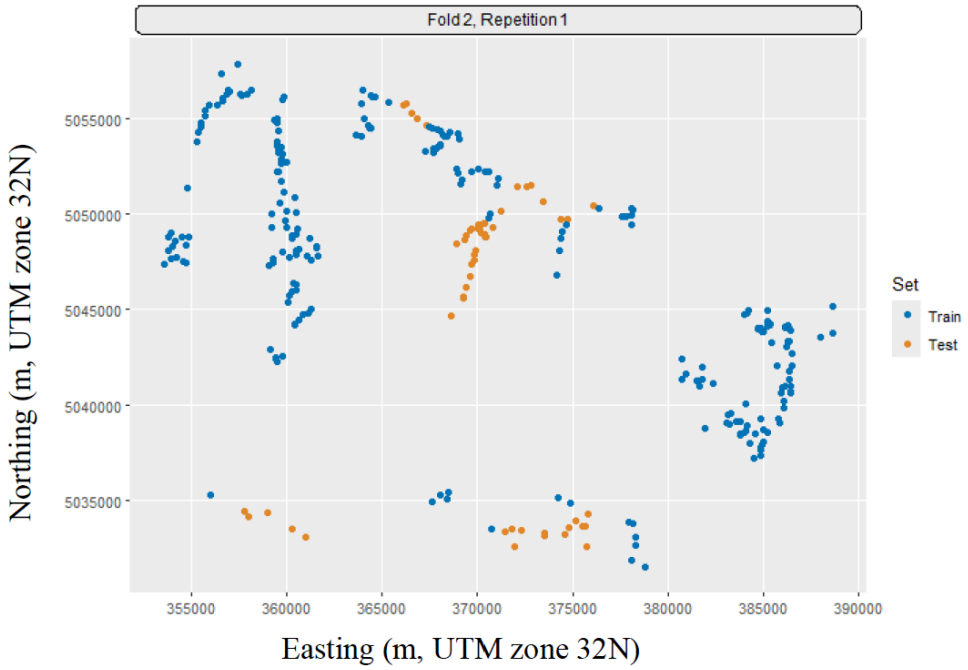

Figure 11: Example of one fold of the spatial block cross-validation used during the RF analysis. Each point represents one of the 283 sampling plots. Blue points are used to train the model while orange points are used to evaluate its predictive performance.

The final model was then trained on the 283 sampling plots and two complementary model-agnostic interpretations from the Interpretable Machine Learning (IML) framework were applied using the R package *iml* (Molnar, 2018). The first one was the permutation-based variable importance using the *FeatureImp* function with classification error as the loss function and 100 repetitions. Each value of each environmental factor previously selected was randomly permuted across all the observations and the increase in classification error relative to the unperturbed model was measured. A big increase in the classification error means that the model relies heavily on this environmental driver. To ensure the stability of the estimation of the importance, it was repeated 100 times. The second method was the partial dependence plots (PDPs) which are computed for each environmental driver using the *FeatureEffect* function with method='pdp'. A PDP shows the marginal effect of a single predictor on the predicted probability of each secondary forest type (the clusters), after averaging out the effects of all other predictors. The PDPs were calculated separately for each forest type class, resulting in a set of eight curves for each predictive variable, illustrating how the predicted probability of belonging to a class varies across the range of values for that variable.

5. Results and discussion

5.1. Secondary forest types

The cluster analysis resulted in the dendrogram shown in Figure 12. The horizontal axis shows the clustering of the 283 plots in eight different groups, separated by the dashed cutting line at height around 19. A table listing the sampling plots in each cluster with the forest structure variable used can be found in Appendix 6. Each colour corresponds to the branches of one cluster. The number of plots for each group is also indicated in the corresponding colour. The vertical axis shows the height. Since standardised data have been used, it has no units. This height in the Ward method represents the increase in within-cluster variance (or inertia) resulting from merging two clusters, in other words, the increase in within-cluster ESS resulting from each step fusion. Two groups merge at a distance level according to their similarities. The higher the height, the more different the two merged groups are.

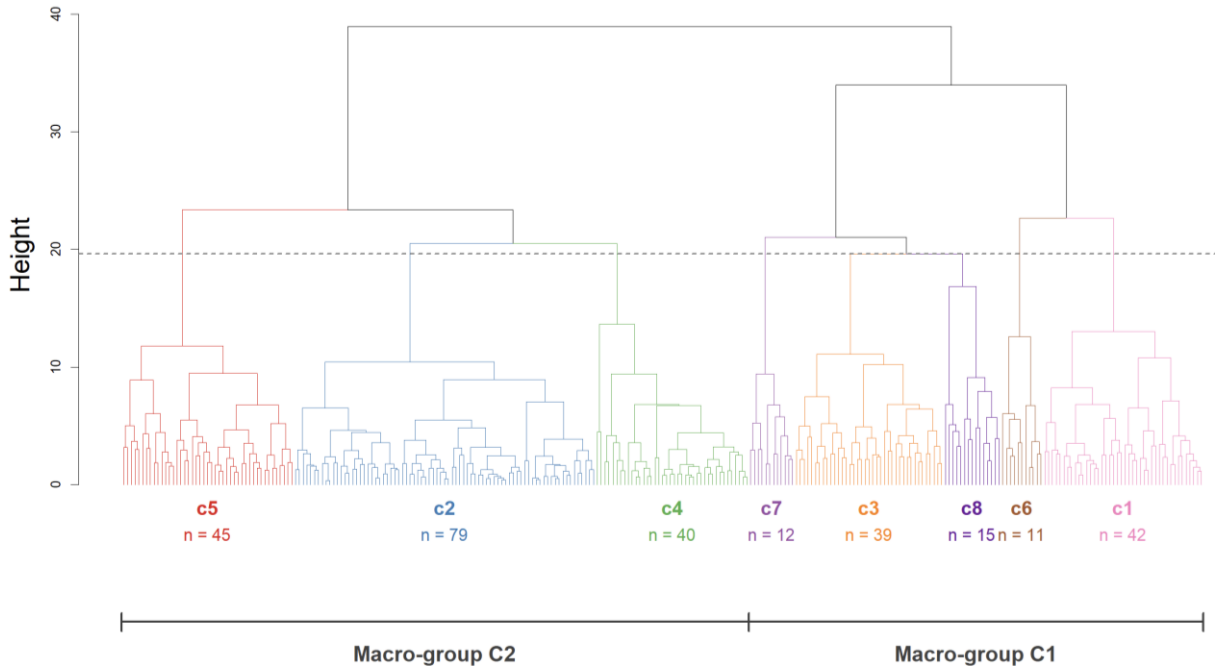

Figure 12: Dendrogram of the hierarchical cluster analysis performed on the 283 sampling plots using Ward's minimum variance method (Ward.D2) with Euclidean distances computed on 17 standardised forest structure variables. The dashed horizontal line at height = 19 indicates the cutting level chosen to define the eight clusters.

5.1.1. Two main macro-groups

The major fusion occurs at the highest level with a height around 38. This indicates that, before describing the 8 different clusters chosen, the clustering description can start with the differentiation of two main macro-groups: the first one (C1) grouping clusters c1, c3, c6, c7, and c8, and the second one (C2) grouping the others (c2, c4, and c5). C2 is composed of 164 sampling plots while C1 is composed of 119. Figure 13 shows the three dominant species in percentage for the two main macro-groups. The first main observation is the very high percentage of plot with European larch (*Larix decidua*) as dominant species in C2. 155 plots in the group (94.5% of the total) are dominated by this species. The two other dominant species are Norway spruce (*Picea abies*) and Swiss stone pine (*Pinus cembra*) with both dominating four plots each. The dominant species in this group are therefore for the most part coniferous trees. Meanwhile, in C1, a mix of broadleaf and coniferous trees makes up the dominant species. Figure 13 shows spruce (26.1%), larch (13.4%) and European ash (*Fraxinus excelsior*) (10.1%)

as the top three dominant species in C1. But this group has also a large series of minority dominant species such as silver fir (*Abies alba*), white birch (*Betula pendula*), sweet chestnut (*Castanea sativa*), common hazel (*Corylus avellana*), European beech (*Fagus sylvatica*), common whitebeam (*Sorbus aria*), etc (Appendix 7 for more details). Based on Figure 13, a first big difference between the two main macro-groups is that the dominant species are mainly coniferous trees in C2 and a mix of broadleaves and coniferous trees in C1.

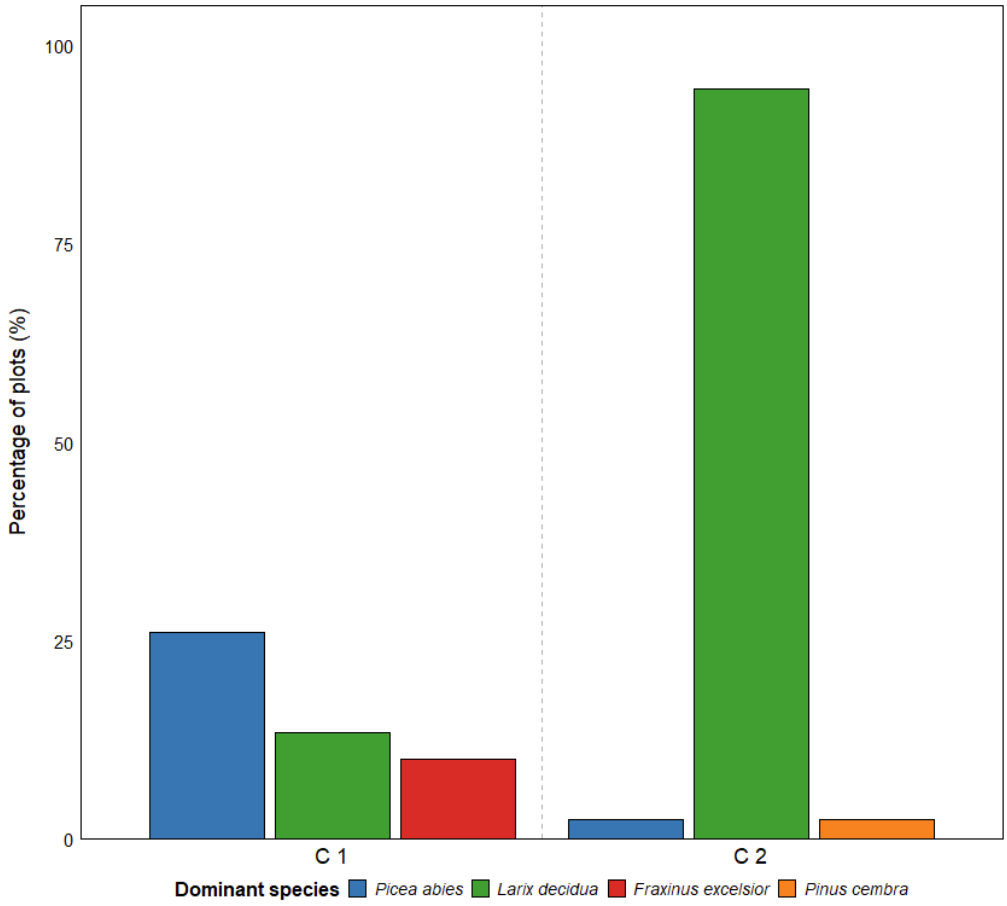

Figure 13: Top three dominant species in percentage for the two main macro-groups. In C1, those three species represent 49.6% of all dominant species while in C2, they represent 99.4%.

Figure 14 shows comparisons of some variables of the forest characteristics between C1 and C2. The mean DBH shows higher values in C2 than in C1. A hypothesis is that forests composed mainly of larch are at more advanced stages of succession than the forests in the group C1. This will be supported by future results. Looking at the broadleaf share (BLF), this result confirms what we observed in Figure 14, that the main difference between C1 and C2 is the composition of the forest. The broadleaves abundance for C1 is 53.7% while for C2 is 3.8%. This is also complemented by the different light tolerance index (LTI) of the two big clusters, with higher values (~ 4) for C2. This is explained by the large dominance of larch in this group, which has a LTI of 4, while in C1 the abundance of shade tolerant species such as beech, fir, or sycamore maple (*Acer pseudoplatanus*) decreases the mean index for the plots. The diversity indices for the regeneration and tree layer are higher in C1, meaning a higher diversity of species in this group. In terms of regeneration density, C1 shows for both seedlings and saplings higher values. C1 has mean values of 17,583 seedlings ha^{-1} and 7,400 saplings ha^{-1} while C2 has 1,950 seedlings ha^{-1} and 1,215 saplings ha^{-1}.

Overall, the cluster analysis first identified two main macro-groups: C2 with larch-dominated forests, with low diversity, low regeneration density and almost no broadleaves, and C1 characterised by a large diversity of species with an important regeneration. This second main group shows also a larger diversity for the nine variables. The first separation of the sampling plots gives on one side homogenous larch forests and on the other side heterogeneous forests with an important diversity.

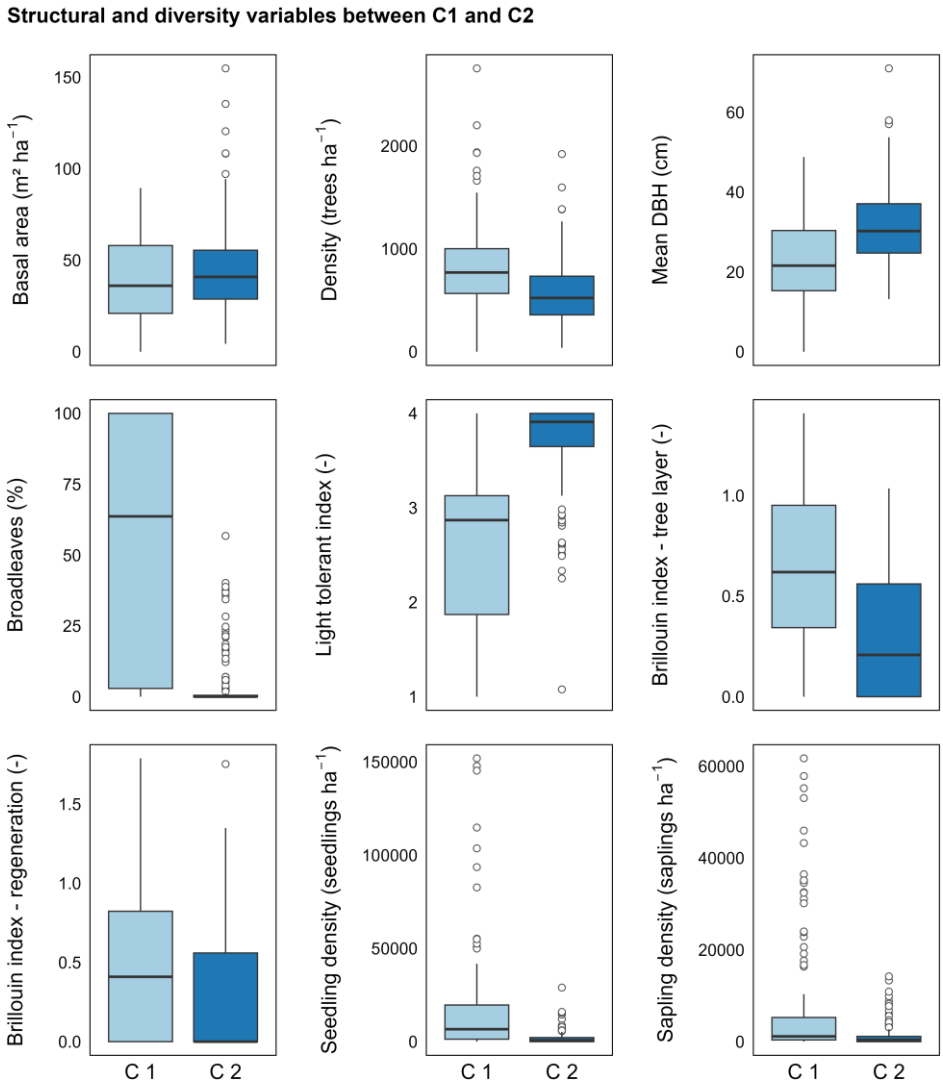

Figure 14: Comparison of nine variables of the forest characteristics between C1 and C2.

5.1.2. Eight different secondary forest types

Within these two main macro-groups, the dendrogram reveals further internal ramifications. A final subdivision of eight different cluster, located with the dashed cutting line (height = 19), has been chosen. This choice of eight clusters is supported by clear discontinuity in fusion height at this level. Furthermore, internal fusions in the clusters stay below 15, meaning a high homogeneity within the clusters and all the fusion between them are above 20. Within C1, five different clusters are identified: c1, c3, c6, c7 and c8. Some of them are very small such as c6 (n = 11) and c7 (n = 12), meaning an important internal homogeneity. Within C2, three clusters are identified: c2, c4 and c5. Those are larger in terms of sample size, especially c2 with 79 sampling plots inside. This size of cluster can bring a large heterogeneity. The following sections describe each of the eight clusters, based on their dominant tree species and some variables of the forest characteristics.

Cluster 1 – Mature spruce-dominated forests

Cluster 1 (c1) encompasses 42 plots, 27 in the Aosta Valley and 15 in Piedmont. Its mean BA is 54.3 m^2 ha^{-1}, and its mean DBH is 30.9 cm. The main dominant species are spruce in 27 plots, larch in 9 plots and silver fir in 4 plots. On average, around 90% of the tree species in the plots are conifers. The mean BA of spruce is 27.3 m^2 ha^{-1}, which represents 50% of the total BA. The light tolerance index in cluster 1 has a mean of 1.95. The surface cover is characterised by 53.9% of litter.

Figure 15 illustrates the typical forests found in c1.

Figure 15: Typical forests found in cluster c1, illustrated by plots 1_P (a) and 67_P (b).

Cluster 2 – Open larch-dominated forests

Cluster 2 (c2) encompasses 79 plots, 70 in the Aosta Valley and 9 in Piedmont. It is characterised mainly by dominance of larch (in 76 out of 79 plots). In terms of BA, this species represents 84% of the trees in the plot. The second dominant species in this cluster is stone pine (2 out of 79 plots). 96% of the trees in the cluster are conifers with an average light tolerance index of 3.75. The structure of the plot is also described by a low density of 547 trees ha^{-1}. This cluster has a Brillouin index for the regeneration of 0.07 as regeneration is mainly composed of larch with few spruce and stone pine. The soils of the plots are covered mainly by grass (45.2%) and shrubs (20.4%).

Figure 16 illustrates the typical forests found in c2.

Figure 16: Typical forests found in cluster c2, illustrated by plots 5_P (a) and 115_P (b).

Cluster 3 – Dense pioneer broadleaves forests

Cluster 3 (c3) encompasses 39 plots, 18 in the Aosta Valley and 21 in Piedmont. It is characterised by a tree density of 1,078 trees ha^{-1} and an average DBH of 17.3 cm. There are many dominant species. The most important are European ash in 7 plots, birch in 6 plots and sweet chestnut in 4 plots. On average, each plot of the cluster is composed of 84% of broadleaves in the tree layer. This cluster is characterised by high diversity in species composition, with Brillouin indices of 0.74 for both tree layer and regeneration. Saplings are abundant (4,794 saplings ha^{-1}).

Figure 17 illustrates the typical forests found in c3.

Figure 17: Typical forests found in cluster c3, illustrated by plots 93_P (a) and 144_P (b).

Cluster 4 – Mature larch-dominated forests

Cluster 4 (c4) encompasses 40 plots, 26 in the Aosta Valley and 14 in Piedmont. The average BA is 72.5 m^2 ha^{-1} and the average DBH is 42.2 cm. The dominant species is larch in 39 plots. 99% of the trees are coniferous, and 92% are larch. The average Brillouin indices are lower, with values of 0.15 in the tree layer and 0.04 for the regeneration. The density of the regeneration is on average 445 saplings ha^{-1} and 789 seedlings ha^{-1}. The soils of the plots are covered mainly by grass (45.3%) and shrubs (20.9%).

Figure 18 illustrates the typical forests found in c4.

Figure 18: Typical forests found in cluster c4, illustrated by plots 97_P (a) and 63_P (b).

Cluster 5 – Larch dominated-forests with active regeneration

Cluster 5 (c5) encompasses 45 plots, 30 in the Aosta Valley and 15 in Piedmont. The forest structure of this cluster is characterised by an average BA of 40.0 m^2 ha^{-1} and an average DBH of 26.6 cm. The dominant species are larch in 40 plots, spruce in 3 plots and stone pine in 2 plots. 92% of the trees are conifers and larch represents 77% of the trees in terms of BA. The average Brillouin index for the regeneration has a value of 0.77 in this cluster.

Figure 19 illustrates the typical forests found in c5.

Figure 19: Typical forests found in cluster c5, illustrated by plots 12_P (a) and 62_P (b).

Cluster 6 – Mature beech-dominated forests

Cluster 6 (c6) encompasses 11 plots, all located in Piedmont. The plots show an average BA of 61.2 m^2 ha^{-1} and density of 966 trees ha^{-1}. The dominant species is beech in 10 out of 11 plots. 89% of the trees are broadleaves and 70% are beech. The light tolerance index gives an average value of 1.48 for this cluster. The regeneration is characterised by a density of 16,444 seedlings ha^{-1} and a Brillouin index of 0.74. The soil cover is dominated by the litter with a percentage of 65%.

Figure 20 illustrates the typical forests found in c6.

Figure 20: Typical forests found in cluster c6, illustrated by plots 140_P (a) and 118_P (b).

Cluster 7 – Pioneer hazel shrublands

Cluster 7 (c7) encompasses 12 plots, all located in Piedmont. The forest structure in this cluster is characterised by a BA of 9.5 m^2 ha^{-1}, an average DBH of 10.6 cm and an average density of 372 trees ha^{-1}. Among the 12 plots of the cluster, four do not have a tree layer. The others are dominated by birch and hazel. The regeneration has densities of 41,970 saplings ha^{-1} and 18,440 seedlings ha^{-1}. Hazel represents 94% of the saplings and 76% of the seedlings in terms of density.

Figure 21 illustrates the typical forests found in c7.

Figure 21: Typical forests found in cluster c7, illustrated by plots 65_P (a) and 78_P (b).

Cluster 8 – Established mixed broadleaves forests with active regeneration

Cluster 8 (c8) encompasses 15 plots, 10 in the Aosta Valley and 5 in Piedmont. Forests in this cluster have an average density of 809 trees ha^{-1}. 71% of the trees are broadleaves. The dominant species are numerous, the main ones being ash (5 plots), larch (3 plots) and sycamore maple (*Acer pseudoplatanus*) (2 plots). The Brillouin index of the tree layer has a value of 0.72. Regeneration represents 22.6% of the soil cover on average. The regeneration density is the highest among clusters, with values of 8,893 saplings ha^{-1} and 70,284 seedlings ha^{-1} with an average Brillouin index of 0.48.

Figure 22 illustrates the typical forests found in c8.

Figure 22: Typical forests found in cluster c8, illustrated by plots 113_P (a) and 29_P (b).

5.1.3. Clusters statistical description

To compare the clusters, the 17 variables (except the DBH sd) are used and hazel BA and the top three dominant species for each cluster were added as informative variables. The top three dominant species per cluster is revealed on Figure 23 (more details with the Table 18 in Appendix 8). Figure 24 shows the boxplots of the ten most important variables of the forest structure for the comparison between the eight clusters. The eight other boxplots can be found in Appendix 10 and the table with the mean and standard deviation values for each variable in Appendix 9.

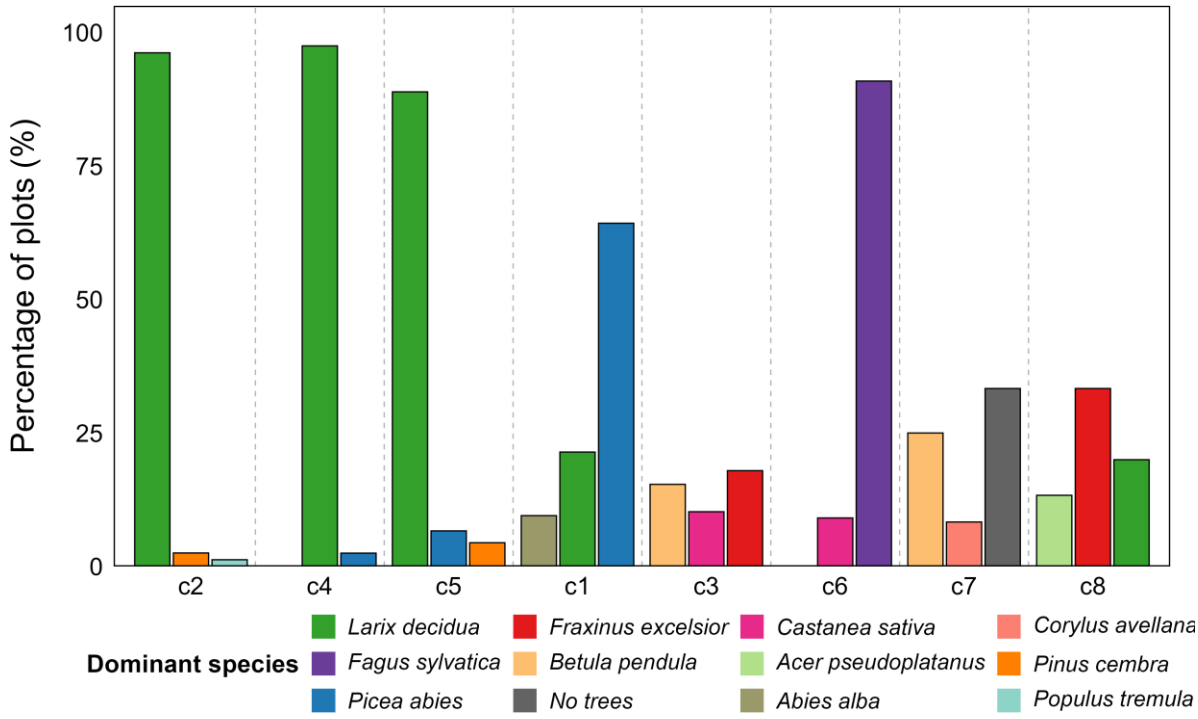

Figure 23: Top three dominant species in the tree layer in percentage for each cluster. Those three species represent 95.2% of all dominant species in c1, 100% in c2, 43.6% in c3, 100% in c4, 100% in c5, 100% in c6, 66.7% in c7, and 66.7% in c8.

The first main observation is the large dominance of larch in c2, c4 and c5, as expected from the macro-groups analysis (section 5.1.1). In particular, only two species are present in c4: larch with highest percentage (97.5%) and spruce (2.5%). c2 and c5 have high percentage of larch too, respectively 96.2% and 88.9% but have also other dominant species such as stone pine or trembling aspen (*Populus tremula*). Apart from the species composition, the biggest differences are found in the structure, species diversity and regeneration layer. Cluster c4 has significantly higher values of mean DBH (42.2 cm), BA (72.5 m^2 ha^{-1}) and larch BA (66.6 m^2 ha^{-1}) compared to c2 (mean DBH: 29.1 cm, BA: 33.3 m^2 ha^{-1}) and c5 (mean DBH: 26.6 cm, BA: 40.0 m^2 ha^{-1}). c2 and c5 show lower and similar values for these structural variables. Those structural differences suggest that c4 presents more mature and long-established secondary larch-dominated forests, in line with the documented changes in larch stands following abandonment in the Southern Alps (see for instance Garbarino et al. 2013). The poor regeneration density and diversity values of c4 are also characteristics of the more mature structure of larch (Schulze et al., 2007).

The main differences for c2 and c5 are in the regeneration characteristics. Cluster c5 shows higher regeneration levels than c2. The mean values of saplings and seedlings densities are

respectively 2,542 and 4,385 individuals ha^{-1} for c5 while c2 has values of 848 saplings ha^{-1} for saplings density and 1,152 seedlings $ha^{-1}$for seedlings density. Another variable that differentiates them is the HB sesa with a mean of 0.07 for c2 and 0.77 for c5. Moreover, regeneration cover shows values nearly four times higher in c5 than in the two other. c5 also shows the highest percentage of broadleaves and tree diversity (HB t).

Based on those differences, some preliminary hypotheses can be formulated. Clusters c2 and c5, with lower structural values (BA and mean DBH), correspond more to younger or less developed stands of larch forests. They are potentially located at higher altitudes, where the conditions do not allow for growth at the same velocity as in the c4 cluster (Schulze et al., 2007). The higher regeneration density and diversity in c5 could be explained by greater proximity to ancient forests serving as seed sources, which encourage the establishment of tree species other than larch (Flinn and Marks, 2007). The distance between seedlings and mature trees is one of the main factors determining forest succession so the presence of established forest stands serving as seed sources could explain the high regeneration values in c5. These hypotheses will be further discussed in the PCA section (5.2). Taken together, c4, c2 and c5 can be interpreted as three stages of a common post-pastoral succession trajectory. c4 and c2 represent old-growth larch stands, distinguished by their elevation, while c5 represents the intermediate stage of an ongoing compositional transition toward shade-tolerant species, of which c1 (spruce-dominated forests) represents the expected late-successional endpoint. These hypotheses will be tested and refined in sections 5.2 and 5.3.

The five other clusters show a larger dominant species diversity than c2, c4 and c5. This group of five clusters can be first divided into two sub-groups based on the dominant species with c1 and c6 showing dominance of few species and c3, c7, and c8 with a high mix of co-dominant species. In the first sub-group, c1 is largely dominated by spruce alongside larch and fir and c6 is dominated by beech which are shade-tolerant species (except larch) that typically dominate the lower montane forests of the Alps at advanced successional stages (Leuschner and Ellenberg, 2017). For c7, there is a small majority (33.3%) of sampling plots without any trees with a diameter higher than 7.5 cm. c3 and c8 have ash as the most widespread dominant species (17.9% and 33.3% respectively) but have a lot of sampling plots with other dominant species such as birch, chestnut, hazel, sycamore or wild cherry (*Prunus avium*). Those species act for the most part as pioneer that colonise abandoned lands and can establish at early or intermediate stages of the succession (San-Miguel-Ayanz et al., 2016; Thomas, 2016). Therefore, the clusters c1 and c6 show dominant species characteristics of mature and long-established forests while c3, c7, and c8 represent earlier stages of secondary succession compared to c1 and c6.

Clusters c1 and c6 differ in an important series of variables. As already said, their dominant species are not the same. Looking at the boxplots (Figure 24), c6 has higher values of BA (61.2 m^2 ha^{-1}) and TPH (966 trees ha^{-1}) than c1 (BA: 54.3 m^2 ha^{-1}, TPH: 678 trees ha^{-1}) while c1 has the largest DBH (c1: 30.9 cm, c6: 26.8 cm). Those differences are mostly explained by the species composition. Cluster c6 is mostly composed of beech and some chestnut which in this area can be predominantly found in coppice form (Figure 20). This species composition is also explaining the difference in broadleaf percentage. c1 is composed in majority by coniferous trees (BLF: 9.3%) while c6 is composed almost exclusively of broadleaved deciduous trees (BLF: 88.7%). The species composing c6 are shade-tolerant species which give a low value of LTI compared to c1. All the sampling plots of c6 are in the Piedmont part of the GPNP. Another large difference is the TPH se, with an average value approximately four times higher for c6. Once again, the species composition can explain this difference as broadleaved species such as beech are known to produce abundant seed pulses during mast years, while the unfavourable germination conditions created by the conifer litter in c1 (acidic humus, allelopathic phenols

already discussed above) further limit seedling establishment (Bernier and Ponge, 1994; Souto et al., 2000). Both different forest types have a very high percentage of litter cover (higher than 50%), but the composition of the litter is not the same due to the different species present. The litter of spruce, larch and fir mainly consists of recalcitrant needles that create more challenging germination conditions. This litter has a slow turnover and produces highly acidic humus forms (Bernier and Ponge, 1994). Furthermore, the phenols released by this humus cause allelopathic effects that are also detrimental to regeneration (Souto et al., 2000). This leads to a lower regeneration in c1 than in c6. One finding that is surprising at first glance is the significant diversity within cluster c6. In beech-dominated forests, low species diversity is expected as this species tends to form dense canopies that absorb most of the light and thereby suppress the establishment of less shade-tolerant species (Leuschner and Ellenberg, 2017). The explanation for the higher diversity found in this study could be that the past forests, managed as coppice, had a higher canopy heterogeneity, allowing more light to reach the ground and promoting understorey diversity (Bartha et al., 2020). This higher diversity therefore reflects the structural legacies of the past forest management.

Clusters c3, c7 and c8 are different from the others as their species composition is mostly made of pioneer species. Those types of secondary forests are typical of newly-established forest on recently abandoned land. However, these young secondary forests can still be distinguished based on several structural parameters. Cluster c7 shows very low values of mean DBH (10.6 cm), TPH (372 trees ha^{-1}) and BA (9.5 m^2 ha^{-1}) compared to all the other clusters, but it is by far the highest in terms of TPH sa with a mean value of 41,970 saplings ha^{-1}. Those saplings are mainly hazel (94%). One third of the sampling plots of this cluster do not have trees with a DBH higher than 7.5 cm. The two dominant species are birch (25%) and hazel (8.3%). Those observations support the hypothesis that the forests of this cluster correspond to the earliest stages of secondary successions and are located on the most recently abandoned land (generally 1, forests established after 2006, or 2, forests established between 1991 and 2006). Clusters c3 and c8 are the two most similar, but they still differ on some structural characteristics. First, their species composition is quite different. c3 is characterised by a higher diversity and a larger share of pioneer species such as ash, birch, and hazel. Therefore, c3 appears to represent a slightly earlier successional stage than c8. The higher TPH mean value (1,078 trees ha^{-1}) and lower DBH (17.3 cm) for c3 is characteristic of the stem exclusion phase of the stand development (Oliver and Larson, 1996). The composition of c8 (ash, larch, and sycamore) proves that this cluster is also composed of newly-established forests, but at more advanced stages of succession than c3. The presence of larch among the dominant species of c8 could suggest a slightly higher altitudinal context for some of the c8 plots, although this will be tested by the PCA results. An important difference between those two is the regeneration density. c8 has mean values (TPH sa: 8,893 saplings ha^{-1}, TPH se: 70,284 seedlings ha^{-1}) that are far higher than c3 (TPH sa: 4,794 saplings ha^{-1}, TPH se: 11,245 seedlings ha^{-1}), especially for the seedlings. Furthermore, c8 has a mean regeneration cover of 22.6%, meaning an active regeneration in the forests of this cluster. The hypothesis is that those forests are at a state just after the stem exclusion. This is explained by the high tree mortality creating gaps in the canopy. This brings more light to the ground favourable for the regeneration (Oliver and Larson, 1996). Based on these differences, c3 is best described as a dense pioneer broadleaves forest in canopy closure and stem exclusion phase, while c8 corresponds to an open mixed broadleaves forest with active and structurally heterogeneous regeneration.

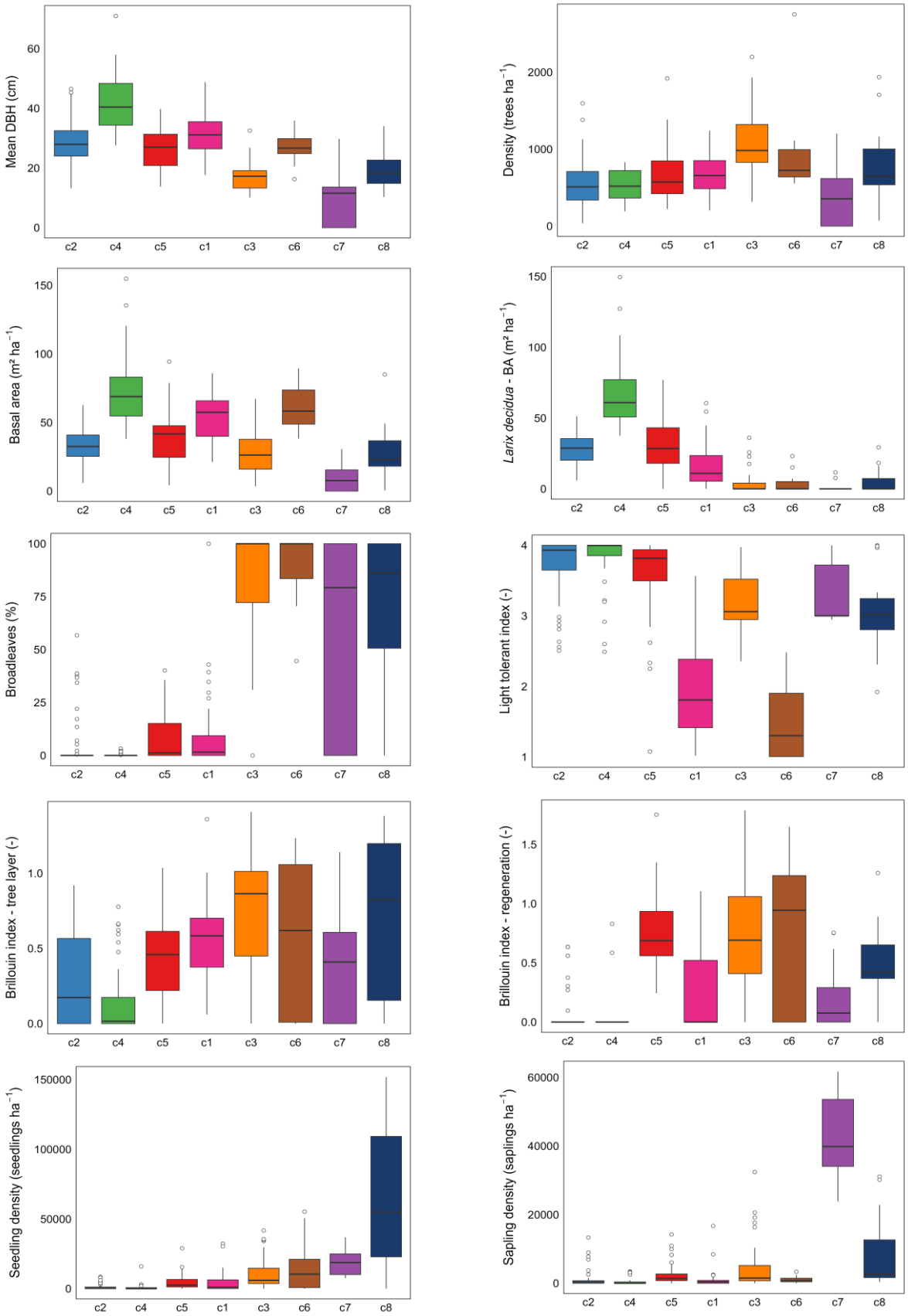

Figure 24: Ten most important forest characteristics to compare the different clusters identified with the cluster analysis.

The mean abandonment period per cluster provides additional support for these interpretations. As a reminder, the abandonment period is variable ranging from 1 (most recently abandoned, classified as dense forest after 2006) to 5 (oldest abandonment, already classified as dense forest before 1954). The pioneer cluster c7 (1.92) show the lowest value, consistent with recent establishment on recently abandoned land, while the mature clusters c1 (3.71) and c6 (3.73) show the highest values, reflecting their longer post-abandonment development. The intermediate clusters c3 (2.77) and c8 (2.67) fall between these extremes, coherent with its intermediate successional position. Within the larch-dominated clusters, the gradient from c2 (2.65) to c5 (2.96) is coherent with the proposed chronosequence, with c5 having been abandoned earlier on average, providing more time for the diversification of its regeneration layer. This ordering of abandonment periods across clusters is therefore broadly consistent with the successional gradient proposed in the preceding sections, reinforcing the ecological plausibility of the interpretations made.

Figure 25 shows the distribution of the eight clusters across the GPNP. The map reveals some clear spatial patterns of the distribution of the different clusters. The larch clusters (c2, c4, and c5) seem to be in the upper sectors of the park's valleys. Those areas correspond to the environmental conditions of the subalpine belt (section 2.1.2), which is the most favourable belt for the establishment of larch forests (Garbarino et al., 2013). In contrast, the five other clusters (c1, c3, c6, c7 and c8) are predominantly located in the valley floor, at lower altitudes, where warmer conditions are more favourable for broadleaves. Cluster c6 is only present in the Piedmont part on south-facing slopes, an unexpected result further explained in section 5.3.3. Clusters c7 and c8 are scattered across the low altitude periphery of the park. This is consistent with the interpretation that these types of secondary forest are in the early stages of establishment in newly abandoned areas.

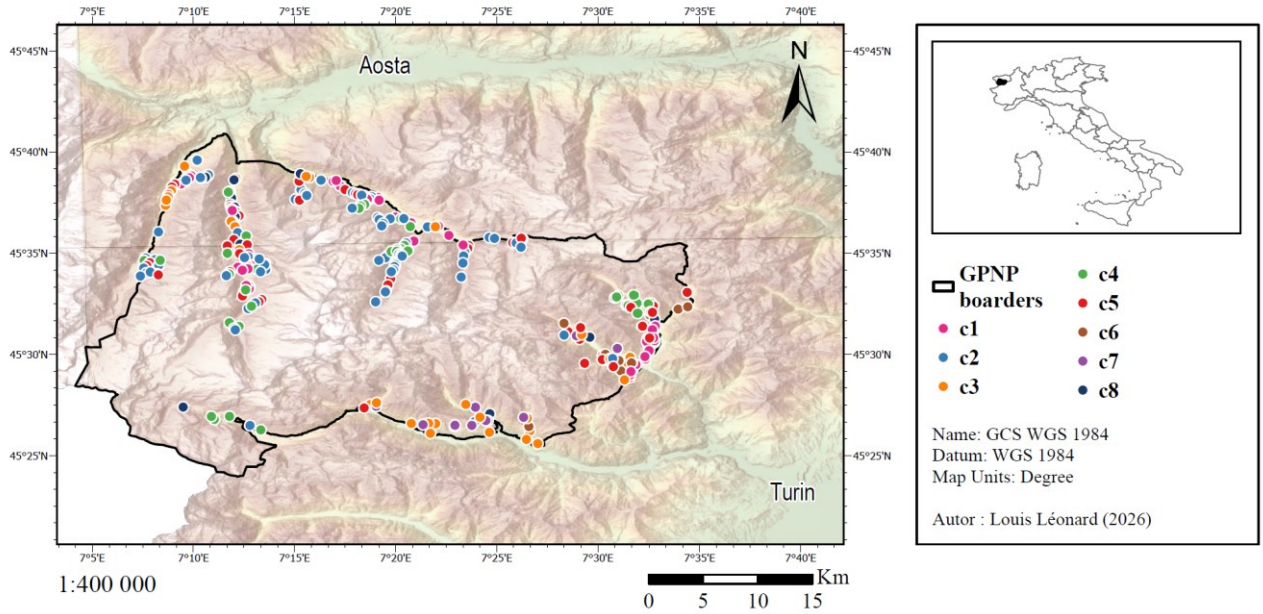

Figure 25: Distribution of the eight different clusters among the GPNP.

The spatial distribution of the different secondary forest types is therefore not random but suggests that interactions with environmental filters at multiple scales (e.g., altitude and thermal gradients), land-use legacies, and abandonment gradients exist. The spatial distribution of those forests is therefore a product of the spatial heterogeneity of these combined factors. This structured spatial distribution is what motivates the multivariate analysis of the following

section. Ordination helps to understand and explain the impact of the different factors on the diversity of secondary forest types and on their spatial distribution.

5.2. Environmental factors explaining secondary forest diversity

The PCA performed on the 15 variables selected (section 4.4.2) produces the ordination space represented in Figure 26, which shows simultaneously the convex hulls delimiting the ordination space occupied by each cluster (i.e., the smallest convex polygon enclosing all plots of a given cluster), and the forest variables. To select the number of significant axes, the two complementary criteria described in section 4.4.2 were used. The broken-stick criterion retained only the first two axes. Only these two have eigenvalues exceeding the expected eigenvalues under a null model (Table 1). The randomisation test based on 9,999 permutations confirmed the high significance of PC1 and PC2 ($p < 0.0001$ for both) and additionally identified PC3 and PC4 as statistically significant ($p < 0.0001$ and $p = 0.004$ respectively) (Appendix 12 for more details). By combining both criteria and considering that PC1 and PC2 together account for 44.71% of the total variance in the dataset (PC1: 26.34% and PC2: 18.37%), the analysis is restricted to those two axes for ecological interpretation. This value, while moderate, is consistent with the complexity of the dataset. The variance is distributed across many axes rather than concentrated in the first two, which is typical of multivariate ecological datasets where no single dominant gradient exists (Borcard et al., 2018). The eight cluster centroids are clearly distributed across the ordination space suggesting that PC1 and PC2 capture the main ecological gradients structuring the secondary forest types identified previously.

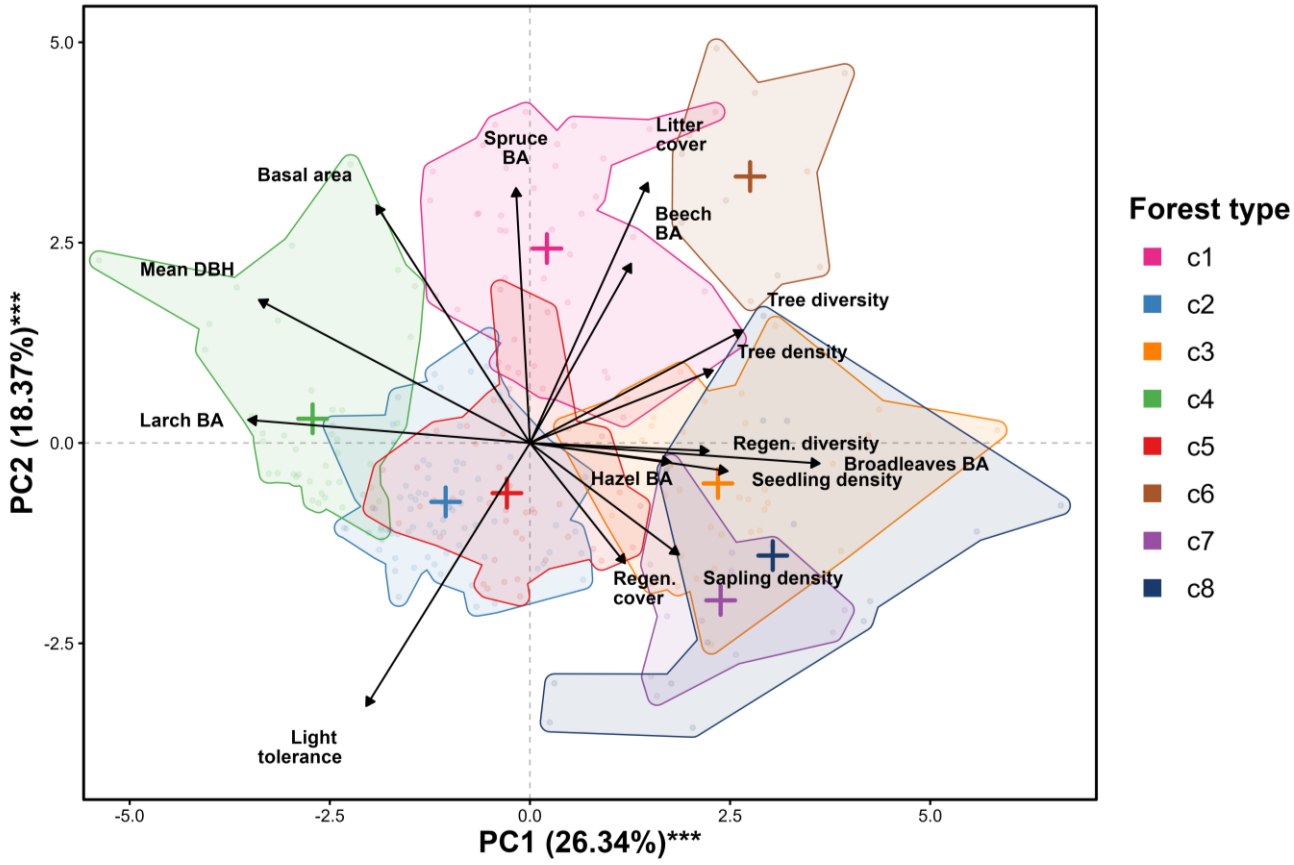

Figure 26: Principal Component Analysis (PCA) biplot of the eight secondary forest types identified in the GPNP (n = 283 plots). The two principal axes PC1 (26.34%) and PC2 (18.37%) together explain 44.71% of the total variance in the 15 forest structure variables. Coloured polygons represent the convex hulls delimiting the ordination space occupied by each of the eight clusters (c1–c8). Crosses indicate cluster centroids. Black arrows

represent the forest structure variables (principal matrix) projected as active variables, with arrow length proportional to the strength of their contribution to the ordination axes.

Table 1: Eigenvalues, variances, and Broken-stick eigenvalues extracted from the PCA for the first ten axes.

Axis	Eigenvalue	% of Variance	Cum. % of Var.	Broken-stick Eigenvalue
1	3.95	26.34	26.34	3.32
2	2.75	18.37	44.71	2.32
3	1.59	10.61	55.31	1.82
4	1.27	8.44	63.75	1.48
5	1.11	7.42	71.17	1.23
6	0.96	6.42	77.60	1.03
7	0.76	5.08	82.68	0.87
8	0.64	4.28	86.96	0.72
9	0.54	3.61	90.57	0.60
10	0.43	2.87	93.44	0.49

5.2.1. Ecological interpretation of the ordination axes

The distribution of the clusters in the ordination space contributes to the understanding of the differences between them. Table 2 helps to more accurately locate the centroids of the eight clusters in the ordination space of the PCA. Their position along the two axes completes the description of section 5.1. Three main groups of clusters are observed on Figure 26, the first corresponds to the macro-group C2, on the negative side of PC1. The clusters of the macro-group C1 can be divided into the two subgroups already identified in the cluster comparison with on one side, c1 and c6 (positive side of PC2), on the other side c3, c7 and c8 (negative side of PC2). The ecological interpretation of the two principal components PC1 and PC2 helps the understanding of the difference between those groups.

Table 2: Coordinates of each cluster's centroid in the ordination space. n = number of sampling plots within the clusters.

Cluster	Forest type	n	PCA Axis 1	PCA Axis 2
c1	Mature Spruce	42	+0.21	+2.43
c2	Mature Larch	79	-1.05	-0.74
c3	Secondary Broadleaves	39	+2.35	-0.51
c4	Larch in Transition	40	-2.72	+0.30
c5	Sparse Larch	45	-0.29	-0.63
c6	Mature Beech	11	+2.75	+3.33
c7	Hazel Shrubland	12	+2.38	-1.96
c8	Pioneer Broadleaves	15	+3.03	-1.41

The first principal component axis (PC1) explains 26.34% of the total variance in the dataset. This axis is primarily driven by a contrast between mixed, broadleaves-dominated stands (positive side of the axis) and larch-dominated stands (negative side). On the negative side, the

strongest contributors are the larch BA (r = -0.783), the mean DBH (r = -0.753), the light tolerance index (LTI) (r = -0.454), and the total BA (r = -0.427). On the positive side of PC1, the strongest contributors from the forest characteristics are broadleaves abundance (BLF) (r = 0.804), tree diversity (HB_t) (r = 0.591), density of seedlings (TPH_se) (r = 0.549), tree density (TPH_t) (r = 0.508), and regeneration diversity (HB_sesa) (r = 0.496). The other variables that contribute to this side but with lower strength are density of saplings (TPH_sa) (r = 0.414), hazel BA (r = 0.391), litter cover (r = 0.327), beech BA (r = 0.281), and the regeneration cover (r = 0.264). All the values of the Pearson correlation coefficients are listed in Table 20 (Appendix 11). On Figure 26, the Pearson correlation coefficients are multiplied by a factor of 4.5 to make the graph easier to read. PC1 represents a species composition gradient that explains the separation between the two macro-groups identified in section 5.1.1.

The larch-dominated clusters (C2) occupy the negative side of the axis while the heterogeneous broadleaves-dominated forests occupy the positive side. Within the larch-dominated clusters (C2), c4 is the cluster having the centroid with the most negative value (- 2.72) while c2 and c5 are much closer to the origin, respectively -1.05 and -0.29. This is reflecting the structural maturity gradient. The mature larch-dominated cluster (c4) is the furthest along the negative axis pulled by its very high BA and mean DBH. c5 is brought closer to the origin by its important regeneration diversity and density, which is consistent with the interpretation of c5 as a larch stand entering the compositional transition toward shade-tolerant successors (Motta et al., 2006; Schulze et al., 2007). It is also consistent with the hypothesis formulated at the section 5.1.3 suggesting that the plots of c5 are closer to older forests providing the seeds needed for the establishment of more diverse species. The lower regeneration diversity of c2 pulled it more on the negative side of PC1, even if the structural characteristics are similar to c5. The ordering of the three larch cluster centroids along PC1 therefore captures not a random distribution but the progressive stages of a post-pastoral chronosequence, from structurally mature but compositionally frozen old-growth larch stands (c4, c2) to a transitional stage with active compositional change (c5), pointing toward the spruce-dominated forests of c1 as the expected late-successional endpoint of this trajectory.

Clusters c3, c6, c7 and c8 have similar values for the coordinates on PC1 (respectively 2.35, 2.75, 2.38 and 3.03). The differences between them operate especially along PC2 and not PC1. The position of c1 near the origin (0.21) reflects the intermediate ecological status of spruce as a shade-tolerant conifer, sharing structural attributes with mature successional stages while remaining compositionally distinct from the broadleaved clusters (Leuschner and Ellenberg, 2017).

The second principal component (PC2) explains 18.37% of the total variance. It represents a gradient of shade tolerance, forest maturity, and successional stages that is largely independent of PC1. On the negative side, the strongest contributor is the light tolerance index (r = -0.729). Regeneration cover (r = -0.334), saplings density (r = -0.310), seedlings density (r = -0.078), abundance of broadleaves (r = -0.057), hazel BA (r = -0.053), and regeneration diversity (r = - 0.022) are also directed toward the negative side of the axis, but to a lesser extent. The strongest positive contributors are litter cover (r = 0.723), spruce BA (r = 0.707), total BA (r = 0.659), and beech BA (r = 0.497). The other variable contributing to the positive side of PC2 are mean DBH (r = 0.397), tree diversity (r = 0.312), tree density (r = 0.201), and larch BA (r = 0.064). Same as for PC1, the Pearson correlation coefficients are multiplied by a factor of 4.5 to make the graph (Figure 26) easier to read. PC2 therefore separates mature established forests (positive side), composed of shade-tolerant species such as beech and spruce with high BA and dense litter cover from young forests (negative side) composed of open stands with light-demanding species and an abundant regeneration. The high positive correlation between

spruce BA, beech BA, total BA and litter cover is an expected result as the mature and advanced forests in mountains are indeed characterised by the domination of those shade-tolerant species and a high BA due to its accumulation during the long development of the stands (Lanta et al., 2023). The higher abundance of litter in those stands is typical of mature forests and may explain the lower regeneration density of those forests. The species dominating younger forests located on the negative side of PC2 are expected to be mainly composed of pioneer species of early successional forests. Pioneer species are characterised by the ease to establish in open conditions with higher light availability, fast growth, low shade tolerance and high reproductive rates (Bennett et al., 2017).

The mature clusters c1 (2.43) and c6 (3.33) occupy the most positive positions, placing them as the most mature among all the clusters. The similarity of their values reflects that mature stages can be reached independently of the dominant species. The mature stage can be reached if the stand has had sufficient time to develop after the abandonment.

At the other end, c7 (-1.96) represents the most recently established stands, characterised by near-total absence of trees with DBH greater than 7.5 cm and high sapling density. Those characteristics are typical of the earliest stages of secondary succession on recently abandoned land (Oliver and Larson, 1996). The position of c7 along PC2 is therefore consistent with the hypothesis made previously which states that c3 and c8 are composed of older forests than c7. c8 (-1.41) and c3 (-0.51) occupy intermediate positions along the PC2 axis. The more negative position of c8 on PC2 than c3 can appear paradoxical with the previous comparison between them which states that c8 represents more advanced successional stage than c3. Their differentiation along PC2 reflects contrasting stand-level dynamics rather than a simple maturity gradient. The more negative position of c8 is due to the high regeneration density of this cluster. c8 is in a gap phase following the stem exclusion where the tree mortality reduces tree density and opens up the canopy creating space for intense regeneration (Oliver and Larson, 1996; Schliemann and Bockheim, 2011). In contrast, c3 is in the stem exclusion phase where the closing canopy suppresses the regeneration and creates an accumulation of litter (c3 has higher value for the litter cover than c8). The litter cover variable pulls the centroid of c3 toward less negative value along this axis. In the comparison of the three pioneer clusters, PC2 represents therefore more a gradient of the canopy openness and the regeneration intensity than the successional stage gradient described previously, which is consistent with the multidimensional and non-linear nature of secondary succession (Poorter et al., 2023).

The three larch-dominated clusters show near-zero values on PC2 (c4: 0.30; c2: -0.74; c5: - 0.63), indicating that their successional stage is not expressed through the compositional shift toward shade-tolerant species captured by this axis, but rather through structural development in BA and mean DBH (Garbarino et al., 2013; Schulze et al., 2007).

The two axes, PC1 and PC2, retain two important and different ecological gradients to differentiate the secondary forest types in mountain landscapes. While PC1 separates larch-dominated from broadleaved stands along a compositional gradient, PC2 separates mature from pioneer stands along a maturity-legacy gradient. The orthogonality between those two axes means that the two ecological gradients are strongly uncorrelated. However, it is important to understand that even if those axes are statistically independent by construction, the ecological gradients captured are not fully independent. The best example is the LTI. This variable contributes strongly to the axes, negatively on PC1 ($r = -0.454$) and on PC2 ($r = -0.729$). This reflects a dependence between species composition (mainly represented on PC1) and shade tolerance (mainly represented on PC2). This is just an example and applies to other variables such as mean DBH, BA, regeneration cover, tree diversity, etc. Nevertheless, those two axes

identified two gradients that are ecologically distinct. The forest characteristics explained on one axis cannot be fully predicted from the ones explained on the other axis. The forest successional stage (PC2) cannot be fully predicted only based on its forest composition (PC1). The two axes capture two partially overlapping but analytically separable ecological gradients in secondary forest variation, one driven by the species composition and the other driven by the successional stage and the light conditions.

5.2.2. Environmental factors

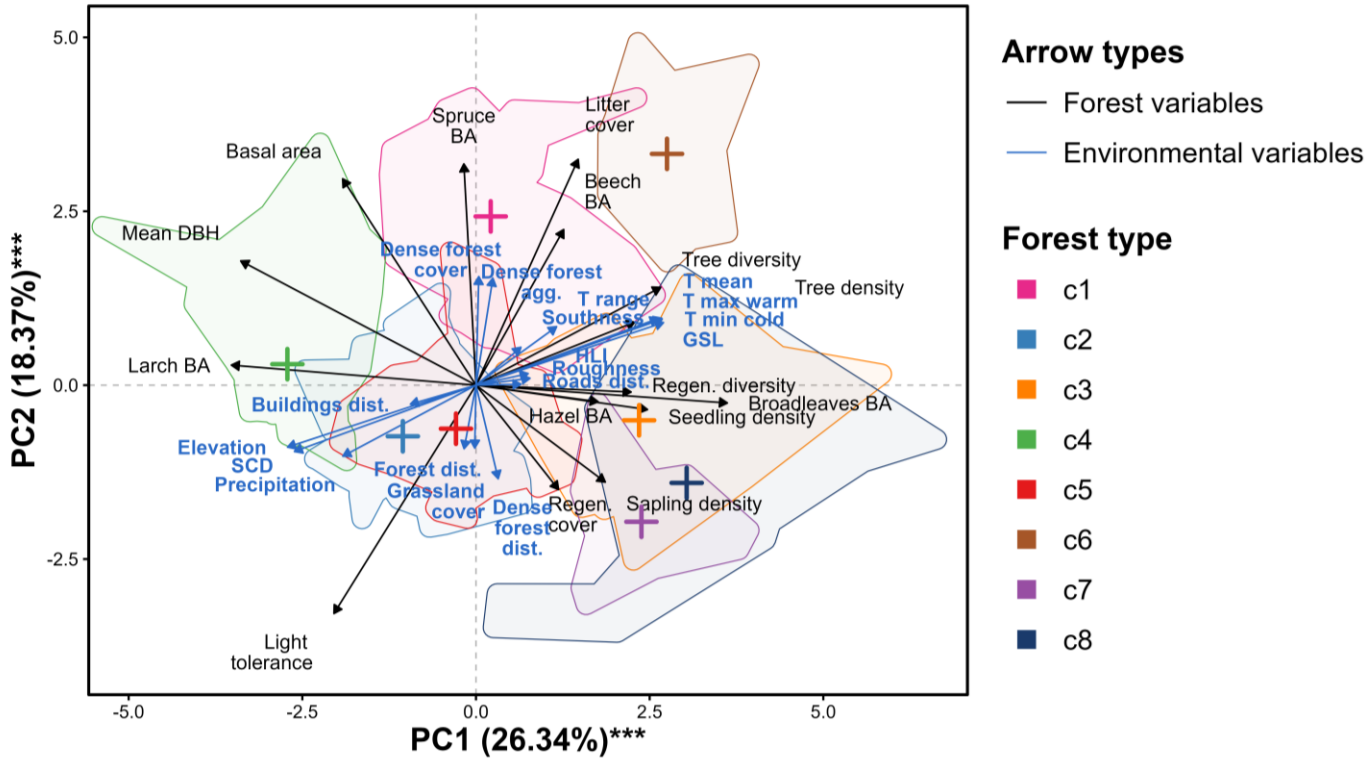

Figure 27: PCA biplot with the passive projection of the environmental variables. Agg.: aggregation, dist.: distance, GSL: Growing Season Length, HLI: Heat Load Index, Regen.: Regeneration, SCD: Snow Cover Days, T: Temperature.

The environmental variables described in section 4 were projected onto the ordination space as passive variables (Figure 27). To describe and quantify their relationships with PC1 and PC2, the Pearson (r) and Kendall (τ) correlation coefficients were used for each variable. Their values are compiled in Table 22 (Appendix 13). The two coefficients show consistent direction and relatively similar magnitudes for all the variables. This indicates that the relations between the environmental predictors and the ordination scores are monotonic, approximately linear, and not substantially influenced by outliers. As the forest variables, a factor of 4.5 is added to their values on the graph to improve readability.

By looking first at the horizontal axis (Figure 27), the first observation is that PC1 seems to be strongly correlated with a thermal-elevation gradient. Among all the environmental variables, seven show absolute values higher than 0.4 for the Pearson coefficient. On the negative side, the elevation shows the strongest negative correlation (r = -0.603) followed by snow cover days (SCD, r = -0.581) and annual precipitation amount (r = -0.426). On the positive side, temperature variables dominate with the minimum temperature of the coldest month (r = 0.600), T mean (r = +0.596), maximum temperature of the warmest month (r = 0.594), and growing

season length (GSL, r = 0.583). Those seven variables describe a consistent thermal-elevation gradient that goes from high altitudes characterised by low temperatures and abundant precipitation on the negative side to lower altitudes with higher temperatures and longer GSL on the positive side. The increasing elevation associated with lower temperature, shorter GSL, higher precipitation and longer snow cover is very coherent (Gobiet et al., 2014; Zandonai et al., 2024).

This gradient is directly used to explain the separation in the ordination space of the two macro-groups of clusters. The negative side of PC1, occupied by larch-dominated clusters (c2, c4 and c5), corresponds therefore to high-altitude subalpine zone described in section 2.1.2 where the conditions (cold temperature, long season of snow cover and short GSL) are favourable for the growth and dominance of larch (Garbarino et al., 2013). Larch is one of the few tree species capable of forming closed-canopy forests at high altitudes in the Alps, owing to its unique combination of frost tolerance, high light requirement and rapid growth on disturbed substrates and mineral soils (Garbarino et al., 2013; Leuschner and Ellenberg, 2017). In contrast, the positive side of PC1, occupied by the other macro-group (C1), corresponds to the lower altitude forest belt zone with warmer temperatures and longer GSL. These conditions are more favourable for the growth of broadleaves such as ash, beech, chestnut, hazel, etc. The four clusters dominated by broadleaved species (c3, c6, c7 and c8) have very similar values on PC1 (ranging from 2.35 to 3.03). This means that they occupy the same places in the thermal-elevation gradient, i.e., warm and low-elevation areas. Among the larch-dominated clusters, the actual mean elevations follow the order c2 > c4 > c5, with respective means of 1,868 m, 1,783 m and 1,720 m a.s.l. This ranking differs from their PC1 ordering, where c4 appears most negative due to its exceptional structural maturity rather than its altitude. c2, despite being the highest cluster on average, is less negative on PC1 than c4 because its lower basal area and higher regeneration diversity partially offset the compositional signal. This illustrates an important limitation of interpreting PC1 positions as direct altitudinal proxies: the structural and compositional variables that define the axis do not map perfectly onto the altitudinal gradient, and the RF analysis provides a more direct quantification of the altitudinal distributions of each cluster. Cluster c1 is placed in the middle of the larch-dominated clusters and the other broadleaved clusters, close to the origin of PC1 (r = 0.21). This position on this axis reflects, above all, the ecological nature of the dominant species in this cluster, spruce. This species is a shade-tolerant conifer that occupies the belts between the subalpine ones dominated by larch and the warm ones dominated by broadleaf species (i.e., to the upper limits of the forest belt and the lower subalpine zone). Spruce is indeed a species that tolerates cooler and wetter conditions than most of broadleaved species but that cannot compete with the larch in the harsh conditions of high altitudes (Leuschner and Ellenberg, 2017; Schulze et al., 2007). The central position of this cluster on PC1 reflects therefore its intermediate altitudinal position.

All the other environmental predictors show much lower correlations with PC1. Some topographic variables are positively associated with PC1 with Pearson coefficient higher than 0.1 (i.e., HLI, r = 0.173; roughness, r = 0.167; southness, r = 0.144; and slope, r = 0.130). This indicates that the broadleaves forests from the macro-group C1 are also associated with sunnier, south-facing and rugged topographic sites. Those variables complement the thermal-elevation gradient and act as secondary predictors. This has an impact on the distribution of the broadleaved forests along the altitudinal gradient. A southern exposure with high HLI can partially compensate for the cold temperature from high altitude and allow those secondary forest types to establish higher than it would be expected based only on the elevation. This leads to the conclusion that PC1 represents therefore a thermal-accumulation gradient more than a thermal-elevation gradient. The anthropogenic predictors show very low correlation with PC1 except the distance to buildings (r = -0.210) and the distance to roads (r = 0.144). The negative

correlations of the distance to buildings indicate that larch-dominated forests tend to be further from human infrastructures. This negative correlation partially reflects the altitudinal gradient captured by the elevation. Human infrastructures are indeed mostly located in the valley floor and to a lesser extent at high altitude. This means that the larch-dominated forests are naturally more distant from the buildings without considering the land use history. The weakness of these correlations with PC1 shows that the anthropogenic factors are not the main ones of the secondary forest differentiation, especially in the differentiation in composition, the ecological gradient identified along PC1 (section 5.2.1).

By looking now at the vertical axis, PC2, the main observation is that this axis seems to be correlated with the land-cover structure. Indeed, five environmental predictors are almost perfectly aligned with the vertical axis, and all of them are landscape variables. As a reminder, as explained in section 4.3.5, the landscape metrics were derived from a 1954 land cover classification. These variables therefore refer to the state of the landscape at the time when some of the secondary successions began. Using historical rather than contemporary landscape metrics is an important methodological choice. It captures the landscape conditions under which secondary succession has started, rather than the current landscape in which secondary forests evolve. These five environmental predictors are the distance to dense forest ($r = -0.299$), grassland cover ($r = -0.203$), distance to both dense and sparse forest ($r = -0.201$) on the negative side of PC2 and the dense forest cover ($r = 0.347$), and dense forest aggregation index ($r = 0.342$) on the positive side. After those landscape variables, some climatic variables show secondary correlation on PC2 such as precipitation ($r = -0.227$), SCD ($r = -0.212$), minimum temperature of the coldest month ($r = 0.200$), T mean ($r = 0.211$), GSL ($r = 0.213$), and the maximum temperature of the warmest month ($r = 0.214$).

The historical landscape variables of 1954 capture two important conditions: the availability of seed sources and the duration since establishment of the secondary forest. Sites surrounded by dense and aggregated forests in 1954 present two characteristics favourable to the development of structurally mature secondary forests. First, they were exposed to more seed sources with the established forests around them. This constitutes a significant advantage for the seedlings establishment of late-successional species (Flinn and Marks, 2007; Hermy and Verheyen, 2007). Second, the presence of dense forest cover surrounding those sites in 1954 is likely indicative of an earlier abandonment of agricultural or pastoral activities. This earlier abandonment is hypothesised to reflect that those sites are in areas with complex topography (steep slopes, far from roads and buildings, high roughness, etc.) which strongly reduced agricultural productivity. These sites have therefore had more time to develop structurally compared to sites that were still actively used as open grasslands in 1954 and were abandoned more recently. Conversely, the sites located in more open areas, dominated by grassland in 1954, were therefore more recently abandoned and have limited seed sources for the forest succession to start. These sites present today forests that are still in earlier stages of forest establishment. The landscape of 1954 therefore acts as an important land-use legacy variable that explains a large part of the variation in the successional stages captured by PC2.

This interpretation is confirmed by the distribution of the cluster centroids along PC2. This gradient shows indeed that the secondary forest maturity and successional stages, the ecological gradient of PC2, are in majority explained by the landscape context (1954) surrounding each plot. The clusters with the structural mature stands, c1 and c6, tend to occur where the environment in 1954 was mainly covered by dense forests, generally well connected. This suggests that those places have a long history of forest continuity. The dense forest aggregation index corroborates the hypothesis that the mature forests found in those two clusters are generally surrounded by aggregated dense forest patches rather than fragmented forests. This

characteristic is a big advantage for the establishment and the persistence of the late successional species found in these forests. c6 shows a higher centroid in PC2 than c1. This is explained by the long history in Piedmont of traditional coppice management for beech and chestnut forests. This intensive land use has maintained continuous forest cover through historical periods. The presence of those coppiced forests provided both important seed sources and early abandonment context that has facilitated c6 to reach earlier mature stages than all the other clusters. For c1, the dense and continuous forest matrix surrounding the plots has similarly facilitated the establishment of spruce, a shade-tolerant species with limited dispersal ability, strongly dependent on the proximity of established seed sources.

In contrast, the clusters composed of pioneer, young forests tend to occur in places that were mainly occupied by grasslands in 1954. Those plots were also further from forests in that period. Those clusters represent young secondary forests recently established on recently abandoned lands. Those forests appear in places where the landscape is today still dominated by open vegetation, with highly fragmented forests. Cluster c7, identified as the youngest and newest established forests, is the most strongly correlated with landscape context dominated by grasslands and fragmented forests. This cluster represents the most recently abandoned sites. The dominant species, common hazel, is a wind-dispersed, highly mobile pioneer able to establish rapidly without depending on the proximity of established forest (Bebi et al., 2017; Tasser and Tappeiner, 2002). c8, with its slightly higher position on PC2, seems to occur in landscapes that were less open in 1954 with a higher forest proximity than c7. The higher species diversity in c8 than in c7 confirms this hypothesis with a greater access to forest seed sources at the time of the establishment (Flinn and Marks, 2007). c3 is positioned closer to the origin on PC2, meaning that the environments surrounding those plots were already partially covered by forest. This partial forest context provided a moderate seed source and an earlier abandonment stage compared to c7 and c8. This result illustrates the limits of the 1954 landscape gradient for differentiating c3 and c8 in detail. Both clusters occupy relatively open landscape contexts in 1954, and the small difference in their PC2 positions along the landscape gradient does not straightforwardly reflect their successional advancement, which, as discussed in section 5.2.1, is better explained by stand-level structural dynamics (stem exclusion vs. gap phase) than by their historical landscape context.

Within the larch-dominated clusters, the three centroids show near zero values on PC2 (c4: 0.30, c2: -0.74, c5: -0.63), indicating that their successional stage is not captured by the historical landscape gradient of PC2. This is coherent with the previous results and discussion. The maturity of larch-dominated forests is expressed more through structural development (higher DBH and BA) than a compositional shift to shade-tolerant species, which is the gradient captured by PC2. In addition, the high-altitude subalpine zone occupied by those three clusters has historically maintained a relatively continuous and homogeneous mosaic of pastures and larch forests (Garbarino et al., 2013). The landscape gradient of 1954 captured by PC2 is therefore less informative for the three clusters. Their successional trajectory is primarily governed by the climatic constraints captured by PC1.

5.3. Relative importance of the environmental factors

5.3.1. Variables selection

As described in section 4.4.3, a variable selection was done before training the RF model. 14 variables of all those in the secondary environmental matrix were retained after the two-step selection. The RFE procedure has first retained 23 variables based on their contribution to classification accuracy under spatial block cross-validation. The second step of the selection, a

subsequent collinearity filtering step, has removed variables with pairwise Pearson correlations exceeding 0.7. This has reduced the final selection to a set of 14 environmental variables distributed in four main categories: climate (annual precipitation amount and mean diurnal temperature range), topography/terrain context (elevation, slope, southness, eastness, TPI and TWI), anthropogenic variables (distances to roads and buildings), and landscape metrics (dense forest cover, distance to dense forest, grassland cover and grassland patch density).

The second step of the selection has mainly removed climatic variables such as mean annual temperature, minimum temperature of the coldest month, maximum temperature of the warmest month, growing season length, and snow cover duration. Those variables are indeed strongly collinear with the elevation ($r > 0.7$), which encompasses the bulk of their predictive information. This selection is consistent with the PCA results. Figure 27 shows clearly the high collinearity between the elevation and those variables. Altogether, they describe the thermal-accumulation gradient discussed previously. The variable selection has retained the elevation because the collinearity-filtering algorithm identifies this variable as having the lowest average correlation across the full predictor set, which minimises global redundancy. Indeed, elevation shows weaker correlation with topographic variables and is therefore retained as the representative of the thermal-accumulation gradient. From an ecological point of view, elevation is also a more integrative and measurement-error-free predictor than interpolated climatic variables, capturing not only thermal conditions but also precipitation regime, snow cover duration and historical land use patterns in a single variable (Körner, 2007). It should be noted, however, that this integrative nature of elevation makes it difficult to separate the climatic signal from land-use legacy effects, a limitation discussed further in section 7.

The 14 variables selected by the two-step method partially overlap with those retained as informative in the PCA (Appendix 5). Among the topographic variables, elevation, slope and southness were already used in the PCA while eastness, TPI and TWI are new factors identified in the RF analysis. This difference is expected based on the differences between PCA and RF. While the PCA identified linear correlations between environmental variables and ordination scores, the RF can detect non-linear and threshold-based relationships that may be invisible to a correlation-based approach. The three new factors may capture non-linear patterns related to the previously identified secondary forest clusters. For the landscape metrics, three of the four retained land-cover variables were also identified as informative in the PCA (dense forest cover, distance to dense forest and grassland cover). The grassland PD is a new variable providing complementary information on the spatial configuration of the 1954 landscape. The two anthropogenic variables retained confirm the minor but non-negligible role of human proximity in structuring secondary forest types, consistent with their weak correlations with PC1 in the PCA. Some of the environmental variables retained in the PCA were not retained in the RF. If they were eliminated by the RFE procedure, it indicates that they do not contribute independently to the classification accuracy of the model once other variables are included. This suggests that the variables retained are sufficient to distinguish the eight secondary forest clusters.

These differences between the PCA and the RF reflect the complementarity of the two methods: the PCA identifies all variables that correlate with the main ecological gradients, regardless of their redundancy, while the RF selection procedure retains only the subset that maximises predictive performance with minimal collinearity to improve ecological interpretability. The 14 variables retained cover the same ecological gradients identified with the PCA. The overlap between the two analyses improves the ecological consistency of the predictor set, while the differences highlight the complementarity of the two methods in characterising the environmental determinants of secondary forest diversity in the GPNP.

The RF classifier performed with the 14 selected variables achieved a spatially cross-validated overall accuracy of 39.8 %, corresponding to a classification error of 60.2%. Although moderate in absolute terms, this result must be interpreted in the context of an eight-class classification problem, for which a random baseline would yield only 12.5 % accuracy, placing the model at approximately 3.2 times above chance. The use of spatial block cross-validation (section 4.4.3) further ensures that this estimate is conservative, as it prevents the model from exploiting local spatial autocorrelation between training and test plots (Valavi et al., 2019). Part of the classification error is also attributable to the ecological proximity of several clusters: types representing adjacent successional stages within the same macro-group share similar environmental conditions, making them inherently harder to discriminate from environmental predictors alone.

5.3.2. Variables importance

The permutation-based variable importance computed on the final RF model reveals the dominance of one single predictor, the elevation (Figure 28). The 13 other environmental predictors selected have importance values below 0.1. This means that all those predictors result in a classification error lower than this value during random shuffling.

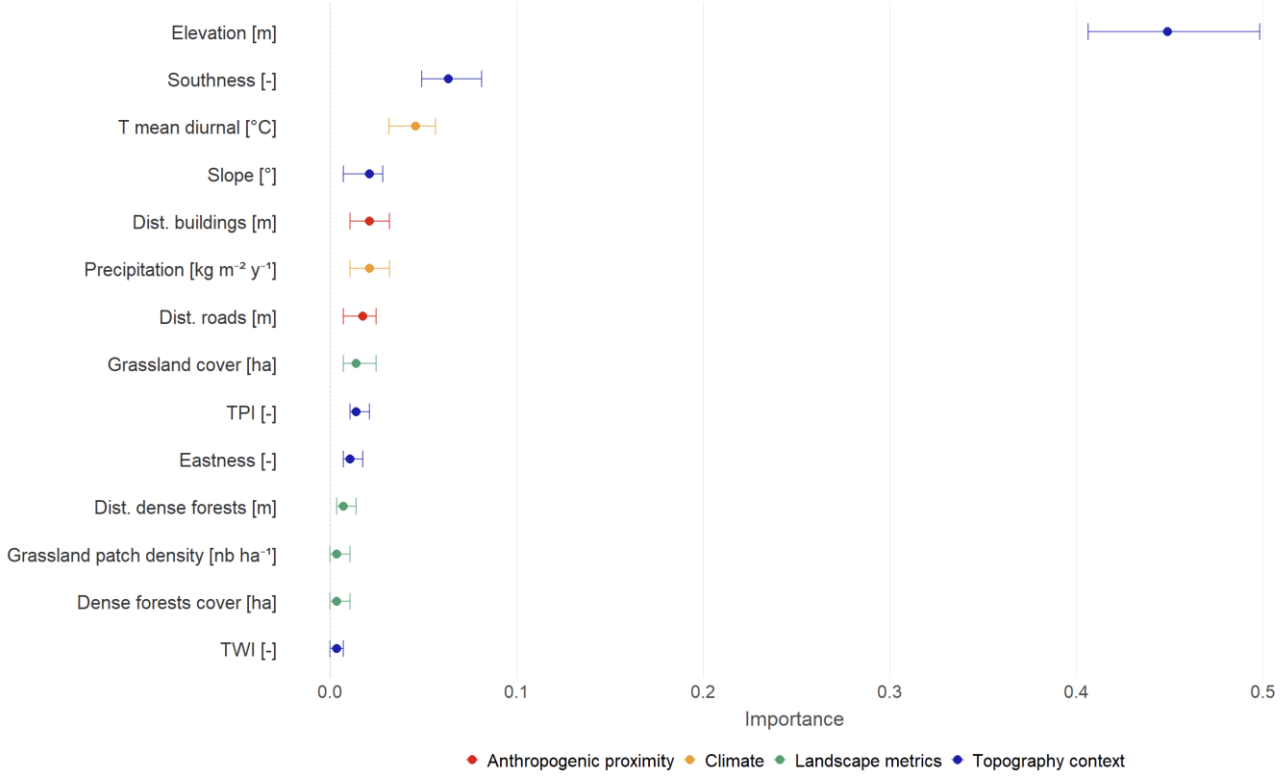

Figure 28: Permutation-based variable importance of the 14 environmental predictors retained. Error bars indicate the standard deviation across the five spatial folds. TPI = Topographic Position Index; TWI = Topographic Wetness Index; T mean diurnal = mean diurnal air temperature range.

As described, the elevation is the dominant predictor, far ahead of the others, with a permutation importance of 0.449. This environmental predictor is therefore accounting for 64.5% of the total importance across all 14 predictors. This result confirms the central role of the thermal-accumulation gradient already mentioned on numerous occasions in the previous sections. With the PCA, the RF analysis confirms that the elevation is the main predictor of the secondary forest types in the GPNP. This result was ecologically expected: the elevation integrates numerous environmental factors such as the precipitation, the temperature, the snow-cover days and even historical land-use patterns into a single gradient that separates larch-dominated

subalpine forests from broadleaved and mixed forests at lower altitudes, as established in section 5.2.1 (Gobiet et al., 2014; Körner, 2007).

Even with a permutation importance of 0.064, the southness accounts for 9.1% of the total importance, confirming the role of slope aspect as a secondary modulator of the altitudinal gradient. The importance of this predictor is about seven time lower than elevation. As discussed in section 5.2.1, a south exposition can increase the solar radiation received and compensate for the temperature decrease with altitude, having an influence on the upper distribution limits of broadleaves forests. This result shows that the slope aspect acts as a secondary modulator of the altitudinal gradient.

The third predictor is the mean diurnal temperature range with a permutation importance of 0.046, representing 6.6% of the total importance. This variable provides predictive information not fully captured by the elevation. Higher diurnal temperature ranges are typically associated with more continental, less cloudy conditions and with specific topographic positions such as valley floors or ridges with stronger radiation-driven temperature fluctuations. The independent contribution of this variable, beyond what is explained by elevation alone, suggests that local thermal exposure plays a role in determining secondary forest type that is not captured by the altitudinal gradient alone.

Annual precipitation amount, slope and distance to buildings all have a permutation importance of 0.021, representing 3.0% of the total importance. Precipitation adds climatic information not fully captured by elevation such as the orographic effect that creates precipitation gradients across the park independently of altitude while slope contributes topographic information complementary to southness, influencing drainage, soil stability and light availability. The modest yet significant contribution of distance to buildings confirms the non-negligible role of anthropogenic proximity in shaping secondary forest composition.

The remaining eight environmental variables contribute marginally to the model's predictive performance. Their low importance suggests that once elevation and southness are accounted for, the historical landscape context provides little additional discriminating power for predicting which of the eight forest types occurs at a given location. This may reflect the fact that the landscape variables of 1954 are themselves spatially structured in a way that is partly collinear with elevation. The high-elevation landscapes were indeed mainly composed of a combination of larch forests and pastures while the lower-altitude zones showed greater landscape heterogeneity.

Looking finally at the permutation importance by category of variables, the topographic one dominates, representing 80.7% of the total importance, followed by the climatic variables (9.6%). Both anthropogenic and historical landscape variables account for less than 10% (5.6% and 4.1%, respectively). This hierarchy is consistent with the main thermal-accumulation gradient identified with the PCA, but the RF provides a more precise quantification. With the importance result, it can be assumed that, in the GPNP, the type of secondary forest developing at a given location is primarily determined by the position on the altitudinal gradient and then by climate exposure, with historical landscape context and anthropogenic proximity playing a complementary but minor predictive role.

5.3.3. Variables effect

Partial Dependence Plots (PDPs) were computed for each of the selected environmental variables. Those PDPs reveal the marginal effects of the 14 predictors on the predicted

probability of each secondary forest cluster, after averaging out the effects of all other predictors. The graphs show how the predicted probability of belonging to a class varies across the range of values for that variable. Two complementary pieces of information can be read from each PDP. First, the average level of the predicted probability curve for a given cluster reflects the overall prevalence of that cluster in the dataset: clusters with more plots show higher average probabilities than smaller clusters, regardless of the predictor considered. This average level should therefore not be interpreted as an indicator of the strength of the relationship between the predictor and the cluster. Second, and more ecologically informative, is the shape and amplitude of the curve across the range of the predictor: a steeply increasing or decreasing curve indicates that the predictor has a strong marginal effect on the probability of belonging to that cluster, while a flat curve indicates that the predictor has little influence once the effects of all other variables are accounted for. The ecological interpretation of the PDPs therefore focuses primarily on the direction and amplitude of the response curves rather than on their absolute level.

The elevation was identified in the previous section as the most informative variable. Its PDP (Figure 29) clearly discriminates the eight secondary forest clusters along the altitudinal gradient. The three larch-dominated clusters (especially c2 and c4) show increasing probability curves with the elevation while the broadleaves-dominated ones show decreasing probability curves. The PDP of the elevation confirms the fundamental difference between the two main macro-groups C1 and C2 along the thermal-accumulation gradient established in the PCA. 1,600 m a.s.l. seems to be the threshold between these two macro-groups. This value appears to be consistent with those reported in the literature, which range between 1,500 and 1,800 metres a.s.l. (Garbarino et al., 2013; Leuschner and Ellenberg, 2017; Tasser and Tappeiner, 2002). This altitude does not represent a fixed limit, but rather an inflection point at which the probability of broadleaves clusters (C1) decreases and that of larch-dominated clusters (C2) increases most rapidly.

Among the larch-dominated clusters, c2 and c4 show a net higher probability to be predicted at high altitude by the RF model while c5 shows also this trend, though less pronounced than the others. c2 has its peak probability at 2,109 m a.s.l. and its probability curve rises steeply after 1,500 m a.s.l., showing its strong belonging to the subalpine zone. c4 has its peak probability at 1,800 m a.s.l., still showing a belonging to the same zone but lower than c2. The amplitude of the response curve is particularly marked for c2 (probability ranging from 7.8% at the lowest elevations to 45.5% at the highest), confirming its strict belonging to the subalpine zone. This is consistent with the mean elevation values for the two clusters where c2 (1,868 m a.s.l.) was higher than c4 (1,783 m a.s.l.). c5 shows a monotone slightly increasing probability curve. No real peak can be identified for this cluster, preventing a precise optimum from being identified. The more meaningful information for this cluster stays its mean value. The distinction between c2 and c4 is ecologically significant: this partially confirms the hypothesis made in section 5.1.3 that c2 is located at higher altitudes than c4. But for c5, contrary to the hypothesis, it shows the lowest mean value of the three larch clusters (1,720 m a.s.l.). The lower altitude of c5 is consistent with its higher regeneration diversity and its proximity to forest seed sources at lower elevations.

Among the broadleaves-dominated clusters, c3 shows a net preference for the sites of low altitudes (below 1,400 m a.s.l.), with a peak probability at 797 m a.s.l. This confirms that the dense forests of pioneer broadleaves are mainly found at low altitude. The results for c6, c7 and c8 are quite similar. c7 however shows a peak probability at 1,491 m a.s.l., suggesting that some of the recently abandoned sites colonised by common hazel can be found at higher elevations. c1 is also associated with intermediate elevations with its peak at 1,491 m a.s.l., which is

consistent with the important proportion of spruce in this cluster and its ecology as a transitional coniferous species. However, the relatively flat response curve of c1 compared to the other C1 clusters suggests that its altitudinal distribution may also partly reflect historical silvicultural practices, as Norway spruce has been widely favoured by alpine forest management for commercial purposes, potentially decoupling its current distribution from purely climatic controls (Motta and Nola, 2001).

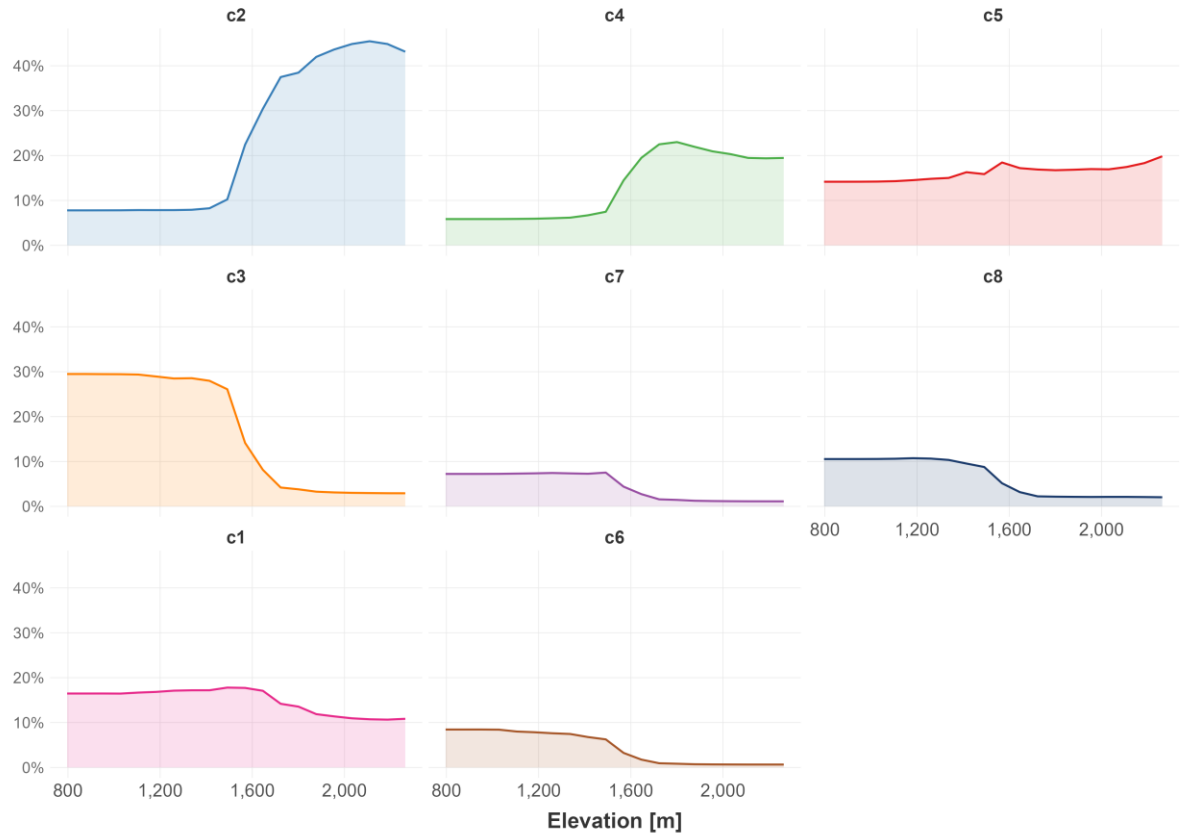

Figure 29: PDPs for the elevation.

The PDPs for southness (Figure 30) reveal some contrasting effects between forest types that are ecologically coherent and complement the elevation gradient. In the first line, c4 is showing an increasing probability curve, meaning a higher probability to be predicted in south-facing slopes while, in the opposite, c2 and c5 show decreasing probability curves. This is an important result meaning that according to the RF model, the mature larch stands tend to be more on south-facing slopes. A greater amount of light on these slopes can favour the structural development of the trees, explaining the greater structural characteristics of this cluster. This contrast with c2 and c5 suggests that slope exposure can play an important role in the succession trajectories of secondary larch forests (Garbarino et al., 2013; Tasser and Tappeiner, 2002). c3 and c7 show a slight tendency to be more located on south-facing slopes, which is consistent with their composition of pioneer, light-demanding species. c6 also shows an increasing probability curve, which is somewhat unexpected given that beech typically favours cooler, north-facing positions in the central European Alps (Leuschner and Ellenberg, 2017). However, all c6 plots are in the Piedmont sector of the GPNP at relatively low elevation where south-facing slopes may still receive sufficient precipitation to support beech establishment. The association of c6 with south-facing slopes in this specific context should therefore be interpreted cautiously and verified with field data on aspect distribution within this cluster. c1 shows a

higher probability on neutral aspects, consistent with its intermediate ecological position already identified. In contrast, c8 shows a slightly decreasing probability curve with southness, which is consistent with its lower proportion of light-demanding species compared to c3.

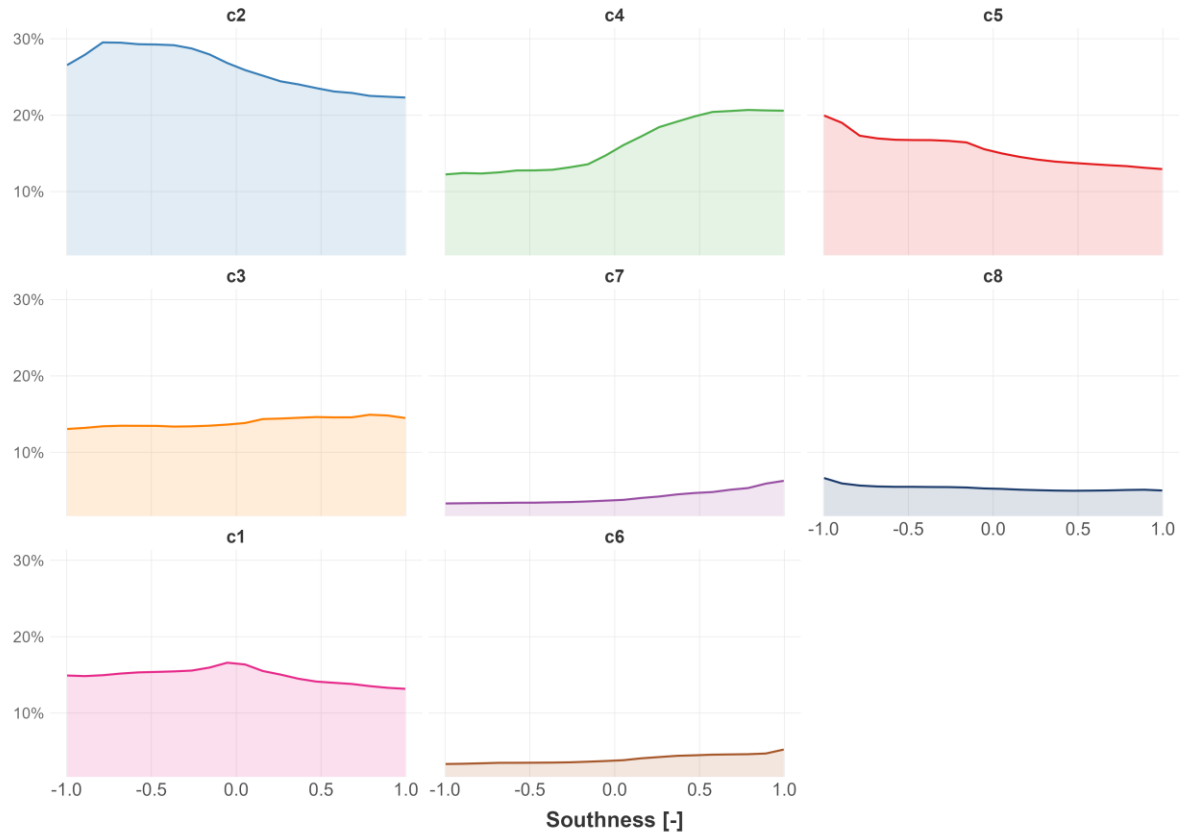

Figure 30: PDPs for the southness.

The PDPs for the mean diurnal temperature range (Figure 31) show less variation in the effects than the two previous variables, reflecting its secondary role as a climatic predictor. Although the amplitudes of the curves are much smaller than the two others, the PDPs stay ecologically interpretable. Three clusters (c2, c3 and c6) show more marked and different responses. c3 displays a decreasing probability with increasing diurnal temperature range while c2 and c6 show the opposite pattern. Those opposite responses are consistent with their topographic distribution. The decreasing probability curve of c3 is consistent with its location in valley-floor sites where atmospheric humidity and forest cover buffer diurnal temperature fluctuations (De Frenne et al., 2019). The increasing probability curves for c2 and c6 reflect two different dimensions of their distribution. In the case of c2, the subalpine larch-dominated forests are subject to more diurnal temperature variation mainly because of their high-elevation distribution (Gobiet et al., 2014). In the case of c6, the distribution in south-facing slopes explains this association to higher diurnal temperature ranges (Zellweger et al., 2019). The remaining clusters show only weak responses, confirming that the mean diurnal temperature range refines the climatic signal captured by elevation rather than identifying an independent ecological gradient, consistent with its modest permutation importance.

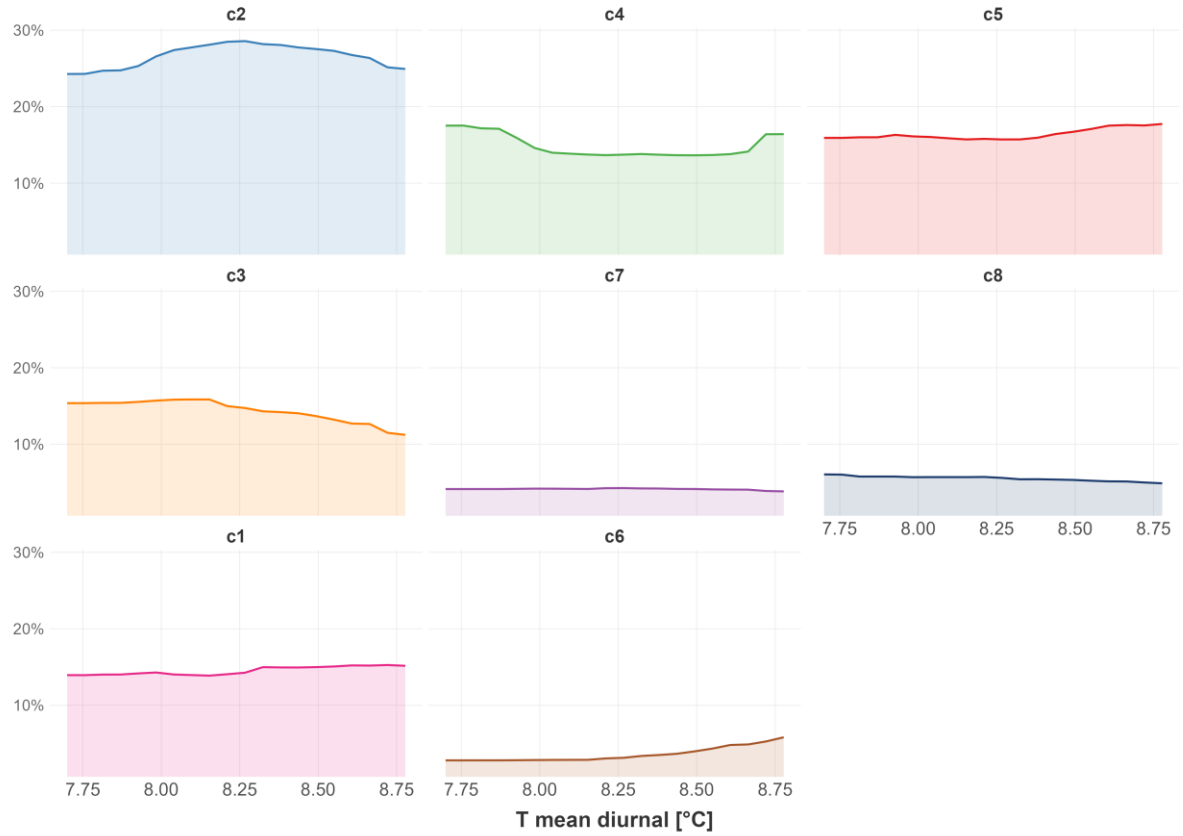

Figure 31: PDPs for the mean diurnal temperature range.

The PDPs for the 11 remaining variables (Appendix 14) show limited responses with very slight variations. This is consistent with the results of the variables importance (section 5.3.2). Indeed, the remaining predictors contribute only marginally to the differentiation between the eight secondary forest clusters. This limited amplitude of the probability curves confirms that the secondary forest types in the GPNP are primarily structured by the climatic-altitudinal gradient and its main topographic modulators.

Nevertheless, a brief mention of the effect of some predictors on some clusters can be done because they show locally visible responses, indicating non-negligible secondary effects. The dense forest cover in 1954 shows a marked positive effect on the probability of c1. This is consistent with the ecology of spruce, a species that requires a high proximity of seed sources for its establishment (result already explained in section 5.2). This result is consistent with the decreasing probability curve with the distance to dense forest. The annual precipitation displays an increasing response for c2. The hypothesis is that this is mainly due to the high-elevation distribution of this cluster. The wetter sites correspond to the high-elevation subalpine valleys and valley heads, places of cold temperatures and abundant snowfalls (Gobiet et al., 2014). This is confirmed by the responses from the other clusters, with those at low and medium altitudes (c1, c3, c6, c7 and c8) showing decreasing probability curves, while the other two larch-dominated clusters show increasing probability curve. Precipitation thus acts here as an indirect spatial marker for the subalpine zone rather than as a direct physiological driver. The remaining variables (eastness, TPI, TWI, slope, distance to buildings, grassland cover, and grassland patch density) show only minor and largely flat partial dependence patterns and are not discussed further here.

5.4. Comparison with previous work

The results presented in the previous sections can be compared to the work of Gontier (2026), which constitutes the immediate precursor of this study, and with the broader literature on post-abandonment forest dynamics in the European Alps.

Despite some differences in the methodology, the two studies share some convergent results. Gontier (2026) has analysed the secondary forests in mountains through 182 plots distributed in the Aosta Valley sector of the GPNP. While the present study has used a PCA completed with a RF analysis, Gontier has performed a Constrained Correspondence Analysis (CCA) combined with Multi-Response Permutation Procedures. Both studies had independently identified an altitudinal-thermal gradient as the dominant axis structuring secondary forest diversity, with anthropogenic and historical landscape variables acting as secondary modulators. Among the secondary forest types identified, both works have revealed three larch-dominated forest types corresponding to different stages of post-pastoral succession: an old-growth larch type without regeneration (c4 in this study, Group 8 in Gontier 2026), a larch type with broadleaved regeneration suggesting active succession (c5 here, Group 9 in Gontier 2026), and a larch–spruce mixed forest (c1 here, Group 10 in Gontier 2026).

However, two important differences can be noticed between the two studies. First, the number of forest types identified differs: ten groups in Gontier (2026) versus eight clusters in this study. This difference reflects both the broader compositional and climatic span captured by the extended dataset and the methodological choice. Some small clusters identified by Gontier (2026) are merged within larger clusters that integrate plots from the two sectors of the GPNP. Second, the relative weight attributed to anthropogenic legacies differs: these variables structure several axes of the CCA in Gontier (2026) while they were not retained in the RF analysis after RFE. This difference does not necessarily mean that the two studies are inconsistent. It reflects the impact of the methodology chosen. The CCA performed was made without prior selection within all the environmental variables while the RF analysis was performed after a two-step selection process. This pre-selection reduces the risk of overfitting and ensures that each retained variable contributes independently to the analysis, at the cost of potentially excluding variables that could be informative. This may partly explain why anthropogenic legacy variables such as terraces and stone clearings, prominent in the CCA of Gontier (2026), were not retained as individual predictors in the present study.

Beyond these methodological considerations, the geographical extension to the Piedmont sector provides three substantive contributions. First, two secondary forest types are essentially restricted to the Piedmont sector: the mature beech-dominated coppice forests (c6), composed of 11 plots all located in Piedmont, and the pioneer hazel shrublands (c7), composed of 12 plots all located in Piedmont. Those two types occupy the lower forest belt of the southern slope of the GPNP, where the climatic conditions (warmer winters, higher humidity) and the historical land-use trajectories (centuries of coppicing) differ from the more continental Aosta Valley sector (Garbarino et al., 2020; Nocentini, 2009). Second, it provides a more balanced representation of the climatic span of the park, which is essential to interpret the role of the altitudinal-thermal gradient: a dataset restricted to the Aosta Valley would have under-represented the lower end of this gradient, possibly biasing the identification of the structuring axes. Third, the extension reveals that the divergence between successional trajectories (conifer-dominated at high elevation versus broadleaves-dominated at lower elevation) operates at the scale of the entire park, supporting the generality of this pattern across different climatic sectors of the western Italian Alps.

6. Conclusion

This master's thesis aimed to characterise the diversity of secondary forest types and to identify the environmental factors determining this diversity. Three main categories were investigated among the environmental factors in this study: climatic, topographic and anthropogenic factors. To answer the research question, the different types of secondary forests were identified based on 283 sampling plots in the Gran Paradiso National Park (GPNP). Within each sampling plot, forest variables were collected to characterise the secondary forests. The environmental variables were determined for each plot through a series of different methods. To address the research question, this study was divided into three main sub-objectives, each addressed using different analytical methods, combining hierarchical cluster analysis, principal component analysis (PCA) and Random Forest (RF) classification.

The first sub-objective was to identify the different secondary forest types in the GPNP based on forest variables relating to the structure, composition and regeneration of stands and identify the ecological gradients that differentiate them. The hierarchical cluster analysis revealed eight structurally and compositionally different types, organised in two macro-groups. The first macro-group (C1) brings together five secondary forest types: mature spruce-dominated forests (c1), dense pioneer broadleaves forests (c3), mature beech-dominated forests (c6), pioneer hazel shrublands (c7), and established mixed broadleaves forests with active regeneration (c8). The second macro-group (C2) gathers three larch-dominated forests: open larch-dominated forests (c2), mature larch-dominated forests (c4) and larch-dominated forests with active regeneration (c5). The clear separation between those eight clusters, combined with their internal homogeneity in terms of forest characteristics (structure, composition and ground cover) indicated that the secondary forests in the GPNP are a mosaic of ecologically meaningful succession trajectories shaped by a series of factors. The PCA revealed that the eight clusters were distributed along two main ecological gradients: a species composition gradient separating the two macro-groups and a maturity-and-legacy gradient separating the mature, well-established stands with dense litter cover from pioneer, newly-established stands.

The second sub-objective was to link these forest types to environmental factors. The passive projection of the environmental factors onto the ordination space of the PCA identified the factors structuring the differences between the secondary forest types. The most important factor was a thermal-accumulation gradient, associated with the species composition axis, linking larch-dominated forests to high elevations characterised by low temperatures, long snow-cover duration, short growing season and high precipitation. The successional stage gradient was primarily associated with landscape legacies from 1954. The pioneer, newly-established stands tended to occur in landscapes dominated by open grasslands in 1954, reflecting more recent abandonment. The combined interpretation of the two gradients shows that each cluster occupies a distinct ecological space that can be defined by the thermal-accumulation gradient and the legacies from 1954. This persistence of historical signals confirms the long-lasting influence of land-use legacies on forest ecosystems in the Alps.

The third sub-objective was to quantify and rank the relative importance of the environmental drivers shaping these forest types. The RF analysis identified the elevation as the only dominant factor with a relative importance of 64.5%, far ahead of the other predictors. This analysis has shown that the climatic and topographic factors accounted for most of the total importance, while anthropogenic and 1954 landscape variables contributed less than 10%. The partial dependence plots confirmed the important effect of the elevation in differentiating the clusters

with secondary factors such as the southness and the mean diurnal temperature range. This hierarchy must however be interpreted in the light of the multicollinearity between elevation and several climatic and anthropogenic variables. The importance value reported for elevation therefore captures a bundle of co-varying climatic, topographic and historical signals rather than a single isolated driver.

Combining the results of the three sub-objectives, it is possible to build a coherent answer to the research question. The diversity of secondary forest types in the GPNP is a result of the combined action of two ecologically distinct processes, allowing these types of forests to be classified based on two criteria: site characteristics and succession trajectory.

The first criterion corresponds broadly to the separation between the two macro-groups. This separation primarily reflects the site effect: the climatic and topographic conditions associated with the altitudinal gradient define distinct ecological envelopes that constrain which tree species can establish and persist. Larch-dominated forests (C2) are restricted to the subalpine zone where cold temperatures, long snow-cover duration and short growing seasons exclude most broadleaved species. Broadleaved and mixed forests (C1) occupy the lower forest belt where warmer conditions and longer growing seasons are compatible with the establishment of shade-tolerant broadleaved species. The two macro-groups therefore do not represent different stages along a common trajectory but rather two fundamentally different trajectories, in two distinct altitudinal zones. The second criterion operates within each macro-group and reflects the successional process. The clusters identified within a macro-group represent different stages along a broadly common post-abandonment trajectory, differentiated by their structural maturity and regeneration dynamics. Within the larch-dominated macro-group C2, the three clusters represent different stages of the same post-pastoral succession trajectory. c4 and c2 represent the old-growth larch-dominated stands that were historically maintained by agro-pastoral activities. They reflect the legacy of centuries of pastoral management that repeatedly suppressed the natural regeneration of shade-tolerant competitors. c2 differs from c4 by its higher mean elevation and the harsher climatic conditions that constrain structural development. c5 represents the intermediate stage of this trajectory: still larch-dominated in its tree layer, it is distinguished by a higher regeneration diversity and density, reflecting the progressive establishment of shade-tolerant species such as spruce. This pattern is consistent with the ongoing compositional transition of these stands toward the late-successional spruce-dominated forests of c1, which represents the expected endpoint of the larch-dominated trajectory. Within macro-group C1, the sequence from c3, c7 and c8 towards c6 similarly reflects a gradient of successional advancement from recently established pioneer stands to structurally mature forests. One notable exception to this within-group logic is c1: although assigned to macro-group C1, the mature spruce-dominated forests it represents are ecologically more consistent with the successional trajectory of macro-group C2.

These two levels of organisation are each associated with a distinct set of environmental drivers. The site-level separation between macro-groups is primarily governed by the thermal-accumulation gradient captured by elevation, which alone accounted for 64.5% of the total variable importance in the Random Forest analysis and structured the main composition axis of the PCA. The successional-stage differentiation within macro-groups is primarily governed by the 1954 landscape legacies: plots surrounded by dense, well-connected forests at the time of abandonment have progressed further along their successional trajectory than plots embedded in open, grassland-dominated landscapes, owing to earlier abandonment and greater proximity to seed sources.

The secondary forest diversity in the GPNP therefore emerges from a hierarchical organisation of two ecological filters. A primary thermal-accumulation filter determines which successional trajectory is possible at a given site. This filter acts primarily based on altitude and secondarily based on slope aspect and diurnal temperature range. The second filter is land-use legacies that determine how far along its trajectory a stand has progressed, by controlling both the availability of seed sources at the time of establishment and the time elapsed since abandonment. This hierarchical framework provides a synthetic answer to the research question: the type of secondary forest developing at a given location in the GPNP is primarily determined by where it is on the thermal-accumulation gradient, and only secondly by its land-use history.

7. Limitations and Prospects

7.1. Limitations and unused data

This master's thesis has several limitations related to both the data that were used and the data that were not used, as well as to the chosen methodology.

Through the sampling methodology, a large series of data were excluded from this work since the starting point. Within this series, the most important data excluded are the soil characteristics and the past and current management of the forests. Soil properties were not included as predictors in this study, primarily due to the absence of a soil map at sufficient spatial resolution covering the entire GPNP. Given that the Aosta Valley and Piedmont sectors may differ in substrate geology with predominantly siliceous substrates in the Aosta Valley and more calcareous substrates in parts of the Piedmont, edaphic factors could contribute to the compositional differences observed between the two sectors, independently of the climatic and topographic gradients. The species composition of the secondary forest types identified in this study reflects not only current environmental gradients but also centuries of forest management practices. Coppicing of beech and chestnut in the Piedmont valleys, selective favouring of Norway spruce by alpine silviculture, and pastoral maintenance of larch-dominated stands are all well-documented practices that have durably shaped current forest composition independently of climatic and topographic conditions (Hermy and Verheyen, 2007; Motta and Nola, 2001; Nocentini, 2009).

Beyond the variables that could not be included, a further limitation concerns the interpretation of one of the key predictors retained in the analysis, the elevation. Although elevation was retained as the single dominant predictor (64.5% of total variable importance), its integrative nature makes it difficult to separate the individual contributions of the co-varying factors it encompasses. Elevation is indeed strongly correlated with climatic variables such as mean annual temperature, growing season length and snow cover duration, but it also co-varies with historical land-use patterns: agricultural and pastoral activities have been abandoned earlier and more extensively at higher elevations. Therefore, the importance attributed to elevation in the Random Forest analysis reflects a bundle of climatic, topographic and historical signals rather than a purely thermal driver. This limitation is common to all studies relying on elevation as a synthetic predictor in mountain ecosystems and does not invalidate the results but calls for caution when attributing the observed forest type distribution to climate alone.

Another limitation of this study is the presence of some sampling biases. Indeed, the sampling protocol was restricted to accessible sites by foot, excluding plots on slopes steeper than 30° and located far from existing trails. This led to an under-representation of remote and steep areas, where secondary succession dynamics are also occurring. Those areas can offer different ecological conditions that may present forest types not captured by the dataset of this study. Those areas are often places of treeline upshift and therefore places of early successional stages with newly-established forests in high altitudes. The low number of sampling plots in c6 (n = 11) and c7 (n = 12) (both all located in the Piedmont sector of the GPNP) can reduce the statistical robustness of their characterisation. An outlier within those clusters can have a major impact on the mean and standard deviation calculated. Within the RF analysis, it can impair the classifier's ability to accurately predict their membership.

One last major limitation identified in this study is that the dataset represents a single period. The successional trajectories such as with clusters c4, c5 and c1 are inferred from interpretation of the results rather than directly observed through repeated measurements.

7.2. Prospects

The results of this master's thesis open several areas for methodological improvement in future research on secondary succession dynamics. The identification of the major limitations makes it possible to develop concrete recommendations regarding the optimal experimental approaches to be adopted in the GPNP.

First, the absence of soil measurement at the plot scale is the most accessible improvement for future studies. Integrating plot-level soil measurements (pH, texture, organic matter content) would allow testing the relative contribution of edaphic versus climatic drivers to secondary forest diversity across the full extent of the GPNP. Second, the integration of the historical management of the plots would make it possible to quantify the relative contribution of forest management legacies to current species composition, independently of the climatic and topographic gradients captured in this study. Third, a denser sampling effort in the Piedmont sector could improve the robustness and the characterisation of the two clusters c6 and c7 and capture the full range of variability within these forest types. Finally, the successional trajectories proposed in this work remain inferred from the results rather than directly observed. Permanent plot monitoring through repeated inventories of representative plots from each cluster, combined with the collection of precise abandonment dates would allow directly testing these trajectories and quantifying the rates of successional change across the different climatic and topographic contexts of the GPNP.

After the prospects at the GPNP scale, this work could be extended to large areas, extending as far as the Alps. The ecological filters identified in this study offer a first understanding of the secondary forest diversity across the Alpine region, but the weight of those filters is likely to vary across the different sectors of the Alps. Replicating the methodology of this study in other National Parks such as the Stelvio National Park in Italy, Mercantour and Vanoise National Park in France, or the National Park Berchtesgaden in Germany would allow testing the generality of the patterns identified and building a comparative framework for secondary forest diversity across the western and central Alps. As temperatures are predicted to severely rise as a result of ongoing climate changes in the Alps, the upper limits of the broadleaved species may be at higher altitudes and potentially changing the primary climatic filter identified. A long-term monitoring of some selected plots to follow these changes would provide valuable empirical data on the pace and direction of these transformations in one of the most biogeographically diverse protected areas of the western Italian Alps.

This study serves as a starting point for identifying the different types of secondary forests in the Alps and the environmental factors that determine this diversity. Whilst certain patterns have been identified, much further research is needed to understand the various dynamics of secondary succession in the Alps.

References

Alberti, G., Peressotti, A., Piussi, P., Zerbi, G., 2009. Structure and stand development of secondary forests in Eastern Prealps (Italy). Dendrochronologia 27, 173–181. https://doi.org/10.1016/j.dendro.2008.02.002

Alberti, G., Peressotti, A., Piussi, P., Zerbi, G., 2008. Forest ecosystem carbon accumulation during a secondary succession in the Eastern Prealps of Italy. For. Int. J. For. Res. 81, 1–11. https://doi.org/10.1093/forestry/cpm026

Anselmetto, N., Sibona, E.M., Meloni, F., Gagliardi, L., Bocca, M., Garbarino, M., 2022. Land Use Modeling Predicts Divergent Patterns of Change Between Upper and Lower Elevations in a Subalpine Watershed of the Alps. Ecosystems 25, 1295–1310. https://doi.org/10.1007/s10021-021-00716-7

Anselmetto, N., Weisberg, P.J., Garbarino, M., 2024. Global change in the European Alps: A century of post-abandonment natural reforestation at the landscape scale. Landsc. Urban Plan. 243, 104973. https://doi.org/10.1016/j.landurbplan.2023.104973

Auer, I., Böhm, R., Jurkovic, A., Lipa, W., Orlik, A., Potzmann, R., Schöner, W., Ungersböck, M., Matulla, C., Briffa, K., Jones, P., Efthymiadis, D., Brunetti, M., Nanni, T., Maugeri, M., Mercalli, L., Mestre, O., Moisselin, J.-M., Begert, M., Müller-Westermeier, G., Kveton, V., Bochnicek, O., Stastny, P., Lapin, M., Szalai, S., Szentimrey, T., Cegnar, T., Dolinar, M., Gajic-Capka, M., Zaninovic, K., Majstorovic, Z., Nieplova, E., 2007. HISTALP—historical instrumental climatological surface time series of the Greater Alpine Region. Int. J. Climatol. 27, 17–46. https://doi.org/10.1002/joc.1377

Bani, L., Luppi, M., Rocchia, E., Dondina, O., Orioli, V., 2019. Winners and losers: How the elevational range of breeding birds on Alps has varied over the past four decades due to climate and habitat changes. Ecol. Evol. 9, 1289–1305. https://doi.org/10.1002/ece3.4838

Bartha, S., Canullo, R., Chelli, S., Campetella, G., 2020. Unimodal Relationships of Understory Alpha and Beta Diversity along Chronosequence in Coppiced and Unmanaged Beech Forests. Diversity 12, 101. https://doi.org/10.3390/d12030101

Baumann, E., Weiser, F., Chiarucci, A., Jentsch, A., Dengler, J., 2016. Diversity and functional composition of alpine grasslands along an elevational transect in the Gran Paradiso National Park (NW Italy). https://doi.org/10.14471/2016.36.015

Bebi, P., Kulakowski, D., Rixen, C., 2009. Snow avalanche disturbances in forest ecosystems-State of research and implications for management. For. Ecol. Manag. 257, 1883–1892. https://doi.org/10.1016/j.foreco.2009.01.050

Bebi, P., Seidl, R., Motta, R., Fuhr, M., Firm, D., Krumm, F., Conedera, M., Ginzler, C., Wohlgemuth, T., Kulakowski, D., 2017. Changes of forest cover and disturbance regimes in the mountain forests of the Alps. For. Ecol. Manag., Ecology of Mountain Forest Ecosystems in Europe 388, 43–56. https://doi.org/10.1016/j.foreco.2016.10.028

Becker, M., Schratz, P., Lang, M., Bischl, B., Zobolas, J., 2025. mlr3fselect: Feature Selection for "mlr3."

Bennett, J.A., Maherali, H., Reinhart, K.O., Lekberg, Y., Hart, M.M., Klironomos, J., 2017. Plant-soil feedbacks and mycorrhizal type influence temperate forest population dynamics. Science 355, 181–184. https://doi.org/10.1126/science.aai8212

Bernier, N., Ponge, J.F., 1994. Humus form dynamics during the sylvogenetic cycle in a mountain spruce forest. Soil Biol. Biochem. 26, 183–220. https://doi.org/10.1016/0038-0717(94)90161-9

Bita-Nicolae, C., Yildiz, F., Kaya, O., 2023. Exploring the Biodiversity and Conservation Value of Alpine Grasslands in the Bucegi Massif, Romanian Carpathians. Sustainability 15, 12643. https://doi.org/10.3390/su151612643

Bohner, A., Karrer, J., Walcher, R., Brandl, D., Michel, K., Arnberger, A., Frank, T., Zaller, J.G., 2019. Ecological responses of semi-natural grasslands to abandonment: case studies in three mountain regions in the Eastern Alps. Folia Geobot. 54, 211–225. https://doi.org/10.1007/s12224-019-09355-2

Bohner, A., Starlinger, F., Koutecky, P., 2012. Vegetation changes in an abandoned montane grassland, compared to changes in a habitat with low-intensity sheep grazing – a case study in Styria, Austria. Ecomont J. Prot. Mt. Areas Res. 4, 5–12. https://doi.org/10.1553/eco.mont-4-2s5

Borcard, D., Gillet, F., Legendre, P., 2018. Numerical Ecology with R, Use R! Springer International Publishing, Cham. https://doi.org/10.1007/978-3-319-71404-2

Botero, C.A., Dor, R., McCain, C.M., Safran, R.J., 2014. Environmental harshness is positively correlated with intraspecific divergence in mammals and birds. Mol. Ecol. 23, 259–268. https://doi.org/10.1111/mec.12572

Breiman, L., 2001. Random Forests. Mach. Learn. 45, 5–32. https://doi.org/10.1023/A:1010933404324

Brun, P., Zimmermann, N.E., Hari, C., Pellissier, L., Karger, D.N., 2022. CHELSA-BIOCLIM+ A novel set of global climate-related predictors at kilometre-resolution. https://doi.org/10.16904/ENVIDAT.332

Brunetti, M., Lentini, G., Maugeri, M., Nanni, T., Simolo, C., Spinoni, J., 2009. 1961–1990 high-resolution Northern and Central Italy monthly precipitation climatologies, in: Advances in Science and Research. Presented at the 8th EMS Annual Meeting and 7th European Conference on Applied Climatology 2008 -, Copernicus GmbH, pp. 73–78. https://doi.org/10.5194/asr-3-73-2009

Campagnaro, T., Brundu, G., Sitzia, T., 2018. Five major invasive alien tree species in European Union forest habitat types of the Alpine and Continental biogeographical regions. J. Nat. Conserv. 43, 227–238. https://doi.org/10.1016/j.jnc.2017.07.007

Caso, F., Nerone, S., Petroccia, A., Bonasera, M., 2021. Geology of the southern Gran Paradiso Massif and Lower Piedmont Zone contact area (middle Ala Valley, Western Alps, Italy). J. Maps 17, 237–246. https://doi.org/10.1080/17445647.2021.1911869

Chan, W.-P., Lenoir, J., Mai, G.-S., Kuo, H.-C., Chen, I.-C., Shen, S.-F., 2024. Climate velocities and species tracking in global mountain regions. Nature 629, 114–120. https://doi.org/10.1038/s41586-024-07264-9

Chazdon, R.L., Lindenmayer, D., Guariguata, M.R., Crouzeilles, R., Rey Benayas, J.M., Lazos Chavero, E., 2020. Fostering natural forest regeneration on former agricultural land through economic and policy interventions. Environ. Res. Lett. 15, 043002. https://doi.org/10.1088/1748-9326/ab79e6

Clark, A.T., Knops, J.M.H., Tilman, D., 2019. Contingent factors explain average divergence in functional composition over 88 years of old field succession. J. Ecol. 107, 545–558. https://doi.org/10.1111/1365-2745.13070

Clements, F.E. (Frederic E., 1916. Plant succession; an analysis of the development of vegetation. Washington, Carnegie Institution of Washington.

Connell, J.H., Slatyer, R.O., 1977. Mechanisms of Succession in Natural Communities and Their Role in Community Stability and Organization. Am. Nat. 111, 1119–1144. https://doi.org/10.1086/283241

Crawford, C.L., Yin, H., Radeloff, V.C., Wilcove, D.S., 2022. Rural land abandonment is too ephemeral to provide major benefits for biodiversity and climate. Sci. Adv. 8, eabm8999. https://doi.org/10.1126/sciadv.abm8999

Cutler, D.R., Edwards Jr., T.C., Beard, K.H., Cutler, A., Hess, K.T., Gibson, J., Lawler, J.J., 2007. Random Forests for Classification in Ecology. Ecology 88, 2783–2792. https://doi.org/10.1890/07-0539.1

D'Amico, M., Pintaldi, E., Sapino, E., Colombo, N., Quaglino, E., Stanchi, S., Navillod, E., Rocco, R., Freppaz, M., 2020. Soil types of Aosta Valley. J. Maps 16, 755–765. https://doi.org/10.1080/17445647.2020.1821803

Dax, T., Schroll, K., Machold, I., Derszniak-Noirjean, M., Schuh, B., Gaupp-Berghausen, M., 2021. Land Abandonment in Mountain Areas of the EU: An Inevitable Side Effect of Farming Modernization and Neglected Threat to Sustainable Land Use. Land 10, 591. https://doi.org/10.3390/land10060591

De Frenne, P., Baeten, L., Graae, B.J., Brunet, J., Wulf, M., Orczewska, A., Kolb, A., Jansen, I., Jamoneau, A., Jacquemyn, H., Hermy, M., Diekmann, M., De Schrijver, A., De Sanctis, M., Decocq, G., Cousins, S.A.O., Verheyen, K., 2011. Interregional variation in the floristic recovery of post-agricultural forests. J. Ecol. 99, 600–609. https://doi.org/10.1111/j.1365-2745.2010.01768.x

De Frenne, P., Zellweger, F., Rodríguez-Sánchez, F., Scheffers, B.R., Hylander, K., Luoto, M., Vellend, M., Verheyen, K., Lenoir, J., 2019. Global buffering of temperatures under forest canopies. Nat. Ecol. Evol. 3, 744–749. https://doi.org/10.1038/s41559-019-0842-1

De Giuli, M., Winkler, M., Deola, T., Henschel, J., Sass, O., Wolff, P., Jentsch, A., 2024. Arrested Succession on Fire-Affected Slopes in the Krummholz Zone and Subalpine Forest of the Northern Limestone Alps. Diversity 16, 366. https://doi.org/10.3390/d16070366

De Reu, J., Bourgeois, J., Bats, M., Zwertvaegher, A., Gelorini, V., De Smedt, P., Chu, W., Antrop, M., De Maeyer, P., Finke, P., Van Meirvenne, M., Verniers, J., Crombé, P., 2013. Application of the topographic position index to heterogeneous landscapes. Geomorphology 186, 39–49. https://doi.org/10.1016/j.geomorph.2012.12.015

Decocq, G., Houet, T., Cevasco, R., Chauchard, S., de Conférences, M., Nancy, U., Gauquelin, T., Univ, A.-M., Tatoni, T., Univ, A.-M., Bergès, L., 2018. Historical ecology of Mediterranean forests: drivers of forest cover change and effects of past land use on current soils and vegetation.

Dziomber, I., Gobet, E., Leunda, M., Gurtner, L., Vogel, H., Tournier, N., Damanik, A., Szidat, S., Tinner, W., Schwörer, C., 2024. Palaeoecological multiproxy reconstruction captures long-term climatic and anthropogenic impacts on vegetation dynamics in the Rhaetian Alps. Rev. Palaeobot. Palynol. 321, 105020. https://doi.org/10.1016/j.revpalbo.2023.105020

Egarter Vigl, L., Tasser, E., Schirpke, U., Tappeiner, U., 2017. Using land use/land cover trajectories to uncover ecosystem service patterns across the Alps. Reg. Environ. Change 17, 2237–2250. https://doi.org/10.1007/s10113-017-1132-6

Ellis, E.C., Kaplan, J.O., Fuller, D.Q., Vavrus, S., Klein Goldewijk, K., Verburg, P.H., 2013. Used planet: A global history. Proc. Natl. Acad. Sci. 110, 7978–7985. https://doi.org/10.1073/pnas.1217241110

Facelli, J.M., Pickett, S.T.A., 1991. Plant litter: Its dynamics and effects on plant community structure. Bot. Rev. 57, 1–32. https://doi.org/10.1007/BF02858763

FAO (Ed.), 2006. Food aid for food security?, The state of food and agriculture. FAO, Rome.

FAO, 2000. Global forest resources assessment. 2000. FAO forestry paper.

Ferretti, F., Sboarina, C., Tattoni, C., Vitti, A., Zatelli, P., Geri, F., Pompei, E., Ciolli, M., 2018. The 1936 Italian Kingdom Forest Map reviewed: a dataset for landscape and ecological research. Ann. Silvic. Res. 42. https://doi.org/10.12899/asr-1411

Finegan, B., 1984. Forest succession. Nature 312, 109–114. https://doi.org/10.1038/312109a0

Flinn, K.M., Marks, P.L., 2007. Agricultural Legacies in Forest Environments: Tree Communities, Soil Properties, and Light Availability. Ecol. Appl. 17, 452–463. https://doi.org/10.1890/05-1963

Foster, D., Swanson, F., Aber, J., Burke, I., Brokaw, N., Tilman, D., Knapp, A., 2003. The Importance of Land-Use Legacies to Ecology and Conservation. BioScience 53, 77. https://doi.org/10.1641/0006-3568(2003)053%5B0077:TIOLUL%5D2.0.CO;2

Franklin, J.F., Lindenmayer, D., MacMahon, J.A., McKee, A., Magnuson, J., Perry, D.A., Waide, R., Foster, D., 2000. Threads of Continuity: There are immense differences between even-aged silvicultural disturbances (especially clearcutting) and natural disturbances, such as windthrow, wildfire, and even volcanic eruptions. Conserv. Pract. 1, 8–17. https://doi.org/10.1111/j.1526-4629.2000.tb00155.x

Gafur, A., Jensen, J.R., Borggaard, O.K., Petersen, L., 2003. Runoff and losses of soil and nutrients from small watersheds under shifting cultivation (Jhum) in the Chittagong Hill Tracts of Bangladesh. J. Hydrol. 274, 30–46. https://doi.org/10.1016/S0022-1694(02)00351-7

Garbarino, M., Lingua, E., Subira, M., Motta, R., 2011. The larch wood pasture: Structure and dynamics of a cultural landscape. Eur. J. For. Res. 130, 491–502. https://doi.org/10.1007/s10342-010-0437-5

Garbarino, M., Lingua, E., Weisberg, P.J., Bottero, A., Meloni, F., Motta, R., 2013. Land-use history and topographic gradients as driving factors of subalpine Larix decidua forests. Landsc. Ecol. 28, 805–817. https://doi.org/10.1007/s10980-012-9792-6

Garbarino, M., Morresi, D., Urbinati, C., Malandra, F., Motta, R., Sibona, E.M., Vitali, A., Weisberg, P.J., 2020. Contrasting land use legacy effects on forest landscape dynamics in the Italian Alps and the Apennines. Landsc. Ecol. 35, 2679–2694. https://doi.org/10.1007/s10980-020-01013-9

Gavrichkova, O., Pretto, G., Brugnoli, E., Chiti, T., Ivashchenko, K.V., Mattioni, M., Moscatelli, M.C., Scartazza, A., Calfapietra, C., 2022. Consequences of Grazing Cessation for Soil Environment and Vegetation in a Subalpine Grassland Ecosystem. Plants 11, 2121. https://doi.org/10.3390/plants11162121

Gehrig-Fasel, J., Guisan, A., Zimmermann, N.E., 2007. Tree line shifts in the Swiss Alps: Climate change or land abandonment? J. Veg. Sci. 18, 571–582. https://doi.org/10.1111/j.1654-1103.2007.tb02571.x

Gelabert, P.J., Rodrigues, M., Vidal-Macua, J.J., Ameztegui, A., Vega-Garcia, C., 2022. Spatially explicit modeling of the probability of land abandonment in the Spanish Pyrenees. Landsc. Urban Plan. 226, 104487. https://doi.org/10.1016/j.landurbplan.2022.104487

Gerhardt, F., Foster, D.R., 2002. Physiographical and historical effects on forest vegetation in central New England, USA. J. Biogeogr. 29, 1421–1437. https://doi.org/10.1046/j.1365-2699.2002.00763.x

Gilck, F., Poschlod, P., 2021. The history of human land use activities in the Northern Alps since the Neolithic Age. A reconstruction of vegetation and fire history in the Mangfall Mountains (Bavaria, Germany). The Holocene 31, 579–591. https://doi.org/10.1177/0959683620981701

Gobiet, A., Kotlarski, S., Beniston, M., Heinrich, G., Rajczak, J., Stoffel, M., 2014. 21st century climate change in the European Alps—A review. Sci. Total Environ. 493, 1138–1151. https://doi.org/10.1016/j.scitotenv.2013.07.050

Gontier, A., 2026. Newly-established forests in the Aosta Valley side of the Gran Paradiso National Park: structural and compositional characterisation (Master's thesis). Università degli Studi di Torino, Turin, Italy.

Gran Paradiso National Park | Alps, Wildlife, Nature | Britannica [WWW Document], n.d. URL https://www.britannica.com/place/Gran-Paradiso-National-Park (accessed 2.10.26).

Harper, J.L., 1977. Population biology of plants. Academic Press, London ; New York.
Harsch, M.A., Hulme, P.E., McGlone, M.S., Duncan, R.P., 2009. Are treelines advancing? A global meta-analysis of treeline response to climate warming. Ecol. Lett. 12, 1040–1049. https://doi.org/10.1111/j.1461-0248.2009.01355.x
Hermy, M., Honnay, O., Firbank, L., Grashof-Bokdam, C., Lawesson, J.E., 1999. An ecological comparison between ancient and other forest plant species of Europe, and the implications for forest conservation. Biol. Conserv. 91, 9–22. https://doi.org/10.1016/S0006-3207(99)00045-2
Hermy, M., Verheyen, K., 2007. Legacies of the past in the present-day forest biodiversity: a review of past land-use effects on forest plant species composition and diversity. Ecol. Res. 22, 361–371. https://doi.org/10.1007/s11284-007-0354-3
Hesselbarth, M., Sciaini, M., With, K., Wiegand, K., Nowosad, J., 2019. landscapemetrics : an open-source R tool to calculate landscape metrics. Ecography 42, 1648–1657. https://doi.org/10.1111/ecog.04617
Hijmans, R.J., Brown, A., Barbosa, M., 2020. terra: Spatial Data Analysis. https://doi.org/10.32614/CRAN.package.terra
Histoire [WWW Document], n.d. URL https://www.pngp.it/fr/visitez-le-parc/histoire-old (accessed 2.10.26).
Hoffmann, S., Steiner, L., Schweiger, A.H., Chiarucci, A., Benner, J., Provenzale, A., Beierkuhnlein, C., 2019. Data on alpine grassland diversity in Gran Paradiso National Park, Italy. Data Brief 24, 103942. https://doi.org/10.1016/j.dib.2019.103942
Honnay, O., Hermy, M., Coppin, P., 1999. Impact of habitat quality on forest plant species colonization. For. Ecol. Manag. 115, 157–170. https://doi.org/10.1016/S0378-1127(98)00396-X
Hunsaker, C.T., Levine, D.A., 1995. Hierarchical Approaches to the Study of Water Quality in Rivers. BioScience 45, 193–203. https://doi.org/10.2307/1312558
Jackson, D.A., 1993. Stopping Rules in Principal Components Analysis: A Comparison of Heuristical and Statistical Approaches. Ecology 74, 2204–2214. https://doi.org/10.2307/1939574
Jactel, H., Bauhus, J., Boberg, J., Bonal, D., Castagneyrol, B., Gardiner, B., Gonzalez-Olabarria, J.R., Koricheva, J., Meurisse, N., Brockerhoff, E.G., 2017. Tree Diversity Drives Forest Stand Resistance to Natural Disturbances. Curr. For. Rep. 3, 223–243. https://doi.org/10.1007/s40725-017-0064-1
Jakovac, C.C., Junqueira, A.B., Crouzeilles, R., Peña-Claros, M., Mesquita, R.C.G., Bongers, F., 2021. The role of land-use history in driving successional pathways and its implications for the restoration of tropical forests. Biol. Rev. 96, 1114–1134. https://doi.org/10.1111/brv.12694
Karger, D.N., Conrad, O., Böhner, J., Kawohl, T., Kreft, H., Soria-Auza, R.W., Zimmermann, N.E., Linder, H.P., Kessler, M., 2017a. Climatologies at high resolution for the earth's land surface areas. Sci. Data 4, 170122. https://doi.org/10.1038/sdata.2017.122
Karger, D.N., Conrad, O., Böhner, J., Kawohl, T., Kreft, H., Soria-Auza, R.W., Zimmermann, N.E., Linder, H.P., Kessler, M., 2017b. Climatologies at high resolution for the earth's land surface areas. Sci. Data 4, 170122. https://doi.org/10.1038/sdata.2017.122
Knüsel, S., Conedera, M., Rigling, A., Fonti, P., Wunder, J., 2015. A tree-ring perspective on the invasion of *Ailanthus altissima* in protection forests. For. Ecol. Manag. 354, 334–343. https://doi.org/10.1016/j.foreco.2015.05.010
Koerner, W., Dambrine, E., Dupouey, J.L., Benoît, M., 1999. δ 15 N of forest soil and understorey vegetation reflect the former agricultural land use. Oecologia 121, 421–425. https://doi.org/10.1007/s004420050947

Kopecký, M., Macek, M., Wild, J., 2021. Topographic Wetness Index calculation guidelines based on measured soil moisture and plant species composition. Sci. Total Environ. 757, 143785. https://doi.org/10.1016/j.scitotenv.2020.143785

Körner, C., 2007. The use of 'altitude' in ecological research. Trends Ecol. Evol. 22, 569–574. https://doi.org/10.1016/j.tree.2007.09.006

Kuhn, M., 2008. Building Predictive Models in *R* Using the **caret** Package. J. Stat. Softw. 28. https://doi.org/10.18637/jss.v028.i05

Kulakowski, D., Bebi, P., Rixen, C., 2010. The interacting effects of land use change, climate change and suppression of natural disturbances on landscape forest structure in the Swiss Alps. Oikos 120, 216–225. https://doi.org/10.1111/j.1600-0706.2010.18726.x

Kutschera, W., Patzelt, G., Wild, E.M., Haas-Jettmar, B., Kofler, W., Lippert, A., Oeggl, K., Pak, E., Priller, A., Steier, P., Wahlmüller-Oeggl, N., Zanesco, A., 2014. Evidence for Early Human Presence at High Altitudes in the Ötztal Alps (Austria/Italy). Radiocarbon 56, 923–947. https://doi.org/10.2458/56.17919

Lang, M., Binder, M., Richter, J., Schratz, P., Pfisterer, F., Coors, S., Au, Q., Casalicchio, G., Kotthoff, L., Bischl, B., 2019. mlr3: A modern object-oriented machine learning framework in R. J. Open Source Softw. 4, 1903. https://doi.org/10.21105/joss.01903

Lanta, V., Mudrák, O., Dvorský, M., Bartoš, M., Šebek, P., Čížek, L., Doležal, J., 2023. Multifaceted diversity changes reveal community assembly mechanisms during early stages of post-logging forest succession. Plant Ecol. 224, 335–347. https://doi.org/10.1007/s11258-023-01306-4

Larson, J., Lidberg, W., Ågren, A.M., Laudon, H., 2022. Predicting soil moisture conditions across a heterogeneous boreal catchment using terrain indices. Hydrol. Earth Syst. Sci. 26, 4837–4851. https://doi.org/10.5194/hess-26-4837-2022

Lavorel, S., Grigulis, K., Leitinger, G., Kohler, M., Schirpke, U., Tappeiner, U., 2019. Historical trajectories in land use pattern and grassland ecosystem services in two European alpine landscapes. Reg. Environ. Change 17, 2251–2264. https://doi.org/10.1007/s10113-017-1207-4

Lavorel, S., Grigulis, K., Leitinger, G., Kohler, M., Schirpke, U., Tappeiner, U., 2017. Historical trajectories in land use pattern and grassland ecosystem services in two European alpine landscapes. Reg. Environ. Change 17, 2251–2264. https://doi.org/10.1007/s10113-017-1207-4

Lazzaro, L., Mazza, G., d'Errico, G., Fabiani, A., Giuliani, C., Inghilesi, A.F., Lagomarsino, A., Landi, S., Lastrucci, L., Pastorelli, R., Roversi, P.F., Torrini, G., Tricarico, E., Foggi, B., 2018. How ecosystems change following invasion by *Robinia pseudoacacia*: Insights from soil chemical properties and soil microbial, nematode, microarthropod and plant communities. Sci. Total Environ. 622–623, 1509–1518. https://doi.org/10.1016/j.scitotenv.2017.10.017

Legendre, P., Legendre, L., 2012. Numerical ecology, Third English edition. ed, Developments in environmental modelling. Elsevier, Amsterdam.

Leuschner, C., Ellenberg, H., 2017. Ecology of Central European Forests: Vegetation Ecology of Central Europe, Volume I. Springer International Publishing, Cham. https://doi.org/10.1007/978-3-319-43042-3

Lindborg, R., Eriksson, O., 2004. Effects of Restoration on Plant Species Richness and Composition in Scandinavian Semi-Natural Grasslands. Restor. Ecol. 12, 318–326. https://doi.org/10.1111/j.1061-2971.2004.00334.x

MacDonald, D., Crabtree, J.R., Wiesinger, G., Dax, T., Stamou, N., Fleury, P., Gutierrez Lazpita, J., Gibon, A., 2000. Agricultural abandonment in mountain areas of Europe: Environmental consequences and policy response. J. Environ. Manage. 59, 47–69. https://doi.org/10.1006/jema.1999.0335

Malandra, F., Vitali, A., Urbinati, C., Weisberg, P.J., Garbarino, M., 2019. Patterns and drivers of forest landscape change in the Apennines range, Italy. Reg. Environ. Change 19, 1973–1985. https://doi.org/10.1007/s10113-019-01531-6

Marengo, G., Anselmetto, N., Barberis, D., Lombardi, G., Lonati, M., Garbarino, M., 2025. Land-use legacy drives post-abandonment forest structure and understory in the western Alps. Landsc. Urban Plan. 259, 105357. https://doi.org/10.1016/j.landurbplan.2025.105357

Marzano, R., Garbarino, M., Marcolin, E., Pividori, M., Lingua, E., 2013. Deadwood anisotropic facilitation on seedling establishment after a stand-replacing wildfire in Aosta Valley (NW Italy). Ecol. Eng. 51, 117–122. https://doi.org/10.1016/j.ecoleng.2012.12.030

Marzini, S., Tasser, E., Wellstein, C., Albrich, K., Rammer, W., Mina, M., 2025. Future expansion of upper forest-grassland ecotone under land-use and climate change in the Eastern Alps. Landsc. Ecol. 40, 55. https://doi.org/10.1007/s10980-025-02070-8

Mather, A.S., 1992. The Forest Transition. Area 24, 367–379.

Mather, A.S., Fairbairn, J., Needle, C.L., 1999. The course and drivers of the forest transition: The case of France. J. Rural Stud. 15, 65–90. https://doi.org/10.1016/S0743-0167(98)00023-0

Maxwell, A.E., Shobe, C.M., 2022. Land-surface parameters for spatial predictive mapping and modeling. Earth-Sci. Rev. 226, 103944. https://doi.org/10.1016/j.earscirev.2022.103944

McCune, B., Mefford, M.J., 2016. PC-ORD: Multivariate Analysis of Ecological Data, Version 7.0 for Windows. Corvallis, Oregon, U.S.A.

McElhinny, C., Gibbons, P., Brack, C., 2006. An objective and quantitative methodology for constructing an index of stand structural complexity. For. Ecol. Manag. 235, 54–71. https://doi.org/10.1016/j.foreco.2006.07.024

McElhinny, C., Gibbons, P., Brack, C., Bauhus, J., 2005. Forest and woodland stand structural complexity: Its definition and measurement. For. Ecol. Manag. 218, 1–24. https://doi.org/10.1016/j.foreco.2005.08.034

Meli, P., Holl, K.D., Benayas, J.M.R., Jones, H.P., Jones, P.C., Montoya, D., Mateos, D.M., 2017. A global review of past land use, climate, and active vs. passive restoration effects on forest recovery. PLOS ONE 12, e0171368. https://doi.org/10.1371/journal.pone.0171368

Mietkiewicz, N., Kulakowski, D., Rogan, J., Bebi, P., 2017. Long-term change in sub-alpine forest cover, tree line and species composition in the Swiss Alps. J. Veg. Sci. 28, 951–964. https://doi.org/10.1111/jvs.12561

Molnar, C., 2018. iml: An R package for Interpretable Machine Learning. J. Open Source Softw. 3, 786. https://doi.org/10.21105/joss.00786

Monteiro, A.T., Fava, F., Hiltbrunner, E., Della Marianna, G., Bocchi, S., 2011. Assessment of land cover changes and spatial drivers behind loss of permanent meadows in the lowlands of Italian Alps. Landsc. Urban Plan. 100, 287–294. https://doi.org/10.1016/j.landurbplan.2010.12.015

Morgese, S., Casale, F., Movedi, E., Confalonieri, R., Bocchiola, D., 2024. Modelling the effects of potential climate change on the dynamics of multi-species mountain pastures: A case study in Gran Paradiso National Park, Italy. Agric. Syst. 217, 103942. https://doi.org/10.1016/j.agsy.2024.103942

Moser, D., Dullinger, S., Englisch, T., Niklfeld, H., Plutzar, C., Sauberer, N., Zechmeister, H.G., Grabherr, G., 2005. Environmental determinants of vascular plant species richness in the Austrian Alps. J. Biogeogr. 32, 1117–1127. https://doi.org/10.1111/j.1365-2699.2005.01265.x

Motta, R., Berretti, R., Lingua, E., Piussi, P., 2006. Coarse woody debris, forest structure and regeneration in the Valbona Forest Reserve, Paneveggio, Italian Alps. For. Ecol. Manag. 235, 155–163. https://doi.org/10.1016/j.foreco.2006.08.007

Motta, R., Lingua, E., 2005. Human impact on size, age, and spatial structure in a mixed European larch and Swiss stone pine forest in the Western Italian Alps. Can. J. For. Res. 35, 1809–1820. https://doi.org/10.1139/x05-107

Motta, R., Nola, P., 2001. Growth trends and dynamics in sub-alpine forest stands in the Varaita Valley (Piedmont, Italy) and their relationships with human activities and global change. J. Veg. Sci. 12, 219–230. https://doi.org/10.2307/3236606

Muigg, B., Haneca, K., Tegel, W., Grünewald, M., Bernard, V., Bleicher, N., Blondel, F., Bolliger, M., Broich, M., Couturier, Y., van Daalen, S., Domínguez-Delmás, M., Girardclos, O., Herzig, F., Langenegger, F., Le Digol, Y., Nelle, O., Nicolussi, K., Oberhänsli, M., Perrault, C., Rzepecki, A., Vorst, Y., Weidemüller, J., Westphal, T., Seim, A., 2025. Woodlands of Antiquity: A millennium of dendrochronological data on forest exploitation and timber economy between the Alps and the Atlantic. Proc. Natl. Acad. Sci. 122, e2516240122. https://doi.org/10.1073/pnas.2516240122

Munroe, D.K., van Berkel, D.B., Verburg, P.H., Olson, J.L., 2013. Alternative trajectories of land abandonment: causes, consequences and research challenges. Curr. Opin. Environ. Sustain., Human settlements and industrial systems 5, 471–476. https://doi.org/10.1016/j.cosust.2013.06.010

Murtagh, F., Legendre, P., 2014. Ward's Hierarchical Agglomerative Clustering Method: Which Algorithms Implement Ward's Criterion? J. Classif. 31, 274–295. https://doi.org/10.1007/s00357-014-9161-z

Nocentini, S., 2009. Structure and management of beech (Fagus sylvatica L.) forests in Italy. IForest - Biogeosciences For. 2, 105–113. https://doi.org/10.3832/ifor0499-002

Oliver, C.D., Larson, B.C., 1996. Forest stand dynamics, Update ed. ed. Wiley, New York.

Otero, I., Marull, J., Tello, E., Diana, G.L., Pons, M., Coll, F., Boada, M., 2015. Land abandonment, landscape, and biodiversity: questioning the restorative character of the forest transition in the Mediterranean. Ecol. Soc. 20.

Parco Nazionale Gran Paradiso: L'Espace Protégé [WWW Document], n.d. URL https://www.parks.it/parco.nazionale.gran.paradiso/Fpar.php?utm_source=chatgpt.com (accessed 2.19.26).

Parisi, A., di Valdengo, F.A., Baneschi, I., Baronetti, A., Boiani, M.V., Catania, M., Lenzi, S., Magnani, M., Mosca, P., Provenzale, A., Raco, B., Vivaldo, G., Giamberini, M., 2024. Carbon dioxide fluxes in Alpine grasslands at the Nivolet Plain, Gran Paradiso National Park, Italy 2017–2023. Sci. Data 11, 652. https://doi.org/10.1038/s41597-024-03374-1

Pedersen, N.K., Schmidt, I.K., Kepfer-Rojas, S., 2023. Drivers of tree colonization, species richness, and structural variation during the initial three decades of natural forest colonization in abandoned agricultural soils. For. Ecol. Manag. 543, 121138. https://doi.org/10.1016/j.foreco.2023.121138

Peel, M.C., Finlayson, B.L., McMahon, T.A., 2007. Updated world map of the Köppen-Geiger climate classification. Hydrol. Earth Syst. Sci. 11, 1633–1644. https://doi.org/10.5194/hess-11-1633-2007

Peres-Neto, P.R., Jackson, D.A., Somers, K.M., 2005. How many principal components? stopping rules for determining the number of non-trivial axes revisited. Comput. Stat. Data Anal. 49, 974–997. https://doi.org/10.1016/j.csda.2004.06.015

Perpiña Castillo, C., Jacobs-Crisioni, C., Diogo, V., Lavalle, C., 2021. Modelling agricultural land abandonment in a fine spatial resolution multi-level land-use model: An application for the EU. Environ. Model. Softw. 136, 104946. https://doi.org/10.1016/j.envsoft.2020.104946

Petitpierre, B., McDougall, K., Seipel, T., Broennimann, O., Guisan, A., Kueffer, C., 2016. Will climate change increase the risk of plant invasions into mountains? Ecol. Appl. 26, 530–544. https://doi.org/10.1890/14-1871

Pielou, E.C., 1975. Ecological diversity. Wiley, New York.

Plieninger, T., Draux, H., Fagerholm, N., Bieling, C., Bürgi, M., Kizos, T., Kuemmerle, T., Primdahl, J., Verburg, P.H., 2016. The driving forces of landscape change in Europe: A systematic review of the evidence. Land Use Policy 57, 204–214. https://doi.org/10.1016/j.landusepol.2016.04.040

Poorter, L., Amissah, L., Bongers, F., Hordijk, I., Kok, J., Laurance, S.G.W., Lohbeck, M., Martínez-Ramos, M., Matsuo, T., Meave, J.A., Muñoz, R., Peña-Claros, M., van der Sande, M.T., 2023. Successional theories. Biol. Rev. 98, 2049–2077. https://doi.org/10.1111/brv.12995

Poorter, L., Van Der Sande, M.T., Amissah, L., Bongers, F., Hordijk, I., Kok, J., Laurance, S.G.W., Martínez-Ramos, M., Matsuo, T., Meave, J.A., Muñoz, R., Peña-Claros, M., Van Breugel, M., Herault, B., Jakovac, C.C., Lebrija-Trejos, E., Norden, N., Lohbeck, M., 2024. A comprehensive framework for vegetation succession. Ecosphere 15, e4794. https://doi.org/10.1002/ecs2.4794

Pornaro, C., Schneider, M.K., Macolino, S., 2013. Plant species loss due to forest succession in Alpine pastures depends on site conditions and observation scale. Biol. Conserv. 161, 213–222. https://doi.org/10.1016/j.biocon.2013.02.019

Poussin, C., Guigoz, Y., Palazzi, E., Terzago, S., Chatenoux, B., Giuliani, G., 2019. Snow Cover Evolution in the Gran Paradiso National Park, Italian Alps, Using the Earth Observation Data Cube. Data 4, 138. https://doi.org/10.3390/data4040138

Praeg, N., Steinwandter, M., Urbach, D., Snethlage, M.A., Alves, R.P., Apple, M.E., Bilovitz, P., Britton, A.J., Bruni, E.P., Chen, T., Dumack, K., Fernandez-Mendoza, F., Freppaz, M., Frey, B., Fromin, N., Geisen, S., Grube, M., Guariento, E., Guisan, A., Ji, Q., Jiménez, J.J., Maier, S., Malard, L.A., Minor, M.A., Mc Lean, C.C., Mitchell, E.A.D., Peham, T., Pizzolotto, R., Taylor, A.F.S., Vernon, P., van Tol, J.J., Wu, D., Wu, Y., Xie, Z., Weber, B., Illmer, P., Seeber, J., 2025. Biodiversity in mountain soils above the treeline. Biol. Rev. Camb. Philos. Soc. 100, 1877–1949. https://doi.org/10.1111/brv.70028

R Core Team, 2023. R: A Language and Environment for Statistical Computing.

Rebele, F., 2013. Differential succession towards woodland along a nutrient gradient. Appl. Veg. Sci. 16, 365–378. https://doi.org/10.1111/avsc.12006

Richiardi, C., Siniscalco, C., Garbarino, M., Adamo, M., 2025. Unravelling decades of habitat dynamics in protected areas: A hierarchical approach applied to the Gran Paradiso National Park (NW Italy). Environ. Monit. Assess. 197. https://doi.org/10.1007/s10661-025-14669-0

Ridding, L.E., Watson, S.C.L., Newton, A.C., Rowland, C.S., Bullock, J.M., 2020. Ongoing, but slowing, habitat loss in a rural landscape over 85 years. Landsc. Ecol. 35, 257–273. https://doi.org/10.1007/s10980-019-00944-2

Roberts, D.R., Bahn, V., Ciuti, S., Boyce, M.S., Elith, J., Guillera-Arroita, G., Hauenstein, S., Lahoz-Monfort, J.J., Schröder, B., Thuiller, W., Warton, D.I., Wintle, B.A., Hartig, F., Dormann, C.F., 2017. Cross-validation strategies for data with temporal, spatial, hierarchical, or phylogenetic structure. Ecography 40, 913–929. https://doi.org/10.1111/ecog.02881

Roberts, N., Fyfe, R.M., Woodbridge, J., Gaillard, M.-J., Davis, B.A.S., Kaplan, J.O., Marquer, L., Mazier, F., Nielsen, A.B., Sugita, S., Trondman, A.-K., Leydet, M., 2018. Europe's lost forests: a pollen-based synthesis for the last 11,000 years. Sci. Rep. 8, 716. https://doi.org/10.1038/s41598-017-18646-7

Rochefort, R.M., Peterson, D.L., 1996. Temporal and Spatial Distribution of Trees in Subalpine Meadows of Mount Rainier National Park, Washington, U.S.A. Arct. Alp. Res. 28, 52–59. https://doi.org/10.2307/1552085

San-Miguel-Ayanz, J., De Rigo, D., Caudullo, G., Houston Durrant, T., Mauri, A., European Commission (Eds.), 2016. European atlas of forest tree species. Publications Office, Luxembourg. https://doi.org/10.2788/4251

Schliemann, S.A., Bockheim, J.G., 2011. Methods for studying treefall gaps: A review. For. Ecol. Manag. 261, 1143–1151. https://doi.org/10.1016/j.foreco.2011.01.011

Schratz, P., Becker, M., Lang, M., Brenning, A., 2021. mlr3spatiotempcv: Spatiotemporal resampling methods for machine learning in R. https://doi.org/10.48550/ARXIV.2110.12674

Schulze, E.-D., Mischì, G., Asche, G., Börner, A., 2007. Land-use history and succession of *Larix decidua* in the Southern Alps of Italy–An essay based on a cultural history study of Roswitha Asche. Flora - Morphol. Distrib. Funct. Ecol. Plants 202, 705–713. https://doi.org/10.1016/j.flora.2007.05.003

Schweizer, P.E., Matlack, G.R., 2014. Factors driving land use change and forest distribution on the coastal plain of Mississippi, USA. Landsc. Urban Plan. 121, 55–64. https://doi.org/10.1016/j.landurbplan.2013.09.003

Scridel, D., Tenan, S., Brambilla, M., Celva, R., Forti, A., Fracasso, I., Volcan, G., Dorigatti, E., Anderle, M., Marchesini, A., Crestanello, B., Vernesi, C., Pedrini, P., Partel, P., 2022. Early-succession secondary forests following agropastoral abandonment are key winter habitats for the conservation of a priority bird in the European Alps. Eur. J. For. Res. 141, 1029–1043. https://doi.org/10.1007/s10342-022-01485-1

Seidl, R., Thom, D., Kautz, M., Martin-Benito, D., Peltoniemi, M., Vacchiano, G., Wild, J., Ascoli, D., Petr, M., Honkaniemi, J., Lexer, M.J., Trotsiuk, V., Mairota, P., Svoboda, M., Fabrika, M., Nagel, T.A., Reyer, C.P.O., 2017. Forest disturbances under climate change. Nat. Clim. Change 7, 395–402. https://doi.org/10.1038/nclimate3303

Sella, L., Ragazzi, E., Francesca Silvia Rota, Maria Adamo, Andrea Scartazza, Maddalena Pennisi, 2025. Interdisciplinary Research in Critical Zone Studies: The Analysis of Land Use Change in the Italian Alps. Sci. Reg. 161–188. https://doi.org/10.14650/112148

Sitzia, T., Semenzato, P., Trentanovi, G., 2010. Natural reforestation is changing spatial patterns of rural mountain and hill landscapes: A global overview. For. Ecol. Manag. 259, 1354–1362. https://doi.org/10.1016/j.foreco.2010.01.048

Smit, R., Olff, H., 1998. Woody species colonisation in relation to habitat productivity. Plant Ecol. 139, 203–209. https://doi.org/10.1023/A:1009750216223

Snell, R.S., Peringer, A., Frank, V., Bugmann, H., 2022. Management-based mitigation of the impacts of climate-driven woody encroachment in high elevation pasture woodlands. J. Appl. Ecol. 59, 1925–1936. https://doi.org/10.1111/1365-2664.14199

Souto, C., Pellissier, F., Chiapusio, G., 2000. Allelopathic Effects of Humus Phenolics on Growth and Respiration of Mycorrhizal Fungi. J. Chem. Ecol. 26, 2015–2023. https://doi.org/10.1023/A:1005551912405

Statuto, D., Cillis, G., Picuno, P., 2017. Using Historical Maps within a GIS to Analyze Two Centuries of Rural Landscape Changes in Southern Italy. Land 6, 65. https://doi.org/10.3390/land6030065

Taillefumier, F., Piégay, H., 2003. Contemporary land use changes in prealpine Mediterranean mountains: a multivariate GIS-based approach applied to two municipalities in the Southern French Prealps. CATENA, Geomorphic Responses to Land Use Changes 51, 267–296. https://doi.org/10.1016/S0341-8162(02)00168-6

Tappeiner, U., Borsdorf, A., Tasser, E., Schönthaler, K. (Eds.), 2008. Alpenatlas: society, economy, environment = Atlas des Alpes = Atlante delle Alpi = Atlas Alp = Mapping the Alps. Spektrum Akademischer Verlag, Heidelberg.

Tasser, E., Leitinger, G., Tappeiner, U., 2017. Climate change versus land-use change—What affects the mountain landscapes more? Land Use Policy 60, 60–72. https://doi.org/10.1016/j.landusepol.2016.10.019

Tasser, E., Ruffini, F.V., Tappeiner, U., 2009. An integrative approach for analysing landscape dynamics in diverse cultivated and natural mountain areas. Landsc. Ecol. 24, 611–628. https://doi.org/10.1007/s10980-009-9337-9

Tasser, E., Tappeiner, U., 2002. Impact of land use changes on mountain vegetation. Appl. Veg. Sci. 5, 173–184. https://doi.org/10.1111/j.1654-109X.2002.tb00547.x

Tasser, E., Tappeiner, U., Cernusca, A., 2005. Ecological Effects of Land-use Changes in the European Alps, in: Huber, U.M., Bugmann, H.K.M., Reasoner, M.A. (Eds.), Global Change and Mountain Regions, Advances in Global Change Research. Springer Netherlands, Dordrecht, pp. 409–420. https://doi.org/10.1007/1-4020-3508-X_41

Tasser, E., Walde, J., Tappeiner, U., Teutsch, A., Noggler, W., 2007. Land-use changes and natural reforestation in the Eastern Central Alps. Agric. Ecosyst. Environ. 118, 115–129. https://doi.org/10.1016/j.agee.2006.05.004

Theissen, T., Otte, A., Waldhardt, R., 2022. High-Mountain Landscape Classification to Analyze Patterns of Land Use and Potential Natural Vegetation. Land 11, 1085. https://doi.org/10.3390/land11071085

Thom, D., Rammer, W., Garstenauer, R., Seidl, R., 2018. Legacies of past land use have a stronger effect on forest carbon exchange than future climate change in a temperate forest landscape. Biogeosciences 15, 5699–5713. https://doi.org/10.5194/bg-15-5699-2018

Thomas, P.A., 2016. Biological Flora of the British Isles: *Fraxinus excelsior*. J. Ecol. 104, 1158–1209. https://doi.org/10.1111/1365-2745.12566

Tiberti, R., Tartari, G.A., Marchetto, A., 2010. Geomorphology and hydrochemistry of 12 Alpine lakes in the Gran Paradiso National Park, Italy. J. Limnol. 69, 242. https://doi.org/10.4081/jlimnol.2010.242

Tilman, D., Downing, J.A., 1994. Biodiversity and stability in grasslands. Nature 367, 363–365. https://doi.org/10.1038/367363a0

Trevisani, S., Teza, G., Guth, P.L., 2023. Hacking the topographic ruggedness index. Geomorphology 439, 108838. https://doi.org/10.1016/j.geomorph.2023.108838

Ustaoglu, E., 2018. Farmland abandonment in Europe: an overview of drivers, consequences, and assessment of the sustainability implications. Environ. Rev. 26, 396–416. https://doi.org/10.1139/er-2018-0001

Vacchiano, G., Maggioni, M., Perseghin, G., Motta, R., 2015. Effect of avalanche frequency on forest ecosystem services in a spruce–fir mountain forest. Cold Reg. Sci. Technol. 115, 9–21. https://doi.org/10.1016/j.coldregions.2015.03.004

Valavi, R., Elith, J., Lahoz-Monfort, J.J., Guillera-Arroita, G., 2019. BLOCK CV : An R package for generating spatially or environmentally separated folds for *k* -fold cross-validation of species distribution models. Methods Ecol. Evol. 10, 225–232. https://doi.org/10.1111/2041-210X.13107

Van Uytvanck, J., Decleer, K., Hoffmann, M., 2008. Establishment patterns of woody species in low intensity-grazed pastures after the cessation of intensive agricultural use. For. Ecol. Manag. 256, 106–113. https://doi.org/10.1016/j.foreco.2008.04.008

Venturi, M., Piras, F., Corrieri, F., Martinez Aguilar, E.A., Santoro, A., 2022. The multifunctional role of linear features in traditional silvopastoral systems: the sabana de morro in Dolores (El Salvador) and the pastures with carob trees in Ragusa (Italy). Biodivers. Conserv. 31, 2315–2327. https://doi.org/10.1007/s10531-021-02220-9

Verhulst, J., Báldi, A., Kleijn, D., 2004. Relationship between land-use intensity and species richness and abundance of birds in Hungary. Agric. Ecosyst. Environ. 104, 465–473. https://doi.org/10.1016/j.agee.2004.01.043

von Scheffer, C., Lange, A., Vleeschouwer, F., Schrautzer, J., Unkel, I., 2019. 6200 years of human activities and environmental change in the northern central Alps. EG Quat. Sci. J. 68, 13–28. https://doi.org/10.5194/egqsj-68-13-2019

Ward, J.H., 1963. Hierarchical Grouping to Optimize an Objective Function. J. Am. Stat. Assoc. 58, 236–244. https://doi.org/10.2307/2282967

Wickham, J.D., Jones, K.B., PhD, K.R., Wade, T.G., O'Neill, R.V., 1999. Transitions in forest fragmentation: implications for restoration opportunities at regional scales. Landsc. Ecol. 14 337-145 1999.

Zandonai, A., Fontana, V., Klotz, J., Bertoldi, G., Crepaz, H., Tappeiner, U., Niedrist, G., 2024. Six years of high-resolution climatic data collected along an elevation gradient in the Italian Alps. Sci. Data 11, 751. https://doi.org/10.1038/s41597-024-03580-x

Zellweger, F., Coomes, D., Lenoir, J., Depauw, L., Maes, S.L., Wulf, M., Kirby, K.J., Brunet, J., Kopecký, M., Máliš, F., Schmidt, W., Heinrichs, S., den Ouden, J., Jaroszewicz, B., Buyse, G., Spicher, F., Verheyen, K., De Frenne, P., 2019. Seasonal drivers of understorey temperature buffering in temperate deciduous forests across Europe. Glob. Ecol. Biogeogr. 28, 1774–1786. https://doi.org/10.1111/geb.12991

Appendix

Appendix 1: Environmental variables

Table 3: Environmental variables of the second matrix and their description.

Variable	Description
FID	ID of the plot (GIS derived); P = Piedmont, AV = Aosta Valley
Region	Region: Aosta Valley or Piedmont
Valley	Valley name (Orco, Soana, Valgrisenche, …)
Aband_stage	Abandonment stage
LC54	Land cover in 1954
Dist_dense_forests [m]	Euclidean distance to the nearest dense forest patch - 1954 land cover [m]
Dist_sparse_forests [m]	Euclidean distance to the nearest sparse forest patch - 1954 land cover [m]
Dist_min_forests [m]	Euclidean distance to the nearest forest (dense or sparse) - 1954 land cover [m]
Road_dist [m]	Euclidean distance to the nearest road [m]
Build_dist [m]	Euclidean distance to the nearest building [m]
dense_forests_ca	Cover of dense forest within a 100 m buffer [ha]
sparse_forests_ca	Cover of sparse forest within a 100 m buffer [ha]
grassland_ca	Cover of grassland within a 100 m buffer [ha]
unvegetated_ca	Cover of unvegetated land within a 100 m buffer [ha]
anthropic_ca	Cover of anthropic land within a 100 m buffer [ha]
sidi	Simpson diversity index at landscape scale within a 100 m buffer [/]
ai	Aggregation index at landscape scale within a 100 m buffer [%]
dense_forests_ai	Aggregation index for dense forest class within a 100 m buffer [%]
sparse_forests_ai	Aggregation index for sparse forest class within a 100 m buffer [%]
grassland_ai	Aggregation index for grassland class within a 100 m buffer [%]
unvegetated_ai	Aggregation index for unvegetated class within a 100 m buffer [%]
anthropic_ai	Aggregation index for anthropic class within a 100 m buffer [%]
ed	Edge density at landscape scale within a 100 m buffer [m/ha]
dense_forests_ed	Edge density for dense forest class within a 100 m buffer [m/ha]
sparse_forests_ed	Edge density for sparse forest class within a 100 m buffer [m/ha]
grassland_ed	Edge density for grassland class within a 100 m buffer [m/ha]
unvegetated_ed	Edge density for unvegetated class within a 100 m buffer [m/ha]
anthropic_ed	Edge density for anthropic class within a 100 m buffer [m/ha]
pd	Patch density at landscape scale within a 100 m buffer [nb/ha]
dense_forests_pd	Patch density for dense forest class within a 100 m buffer [nb/ha]
sparse_forests_pd	Patch density for sparse forest class within a 100 m buffer [nb/ha]

Variable	Description
grassland_pd	Patch density for grassland class within a 100 m buffer [nb/ha]
unvegetated_pd	Patch density for unvegetated class within a 100 m buffer [nb/ha]
anthropic_pd	Patch density for anthropic class within a 100 m buffer [nb/ha]
Elevation [m]	Mean elevation within a 10 m buffer around the plot, extracted from DTM [m]
Slope [°]	Mean slope within a 10 m buffer around the plot, extracted from DTM [°]
Eastness	East exposition of aspect (sin(aspect)) [-]
Southness	South exposition component of aspect (cos(aspect)) [-]
TPI	Topographic Position Index within a 10 m buffer, extracted from DTM [/]
Roughness	Terrain roughness within a 10 m buffer, extracted from DTM [/]
HLI	Heat Load Index [/]: HLI = 1.452 - cos(aspect°), extracted from DTM
TRI	Topographic Ruggedness Index within a 10 m buffer, extracted from DTM [/]
TWI	Topographic Wetness Index within a 10 m buffer, extracted from DTM [/]
CHELSA_bio1	Mean annual air temperature [°C] — CHELSA dataset
CHELSA_bio2	Mean diurnal air temperature range [°C] — CHELSA dataset
CHELSA_bio5	Mean daily maximum air temperature of the warmest month [°C] — CHELSA dataset
CHELSA_bio6	Mean daily minimum air temperature of the coldest month [°C] — CHELSA dataset
CHELSA_bio12	Annual precipitation amount [kg m^{-2} y^{-1}] — CHELSA dataset
CHELSA_gsl	Growing season length (TREELIM) [nb of days] — CHELSA dataset
CHELSA_gdd0	Heat sum above 0°C accumulated over 1 year [°C] — CHELSA dataset
CHELSA_scd	Number of days with snow cover (TREELIM snowpack model) [nb of days] — CHELSA dataset

Appendix 2: Land-cover map of 1954.

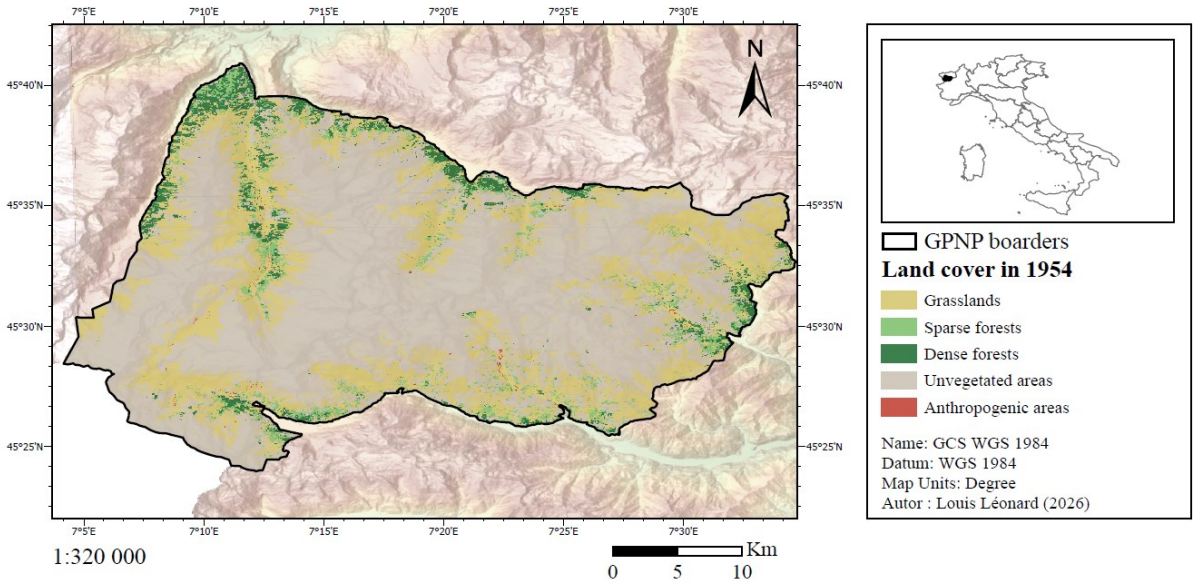

Figure 32: Land-cover map of the GPNP in 1954. Land cover is classified into grasslands, sparse forests, dense forests, unvegetated areas, and anthropogenic areas.

Appendix 3: DTM map

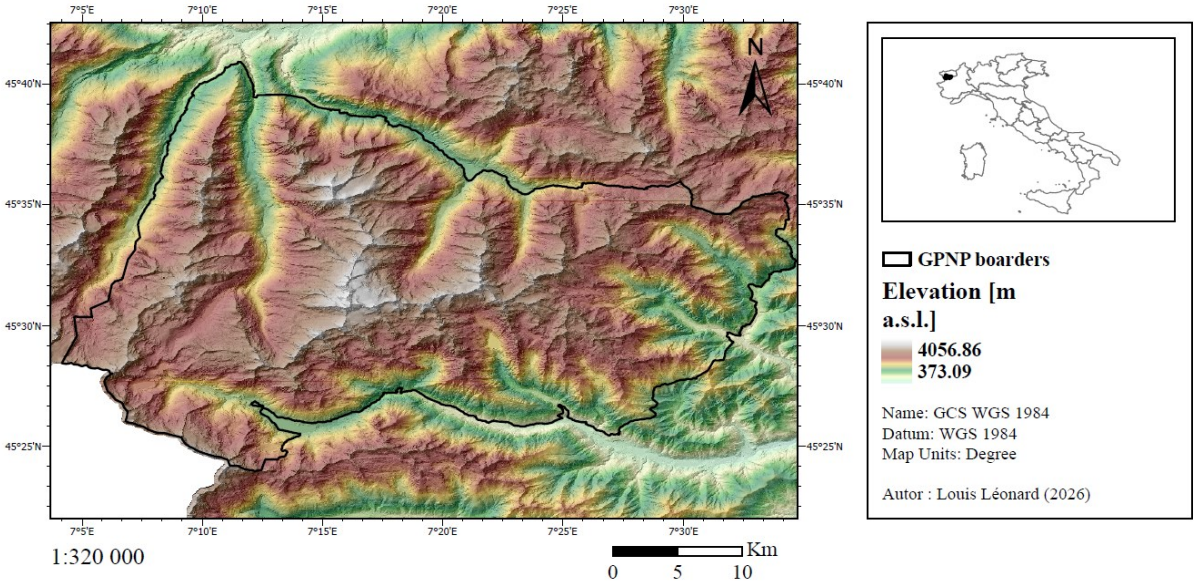

Figure 33: Digital terrain model of the GPNP. Elevation ranges from 373 to 4,057 m a.s.l., highlighting the pronounced topographic variability of the area. The DTM extent slightly exceeds the park boundaries.

Appendix 4: Plots and their forest variables

Table 4: Forest variables (1).

Plot	DBH avg (cm)	DBH sd (cm)	BA (m^2 ha^{-1})	TPH (n ha^{-1})	BLF (%)	LTI (-)	TPH se (n ha^{-1})	TPH sd (n ha^{-1})	HB t (-)	HB se,sd (-)	HB se (-)	HB sd (-)	Litter cover (%)	Regen cover (%)	Larch BA (m^2 ha^{-1})	Spruce BA (m^2 ha^{-1})	Beech BA (m^2 ha^{-1})	Hazel Ba (m^2 ha^{-1})
1_P	32.06	14.11	84.38	881.41	39.35	2.38	0.00	391.74	0.95	0.00	0.00	0.00	78.0	1.0	38.74	12.43	33.21	0.00
2_P	44.50	0.00	5.98	38.44	0.00	4.00	0.00	2,562.58	0.00	0.00	0.00	0.00	0.0	10.0	5.98	0.00	0.00	0.00
3_P	26.50	11.34	63.15	973.27	63.65	3.50	16,421.38	6,007.82	1.34	1.23	1.25	0.00	49.0	1.0	22.80	0.16	0.00	0.00
4_P	37.82	8.86	85.00	719.03	0.00	4.00	2,178.87	0.00	0.00	0.00	0.00	0.00	10.0	1.0	85.00	0.00	0.00	0.00
5_P	40.67	11.55	17.35	126.78	0.00	4.00	5,634.64	8,921.51	0.00	0.00	0.00	0.00	2.0	1.0	17.35	0.00	0.00	0.00
6_P	16.63	6.08	12.65	517.12	100.00	2.98	5,362.71	4,596.61	0.18	0.96	1.09	0.45	0.0	5.0	0.00	0.00	0.00	0.00
12_P	29.71	14.55	78.74	926.92	2.33	3.98	3,635.00	2,423.33	0.09	0.90	0.00	0.56	1.0	1.0	76.91	0.00	0.00	0.00
16_P	18.22	9.24	31.61	970.67	86.99	3.84	34,215.12	9,669.49	0.80	1.37	1.30	0.00	30.0	1.0	4.11	0.00	0.00	1.08
19_P	35.88	15.59	80.16	671.99	44.62	1.92	19,555.19	2,488.84	1.17	1.65	1.52	0.95	55.0	3.0	23.11	21.28	31.68	0.00
20_P	0.00	0.00	0.00	0.00	0.00	3.00	18,723.92	32,543.95	0.00	0.62	0.70	0.54	1.0	10.0	0.00	0.00	0.00	0.00
22_P	13.83	7.17	36.74	1,937.04	100.00	3.16	93,557.51	5,270.85	1.22	0.49	0.41	0.00	10.0	2.0	0.00	0.00	0.00	13.49
24_P	28.04	11.95	55.66	767.50	2.55	3.97	710.65	0.00	0.11	0.00	0.00	0.00	2.0	1.0	54.24	0.00	0.00	0.00
26_P	27.56	15.68	47.20	606.13	0.00	4.00	0.00	748.31	0.00	0.00	0.00	0.00	2.0	3.0	47.20	0.00	0.00	0.00
27_P	26.11	10.46	35.65	578.12	28.30	3.47	12,133.43	0.00	0.63	1.17	1.17	0.00	3.0	1.0	25.56	0.00	0.00	0.14
29_P	20.12	7.24	22.47	629.69	100.00	2.69	103,637.13	16,616.92	0.78	1.26	1.20	0.00	55.0	2.0	0.00	0.00	1.36	0.00
30_P	12.27	5.14	20.70	1,495.29	100.00	3.00	2,431.37	5,267.96	1.00	0.00	0.00	0.00	59.0	1.0	0.00	0.00	0.00	7.61
31_P	26.67	10.34	55.00	860.04	0.47	2.51	1,102.61	0.00	0.79	0.00	0.00	0.00	10.0	1.0	27.48	2.27	0.00	0.00
34_P	12.30	3.91	15.35	1,176.91	100.00	3.04	24,172.29	20,605.89	1.00	0.70	0.96	0.00	61.0	2.0	0.00	0.00	0.00	0.00
35_P	26.64	12.39	48.69	724.30	100.00	1.00	1,532.90	1,149.68	0.00	0.00	0.00	0.00	46.0	1.0	0.00	0.00	48.69	0.00
37_P	11.90	4.98	19.54	1,499.86	85.40	3.10	3,703.35	0.00	1.03	0.66	0.66	0.00	5.0	1.0	2.85	0.00	0.00	0.00
39_P	18.61	10.78	36.62	1,017.33	100.00	2.31	147,755.58	31,085.19	0.83	0.89	0.64	0.00	20.0	10.0	0.00	0.00	0.00	2.45
42_P	39.64	10.56	68.80	522.93	0.00	4.00	0.00	0.00	0.00	0.00	0.00	0.00	1.0	1.0	68.80	0.00	0.00	0.00
44_P	20.64	12.15	20.83	473.49	23.38	3.77	7,652.36	0.00	0.47	0.68	0.68	0.00	2.0	3.0	15.96	0.00	0.00	0.00
45_P	31.57	19.59	62.42	586.79	22.11	1.40	12,170.36	869.31	0.88	1.04	0.97	0.00	67.0	1.0	6.22	42.40	10.78	0.48
49_P	34.07	23.00	30.41	239.88	3.50	3.96	25,892.13	22,846.00	0.12	0.67	0.67	0.67	5.0	45.0	29.35	0.00	0.00	0.00
51_P	27.75	6.24	19.29	305.43	0.00	4.00	8,484.21	848.42	0.00	0.30	0.00	0.00	3.0	1.0	19.29	0.00	0.00	0.00
56_P	36.81	10.62	55.39	483.45	0.00	4.00	0.00	0.00	0.00	0.00	0.00	0.00	1.0	0.0	55.39	0.00	0.00	0.00
60_P	17.33	8.93	52.30	1,759.28	31.00	3.72	22,230.55	1,149.86	0.71	1.33	1.28	0.00	15.0	1.0	36.09	0.00	0.00	0.79
62_P	18.31	10.36	37.12	1,076.98	40.16	3.76	8,252.70	9,903.24	1.04	0.65	0.86	0.38	10.0	2.0	22.21	0.00	0.00	0.40
63_P	41.53	20.58	86.01	516.48	1.02	3.99	3,060.65	0.00	0.05	0.00	0.00	0.00	3.0	1.0	85.13	0.00	0.00	0.00
65_P	9.75	2.47	0.75	97.31	100.00	3.00	27,571.04	43,248.69	0.00	0.00	0.00	0.00	30.0	10.0	0.00	0.00	0.00	0.00
66_P	25.44	15.53	66.13	958.03	29.66	1.45	851.59	425.79	1.00	0.00	0.00	0.00	67.0	1.0	6.09	0.00	8.43	0.00
67_P	21.87	12.08	43.30	892.42	4.19	1.27	32,334.08	0.00	0.35	0.79	0.79	0.00	4.0	1.0	2.74	0.00	0.00	0.00
70_P	33.54	15.99	51.67	483.42	0.00	4.00	0.00	0.00	0.00	0.00	0.00	0.00	2.0	0.0	51.67	0.00	0.00	0.00
72_P	24.65	21.11	48.90	606.53	100.00	1.89	22,596.15	792.85	0.95	1.21	1.21	0.00	59.0	1.0	0.00	0.00	24.23	0.00
73_P	46.22	10.82	63.36	360.05	0.00	4.00	0.00	0.00	0.00	0.00	0.00	0.00	2.0	1.0	63.36	0.00	0.00	0.00
74_P	33.96	14.92	44.92	421.39	0.00	4.00	3,511.59	0.00	0.00	0.93	0.93	0.00	2.0	1.0	44.92	0.00	0.00	0.00
75_P	26.62	19.46	24.30	299.90	37.69	3.97	7,914.12	13,329.04	0.66	0.10	0.21	0.00	13.0	2.0	15.26	0.00	0.00	0.72
76_P	12.78	5.82	33.92	2,198.91	100.00	2.69	34,903.34	32,410.24	1.14	0.91	0.99	0.00	47.0	1.0	0.00	0.00	5.20	5.08
77_P	13.77	10.38	44.53	1,920.05	35.67	3.65	6,716.21	3,950.71	0.63	0.35	0.22	0.50	2.0	1.0	28.64	0.00	0.00	0.00
78_P	0.00	0.00	0.00	0.00	0.00	3.00	18,855.60	61,709.23	0.00	0.00	0.00	0.00	65.0	1.0	0.00	0.00	0.00	0.00
79_P	30.17	14.90	26.66	306.47	0.00	4.00	378.36	756.73	0.00	0.63	0.00	0.00	20.0	1.0	26.66	0.00	0.00	0.00
81_P	11.71	6.30	9.44	689.59	100.00	3.00	22,085.02	45,972.89	0.50	0.75	1.45	0.00	20.0	1.0	0.00	0.00	0.00	3.19
82_P	29.75	14.99	30.51	357.42	30.95	2.95	12,310.99	55,200.89	1.14	0.04	0.14	0.00	45.0	1.0	11.62	9.44	0.00	0.00
84_P	20.00	9.24	36.06	952.74	100.00	3.12	35,569.02	1,270.32	0.86	0.73	0.72	0.00	30.0	1.0	0.00	0.00	0.00	0.00
85_P	24.44	10.80	19.40	352.22	58.56	4.00	24,785.93	53,050.58	0.64	0.10	0.24	0.00	20.0	1.0	7.67	0.00	0.00	0.00
87_P	0.00	0.00	0.00	0.00	0.00	3.00	7,497.53	34,571.96	0.00	0.06	0.21	0.00	73.0	1.0	0.00	0.00	0.00	0.00

Table 5: Forest variables (2).

Plot	DBH avg (cm)	DBH sd (cm)	BA ($m^2 ha^{-1}$)	TPH (n ha^{-1})	BLF (%)	LTI (-)	TPH se (n ha^{-1})	TPH sd (n ha^{-1})	HB t (-)	HB se (-)	HB sd (-)	Litter cover (%)	Regen cover (%)	Larch BA ($m^2 ha^{-1}$)	Spruce BA ($m^2 ha^{-1}$)	Beech BA ($m^2 ha^{-1}$)	Hazel Ba ($m^2 ha^{-1}$)
88_P	0.00	0.00	0.00	0.00	0.00	3.00	36,849.22	36,457.20	0.00	0.31	0.00	5.0	1.0	0.00	0.00	0.00	0.00
90_P	15.14	8.74	21.37	900.51	94.89	3.32	26,681.91	17,629.12	1.00	1.02	0.00	10.0	1.0	1.09	0.00	0.00	4.62
91_P	33.03	17.16	78.84	733.00	3.26	3.97	1,285.97	3,429.24	0.13	0.00	0.00	1.0	1.0	76.27	0.00	0.00	0.00
92_P	13.55	3.37	12.37	809.88	100.00	3.00	7,198.90	10,348.42	0.48	0.47	0.68	25.0	1.0	0.00	0.00	0.00	0.00
93_P	17.95	9.97	49.65	1,508.76	100.00	2.35	6,877.52	1,719.38	0.61	1.11	0.78	79.0	1.0	0.00	0.00	0.00	0.00
94_P	12.75	10.21	12.79	634.89	100.00	3.72	25,395.78	57,845.94	0.60	0.75	1.56	30.0	2.0	0.00	0.00	0.00	1.32
95_P	13.00	5.11	29.49	1,931.34	100.00	2.81	13,284.38	16,350.00	1.01	0.98	0.88	60.0	1.0	0.00	0.00	0.00	1.53
96_P	13.64	10.76	14.13	613.18	100.00	3.85	9,246.42	23,846.04	0.45	0.13	0.34	50.0	1.0	0.00	0.00	0.00	2.05
97_P	57.65	19.56	108.21	375.65	0.00	4.00	2,086.92	2,504.30	0.00	0.59	0.67	30.0	1.0	108.21	0.00	0.00	0.00
98_P	31.23	8.35	45.20	553.52	100.00	1.00	10,408.13	473.10	0.00	1.03	0.99	69.0	1.0	0.00	0.00	45.20	0.00
99_P	18.70	7.49	29.31	924.02	100.00	2.57	1,140.76	1,140.76	0.62	0.69	0.00	0.0	0.0	0.00	0.00	0.00	0.00
100_P	17.81	14.25	51.06	1,265.50	6.53	3.93	2,267.93	4,535.85	0.25	0.24	0.00	1.0	1.0	47.72	0.00	0.00	1.90
101_P	14.64	10.51	22.80	906.60	20.99	3.73	8,461.61	6,044.01	0.62	0.92	1.09	10.0	2.0	18.01	0.00	0.00	1.26
102_P	13.58	6.64	21.42	1,200.15	100.00	3.72	7,556.51	24,003.02	0.69	0.00	0.00	31.0	2.0	0.00	0.00	0.00	2.99
103_P	26.19	18.60	25.48	328.16	0.00	4.00	2,278.86	1,367.31	0.00	0.00	0.00	2.0	1.0	25.48	0.00	0.00	0.00
104_P	21.40	13.33	28.69	585.60	100.00	1.51	433.78	433.78	0.49	0.00	0.00	69.0	1.0	0.00	0.00	23.44	0.00
105_P	28.86	17.77	51.24	576.87	70.49	2.48	50,564.72	1,780.45	1.23	0.94	0.85	58.0	5.0	15.12	0.00	20.81	0.50
106_P	11.39	3.37	5.78	527.12	100.00	3.00	10,412.21	35,141.20	0.37	0.00	0.00	37.0	1.0	0.00	0.00	0.00	0.00
107_P	25.00	14.06	71.33	1,113.62	89.47	1.30	2,209.56	441.91	0.32	0.69	0.67	80.0	1.0	7.20	0.31	63.82	0.00
108_P	19.22	18.26	58.39	1,076.97	9.51	1.20	13,295.89	8,420.73	0.32	1.11	1.00	55.0	1.0	0.00	0.00	0.00	4.39
110_P	22.07	10.25	45.89	993.07	100.00	3.01	29,677.85	0.00	0.40	0.33	0.33	40.0	1.0	0.00	0.00	0.00	0.58
111_P	26.53	16.19	76.01	1,010.77	77.59	1.12	0.00	374.36	0.62	0.00	0.00	76.0	1.0	3.06	13.16	58.98	0.00
112_P	34.53	15.84	62.41	521.94	0.00	4.00	0.00	412.54	0.00	0.00	0.00	1.0	1.0	62.41	0.00	0.00	0.00
113_P	28.11	18.90	49.15	557.99	15.16	1.92	151,897.20	2,657.09	0.91	0.71	0.66	35.0	5.0	10.64	31.05	0.29	0.73
114_P	20.52	8.95	38.25	977.99	100.00	1.36	18,807.58	3,343.57	0.65	1.26	1.04	67.0	1.0	0.00	0.00	25.37	0.19
115_P	23.33	14.68	62.66	1,060.91	22.03	3.78	4,471.29	6,910.17	0.60	0.00	0.00	2.0	1.0	48.86	0.00	0.00	0.00
116_P	20.83	19.33	22.37	371.98	5.98	3.94	8,725.46	4,133.11	0.19	1.05	0.62	2.0	1.0	21.03	0.00	0.00	0.00
117_P	32.42	31.51	66.57	432.21	1.34	1.02	12,405.99	0.00	0.06	0.28	0.00	63.0	2.0	0.00	65.67	0.26	0.16
118_P	16.27	6.32	65.72	2,751.77	100.00	1.01	0.00	794.16	0.02	0.00	0.00	79.0	1.0	0.00	0.00	65.47	0.00
119_P	13.88	6.64	24.45	1,323.35	71.35	3.14	12,030.47	19,159.64	1.10	0.33	0.67	20.0	2.0	6.75	0.00	0.00	1.66
121_P	32.52	13.87	67.21	689.52	100.00	3.06	2,553.76	0.00	0.20	0.41	0.41	20.0	1.0	0.00	0.00	0.00	0.00
122_P	18.03	10.27	19.18	575.81	100.00	3.69	2,799.09	0.00	0.57	0.41	0.41	0.0	10.0	0.00	0.00	0.00	0.38
123_P	50.32	20.34	108.41	473.30	0.00	4.00	375.64	0.00	0.00	0.00	0.00	50.0	1.0	108.41	0.00	0.00	0.00
124_P	28.94	19.57	64.95	690.32	15.99	3.56	4,060.72	16,694.07	0.46	0.00	0.00	67.0	1.0	54.56	0.00	8.97	1.42
125_P	28.89	26.46	47.07	411.38	6.25	3.94	6,602.38	14,220.51	0.20	0.46	0.43	5.0	1.0	44.13	0.00	0.00	0.00
126_P	43.62	19.94	49.98	282.71	0.31	4.00	0.00	785.31	0.01	0.00	0.00	2.0	1.0	49.83	0.00	0.00	0.16
127_P	37.14	11.66	58.51	494.77	0.80	3.99	14,528.91	8,246.14	0.03	0.42	0.40	2.0	1.0	58.04	0.00	0.00	0.00
128_P	37.67	29.10	60.91	357.04	7.69	1.66	6,611.83	1,763.16	0.72	0.86	0.89	61.0	2.0	13.48	42.74	4.69	0.00
129_P	23.85	14.65	73.57	1,208.12	42.91	1.86	9,446.17	2,485.83	1.36	0.56	0.62	76.0	1.0	6.49	35.51	13.02	0.00
130_P	28.21	14.15	74.94	966.23	34.77	2.29	11,183.27	0.00	1.00	0.00	0.00	70.0	1.0	32.28	16.61	26.05	0.00
131_P	22.64	15.22	71.83	1,240.92	26.99	2.87	0.00	1,253.45	0.83	0.00	0.00	84.0	1.0	44.76	7.68	19.39	0.00
132_P	24.86	20.10	53.57	682.47	7.03	3.71	2,527.66	2,527.66	0.48	0.83	1.24	34.0	1.0	45.92	3.88	0.00	2.53
133_P	31.94	27.79	45.95	342.59	4.48	1.02	30,452.38	1,268.85	0.17	0.71	0.61	64.0	1.0	0.00	43.89	1.53	0.53
135_P	18.58	11.50	44.54	1,198.37	16.43	3.97	3,550.72	2,663.04	0.47	0.69	0.38	5.0	1.0	37.22	0.00	0.00	0.00
136_P	30.03	16.81	89.40	973.34	93.88	2.18	55,213.06	0.00	1.20	1.37	1.37	62.0	1.0	0.00	5.47	31.35	0.00
137_P	31.56	17.81	66.85	657.88	9.20	1.51	3,654.90	1,827.45	0.59	0.45	0.56	59.0	1.0	7.35	53.35	0.00	0.00
138_P	15.43	9.62	21.99	856.99	80.79	3.76	5,382.04	6,210.05	1.00	0.49	0.79	15.0	2.0	4.23	0.00	0.00	2.69
139_P	22.15	19.96	42.45	624.67	6.99	3.84	4,082.84	7,757.40	0.37	0.00	0.00	10.0	1.0	37.96	1.52	0.00	2.23
140_P	29.64	15.29	58.33	675.73	100.00	1.00	0.00	417.11	0.00	0.00	0.00	63.0	1.0	0.00	0.00	58.33	0.00
141_P	21.62	15.81	43.44	784.60	15.12	3.85	7,410.08	10,897.17	0.46	0.55	0.65	0.44	2.0	1.0	36.87	0.00	0.00	0.00

Table 6: Forest variables (3).

Plot	DBH avg (cm)	DBH sd (cm)	BA (m^2 ha^{-1})	TPH (n ha^{-1})	BLF (%)	LTI (-)	TPH se (n ha^{-1})	TPH sd (n ha^{-1})	HB t (-)	HB se (-)	HB sd (-)	Litter cover (%)	Regen cover (%)	Larch BA (m^2 ha^{-1})	Spruce BA (m^2 ha^{-1})	Beech BA (m^2 ha^{-1})	Hazel Ba (m^2 ha^{-1})
142_P	33.38	20.12	57.69	494.67	4.40	1.13	15,114.82	458.02	0.16	0.89	0.00	5.0	2.0	0.00	0.00	0.00	0.00
143_P	20.44	12.86	28.63	634.73	24.73	3.72	28,993.79	1,959.04	0.56	0.54	0.50	5.0	1.0	21.55	0.00	0.00	0.00
144_P	24.14	9.88	63.44	1,192.67	100.00	3.00	5,797.68	3,312.96	0.00	0.18	0.00	45.0	1.0	0.00	0.00	0.00	0.00
145_P	11.67	6.79	11.38	805.96	72.88	3.60	5,970.10	2,985.05	0.89	0.55	0.41	5.0	1.0	3.09	0.00	0.00	0.00
6_AV	31.13	12.31	50.60	664.82	0.00	1.76	2,462.29	0.00	0.53	0.00	0.00	77.0	1.0	12.89	37.72	0.00	0.00
7_AV	35.52	14.57	62.18	627.44	0.00	2.17	0.00	0.00	0.63	0.00	0.00	52.0	1.0	24.33	37.85	0.00	0.00
11_AV	31.82	10.55	28.77	361.82	0.00	4.00	0.00	0.00	0.00	0.00	0.00	2.5	5.0	28.77	0.00	0.00	0.00
13_AV	13.94	5.50	3.57	234.10	0.00	4.00	1,734.07	2,167.58	0.00	0.00	0.00	0.0	40.0	3.57	0.00	0.00	0.00
18_AV	10.31	2.23	12.91	1,545.21	100.00	3.00	357.69	1,073.07	0.06	0.00	0.00	2.5	2.5	0.00	0.00	0.00	0.00
19_AV	38.44	18.01	20.88	179.96	0.00	4.00	799.83	399.92	0.00	0.00	0.00	5.0	1.0	20.88	0.00	0.00	0.00
20_V	18.28	6.63	17.09	651.00	100.00	3.99	0.00	30,138.84	0.04	0.00	0.00	10.0	25.0	0.00	0.00	0.00	0.00
24_AV	23.26	9.61	27.43	645.43	17.19	3.25	0.00	398.41	0.79	0.00	0.00	30.0	2.5	17.39	5.33	0.00	0.00
28_AV	19.59	10.08	35.11	1,164.38	62.60	2.41	49,901.79	2,587.50	1.24	0.63	0.51	17.5	12.5	0.00	13.13	0.00	0.74
33_AV	30.84	12.18	32.75	438.32	0.00	1.31	3,371.67	0.00	0.28	0.53	0.00	70.5	5.0	3.34	29.41	0.00	0.00
34_AV	35.03	22.63	41.95	435.38	15.34	3.91	7,814.50	5,581.78	0.51	1.35	0.51	20.0	12.5	34.75	0.76	0.00	0.32
46_AV	21.56	7.58	28.10	769.56	5.59	1.88	3,109.33	2,332.00	0.64	0.68	0.00	20.0	2.5	6.64	19.89	0.00	0.00
47_AV	30.95	12.50	73.17	972.74	5.48	3.94	15,491.83	4,683.58	0.29	1.04	0.95	1.01	20.0	27.5	67.81	1.35	0.00
50_AV	14.89	5.83	28.91	1,660.61	84.05	3.63	5,426.84	723.58	1.07	1.00	0.86	0.69	10.0	5.0	4.61	0.00	0.00
51_AV	18.07	6.45	26.60	1,037.22	100.00	3.00	0.00	0.00	0.00	0.00	0.00	0.00	10.0	0.0	0.00	0.00	0.00
53_AV	33.72	13.15	47.00	526.18	0.00	3.13	899.45	899.45	0.94	0.69	0.69	25.0	1.0	23.96	8.98	0.00	0.00
54_AV	30.34	11.67	24.30	336.11	0.00	3.65	0.00	0.00	0.47	0.00	0.00	2.5	1.0	20.16	2.22	0.00	0.00
56_AV	17.75	7.22	23.99	969.76	64.23	2.80	3,848.26	1,154.48	0.97	0.27	0.00	15.0	5.0	4.01	4.57	0.00	0.00
60_AV	25.40	8.66	31.94	630.48	5.25	3.85	0.00	412.08	0.33	0.00	0.00	20.0	2.5	28.66	1.61	0.00	0.00
61_AV	22.10	9.15	29.03	757.05	0.00	3.89	0.00	801.11	0.30	0.00	0.00	30.0	1.0	25.83	0.00	0.00	0.00
62_AV	22.09	15.01	32.49	847.79	12.22	4.00	5,275.13	2,260.77	0.32	1.75	1.01	22.5	15.0	28.52	0.00	0.00	0.00
64_AV	13.62	5.91	10.33	708.68	62.23	2.87	8,232.10	357.92	0.84	1.79	0.00	37.5	10.0	0.00	3.90	0.00	0.00
65_AV	25.50	13.66	33.90	663.45	0.00	3.68	819.07	409.54	0.57	0.63	0.00	20.0	1.0	23.16	0.00	0.00	0.00
67_AV	48.77	24.86	38.29	205.00	0.00	1.62	379.63	0.00	0.46	0.00	0.00	15.0	1.0	7.88	30.41	0.00	0.00
68_AV	15.73	6.91	19.19	987.11	73.94	2.98	52,570.41	1,512.82	1.38	0.55	0.56	10.0	17.5	3.93	1.07	0.00	0.00
70_AV	30.68	19.79	34.09	460.97	0.00	1.46	1,097.55	731.70	0.38	0.00	0.00	15.0	5.0	5.24	28.85	0.00	0.00
71_AV	25.46	11.50	17.35	340.93	0.00	3.86	1,136.44	378.81	0.33	0.56	0.00	5.0	1.0	14.94	0.00	0.00	0.00
72_AV	30.29	13.05	42.59	591.04	0.00	2.81	0.00	0.00	0.62	0.00	0.00	49.5	1.0	25.70	16.89	0.00	0.00
73_AV	39.48	23.38	34.16	279.02	2.18	3.73	5,037.82	0.00	0.32	0.00	0.00	10.0	5.0	30.61	2.80	0.00	0.00
75_AV	13.69	4.99	20.35	1,381.83	0.00	4.00	426.49	1,279.47	0.00	0.56	0.00	36.5	15.0	20.35	0.00	0.00	0.00
82_AV	25.94	15.19	34.90	660.21	0.00	2.80	431.51	431.51	0.62	0.00	0.00	45.0	2.5	20.95	13.94	0.00	0.00
87_AV	13.62	5.95	7.53	516.96	100.00	3.02	19,745.05	1,795.00	0.19	0.36	0.67	5.0	30.0	0.00	0.00	0.00	0.00
90_AV	18.50	8.00	12.83	476.99	71.54	3.20	14,006.98	1,514.27	0.70	0.56	0.21	37.5	2.5	3.65	0.00	0.00	0.00
91_AV	31.09	11.48	33.62	442.84	0.00	4.00	0.00	410.03	0.00	0.00	0.00	10.0	1.0	33.62	0.00	0.00	0.00
93_AV	35.52	16.85	71.32	719.59	0.28	3.91	0.00	0.00	0.13	0.00	0.00	33.0	1.0	69.00	2.12	0.00	0.00
94_AV	10.51	2.69	5.56	640.86	100.00	2.93	2,492.23	4,984.46	0.15	0.98	0.89	7.5	2.5	0.00	0.00	0.00	0.00
95_AV	17.36	7.66	20.13	850.00	86.11	3.13	114,785.94	5,448.70	1.17	0.39	1.08	10.0	35.0	2.80	0.00	0.00	0.00
97_AV	13.19	6.53	21.80	1,595.83	0.00	4.00	0.00	3,711.23	0.00	0.00	0.00	32.0	25.0	21.80	0.00	0.00	0.00
104_AV	25.19	13.40	85.07	1,707.44	79.54	3.10	82,687.16	1,073.86	1.25	0.38	0.00	10.0	20.0	16.40	1.01	0.00	0.00
108_AV	39.29	22.01	55.15	454.88	18.57	3.83	6,137.32	1,083.06	0.63	1.34	1.00	20.0	2.5	43.38	1.53	0.00	0.00
110_AV	17.17	6.40	26.26	1,133.84	100.00	3.83	41,754.12	719.90	0.36	0.61	0.57	10.0	10.0	0.00	0.00	0.00	0.00
111_AV	29.97	13.74	19.63	278.12	21.33	3.57	1,324.38	1,324.38	0.44	1.01	0.63	5.0	2.5	15.44	0.00	0.00	0.00
112_AV	17.64	5.81	23.11	945.84	100.00	3.33	145,318.83	362.39	0.67	0.41	0.00	2.5	30.0	0.00	0.00	0.00	0.00
115_AV	24.41	10.89	33.36	712.79	0.00	3.88	377.14	754.27	0.26	0.00	0.00	30.0	2.5	30.70	0.64	0.00	0.00
116_AV	39.22	11.60	43.15	357.09	0.00	1.91	3,967.65	0.00	0.57	0.00	0.00	70.5	2.5	13.10	30.05	0.00	0.00
119_AV	23.27	8.42	38.93	915.23	0.00	3.77	813.53	0.00	0.23	0.00	0.00	32.5	1.0	35.98	2.95	0.00	0.00

Table 7: Forest variables (4).

Plot	DBH avg (cm)	DBH sd (cm)	BA (m^2 ha^{-1})	TPH (n ha^{-1})	BLF (%)	LTI (-)	TPH se (n ha^{-1})	TPH sa (n ha^{-1})	HB t (-)	HB sesa (-)	HB se (-)	HB sa (-)	Litter cover (%)	Regen cover (%)	Larch BA (m^2 ha^{-1})	Spruce BA (m^2 ha^{-1})	Beech BA (m^2 ha^{-1})	Hazel Ba (m^2 ha^{-1})
120_AV	25.83	13.10	56.95	1,087.29	49.91	3.43	8,883.07	1,065.97	1.15	1.41	1.28	0.63	20.0	7.5	25.77	2.76	0.00	0.00
122_AV	27.74	15.62	35.00	578.97	0.00	4.00	3,216.53	357.39	0.00	0.00	0.00	0.00	15.0	2.5	35.00	0.00	0.00	0.00
125_AV	26.32	9.23	43.13	792.71	59.26	2.95	7,206.45	800.72	0.91	0.64	0.56	0.69	44.0	2.5	17.57	0.00	0.00	0.00
127_AV	38.17	20.58	50.47	441.06	2.33	1.53	753.95	0.00	0.48	0.00	0.00	0.00	73.0	0.0	7.79	41.50	0.00	0.00
128_AV	31.81	14.14	34.42	433.05	0.00	4.00	0.00	437.42	0.00	0.00	0.00	0.00	40.0	2.5	34.42	0.00	0.00	0.00
129_AV	18.03	8.79	24.23	948.98	79.71	3.54	3,635.96	5,090.34	1.02	1.53	1.28	0.82	20.5	15.0	4.92	0.00	0.00	0.00
130_AV	23.06	8.89	18.47	442.24	0.00	4.00	3,401.83	1,511.93	0.00	0.00	0.00	0.00	17.5	12.5	18.47	0.00	0.00	0.00
132_AV	39.99	15.40	74.35	592.01	9.39	2.39	0.00	0.00	0.87	0.00	0.00	0.00	78.0	1.0	27.41	39.96	0.00	0.00
133_AV	40.44	14.17	76.18	593.15	0.00	2.60	0.00	387.68	0.66	0.00	0.00	0.00	10.0	0.0	40.62	35.56	0.00	0.00
134_AV	23.30	10.80	30.15	707.15	0.00	3.96	357.15	0.00	0.05	0.00	0.00	0.00	30.0	1.0	29.71	0.43	0.00	0.00
135_AV	22.81	12.23	25.16	615.67	36.79	3.58	1,520.17	760.08	0.78	0.63	0.00	0.00	2.5	5.0	15.90	0.00	0.00	0.00
136_AV	22.19	13.45	28.83	745.43	56.74	3.99	2,880.91	360.11	0.65	0.00	0.00	0.00	10.0	1.0	12.47	0.00	0.00	0.00
138_AV	52.85	19.15	42.01	191.48	0.00	4.00	0.00	0.00	0.00	0.00	0.00	0.00	15.0	0.0	42.01	0.00	0.00	0.00
142_AV	36.52	19.44	64.99	620.40	0.00	1.41	0.00	0.00	0.37	0.00	0.00	0.00	63.0	1.0	8.93	56.07	0.00	0.00
143_AV	19.16	10.14	8.85	306.96	3.03	4.00	1,515.84	1,894.79	0.08	0.85	1.03	0.50	10.0	2.5	8.59	0.00	0.00	0.00
146_AV	21.56	10.49	12.96	354.78	0.00	3.84	2,759.44	394.21	0.34	0.38	0.41	0.00	2.5	5.0	10.93	0.00	0.00	0.00
148_AV	21.33	9.32	29.64	829.28	0.00	2.67	7,371.38	737.14	0.62	0.00	0.00	0.00	40.0	2.5	16.54	13.11	0.00	0.00
151_AV	36.86	13.91	33.08	310.02	0.00	2.56	382.75	0.00	0.63	0.00	0.00	0.00	30.0	2.5	17.18	15.90	0.00	0.00
152_AV	26.98	13.42	46.09	806.11	0.00	2.62	0.00	895.68	0.64	0.69	0.00	0.69	52.0	1.0	24.88	21.21	0.00	0.00
155_AV	24.12	9.15	38.16	835.01	0.00	3.97	2,319.48	0.00	0.09	0.00	0.00	0.00	7.5	1.0	37.17	0.00	0.00	0.00
156_AV	27.48	11.80	37.71	635.84	38.67	2.91	54,949.50	1,177.49	1.05	0.42	0.41	0.00	22.5	20.0	18.35	4.78	0.00	0.00
158_AV	31.31	17.56	63.87	829.65	0.00	3.85	737.47	0.00	0.39	0.69	0.69	0.00	2.5	1.0	54.22	0.00	0.00	0.00
159_AV	28.30	18.52	17.92	284.91	17.55	3.82	2,769.99	1,978.56	0.39	0.56	0.60	0.50	0.0	1.0	14.77	0.00	0.00	0.00
160_AV	17.06	4.14	7.85	343.44	0.00	4.00	0.00	381.60	0.00	0.00	0.00	0.00	5.0	2.5	7.85	0.00	0.00	0.00
161_AV	46.67	21.87	59.35	347.00	0.00	4.00	0.00	385.55	0.00	0.00	0.00	0.00	21.5	1.0	59.35	0.00	0.00	0.00
164_AV	29.65	13.55	38.09	551.80	0.00	2.84	408.74	1,226.22	0.61	0.56	0.00	0.63	5.0	5.0	23.41	14.68	0.00	0.00
166_AV	26.79	11.18	47.83	848.36	95.12	2.50	9,818.93	392.76	0.69	0.00	0.00	0.00	15.0	10.0	0.00	2.33	0.00	0.00
168_AV	33.65	7.32	74.00	831.91	0.00	3.83	0.00	0.00	0.20	0.00	0.00	0.00	2.5	0.0	69.82	4.18	0.00	0.00
169_AV	38.17	15.87	43.56	380.60	0.00	3.97	1,922.21	768.88	0.04	1.27	1.33	0.00	15.0	5.0	43.14	0.42	0.00	0.00
170_AV	37.04	15.35	52.77	489.70	0.00	4.00	0.00	0.00	0.00	0.00	0.00	0.00	15.0	1.0	52.77	0.00	0.00	0.00
171_AV	44.02	16.75	52.38	344.19	0.00	4.00	0.00	0.00	0.00	0.00	0.00	0.00	10.0	1.0	52.38	0.00	0.00	0.00
174_AV	26.58	11.12	33.99	612.49	0.00	4.00	0.00	0.00	0.00	0.00	0.00	0.00	35.5	1.0	33.99	0.00	0.00	0.00
175_AV	27.75	9.30	51.95	858.99	5.63	1.99	5,394.62	414.97	0.75	0.00	0.00	0.00	41.5	1.0	16.21	32.82	0.00	0.00
176_AV	25.54	9.54	47.46	926.44	0.00	3.97	1,906.25	762.50	0.04	0.00	0.00	0.00	20.0	2.5	47.00	0.46	0.00	0.00
178_AV	20.28	10.59	12.63	390.83	38.79	3.61	0.00	1,579.12	0.55	0.00	0.00	0.00	2.5	2.5	7.73	0.00	0.00	0.00
179_AV	28.74	8.52	37.58	579.16	0.00	3.67	0.00	0.00	0.30	0.00	0.00	0.00	15.0	0.0	33.48	4.11	0.00	0.00
181_AV	29.09	13.97	41.71	627.74	0.00	3.95	410.29	0.00	0.07	0.00	0.00	0.00	25.0	5.0	40.97	0.74	0.00	0.00
182_AV	32.78	22.51	61.77	732.11	2.09	3.74	1,220.18	3,253.81	0.36	0.00	0.00	0.00	25.0	1.0	55.18	4.83	0.00	0.00
183_AV	28.64	13.96	35.57	552.05	0.00	3.99	0.00	0.00	0.03	0.00	0.00	0.00	5.0	1.0	35.31	0.00	0.00	0.00
186_AV	19.12	7.78	23.82	829.45	0.00	4.00	0.00	0.00	0.00	0.00	0.00	0.00	30.0	1.0	23.82	0.00	0.00	0.00
187_AV	35.97	14.73	60.98	600.00	0.00	3.65	0.00	0.00	0.64	0.00	0.00	0.00	2.5	0.0	43.50	1.95	0.00	0.00
188_AV	32.28	18.41	39.82	486.74	0.00	3.82	1,802.73	0.00	0.40	0.50	0.50	0.00	5.0	1.0	34.39	0.96	0.00	0.00
189_AV	24.02	8.74	51.20	1,129.69	0.00	4.00	965.55	0.00	0.00	0.00	0.00	0.00	35.0	2.5	51.20	0.00	0.00	0.00
194_AV	31.40	14.09	44.93	580.16	0.00	3.29	1,208.67	0.00	0.52	0.63	0.63	0.00	15.0	1.0	34.15	10.60	0.00	0.00
195_AV	37.17	8.01	50.20	462.48	0.00	1.26	0.00	0.00	0.26	0.00	0.00	0.00	75.0	0.0	4.38	45.82	0.00	0.00
196_AV	31.73	15.83	18.84	238.26	0.00	3.99	5,735.81	0.00	0.04	0.27	0.27	0.00	10.0	5.0	18.59	0.00	0.00	0.00
202_AV	32.25	13.87	31.18	381.61	0.00	4.00	0.00	0.00	0.00	0.00	0.00	0.00	10.0	0.0	31.18	0.00	0.00	0.00
203_AV	26.38	9.96	57.13	1,045.30	0.00	3.07	414.80	0.00	0.58	0.00	0.00	0.00	78.0	1.0	39.35	17.77	0.00	0.00
204_AV	27.61	8.07	49.48	826.30	0.00	3.98	1,530.18	0.00	0.02	0.56	0.56	0.00	10.0	0.0	49.21	0.27	0.00	0.00
205_AV	31.08	9.79	61.91	816.19	0.00	2.35	0.00	394.30	0.65	0.00	0.00	0.00	64.5	1.0	27.83	34.07	0.00	0.00

Table 8: Forest variables (5).

Plot	DBH avg (cm)	DBH sd (cm)	BA (m^2 ha^{-1})	TPH (n ha^{-1})	BLF (%)	LTI (-)	TPH se (n ha^{-1})	TPH sa (n ha^{-1})	HB t (-)	HB se&sa (-)	HB se (-)	HB sa (-)	Litter cover (%)	Regen cover (%)	Larch BA (m^2 ha^{-1})	Spruce BA (m^2 ha^{-1})	Beech BA (m^2 ha^{-1})	Hazel Ba (m^2 ha^{-1})
206_AV	36.57	15.95	78.28	745.45	0.00	3.31	0.00	0.00	0.59	0.00	0.00	0.00	70.5	1.0	24.17	0.00	0.00	0.00
207_AV	17.24	7.44	33.33	1,427.91	73.27	2.95	1,081.75	0.00	1.06	1.09	1.09	0.00	40.0	1.0	2.58	6.33	0.00	0.00
208_AV	29.98	17.13	25.47	360.94	0.57	3.48	364.59	364.59	0.42	0.00	0.00	0.00	5.0	2.5	20.89	4.44	0.00	0.00
213_AV	33.83	20.20	68.98	767.50	0.00	3.22	0.00	0.00	0.54	0.00	0.00	0.00	28.5	1.0	51.05	17.93	0.00	0.00
214_AV	32.73	8.17	30.20	358.91	0.00	4.00	398.79	0.00	0.00	0.00	0.00	0.00	13.0	1.0	30.20	0.00	0.00	0.00
215_AV	35.46	14.69	85.86	869.39	0.20	3.12	6,687.59	0.00	0.59	0.00	0.00	0.00	83.0	1.0	60.52	25.17	0.00	0.00
216_AV	41.97	16.89	48.60	351.25	0.00	3.40	433.64	0.00	0.64	0.00	0.00	0.00	22.5	0.0	36.48	8.48	0.00	0.00
217_AV	32.01	9.31	38.86	482.98	0.00	3.18	4,128.03	0.00	0.54	0.50	0.50	0.00	60.0	1.0	28.21	10.65	0.00	0.00
218_AV	23.81	11.28	47.65	1,070.15	0.00	3.50	0.00	1,150.69	0.41	0.63	0.00	0.63	40.0	1.0	39.73	7.92	0.00	0.00
220_AV	27.92	10.27	32.51	530.94	0.00	3.93	0.00	0.00	0.08	0.00	0.00	0.00	5.0	0.0	31.76	0.75	0.00	0.00
221_AV	33.32	12.93	32.39	371.48	0.00	3.95	1,125.70	375.23	0.15	0.00	0.00	0.00	2.5	1.0	30.87	0.00	0.00	0.00
222_AV	26.20	16.50	24.75	459.16	0.00	3.97	364.41	364.41	0.11	0.00	0.00	0.00	2.5	1.0	23.90	0.00	0.00	0.00
224_AV	70.96	52.28	135.40	342.36	0.00	3.82	0.00	380.40	0.21	0.00	0.00	0.00	20.0	1.0	127.27	8.12	0.00	0.00
235_AV	24.36	13.13	51.97	1,114.76	0.00	3.99	0.00	1,092.90	0.02	0.63	0.00	0.63	10.0	2.5	51.71	0.26	0.00	0.00
239_AV	19.50	8.33	15.30	512.46	0.00	4.00	1,423.50	355.88	0.00	0.50	0.56	0.00	5.0	2.5	15.30	0.00	0.00	0.00
243_AV	33.84	12.90	69.21	769.55	0.00	3.93	356.27	0.00	0.10	0.00	0.00	0.00	10.0	1.0	67.51	1.70	0.00	0.00
248_AV	24.10	10.95	14.24	312.11	0.00	3.93	770.65	2,697.27	0.18	0.33	0.69	0.41	2.5	2.5	13.25	0.00	0.00	0.00
249_AV	28.89	13.59	39.65	604.95	0.00	3.58	373.42	746.85	0.63	0.63	0.00	0.69	20.0	1.0	23.03	0.00	0.00	0.00
250_AV	25.02	11.78	20.18	410.30	0.00	2.63	0.00	0.00	0.60	0.00	0.00	0.00	10.0	1.0	10.98	9.20	0.00	0.00
253_AV	28.12	13.83	44.20	711.74	0.00	3.84	1,078.40	718.93	0.17	0.00	0.00	0.00	32.5	1.0	41.91	2.29	0.00	0.00
255_AV	44.85	18.19	27.13	171.68	0.00	4.00	0.00	0.00	0.00	0.00	0.00	0.00	5.0	1.0	27.13	0.00	0.00	0.00
263_AV	40.20	15.31	36.56	288.09	0.00	4.00	0.00	0.00	0.00	0.00	0.00	0.00	0.0	1.0	36.56	0.00	0.00	0.00
264_AV	30.75	14.76	49.75	670.02	10.50	2.51	3,308.77	413.60	0.93	0.85	0.73	0.00	42.5	2.5	21.59	22.94	0.00	0.00
266_AV	11.81	4.41	3.46	316.10	100.00	3.57	4,292.69	3,121.96	0.42	0.69	0.47	0.38	20.0	5.0	0.00	0.00	0.00	0.00
275_AV	28.88	13.63	46.24	705.78	0.00	2.87	4,127.35	0.00	0.62	0.00	0.00	0.00	30.0	2.5	28.77	17.47	0.00	0.00
276_AV	32.54	20.70	18.35	220.54	3.86	1.08	1,633.62	1,633.62	0.12	1.25	1.04	0.56	0.0	10.0	0.00	17.64	0.00	0.00
286_AV	14.15	5.67	4.35	276.48	0.00	3.25	1,755.42	1,755.42	0.52	1.07	1.04	0.56	15.0	5.0	2.86	0.88	0.00	0.00
287_AV	20.83	10.93	38.61	1,133.33	0.42	3.89	1,218.64	1,624.85	0.22	1.27	0.63	0.56	15.0	2.5	36.26	0.96	0.00	0.00
288_AV	19.83	10.00	27.39	886.81	13.43	3.60	2,758.95	394.14	0.92	0.38	0.00	0.00	25.0	2.5	14.48	0.81	0.00	0.00
289_AV	20.03	10.24	35.19	1,116.40	54.65	2.45	4,378.04	729.67	1.41	0.41	0.29	0.69	15.0	10.0	3.53	12.43	0.00	0.00
292_AV	29.80	15.63	24.59	352.48	0.00	3.50	1,566.57	783.29	0.62	0.69	0.56	0.00	7.5	1.0	12.20	0.00	0.00	0.00
294_AV	17.66	9.08	21.23	866.82	0.00	1.72	0.00	875.57	0.47	0.00	0.00	0.00	45.0	7.5	5.07	16.17	0.00	0.00
296_AV	41.26	10.65	49.02	366.74	0.00	4.00	0.00	0.00	0.00	0.00	0.00	0.00	15.0	1.0	49.02	0.00	0.00	0.00
298_AV	30.72	18.48	61.44	828.86	1.86	1.85	767.46	1,151.19	0.62	0.95	0.69	0.63	30.0	1.0	16.72	43.58	0.00	0.00
299_AV	43.67	15.44	72.12	481.44	0.00	3.86	82.97	0.00	0.17	0.00	0.00	0.00	35.0	1.0	68.76	3.36	0.00	0.00
300_AV	24.81	13.91	44.40	917.98	0.00	3.73	1,133.31	377.77	0.27	0.56	0.00	0.00	68.0	1.0	40.36	4.04	0.00	0.00
301_AV	19.51	6.51	39.45	1,318.93	0.00	3.25	3,663.70	366.37	0.94	1.24	1.22	0.00	30.0	7.5	9.76	9.87	0.00	0.00
307_AV	31.51	15.36	59.90	768.31	0.00	2.33	4,656.39	776.07	0.65	0.26	0.00	0.69	25.0	4.0	26.62	33.28	0.00	0.00
308_AV	36.21	13.58	74.92	727.41	0.00	3.87	0.00	0.00	0.16	0.00	0.00	0.00	25.0	1.0	71.71	3.22	0.00	0.00
309_AV	46.72	14.70	83.73	488.34	0.00	4.00	0.00	417.39	0.00	0.00	0.00	0.00	17.5	1.0	83.73	0.00	0.00	0.00
310_AV	41.13	3.63	32.33	243.28	0.00	4.00	0.00	450.52	0.00	0.00	0.00	0.00	26.0	1.0	32.33	0.00	0.00	0.00
311_AV	38.24	10.69	33.42	290.97	0.00	3.18	0.00	359.22	0.53	0.00	0.00	0.00	15.0	1.0	24.32	9.10	0.00	0.00
313_AV	35.38	20.50	47.97	487.89	0.00	3.30	0.00	387.21	0.57	0.00	0.00	0.00	30.0	2.5	14.52	0.00	0.00	0.00
320_AV	37.67	15.93	70.82	635.44	0.00	2.92	0.00	830.64	0.62	0.00	0.00	0.00	35.5	1.0	45.22	25.60	0.00	0.00
321_AV	26.58	11.85	33.23	598.96	0.00	2.50	950.72	475.36	0.84	0.00	0.00	0.00	32.5	1.0	14.49	15.62	0.00	0.00
323_AV	48.24	18.33	120.45	659.09	0.00	3.20	1,927.16	385.43	0.78	0.00	0.00	0.00	2.5	2.5	81.54	28.77	0.00	0.00
325_AV	39.78	15.20	71.30	573.83	1.22	3.40	2,975.41	4,250.59	0.60	0.66	0.68	0.53	7.5	20.0	55.16	13.49	0.00	0.00
326_AV	57.00	13.52	49.54	194.16	0.00	4.00	862.92	0.00	0.00	0.00	0.00	0.00	5.0	1.0	49.54	0.00	0.00	0.00
327_AV	39.30	13.65	90.08	742.56	0.00	4.00	0.00	0.00	0.00	0.00	0.00	0.00	2.5	0.0	90.08	0.00	0.00	0.00
328_AV	23.86	12.58	11.99	268.27	34.34	3.71	5,961.53	1,117.79	0.67	0.00	0.00	0.00	1.0	5.0	7.87	0.00	0.00	0.00

Table 9: Forest variables (6).

Plot	DBH avg (cm)	DBH sd (cm)	BA (m^2 ha^{-1})	TPH (n ha^{-1})	BLF (%)	LTI (-)	TPH se (n ha^{-1})	TPH sd (n ha^{-1})	HB t (-)	HB sd (-)	HB se (-)	HB sd (-)	Litter cover (%)	Regen cover (%)	Larch BA (m^2 ha^{-1})	Spruce BA (m^2 ha^{-1})	Beech BA (m^2 ha^{-1})	Hazel Ba (m^2 ha^{-1})
331_AV	14.68	5.16	16.63	983.09	100.00	3.30	15,292.51	1,747.71	1.03	0.80	0.60	0.69	15.0	10.0	0.00	0.00	0.00	0.00
334_AV	10.25	0.35	0.59	70.86	100.00	3.00	9,842.30	8,661.22	0.00	0.00	0.00	0.00	0.0	45.0	0.00	0.00	0.00	0.00
335_AV	10.08	1.68	8.05	1,008.77	100.00	3.97	5,811.84	3,321.05	0.07	1.06	0.99	0.00	5.0	15.0	0.00	0.00	0.00	0.00
340_AV	34.76	13.64	62.37	657.06	0.00	1.94	0.00	0.00	0.59	0.00	0.00	0.00	37.5	0.0	19.45	42.92	0.00	0.00
341_AV	44.75	17.55	68.31	434.37	1.80	1.29	0.00	0.00	0.34	0.00	0.00	0.00	10.0	0.0	5.89	61.19	0.00	0.00
343_AV	32.17	13.63	55.94	688.28	0.00	3.13	899.71	0.00	0.56	0.00	0.00	0.00	20.0	1.0	39.80	16.13	0.00	0.00
344_AV	51.76	39.73	154.79	735.64	1.81	3.93	15,958.35	3,113.82	0.16	0.83	0.80	0.00	30.0	5.0	149.51	2.48	0.00	2.65
346_AV	38.57	12.27	60.94	521.52	0.00	3.68	0.00	0.00	0.59	0.00	0.00	0.00	20.0	1.0	41.49	0.00	0.00	0.00
349_AV	31.05	16.89	56.41	744.99	0.00	4.00	0.00	413.89	0.00	0.00	0.00	0.00	17.5	5.0	56.41	0.00	0.00	0.00
350_AV	32.75	18.03	52.44	622.50	0.00	4.00	0.00	384.26	0.02	0.00	0.00	0.00	30.0	1.0	52.22	0.00	0.00	0.00
351_AV	23.97	15.27	10.53	233.30	0.00	3.83	1,110.93	740.62	0.34	0.00	0.00	0.00	5.0	15.0	8.76	0.00	0.00	0.00
362_AV	29.44	18.97	94.31	1,385.34	0.00	3.32	832.04	832.04	0.60	0.69	0.00	0.00	2.5	5.0	30.20	0.00	0.00	0.00
363_AV	26.93	13.73	48.11	844.60	0.00	3.65	360.94	0.00	0.62	0.00	0.00	0.00	10.0	1.0	35.80	2.21	0.00	0.00
364_AV	27.39	12.74	45.29	768.67	0.00	3.65	371.34	0.00	0.60	0.00	0.00	0.00	10.0	2.5	34.83	2.77	0.00	0.00
368_AV	27.26	11.54	33.49	573.86	0.00	1.27	375.07	375.07	0.26	0.00	0.00	0.00	49.0	2.5	3.06	30.42	0.00	0.00
370_AV	21.39	8.39	32.46	903.07	0.00	3.99	0.00	1,543.72	0.02	0.00	0.00	0.00	2.5	2.5	32.29	0.00	0.00	0.00
371_AV	57.93	23.14	82.89	314.46	0.00	2.49	0.00	0.00	0.66	0.00	0.00	0.00	45.0	1.0	41.18	41.71	0.00	0.00
372_AV	49.75	19.39	38.00	195.47	0.00	3.97	723.95	0.00	0.04	0.00	0.00	0.00	5.0	2.5	37.57	0.43	0.00	0.00
376_AV	26.61	10.15	24.81	445.98	5.91	2.25	2,831.64	1,415.82	0.75	0.87	0.56	0.69	20.0	15.0	9.19	14.15	0.00	0.00
377_AV	28.62	10.00	28.76	447.04	0.00	3.60	0.00	1,146.26	0.47	0.00	0.00	0.00	5.0	2.5	23.85	3.36	0.00	0.00
378_AV	30.59	12.44	40.06	544.95	0.00	2.93	756.88	0.00	0.88	0.00	0.00	0.00	25.0	1.0	21.97	12.43	0.00	0.00
379_AV	53.71	31.68	56.50	249.35	0.00	3.67	0.00	0.00	0.59	0.00	0.00	0.00	2.5	0.0	37.92	0.00	0.00	0.00
386_AV	26.87	15.12	30.45	536.85	0.00	3.91	745.62	372.81	0.25	0.63	0.00	0.00	10.0	1.0	27.76	0.00	0.00	0.00
387_AV	45.26	15.93	46.42	288.54	0.00	2.98	0.00	458.00	0.87	0.00	0.00	0.00	17.5	1.0	12.65	6.70	0.00	0.00
388_AV	23.73	8.15	22.55	510.08	0.00	3.76	708.45	354.22	0.23	0.00	0.00	0.00	5.0	2.5	20.72	1.83	0.00	0.00
389_AV	30.96	14.61	41.69	553.57	0.00	3.83	1,447.24	361.81	0.40	0.67	0.69	0.00	10.0	2.5	34.80	0.00	0.00	0.00
392_AV	30.86	10.74	37.62	502.99	0.00	4.00	0.00	0.00	0.00	0.00	0.00	0.00	5.0	0.0	37.62	0.00	0.00	0.00
397_AV	46.49	13.67	55.88	329.21	0.00	3.63	0.00	0.00	0.34	0.00	0.00	0.00	10.0	1.0	48.98	6.90	0.00	0.00
403_AV	22.18	7.96	34.65	897.16	0.00	3.90	0.00	0.00	0.11	0.00	0.00	0.00	2.5	1.0	33.52	1.13	0.00	0.00
408_AV	36.02	14.05	55.45	544.10	0.00	1.42	403.04	0.00	0.37	0.00	0.00	0.00	37.0	12.5	7.85	47.60	0.00	0.00
410_AV	48.75	16.20	97.10	520.29	0.00	3.48	0.00	0.00	0.48	0.00	0.00	0.00	10.0	1.0	79.73	16.37	0.00	0.00
411_AV	36.28	16.88	33.11	320.35	0.00	4.00	0.00	0.00	0.00	0.00	0.00	0.00	20.0	1.0	33.11	0.00	0.00	0.00
412_AV	28.40	11.12	35.68	563.08	0.00	4.00	0.00	0.00	0.00	0.00	0.00	0.00	25.0	2.5	35.68	0.00	0.00	0.00
415_AV	40.38	22.20	66.30	517.67	0.00	4.00	0.00	0.00	0.00	0.00	0.00	0.00	1.0	1.0	66.30	0.00	0.00	0.00
416_AV	34.23	12.82	36.14	392.67	0.00	4.00	0.00	0.00	0.00	0.00	0.00	0.00	2.5	1.0	36.14	0.00	0.00	0.00
417_AV	33.57	13.58	30.72	347.01	0.00	4.00	771.13	385.56	0.00	0.00	0.00	0.00	5.0	1.0	30.72	0.00	0.00	0.00

Appendix 5: Environmental variables selected for the RF analysis

Table 10: Environmental variables (1).

Plot	Elevation (m a.s.l.)	Precipitation (kg m⁻² ha⁻¹)	Mean diurnal temperature range (°C)	Slope (°)	Southness (-)	Eastness (-)	TPI (-)	TWI (-)	Distance to buildings (m)	Distance to roads (m)	Dense forest cover (ha)	Distance to dense forest (m)	Grassland cover (ha)	Grassland patch density (nb ha⁻¹)
1_P	1,306.98	1,074.78	8.74	24.65	-0.10	0.99	0.02	5.78	270.72	26.75	3.37	0.00	0.07	29.06
2_P	1,646.34	1,366.33	8.70	32.72	-0.96	0.25	0.12	3.09	348.14	153.42	0.76	9.99	0.21	116.26
3_P	971.23	1,221.89	8.70	27.45	0.25	-0.96	0.10	3.63	273.32	34.40	0.81	31.58	1.98	58.13
4_P	1,377.68	1,314.27	8.73	6.77	0.56	0.82	0.03	4.57	191.15	22.12	0.00	507.35	2.75	29.15
5_P	1,658.50	1,366.33	8.70	40.63	0.05	0.95	-0.35	4.86	443.96	395.94	0.03	89.88	0.69	86.44
6_P	1,340.04	1,280.16	7.95	23.06	0.96	0.23	-0.03	4.53	156.88	22.81	0.00	196.96	3.15	29.15
12_P	1,406.93	1,314.27	8.73	51.27	-0.65	0.75	-0.31	4.20	88.66	38.05	0.00	190.79	2.21	87.45
16_P	1,330.14	1,451.01	8.70	20.37	-0.26	0.84	0.25	3.18	472.50	10.63	0.82	58.23	0.33	115.59
19_P	1,199.21	1,229.66	8.75	7.98	0.31	0.90	-0.02	6.09	127.16	25.24	0.37	49.93	2.84	87.70
20_P	1,637.45	1,366.33	8.70	39.58	-0.86	-0.02	-0.99	4.69	416.07	370.15	0.00	139.81	0.74	58.13
22_P	1,261.72	1,463.25	8.69	36.93	0.85	-0.51	0.21	4.26	186.38	207.21	0.05	85.32	0.67	86.94
24_P	1,357.71	1,314.27	8.73	9.95	0.23	0.38	0.33	3.91	54.50	35.80	0.00	260.41	3.50	28.57
26_P	1,618.80	1,404.60	7.71	22.47	0.94	-0.29	-0.15	4.62	233.88	40.02	0.28	76.05	0.74	58.13
27_P	1,187.79	1,600.23	8.65	7.35	0.24	0.92	-0.05	5.78	145.57	59.43	0.00	155.35	1.30	29.23
29_P	1,190.49	1,145.07	8.72	36.90	0.78	-0.62	0.00	4.19	175.73	13.45	0.94	0.00	1.96	67.98
30_P	1,246.09	1,268.01	8.70	30.30	-0.77	0.63	0.06	3.82	322.35	603.74	1.38	29.96	0.00	0.00
31_P	1,141.60	1,268.01	8.70	19.18	-0.84	0.30	0.49	3.47	245.04	40.86	2.43	0.00	0.12	58.30
34_P	1,131.52	1,161.74	8.45	25.93	0.78	0.61	0.11	4.42	191.76	813.73	0.34	58.23	1.29	145.74
35_P	1,236.68	1,243.44	8.46	24.65	0.67	-0.72	-0.16	3.89	248.72	826.08	0.27	69.91	0.27	87.19
37_P	1,456.86	1,386.29	8.70	39.80	-0.80	-0.59	0.06	3.59	32.85	16.83	0.03	94.74	2.57	29.23
39_P	1,218.31	1,268.54	8.34	31.41	0.89	-0.45	-0.10	5.01	280.13	17.38	0.00	622.85	1.87	58.47
42_P	1,652.93	1,366.33	8.70	34.46	-0.98	-0.17	-0.10	4.14	375.75	243.80	0.48	50.92	0.92	58.81
44_P	1,759.43	1,716.19	8.60	42.15	-0.99	-0.13	0.10	3.73	170.65	284.19	0.00	365.70	0.00	0.00
45_P	1,490.09	1,178.56	8.70	37.34	-0.07	0.98	-0.34	4.96	189.05	32.44	1.00	22.33	0.10	57.96
49_P	1,890.59	1,647.38	7.70	23.06	-0.96	-0.15	0.16	4.35	98.61	75.27	0.00	678.05	3.05	57.96
51_P	1,614.42	1,350.66	7.70	33.61	0.65	-0.76	0.19	5.68	76.21	42.93	0.02	22.33	0.01	43.60
56_P	1,653.08	1,350.66	7.70	31.62	0.88	-0.46	0.03	4.18	184.24	223.68	2.03	0.00	0.04	29.06
60_P	1,461.80	1,451.01	8.70	25.53	-0.44	0.89	-0.05	4.96	318.49	717.54	0.52	66.99	1.58	57.96
62_P	1,379.53	1,268.01	8.70	31.61	-0.77	0.63	0.11	5.17	439.38	594.76	0.38	22.33	0.68	86.94
63_P	1,809.01	1,470.91	7.70	21.37	-0.92	-0.39	-0.08	5.20	225.94	16.13	3.28	0.00	0.14	87.19
65_P	1,151.28	1,152.49	8.33	48.38	-0.83	0.50	0.74	2.71	127.85	166.97	0.00	339.69	1.08	145.32
66_P	949.42	1,118.88	8.70	33.94	-0.87	0.49	0.07	4.10	81.76	103.29	2.60	0.00	0.11	35.68
67_P	1,312.36	1,386.29	8.70	35.88	-0.68	-0.72	0.17	3.57	451.29	16.24	2.07	0.00	0.38	145.74
70_P	1,778.26	1,470.91	7.70	29.58	-0.75	0.66	-0.11	4.91	205.67	20.39	2.73	0.00	0.00	0.00
72_P	1,497.27	1,709.58	8.61	26.07	1.00	0.07	-0.07	5.03	32.55	47.03	0.00	385.87	1.91	57.96
73_P	1,645.01	1,314.27	8.73	36.65	0.81	0.57	0.12	3.30	126.26	31.97	0.00	357.98	1.28	115.59
74_P	1,564.67	1,463.12	8.77	26.50	-0.15	0.98	0.10	4.80	245.77	162.50	0.03	100.36	2.61	29.15
75_P	1,610.05	1,169.28	8.27	32.09	0.93	0.36	0.11	3.63	218.25	270.83	0.00	101.84	1.15	144.90
76_P	1,500.64	1,325.13	8.47	41.80	0.20	-0.91	-0.15	2.78	175.16	627.64	0.00	760.54	1.50	116.94
77_P	1,611.31	1,783.22	8.62	27.43	0.73	0.67	-0.08	4.48	477.88	197.06	0.00	369.63	0.45	86.94
78_P	1,461.34	1,193.82	8.21	34.69	1.00	-0.02	0.15	5.73	348.21	4.31	0.00	450.39	0.80	58.13
79_P	1,706.10	1,716.19	8.60	22.17	0.62	0.78	0.01	5.00	29.17	9.08	0.00	402.57	1.35	85.46
81_P	1,376.49	1,540.09	8.65	36.99	0.88	0.47	-0.02	4.29	323.51	301.51	0.82	36.01	0.24	87.19
82_P	1,504.97	1,169.28	8.27	29.40	0.94	0.34	-0.11	3.60	261.15	2.18	0.00	192.09	3.21	29.06
84_P	1,066.19	1,167.03	8.07	33.00	0.90	0.41	-0.20	5.16	268.61	305.52	1.33	14.12	0.14	29.15
85_P	1,487.81	1,276.97	7.97	34.98	0.83	-0.54	0.11	3.87	224.83	179.42	0.00	121.90	2.07	29.23
87_P	1,240.43	1,152.49	8.33	35.80	-0.13	0.96	-0.26	5.36	202.02	237.19	0.00	467.55	0.50	174.39

Table 11: Environmental variables (2).

Plot	Elevation (m a.s.l.)	Precipitation (kg m⁻² ha⁻¹)	Mean diurnal temperature range (°C)	Slope (°)	Southness (-)	Eastness (-)	TPI (-)	TWI (-)	Distance to buildings (m)	Distance to roads (m)	Dense forest cover (ha)	Distance to dense forest (m)	Grassland cover (ha)	Grassland patch density (plt ha⁻¹)
88_P	1,517.46	1,193.82	8.21	30.22	0.97	-0.10	0.06	3.12	320.08	75.70	0.00	531.63	0.78	58.13
90_P	1,487.06	1,202.98	8.15	37.86	0.89	-0.41	-0.03	3.06	476.86	26.84	0.14	89.32	0.75	58.13
91_P	1,716.39	1,346.59	8.70	34.43	-0.87	0.49	0.06	3.79	389.96	383.63	0.14	56.49	0.71	116.26
92_P	1,328.45	1,188.43	8.11	38.65	0.79	0.58	0.07	4.01	305.48	36.04	0.00	127.89	1.47	87.19
93_P	796.54	1,042.91	8.42	36.66	0.78	0.59	0.15	3.25	359.09	439.92	0.18	56.49	0.24	87.19
94_P	1,286.58	1,235.47	8.28	59.73	0.68	-0.72	-0.11	3.41	275.72	284.79	0.09	76.05	3.17	29.06
95_P	1,462.03	1,364.56	8.29	46.05	0.87	0.47	-0.25	3.81	92.69	5.61	0.00	620.45	2.03	29.15
96_P	1,301.26	1,188.43	8.11	42.46	0.97	-0.24	-0.12	2.98	291.73	13.73	0.00	233.14	3.39	29.06
97_P	1,626.96	1,356.15	8.76	31.84	0.50	-0.85	-0.16	4.60	662.88	499.48	0.00	182.24	3.45	28.98
98_P	1,296.25	1,236.40	8.76	41.25	0.96	-0.28	0.00	4.75	165.27	32.19	0.01	72.01	0.31	148.55
99_P	1,229.07	1,540.09	8.65	22.08	0.47	0.88	-0.16	4.61	159.64	9.38	0.14	70.61	0.61	58.30
100_P	1,627.10	1,229.66	8.75	39.59	0.16	-0.97	0.29	2.90	742.46	415.35	0.34	41.18	2.92	28.65
101_P	1,362.21	1,540.09	8.65	29.47	-0.60	0.03	0.03	3.97	41.03	0.84	0.00	119.84	2.56	29.06
102_P	1,540.76	1,246.06	8.42	34.52	0.65	0.75	-0.07	4.48	334.39	374.57	0.00	819.44	3.08	28.98
103_P	1,864.30	1,478.59	8.70	38.23	-0.99	-0.09	-0.15	5.14	677.35	615.65	0.00	290.29	0.05	29.23
104_P	1,091.63	1,343.12	8.70	34.50	-0.72	0.69	0.04	5.12	351.15	85.66	0.87	29.96	2.18	29.15
105_P	1,025.75	1,343.12	8.70	7.46	-0.64	0.74	-0.01	4.95	279.81	33.80	1.43	14.12	1.50	29.06
106_P	1,240.80	1,286.29	8.70	56.87	0.38	-0.93	0.01	3.27	457.26	65.51	0.58	28.25	1.45	87.19
107_P	1,332.09	1,178.56	8.70	37.18	0.57	0.82	0.09	4.99	170.10	23.31	0.20	41.18	2.42	145.32
108_P	1,357.68	1,386.29	8.70	37.05	-0.25	-0.97	-0.04	4.76	281.64	0.05	0.46	19.97	2.08	58.30
110_P	857.97	1,105.80	8.31	22.08	0.98	0.17	-0.08	4.44	321.51	274.80	0.46	49.93	1.50	58.30
111_P	1,363.36	1,386.29	8.70	19.09	-0.16	0.98	-0.06	5.01	209.34	591.09	0.35	58.23	0.55	87.70
112_P	1,797.04	1,346.59	8.70	30.11	-0.93	0.36	0.00	4.19	538.05	503.74	0.00	170.65	0.84	87.45
113_P	1,222.93	1,105.51	8.72	36.62	-0.21	0.95	-0.39	5.39	220.98	95.65	1.42	42.37	0.59	87.19
114_P	1,405.23	1,281.66	8.78	32.99	0.96	0.24	-0.33	5.95	141.51	96.05	0.04	98.86	1.49	59.33
115_P	1,576.08	1,451.01	8.70	29.53	-0.49	0.87	0.06	4.77	339.55	597.75	0.56	44.66	0.34	28.98
116_P	1,659.48	1,366.33	8.70	44.59	-0.96	0.07	-0.10	2.75	392.63	361.79	0.00	160.09	0.90	87.45
117_P	1,527.38	1,178.56	8.70	28.95	-0.04	0.95	-0.18	5.67	330.12	149.51	0.43	29.96	0.88	29.15
118_P	1,359.41	1,268.01	8.70	25.77	0.09	0.99	0.23	3.80	320.98	296.97	0.17	63.16	0.58	58.30
119_P	1,161.65	1,152.49	8.33	37.74	-0.66	0.69	0.45	2.48	224.41	216.16	0.00	426.97	1.57	29.06
121_P	897.60	1,167.25	8.09	15.57	0.86	-0.39	-0.16	5.47	162.97	177.35	2.27	0.00	0.00	0.00
122_P	1,448.68	1,276.97	7.97	24.50	0.49	-0.85	0.19	3.21	42.92	18.64	0.00	120.25	1.58	85.95
123_P	1,530.70	1,356.15	8.76	21.76	0.25	-0.96	0.05	4.41	469.36	297.65	0.82	0.00	2.28	29.15
124_P	1,352.97	1,229.66	8.75	37.27	0.64	-0.76	0.04	3.69	387.86	23.01	1.56	0.00	1.70	116.60
125_P	1,400.74	1,229.66	8.75	44.11	0.54	-0.83	0.35	4.00	408.09	74.67	1.39	0.00	1.71	86.69
126_P	1,571.03	1,260.42	8.72	24.67	-0.28	0.93	-0.04	5.18	260.45	27.38	0.92	0.00	0.60	115.92
127_P	1,573.02	1,234.85	8.70	28.23	-0.26	0.91	-0.29	6.18	155.82	44.82	2.41	0.00	0.28	29.15
128_P	1,207.42	1,145.07	8.72	35.83	-0.56	0.71	-0.33	4.75	94.27	31.34	2.85	0.00	0.01	34.82
129_P	1,329.73	1,105.51	8.72	43.97	0.72	0.67	-0.08	2.91	243.27	54.14	2.46	0.00	0.14	29.15
130_P	1,269.02	1,074.78	8.74	35.96	-0.48	0.88	-0.14	3.42	331.62	3.80	3.43	0.00	0.00	0.00
131_P	1,235.29	1,074.78	8.74	31.50	-0.75	0.63	0.31	3.75	324.78	38.88	3.13	0.00	0.08	29.23
132_P	1,384.53	1,074.78	8.74	38.70	-0.42	0.69	-0.74	6.30	317.50	92.99	2.13	0.00	0.30	87.19
133_P	1,165.80	1,060.26	8.74	33.31	-0.51	0.83	-0.43	5.57	410.61	90.26	2.26	0.00	0.76	29.41
135_P	1,370.27	1,343.12	8.70	39.07	-0.84	0.50	0.31	2.71	513.57	79.59	1.83	0.00	0.57	87.19
136_P	1,059.81	1,117.11	8.70	49.87	0.31	0.95	-0.02	3.64	142.11	212.77	1.60	0.00	0.07	35.68
137_P	1,076.35	1,117.11	8.70	40.95	-0.40	0.91	-0.04	3.94	215.81	210.71	3.01	0.00	0.24	29.23
138_P	1,065.43	1,343.12	8.70	34.00	-0.93	-0.34	-0.25	3.23	203.96	104.60	1.63	0.00	0.17	29.06
139_P	1,057.89	1,343.12	8.70	30.14	-0.93	0.37	0.15	3.11	269.07	255.02	2.30	0.00	0.58	29.06
140_P	954.24	1,268.01	8.70	31.96	-0.74	0.67	0.06	4.57	98.41	188.65	2.46	0.00	0.70	58.13
141_P	1,595.40	1,451.01	8.70	35.45	-0.89	0.46	0.03	4.02	236.82	704.56	1.86	0.00	0.38	57.63

Table 12: Environmental variables (3).

Plot	Elevation (m a.s.l.)	Precipitation (kg m^{-2} ha^{-1})	Mean diurnal temperature range (°C)		Slope (°)	Southness (-)	Eastness (-)	TPI (-)	TWI (-)	Distance to buildings (m)	Distance to roads (m)	Dense forest cover (ha)	Distance to dense forest (m)	Grassland cover (ha)	Grassland patch density (nb ha^{-1})
142_P	1,231.95	1,386.39	8.70	40.53	-0.95	0.16	0.61	2.55		385.88	3.44	2.61	9.99	0.46	58.13
143_P	1,192.90	1,200.65	7.92	25.63	0.45	0.88	-0.12	4.46		188.43	12.78	0.47	19.97	0.47	174.89
144_P	968.12	1,038.72	8.44	30.83	0.88	-0.46	0.05	3.76		197.56	236.85	3.17	0.00	0.00	0.00
145_P	1,624.45	1,386.29	8.70	34.37	-0.63	0.71	0.44	2.94		39.17	15.14	0.17	82.35	2.60	57.96
6_AV	1,633.79	1,241.69	8.25	30.64	0.26	-0.96	-0.12	4.83		394.94	35.06	2.29	0.00	0.38	29.15
7_AV	1,664.40	1,241.69	8.25	30.47	0.30	-0.94	0.19	3.23		516.70	25.70	1.84	14.12	1.00	29.23
11_AV	2,156.73	1,224.93	8.26	27.96	-0.60	-0.79	-0.07	5.24		610.24	28.47	0.00	166.21	0.88	87.45
13_AV	2,130.91	1,256.31	8.26	34.19	-1.00	0.06	-0.18	4.66		797.41	30.19	1.00	0.00	1.97	29.15
18_AV	1,182.19	1,105.83	8.25	6.34	-0.69	-0.28	-0.20	7.78		39.76	19.93	1.69	14.12	0.89	87.19
19_AV	2,078.48	1,256.31	8.26	27.35	-0.38	-0.92	-0.12	4.45		925.68	27.84	0.21	58.23	3.24	28.98
20_V	1,380.67	1,123.21	8.30	29.42	-0.95	0.32	0.14	4.18		116.96	60.03	0.07	72.01	2.81	30.48
24_AV	1,616.46	1,322.97	8.20	28.53	-0.08	-0.98	-0.24	5.13		106.50	63.62	0.73	42.37	1.85	116.94
28_AV	1,199.55	1,148.31	8.20	16.97	-0.89	-0.32	0.28	3.51		50.77	13.90	0.33	19.97	2.65	28.81
33_AV	1,538.76	1,322.97	8.20	19.78	-0.12	-0.99	0.00	5.21		431.20	25.37	1.90	14.12	1.17	87.70
34_AV	1,323.79	1,362.19	8.22	16.95	-0.80	-0.55	-0.02	4.11		235.02	70.43	0.59	66.99	2.81	29.41
46_AV	1,739.21	1,237.47	8.30	24.10	-0.92	-0.37	-0.05	3.67		30.62	15.69	1.68	0.00	0.50	29.15
47_AV	1,321.72	1,362.19	8.22	10.65	-0.41	-0.88	-0.08	5.67		126.90	57.38	0.27	9.99	1.97	84.62
50_AV	1,355.95	1,362.19	8.22	11.28	-0.75	-0.65	-0.03	7.19		186.34	41.05	0.22	41.18	2.42	37.28
51_AV	1,327.94	1,190.98	8.20	17.37	0.60	0.79	-0.02	4.78		81.24	135.80	0.14	89.32	3.27	29.23
53_AV	1,898.99	1,389.88	8.29	37.28	-0.67	0.72	0.30	4.04		295.40	15.06	0.90	14.12	0.79	28.98
54_AV	1,832.16	1,357.09	8.22	18.50	-0.97	-0.13	0.14	3.62		22.18	61.72	0.79	29.96	2.02	56.81
56_AV	1,326.33	1,190.98	8.20	22.80	0.17	0.98	0.11	4.37		93.46	110.21	0.00	121.90	3.08	29.15
60_AV	1,916.43	1,312.70	8.30	30.72	-0.68	0.73	0.06	3.50		803.09	19.34	0.18	28.25	0.50	87.45
61_AV	1,991.92	1,382.07	8.25	27.37	-0.95	0.29	-0.12	4.15		30.65	26.06	0.00	119.84	1.84	28.90
62_AV	1,407.45	1,409.08	8.19	19.40	-0.73	-0.68	0.06	5.44		286.10	31.43	1.02	9.99	1.47	39.79
64_AV	1,432.37	1,409.08	8.19	8.83	-0.15	-0.98	-0.03	6.67		155.76	90.56	0.34	14.12	2.82	30.29
65_AV	2,075.48	1,382.07	8.25	30.17	-0.99	0.10	-0.04	3.91		160.36	93.03	0.00	190.79	2.11	87.45
67_AV	1,834.37	1,279.53	8.30	21.07	-0.57	0.82	-0.07	4.27		57.90	42.64	0.00	250.46	2.63	29.06
68_AV	1,331.38	1,190.98	8.20	20.36	-0.50	0.84	0.13	4.14		413.85	66.23	0.00	279.62	2.71	28.81
70_AV	1,432.61	1,246.35	8.30	14.39	0.05	0.84	-0.26	7.06		201.78	24.37	0.00	177.80	1.90	58.30
71_AV	2,196.56	1,357.09	8.22	21.32	-0.98	-0.15	0.18	3.72		600.25	67.20	0.00	424.63	3.37	29.15
72_AV	1,587.70	1,246.35	8.30	23.06	-0.10	0.99	-0.09	7.57		249.96	13.35	1.03	41.18	1.88	28.81
73_AV	1,772.57	1,246.35	8.30	33.62	-0.41	0.87	0.16	4.22		110.87	16.26	0.75	58.23	2.17	87.19
75_AV	1,683.54	1,246.35	8.30	34.99	-0.49	0.86	-0.14	4.08		40.54	15.96	1.16	22.33	2.05	58.47
82_AV	1,780.64	1,369.20	8.30	34.99	-0.62	0.78	-0.12	3.82		39.27	6.65	0.91	22.33	2.05	87.19
87_AV	1,361.05	1,233.38	8.18	9.94	-0.73	0.58	0.15	4.15		360.65	111.36	0.00	219.02	3.42	29.06
90_AV	1,557.20	1,473.97	8.16	20.83	-0.50	-0.87	-0.07	4.90		181.10	12.07	0.65	50.92	2.30	87.19
91_AV	1,864.71	1,369.20	8.30	30.45	0.33	0.93	0.17	2.89		382.49	5.55	0.38	19.97	2.05	86.94
93_AV	1,900.69	1,489.15	8.28	36.28	-0.59	0.80	0.16	3.56		311.94	11.55	0.62	42.37	2.28	29.23
94_AV	1,367.77	1,233.38	8.18	5.49	-0.80	0.43	0.01	5.18		166.83	120.90	0.00	101.84	3.38	29.15
95_AV	1,376.72	1,233.38	8.18	13.93	-0.43	-0.89	-0.15	6.15		131.43	24.81	0.37	29.96	2.63	29.15
97_AV	2,054.62	1,489.15	8.28	30.76	-0.77	0.63	-0.09	4.20		72.92	67.02	0.00	110.30	1.80	87.70
104_AV	1,429.77	1,233.38	8.18	9.83	-0.79	-0.48	0.20	4.67		101.75	41.67	0.27	41.18	2.85	58.13
108_AV	1,414.02	1,233.38	8.18	10.91	-0.86	-0.41	0.25	4.58		56.81	37.49	0.28	9.99	2.47	29.32
110_AV	1,461.39	1,275.25	8.13	9.97	-0.82	-0.43	0.19	3.87		143.17	29.44	0.10	69.91	2.68	58.13
111_AV	1,551.23	1,275.25	8.13	36.80	0.05	-0.98	-0.17	5.72		285.59	6.60	0.54	36.01	2.12	58.30
112_AV	1,482.32	1,275.25	8.13	11.90	0.05	-0.99	-0.08	6.04		61.70	44.82	0.00	120.25	3.43	29.06
115_AV	2,153.61	1,537.74	8.29	20.20	-0.84	0.53	-0.04	5.06		99.45	15.25	0.00	260.41	0.27	116.26
116_AV	1,758.98	1,378.49	8.30	26.72	-0.50	0.86	-0.03	3.76		45.61	27.03	1.43	0.00	1.09	28.98
119_AV	1,928.14	1,378.49	8.30	29.50	-0.84	0.54	0.12	3.78		28.73	11.69	0.31	63.94	2.36	29.06

Table 13: Environmental variables (4).

Plot	Elevation (m a.s.l.)	Precipitation (kg m⁻² ha⁻¹)	Mean diurnal temperature range (°C)		Slope (°)	Southness (-)	Eastness (-)	TPI (-)	TWI (-)	Distance to buildings (m)		Distance to roads (m)		Dense forest cover (ha)		Distance to dense forest (m)		Grassland cover (ha)		Grassland patch density (no ha⁻¹)	
120_AV	1,458.84	1,275.25		8.13	4.31	-0.84	-0.52	0.02	5.19		82.02		18.15		0.00		190.79		3.37		29.15
122_AV	2,156.69	1,537.74		8.29	6.72	-0.80	-0.58	-0.02	6.10		86.45		29.43		0.00		112.98		2.74		29.06
125_AV	1,466.75	1,275.25		8.13	25.40	-0.09	1.00	-0.18	6.86		99.69		116.83		0.00		120.67		3.42		29.15
127_AV	1,531.49	1,332.81		8.32	20.81	-0.37	0.92	-0.11	6.67		361.56		78.93		0.94		29.96		2.13		29.84
128_AV	2,137.76	1,527.38		8.29	35.75	0.49	0.87	-0.05	4.48		242.31		20.39		0.00		235.05		2.88		29.41
129_AV	1,475.91	1,323.61		8.10	13.42	-0.15	0.98	-0.01	4.07		104.58		65.47		0.06		89.32		3.17		29.15
130_AV	2,199.06	1,527.38		8.29	20.48	-0.88	0.39	0.26	4.49		330.44		112.93		0.00		335.70		3.43		29.15
132_AV	1,614.97	1,177.18		8.39	13.97	0.12	0.98	-0.17	4.92		203.96		3.37		0.26		39.95		0.78		99.94
133_AV	1,672.69	1,332.81		8.32	23.96	-0.62	0.78	-0.07	4.93		155.43		69.44		0.44		28.25		2.65		58.13
134_AV	1,638.79	1,177.18		8.39	8.01	-0.86	-0.45	0.03	4.49		117.62		5.64		0.93		9.99		1.18		91.16
135_AV	1,620.16	1,554.79		8.10	15.54	-0.59	-0.65	-0.06	5.50		90.86		113.77		0.36		22.33		1.06		180.13
136_AV	1,505.47	1,323.61		8.10	9.09	-0.73	0.55	-0.13	5.17		326.06		70.67		0.10		80.51		3.32		29.06
138_AV	1,653.28	1,327.26		8.09	33.76	0.55	-0.83	-0.12	4.23		500.58		29.34		0.00		269.82		3.13		29.06
142_AV	1,643.27	1,214.10		8.41	12.60	-0.08	0.98	-0.10	5.38		153.22		20.39		2.21		0.00		0.51		57.30
143_AV	1,725.89	1,370.32		8.08	19.97	-0.86	0.46	0.00	4.39		483.22		39.88		0.84		22.33		1.60		87.45
146_AV	2,250.12	1,497.81		8.60	28.08	-0.90	-0.40	-0.22	3.89		536.16		15.73		1.36		9.99		1.38		29.15
148_AV	1,680.99	1,303.67		8.33	18.20	-0.14	-0.95	0.14	3.50		108.63		70.86		1.35		9.99		1.35		29.06
151_AV	1,731.40	1,478.98		8.29	22.24	0.51	0.83	-0.20	5.17		78.64		40.09		0.08		59.92		0.25		116.26
152_AV	2,010.67	1,412.50		8.04	37.25	-0.09	0.98	-0.29	5.93		338.79		49.11		1.57		0.00		1.25		57.96
155_AV	2,219.63	1,409.37		8.55	22.60	-0.81	-0.56	-0.06	4.47		220.91		31.50		0.13		84.74		2.28		29.06
156_AV	1,572.12	1,370.32		8.08	25.29	-0.17	0.98	-0.01	6.35		155.13		67.61		0.08		29.96		3.39		28.81
158_AV	2,067.65	1,409.37		8.55	16.37	-0.96	0.27	-0.02	4.09		451.06		11.20		1.74		22.33		0.66		87.19
159_AV	1,577.39	1,326.39		8.07	26.01	-0.31	-0.95	0.06	5.70		83.99		53.49		0.00		155.35		2.21		87.70
160_AV	2,117.73	1,409.37		8.55	22.06	-0.94	0.33	-0.07	3.93		319.36		3.91		0.94		19.97		0.72		58.30
161_AV	1,713.55	1,478.98		8.29	22.93	0.25	0.95	-0.06	4.12		242.79		26.82		0.00		170.06		0.56		58.13
164_AV	1,698.01	1,269.44		8.43	29.90	-0.34	-0.93	0.10	4.53		182.28		62.36		0.10		79.89		1.23		115.59
166_AV	1,642.12	1,412.50		8.04	25.28	0.14	0.99	-0.13	5.82		146.27		119.01		0.00		123.53		2.98		58.13
168_AV	1,691.89	1,478.98		8.29	17.22	0.39	0.90	-0.16	7.02		132.22		34.21		0.00		354.20		1.44		29.06
169_AV	1,701.26	1,269.44		8.43	22.47	-0.23	-0.97	-0.10	5.57		133.37		36.72		0.00		176.96		2.74		28.98
170_AV	1,819.68	1,478.98		8.29	38.66	0.38	0.92	0.00	3.57		267.72		39.29		0.00		120.67		0.28		28.98
171_AV	1,727.02	1,478.98		8.29	22.16	0.52	0.85	0.04	4.59		202.41		15.98		0.00		149.80		3.02		29.06
174_AV	1,994.29	1,664.99		8.26	27.69	-0.41	0.89	0.12	3.94		109.99		2.77		0.06		70.61		1.55		144.07
175_AV	1,589.99	1,325.53		8.06	31.57	0.01	-1.00	-0.12	5.29		85.49		33.53		0.00		139.81		3.43		29.15
176_AV	1,709.42	1,269.44		8.43	21.61	0.03	0.99	0.03	5.17		241.88		25.58		0.00		198.23		2.27		29.06
178_AV	1,755.61	1,591.05		8.01	25.20	-0.12	-0.97	-0.11	5.28		258.71		41.95		1.03		28.25		1.72		72.93
179_AV	1,585.30	1,346.36		8.01	8.38	-0.22	-0.96	0.03	4.70		131.05		40.67		0.37		9.99		1.75		116.60
181_AV	2,083.47	1,663.85		8.22	31.02	-0.35	0.92	-0.05	6.07		142.68		97.25		0.00		281.22		3.44		28.98
182_AV	1,768.10	1,591.05		8.01	29.92	-0.31	-0.95	0.01	3.83		139.18		189.98		0.39		0.00		2.35		36.46
183_AV	1,741.67	1,370.77		8.42	30.24	-0.34	0.94	0.10	4.64		598.37		18.50		0.00		166.21		3.03		58.30
186_AV	2,182.14	1,663.85		8.22	32.47	-0.17	0.98	-0.20	4.17		96.73		112.48		0.00		417.28		3.44		29.06
187_AV	2,023.14	1,558.72		8.00	17.37	-0.17	-0.96	-0.11	7.98		520.27		41.03		0.81		39.95		0.67		87.19
188_AV	1,931.36	1,558.72		8.00	9.89	-0.10	-0.96	0.17	4.01		351.23		16.54		0.78		22.33		1.37		28.65
189_AV	2,226.42	1,859.32		8.20	41.89	-0.39	0.92	-0.03	3.35		387.83		373.61		0.00		346.66		3.39		29.41
194_AV	1,886.76	1,591.05		8.01	30.05	-0.17	-0.98	-0.19	4.76		351.00		34.84		0.52		44.66		1.33		29.15
195_AV	1,614.29	1,346.36		8.01	34.06	0.06	0.99	-0.10	6.61		190.54		43.03		0.00		171.81		2.06		87.19
196_AV	2,263.45	1,558.72		8.00	36.60	-0.35	-0.94	0.06	3.24		552.04		20.25		1.11		0.00		1.71		29.23
202_AV	1,768.10	1,370.77		8.42	33.15	-0.22	0.97	0.01	5.03		525.46		15.64		0.00		679.08		3.47		28.81
203_AV	1,669.59	1,346.36		8.01	31.33	0.02	-1.00	0.06	6.00		99.23		125.44		0.02		31.58		1.89		29.41
204_AV	1,852.75	1,591.05		8.01	22.72	-0.27	-0.94	0.13	3.46		286.92		25.80		1.88		9.99		1.35		29.06
205_AV	1,947.93	1,508.87		8.00	25.87	-0.19	0.95	0.17	3.24		133.15		7.83		0.07		79.89		0.67		147.03

Table 14: Environmental variables (5).

Plot	Elevation (m a.s.l.)	Precipitation (kg m⁻² ha⁻¹)	Mean diurnal temperature range (°C)		Slope (°)	Southness (-)	Eastness (-)	TPI (-)	TWI (-)	Distance to buildings (m)	Distance to roads (m)	Dense forest cover (ha)	Distance to dense forest (m)	Grassland cover (ha)	Grassland patch density (nb ha⁻¹)
206_AV	2,225.16	1,390.97		8.02	35.69	-0.03	-1.00	0.04	3.63	523.13	14.27	0.09	49.93	2.05	29.15
207_AV	1,644.72	1,346.36		8.01	10.61	-0.69	-0.63	0.15	5.93	150.55	79.27	0.00	198.23	2.66	57.96
208_AV	1,707.75	1,675.95		8.21	13.33	-0.76	-0.64	-0.09	6.30	70.79	30.57	0.00	291.67	3.21	28.81
213_AV	1,923.21	1,407.83		8.00	23.37	-0.01	-0.95	0.49	3.27	620.69	29.69	2.13	19.97	0.96	88.48
214_AV	1,724.84	1,688.05		8.20	27.74	-0.30	-0.95	0.07	3.78	215.00	83.02	0.00	157.90	2.92	29.15
215_AV	1,669.36	1,389.43		8.00	15.39	-0.18	-0.89	0.16	4.09	165.39	67.54	0.00	113.86	3.40	29.41
216_AV	2,198.50	1,426.24		8.00	35.72	0.24	-0.97	0.17	5.46	964.15	31.18	1.06	0.00	1.70	29.06
217_AV	1,737.99	1,389.43		8.00	31.28	0.40	0.92	-0.10	5.01	165.09	18.11	1.26	41.18	2.12	29.58
218_AV	2,218.98	1,508.87		8.00	22.42	-0.22	0.97	-0.05	5.02	554.05	360.15	0.30	58.23	2.59	28.65
220_AV	1,737.91	1,688.05		8.20	15.49	-0.14	-0.98	0.06	5.40	237.81	56.92	0.00	205.88	3.15	29.06
221_AV	1,997.06	1,603.71		7.98	19.25	-0.38	-0.92	0.00	4.85	587.44	23.07	1.28	19.97	1.54	29.06
222_AV	2,174.37	1,601.01		7.97	12.87	-0.46	-0.80	-0.13	6.43	397.92	35.69	0.00	352.93	2.37	58.13
224_AV	2,217.29	1,508.87		8.00	21.51	0.77	0.63	0.04	5.92	481.06	340.09	0.00	138.74	3.38	29.15
235_AV	1,780.54	1,733.00		8.19	13.89	-0.34	-0.94	-0.02	5.23	537.50	49.44	0.01	102.82	2.35	58.30
239_AV	1,792.31	1,733.00		8.19	5.79	-0.16	0.95	-0.02	5.03	1,061.02	82.32	0.00	210.66	1.66	58.13
243_AV	1,839.20	1,786.68		8.19	4.89	0.25	-0.85	0.02	5.91	591.30	63.76	0.19	66.99	1.62	28.73
248_AV	2,204.59	1,503.55		7.94	22.73	-0.41	-0.85	-0.27	6.07	122.53	46.53	0.00	449.39	2.52	29.06
249_AV	2,161.59	1,503.55		7.94	18.41	-0.19	-0.97	0.18	3.43	121.91	39.34	0.00	280.33	2.68	29.15
250_AV	2,048.59	1,514.31		7.90	32.37	-0.05	-0.99	-0.02	5.38	263.58	16.93	0.26	50.92	2.19	145.32
253_AV	1,855.77	1,514.31		7.90	8.29	-0.13	-0.88	-0.08	5.49	19.84	5.52	0.16	9.99	3.02	29.49
255_AV	1,973.05	1,669.06		7.85	21.62	-0.09	1.00	-0.03	6.30	55.08	74.47	0.00	198.23	2.71	29.06
263_AV	2,035.39	1,256.31		8.26	28.41	-0.72	-0.68	-0.09	5.49	857.75	52.86	0.87	42.37	2.50	29.23
264_AV	1,659.66	1,241.69		8.25	31.02	-0.85	-0.51	0.02	4.52	319.50	25.58	2.54	0.00	0.64	87.45
266_AV	1,386.83	1,123.21		8.30	25.50	-0.96	0.25	0.14	3.78	99.44	57.19	0.36	9.99	1.33	64.48
275_AV	1,628.34	1,282.33		8.23	31.20	-0.75	-0.66	0.12	4.54	65.86	49.23	0.72	0.00	2.09	87.19
276_AV	1,433.91	1,211.22		8.27	28.98	-0.11	0.96	0.10	3.59	25.67	12.30	0.00	236.74	0.00	0.00
286_AV	1,920.35	1,312.70		8.30	36.44	-0.63	0.77	0.15	3.49	621.50	17.68	0.00	110.30	0.17	86.94
287_AV	1,924.39	1,312.70		8.30	29.42	-0.91	0.40	0.09	3.10	454.51	32.67	0.00	236.74	0.46	116.94
288_AV	1,862.54	1,312.70		8.30	28.08	-0.60	0.78	0.39	4.07	210.47	29.17	0.00	299.76	3.12	29.15
289_AV	1,441.68	1,409.08		8.19	13.98	-0.89	-0.42	0.11	5.56	195.77	25.43	2.17	0.00	0.03	82.53
292_AV	2,210.04	1,357.09		8.22	24.43	-0.97	0.20	-0.03	4.80	406.02	46.00	0.00	353.92	2.61	28.73
294_AV	1,504.08	1,369.20		8.30	35.35	-0.97	0.22	0.15	3.07	198.49	66.33	0.25	70.61	1.57	29.15
296_AV	1,864.32	1,369.20		8.30	30.09	-0.66	0.75	-0.03	4.12	370.32	66.43	0.06	90.43	2.93	28.98
298_AV	1,418.11	1,233.38		8.18	22.61	-0.13	0.99	-0.06	4.55	165.78	10.34	0.21	60.75	1.76	176.43
299_AV	1,621.74	1,249.15		8.34	30.75	-0.25	0.97	-0.05	3.53	413.39	48.27	1.78	19.97	1.00	145.32
300_AV	1,556.22	1,249.15		8.34	20.16	-0.71	0.70	0.06	6.11	268.52	66.06	0.41	0.00	2.72	29.06
301_AV	1,632.82	1,177.18		8.39	14.22	0.13	-0.98	-0.02	4.31	268.37	5.37	0.11	89.32	0.00	0.00
307_AV	1,677.69	1,412.50		8.04	23.59	-0.76	0.64	-0.10	6.46	157.62	5.17	0.58	9.99	2.52	57.79
308_AV	1,989.09	1,664.99		8.26	37.54	0.44	0.89	0.14	2.67	226.22	48.48	0.22	31.58	1.22	170.92
309_AV	1,776.07	1,571.98		8.27	31.62	0.59	0.80	0.00	5.61	256.19	27.18	0.08	49.93	2.04	29.32
310_AV	1,634.35	1,346.36		8.01	37.90	-0.16	0.99	0.00	6.92	125.59	75.96	0.07	84.74	3.29	29.06
311_AV	1,693.10	1,552.34		8.26	9.01	0.39	0.90	-0.08	5.75	185.69	6.63	0.00	215.58	1.30	87.19
313_AV	2,185.61	1,390.97		8.02	24.03	0.76	-0.64	-0.11	4.71	610.04	32.43	0.08	28.25	1.50	58.47
320_AV	1,787.30	1,438.23		7.96	31.49	-0.21	-0.97	0.02	3.34	146.48	54.38	0.45	60.75	0.74	29.41
321_AV	1,796.23	1,483.36		7.91	41.19	-0.34	-0.92	0.12	3.94	112.76	20.68	0.00	113.86	0.00	0.00
323_AV	1,980.00	1,483.36		7.91	22.44	-0.02	1.00	0.02	5.55	362.25	21.23	0.00	174.69	0.60	145.32
325_AV	2,089.00	1,555.60		7.92	32.54	-0.34	0.93	-0.12	5.19	309.43	8.77	0.00	290.29	0.80	58.13
326_AV	1,876.09	1,514.31		7.90	35.93	0.00	-1.00	-0.18	5.89	264.73	240.16	1.17	0.00	2.09	28.98
327_AV	2,054.95	1,669.06		7.85	25.92	0.83	0.52	-0.20	4.55	330.79	29.53	0.14	49.93	1.83	58.13
328_AV	1,519.55	1,161.09		8.29	18.78	-0.22	-0.97	-0.06	4.89	36.76	32.80	0.98	44.66	1.49	29.15

Table 15: Environmental variables (6).

Plot	Elevation (m a.s.l.)	Precipitation (kg m⁻² ha⁻¹)	Mean diurnal temperature range (°C)	Slope (°)	Southness (-)	Eastness (-)	TPI (-)	TWI (-)	Distance to buildings (m)	Distance to roads (m)	Dense forest cover (ha)	Distance to dense forest (m)	Grassland cover (ha)	Grassland patch density (nb ha⁻¹)
331_AV	1,324.22	1,182.75	8.29	35.38	0.43	-0.90	0.03	3.63	166.04	24.40	0.92	19.97	0.63	87.19
334_AV	1,191.06	1,084.78	8.30	26.26	-0.78	0.62	-0.04	5.45	43.28	55.76	0.00	212.31	0.24	49.15
335_AV	1,373.91	1,123.21	8.30	30.94	-0.97	0.21	-0.06	5.38	203.41	11.99	0.37	56.49	2.81	58.13
340_AV	1,418.22	1,237.47	8.30	35.02	-1.00	-0.01	-0.10	7.12	507.70	1.99	0.15	59.92	3.29	29.06
341_AV	1,340.28	1,237.47	8.30	36.14	-0.99	0.11	0.03	4.99	307.78	10.30	0.69	9.99	1.97	35.56
343_AV	1,313.27	1,228.68	8.30	38.39	-0.98	0.18	-0.01	6.03	539.92	120.97	1.38	9.99	1.11	58.13
344_AV	1,366.56	1,190.98	8.20	24.52	-0.65	0.76	-0.06	4.47	147.12	213.00	0.38	14.12	2.23	29.15
346_AV	2,074.10	1,382.07	8.25	30.05	-0.88	-0.43	0.12	3.07	206.06	142.36	0.00	141.23	1.75	87.19
349_AV	2,005.94	1,489.15	8.28	30.45	-0.90	0.42	0.03	3.12	90.84	9.78	0.59	14.12	1.12	87.19
350_AV	2,049.53	1,489.15	8.28	21.90	-0.39	0.91	-0.05	4.24	83.72	5.51	0.00	148.46	1.18	87.19
351_AV	2,205.80	1,489.15	8.28	16.59	-0.28	0.95	-0.11	5.19	223.46	23.75	0.00	108.02	1.53	29.15
362_AV	2,198.24	1,497.81	8.60	31.71	-0.93	-0.35	0.14	3.37	581.74	68.25	2.40	0.00	0.12	57.30
363_AV	1,848.53	1,289.94	8.49	10.29	0.76	-0.50	0.11	3.87	133.68	127.60	0.00	125.13	0.01	57.30
364_AV	1,870.37	1,337.54	8.51	17.41	-0.62	-0.78	-0.04	5.91	173.11	62.06	0.92	19.97	0.22	145.32
368_AV	1,642.98	1,269.44	8.43	20.13	-0.72	0.68	0.03	4.69	169.92	5.23	0.24	14.12	0.00	0.00
370_AV	2,145.47	1,450.44	8.57	22.79	-0.97	-0.22	0.08	4.28	234.31	61.32	1.26	9.99	0.88	115.26
371_AV	2,130.20	1,412.50	8.04	24.65	0.68	0.66	0.32	3.30	512.67	45.84	1.95	0.00	0.35	29.15
372_AV	1,702.13	1,478.98	8.29	12.08	-0.03	-0.96	-0.07	6.63	43.47	57.05	0.00	131.35	1.26	57.96
376_AV	1,680.36	1,552.34	8.26	1.82	-0.47	0.83	0.03	5.68	273.68	49.82	0.00	135.83	0.29	116.60
377_AV	1,702.29	1,552.34	8.26	21.60	-0.85	-0.48	0.12	3.68	313.52	82.59	0.00	219.93	1.43	144.07
378_AV	1,925.21	1,390.97	8.02	21.19	-0.76	-0.65	-0.11	5.53	397.13	45.29	0.05	84.74	0.00	0.00
379_AV	2,153.85	1,558.72	8.00	26.46	-0.49	-0.87	-0.08	5.32	184.86	57.54	0.32	28.25	0.43	58.47
386_AV	2,084.84	1,601.01	7.97	17.87	-0.36	-0.92	-0.03	4.40	831.17	84.55	1.42	0.00	0.07	58.30
387_AV	2,080.29	1,426.24	8.00	38.90	-0.68	-0.73	-0.08	4.75	902.54	58.07	3.34	0.00	0.00	0.00
388_AV	1,728.65	1,688.05	8.20	2.43	-0.65	0.42	0.06	5.27	85.55	36.90	0.00	233.14	3.29	29.15
389_AV	2,207.46	1,601.01	7.97	12.67	-0.89	-0.42	0.13	4.44	258.83	40.85	0.00	291.15	0.68	29.15
392_AV	1,920.13	1,603.71	7.98	26.89	-0.23	-0.96	-0.09	6.40	263.27	69.23	1.16	9.99	0.21	44.76
397_AV	2,211.03	1,590.64	8.00	28.98	0.95	0.27	0.04	3.68	360.71	257.28	0.00	209.95	2.51	28.90
403_AV	1,917.79	1,583.46	8.41	27.20	-0.49	0.87	0.05	3.30	420.55	44.14	0.00	445.38	1.02	58.13
408_AV	1,763.93	1,438.23	7.96	28.62	-0.05	0.97	0.21	3.70	228.44	18.42	0.49	0.00	1.40	87.45
410_AV	1,889.73	1,483.36	7.91	30.68	-0.55	0.82	0.09	3.89	247.84	28.56	0.21	44.66	0.62	28.49
411_AV	1,833.33	1,786.68	8.19	4.68	0.18	-0.73	-0.02	7.59	553.99	5.22	0.00	135.83	0.73	87.19
412_AV	1,976.27	1,885.59	8.13	26.75	-0.45	0.89	-0.23	3.95	284.77	28.53	0.00	219.70	0.90	145.32
415_AV	2,026.10	1,669.06	7.85	29.97	-0.18	-0.98	-0.31	5.62	269.18	104.48	0.00	170.06	0.94	85.46
416_AV	1,979.43	1,669.06	7.85	12.34	-0.35	0.87	-0.05	4.48	58.45	81.04	0.00	257.72	1.85	29.23
417_AV	1,991.99	1,669.06	7.85	23.16	-0.62	0.77	0.04	5.81	189.56	121.38	0.00	412.84	2.38	29.06

Appendix 6: Distribution of each plot among the eight cluster

Table 16: List of forest plot IDs constituting each of the eight cluster groups identified by hierarchical cluster analysis. Plot IDs ending in P refer to plots located in the Piedmont region, while IDs ending in AV refer to plots located in the Aosta Valley region. n = number of plots per cluster.

Cluster	n	Plot IDs
c1	42	1_P, 45_P, 66_P, 67_P, 104_P, 108_P, 117_P, 124_P, 128_P, 129_P, 130_P, 131_P, 133_P, 137_P, 142_P, 6_AV, 7_AV, 33_AV, 46_AV, 67_AV, 70_AV, 82_AV,116_AV, 127_AV, 132_AV, 142_AV, 148_AV, 175_AV, 195_AV, 203_AV, 205_AV, 206_AV, 215_AV, 217_AV, 264_AV, 294_AV, 298_AV, 321_AV, 340_AV, 341_AV, 368_AV, 408_AV
c2	79	2_P, 5_P, 31_P, 51_P, 75_P, 79_P, 103_P, 115_P, 139_P, 11_AV, 19_AV, 24_AV, 54_AV, 60_AV, 61_AV, 71_AV, 72_AV, 73_AV, 75_AV, 91_AV, 97_AV, 115_AV, 119_AV, 122_AV, 128_AV, 130_AV, 134_AV, 135_AV, 136_AV, 151_AV, 155_AV, 160_AV, 174_AV, 176_AV, 178_AV, 179_AV, 181_AV, 183_AV, 186_AV, 187_AV, 189_AV, 196_AV, 202_AV, 204_AV, 208_AV, 214_AV, 216_AV, 220_AV, 221_AV, 222_AV, 250_AV, 253_AV, 255_AV, 263_AV, 275_AV, 288_AV, 300_AV, 310_AV, 311_AV, 313_AV, 328_AV, 343_AV, 346_AV, 351_AV, 363_AV, 364_AV, 370_AV, 377_AV, 378_AV, 386_AV, 387_AV, 388_AV, 392_AV, 397_AV, 403_AV, 411_AV, 412_AV, 416_AV, 417_AV
c3	39	3_P, 6_P, 16_P, 30_P, 34_P, 37_P, 60_P, 76_P, 84_P, 90_P, 92_P, 93_P, 95_P, 99_P, 110_P, 119_P, 121_P, 122_P, 138_P, 144_P, 145_P, 18_AV, 50_AV, 51_AV, 56_AV, 64_AV, 90_AV, 94_AV, 110_AV, 120_AV, 125_AV, 129_AV, 166_AV, 207_AV, 266_AV, 289_AV, 301_AV, 331_AV, 335_AV
c4	40	4_P, 24_P, 26_P, 42_P, 56_P, 63_P, 70_P, 73_P, 91_P, 97_P, 112_P, 123_P, 126_P, 93_AV, 133_AV, 138_AV, 161_AV, 168_AV, 170_AV, 171_AV, 182_AV, 213_AV, 224_AV, 243_AV, 296_AV, 299_AV, 308_AV, 309_AV, 320_AV, 323_AV, 326_AV, 327_AV, 344_AV, 349_AV, 350_AV, 371_AV, 372_AV, 379_AV, 410_AV, 415_AV
c5	45	12_P, 27_P, 44_P, 62_P, 74_P, 77_P, 100_P, 101_P, 116_P, 125_P, 127_P, 132_P, 135_P, 141_P, 143_P, 34_AV, 47_AV, 53_AV, 62_AV, 65_AV, 108_AV, 111_AV, 143_AV, 146_AV, 152_AV, 158_AV, 159_AV, 164_AV, 169_AV, 188_AV, 194_AV, 218_AV, 235_AV, 239_AV, 248_AV, 249_AV, 276_AV, 286_AV, 287_AV, 292_AV, 307_AV, 325_AV, 362_AV, 376_AV, 389_AV
c6	11	19_P, 35_P, 72_P, 98_P, 105_P, 107_P, 111_P, 114_P, 118_P, 136_P, 140_P
c7	12	20_P, 65_P, 78_P, 81_P, 82_P, 85_P, 87_P, 88_P, 94_P, 96_P, 102_P, 106_P
c8	15	22_P, 29_P, 39_P, 49_P, 113_P, 13_AV, 20_AV, 28_AV, 68_AV, 87_AV, 95_AV, 104_AV, 112_AV, 156_AV, 334_AV

Appendix 7: Dominant species for the two macro-groups

Table 17: Distribution of the dominant tree species among the main macro-groups C1 and C2.

Dominant species	Cluster 1 – C1	Cluster 2 – C2	Total
Larix decidua	16	155	171
Picea abies	31	4	35
Fraxinus excelsior	12	0	12
Fagus sylvatica	11	0	11
Betula pendula	10	0	10
Castanea sativa	5	0	5
Pinus cembra	1	4	5
No trees	4	0	4
Abies alba	4	0	4
Acer pseudoplatanus	4	0	4
Laburnum anagyroides	4	0	4
Salix caprea	4	0	4
Populus tremula	2	1	3
Prunus avium	3	0	3
Corylus avellana	2	0	2
Sorbus aria	2	0	2
Sorbus aucuparia	2	0	2
Pinus sylvestris	1	0	1
Tilia cordata	1	0	1
Total	**119**	**164**	**283**

Appendix 8: Dominant species for the eight clusters

Table 18: Distribution of the dominant tree species among the eight clusters identified in section 5.1.

Dominant species	Cluster 1 – c1	Cluster 2 – c2	Cluster 3 – c3	Cluster 4 – c4	Cluster 5 – c5	Cluster 6 – c6	Cluster 7 – c7	Cluster 8 – c8	Total
Larix decidua	9	76	3	39	40	0	1	3	171
Picea abies	27	0	2	1	3	0	0	2	35
Fraxinus excelsior	0	0	7	0	0	0	0	5	12
Fagus sylvatica	1	0	0	0	0	10	0	0	11
Betula pendula	0	0	6	0	0	0	3	1	10
Castanea sativa	0	0	4	0	0	1	0	0	5
Pinus cembra	1	2	0	0	2	0	0	0	5
Abies alba	4	0	0	0	0	0	0	0	4
Acer pseudoplatanus	0	0	2	0	0	0	0	2	4
Laburnum anagyroides	0	0	3	0	0	0	1	0	4
No trees	0	0	0	0	0	0	4	0	4
Salix caprea	0	0	4	0	0	0	0	0	4
Populus tremula	0	1	1	0	0	0	0	1	3
Prunus avium	0	0	3	0	0	0	0	0	3
Corylus avellana	0	0	0	0	0	0	1	1	2
Sorbus aria	0	0	1	0	0	0	1	0	2
Sorbus aucuparia	0	0	1	0	0	0	1	0	2
Pinus sylvestris	0	0	1	0	0	0	0	0	1
Tilia cordata	0	0	1	0	0	0	0	0	1
Total	**42**	**79**	**39**	**40**	**45**	**11**	**12**	**15**	**283**

Appendix 9: Mean forest variables for each cluster

Table 19: Mean forest variables for each cluster.

Variables	c1	c2	c3	c4	c5	c6	c7	c8
Basal area (m^2 ha^{-1})	54.27 ± 16.59	33.30 ± 12.37	29.14 ± 16.86	72.49 ± 25.20	40.00 ± 19.16	61.20 ± 16.42	9.52 ± 10.29	28.30 ± 20.85
Density (trees ha^{-1})	678 ± 238	547 ± 280	1,078 ± 406	529 ± 186	671 ± 354	966 ± 623	372 ± 377	809 ± 516
Mean DBH (cm)	30.88 ± 6.75	29.10 ± 7.13	17.31 ± 5.24	42.20 ± 9.45	26.64 ± 6.75	26.84 ± 5.32	10.58 ± 9.69	19.59 ± 6.49
Sapling density (saplings ha^{-1})	1,062 ± 2,833	848 ± 2,117	4,794 ± 7,178	445 ± 926	2,542 ± 3,100	1,096± 1,031	41,970± 12,890	8,893± 10,840
Seedling density (seedlings ha^{-1})	4,699 ± 7,398	1,152 ± 1,895	11,245 ± 11,313	789 ± 2,571	4,385 ± 5,333	16,444 ± 19,982	18,440 ± 9,289	70,284± 54,025
Regeneration cover (%)	1.81 ± 2.21	2.51 ± 3.84	4.03 ± 4.24	1.15 ± 1.09	3.96 ± 5.62	1.55 ± 1.29	2.67 ± 3.45	22.60 ± 14.72
Litter cover (%)	53.90 ± 22.57	15.30 ± 13.30	25.37 ± 20.10	14.41 ± 13.69	11.23 ± 11.37	64.91 ± 10.59	33.92 ± 21.81	14.17 ± 14.66
Brillouin index - tree layer (-)	0.57 ± 0.26	0.27 ± 0.29	0.74 ± 0.39	0.15 ± 0.23	0.42 ± 0.25	0.56 ± 0.52	0.37 ± 0.37	0.72 ± 0.52
Brillouin index - regeneration (-)	0.24 ± 0.37	0.07 ± 0.18	0.74 ± 0.45	0.04 ± 0.16	0.77 ± 0.32	0.74 ± 0.64	0.22 ± 0.30	0.48 ± 0.34
Brillouin index - seedlings (-)	0.21 ± 0.34	0.01 ± 0.07	0.74 ± 0.46	0.04 ± 0.16	0.60 ± 0.43	0.70 ± 0.60	0.41 ± 0.55	0.42 ± 0.31
Brillouin index - saplings (-)	0.05 ± 0.15	0.00 ± 0.00	0.24 ± 0.32	0.00 ± 0.00	0.39 ± 0.32	0.12 ± 0.30	0.05 ± 0.16	0.23 ± 0.36
Broadleaves percentage (%)	9.28 ± 18.41	3.45 ± 10.61	84.13 ± 22.79	0.28 ± 0.76	7.52 ± 10.65	88.73 ± 17.87	57.46 ± 47.45	70.63 ± 37.82
Light tolerance index (-)	1.95 ± 0.69	3.75 ± 0.38	3.17 ± 0.41	3.81 ± 0.38	3.59 ± 0.57	1.48 ± 0.54	3.27 ± 0.42	3.06 ± 0.60
Larix decidua - BA (m^2 ha^{-1})	15.78 ± 15.00	28.01 ± 10.82	4.04 ± 8.03	66.58 ± 24.32	30.68 ± 16.98	4.41 ± 7.81	1.61 ± 3.85	5.67 ± 9.00
Picea abies - BA (m^2 ha^{-1})	27.28 ± 18.42	2.15 ± 4.20	1.09 ± 2.79	4.91 ± 10.44	3.40 ± 7.11	3.66 ± 7.13	0.79 ± 2.73	3.40 ± 8.40
Fagus sylvatica - BA (m^2 ha^{-1})	3.57 ± 8.02	0.00 ± 0.00	0.13 ± 0.83	0.00 ± 0.00	0.00 ± 0.00	43.09 ± 16.99	0.00 ± 0.00	0.11 ± 0.35
Corylus avellana - BA (m^2 ha^{-1})	0.17 ± 0.71	0.04 ± 0.26	0.67 ± 1.64	0.07 ± 0.42	0.15 ± 0.50	0.06 ± 0.16	0.80 ± 1.26	1.16 ± 3.47

Appendix 10: Comparison of the eight remaining forest variables between the eight clusters.

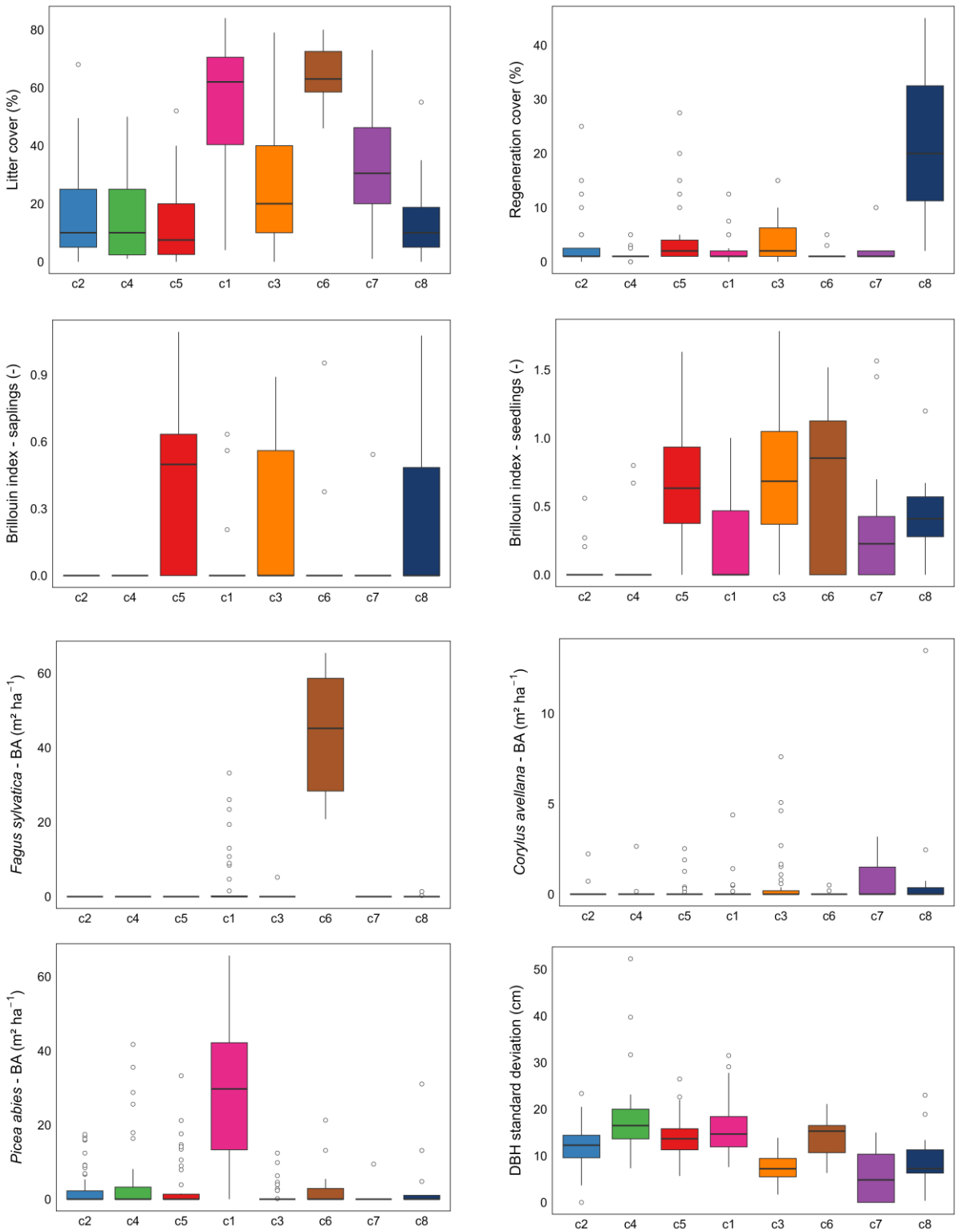

Figure 34: The eight remaining forest characteristics to compare the different clusters identified with the cluster analysis.

Appendix 11: PCA coefficient for the forest variables

Table 20: Pearson coefficients of the 15 forest variables used in the PCA for the two principal component: PC1 and PC2.

	Correlation coefficient [-]	
Variable	**PC1**	**PC2**
Mean DBH [cm]	-0.7527	0.3970
BA [m^2 ha^{-1}]	-0.4266	0.6593
TPH [trees ha^{-1}]	0.5082	0.2016
Spruce BA [m^2 ha^{-1}]	-0.0388	0.7070
Beech BA [m^2 ha^{-1}]	0.2807	0.4973
Hazel BA [m^2 ha^{-1}]	0.3909	-0.0530
Larch BA [m^2 ha^{-1}]	-0.7827	0.0641
BLF [-]	0.8043	-0.0569
LTI [-]	-0.4544	-0.7295
TPH_se [seedlings ha^{-1}]	0.5488	-0.0780
TPH_sa [saplings ha^{-1}]	0.4138	-0.3098
HB_t [-]	0.5911	0.3124
HB_sesa [-]	0.4964	-0.0219
Lit_cov [%]	0.3270	0.7217
Reg_cov [%]	0.2641	-0.3336

Appendix 12: Randomisation results

Table 21: Results of the randomisation test performed with 9,999 permutations. N: number of eigenvalues from randomisations lower than eigenvalue from real data.

		Eigenvalues from randomisations				
Axis	**Eigenvalue from real data**	**Minimum**	**Average**	**Maximum**	**p-value**	**n**
1	3.95	1.27	1.41	1.66	0.0001	0
2	2.75	1.19	1.32	1.49	0.0001	0
3	1.59	1.14	1.25	1.45	0.0001	0
4	1.27	1.09	1.19	1.31	0.0040	39
5	1.11	1.05	1.13	1.23	0.7477	7476
6	0.96	1.00	1.08	1.18	1.0000	9999
7	0.76	0.95	1.03	1.12	1.0000	9999
8	0.64	0.90	0.99	1.06	1.0000	9999
9	0.54	0.84	0.94	1.02	1.0000	9999
10	0.43	0.80	0.90	0.98	1.0000	9999

Appendix 13: PCA coefficient for the environmental variables

Table 22: Pearson (r), coefficient of determination (r^2) and Kendall (tau) correlations between environmental variables and PCA ordination axes 1 and 2 (N = 283).

	Axis 1			Axis 2		
Variable	**r**	**r^2**	**tau**	**r**	**r^2**	**tau**
Dense forest distance	0.071	0.005	-0.020	-0.299	0.089	-0.229
Sparse forest distance	-0.048	0.002	0.015	0.028	0.001	-0.016
Forest distance	-0.004	0.000	0.013	-0.201	0.040	-0.181
Roads distance	0.144	0.021	0.047	0.003	0.000	-0.046
Buildings distance	-0.210	0.044	-0.115	-0.061	0.004	-0.013
Dense forest cover	0.009	0.000	0.059	0.347	0.121	0.233
Sparse forest cover	0.022	0.000	-0.023	0.089	0.008	0.015
Grassland cover	-0.038	0.001	-0.039	-0.203	0.041	-0.128
Unvegetated area cover	0.003	0.000	0.039	-0.140	0.020	-0.099
Anthropogenic cover	-0.006	0.000	0.033	-0.074	0.005	-0.059
Simpson index	0.001	0.000	-0.015	0.022	0.000	0.012
Aggregation index (ai)	-0.079	0.006	-0.031	0.056	0.003	0.019
Edge density (ed)	0.074	0.005	0.027	-0.039	0.002	-0.014
Patch density (pd)	0.102	0.010	0.076	-0.035	0.001	-0.024
Dense forest ai	0.054	0.003	0.033	0.342	0.117	0.251
Sparse forest ai	-0.015	0.000	-0.048	-0.007	0.000	-0.004
Grassland ai	-0.075	0.006	-0.061	-0.114	0.013	-0.094
Unvegetated area ai	0.113	0.013	0.035	-0.080	0.006	-0.029
Anthropogenic area ai	0.050	0.003	0.025	-0.080	0.006	-0.045
Dense forest ed	0.039	0.002	0.062	0.153	0.023	0.161
Sparse forest ed	0.039	0.002	0.013	0.017	0.000	0.007
Grassland ed	0.046	0.002	0.004	-0.093	0.009	-0.032

	Axis 1			Axis 2		
Variable	**r**	**r²**	**tau**	**r**	**r²**	**tau**
Unvegetated area ed	0.065	0.004	0.047	-0.172	0.030	-0.119
Anthropogenic area ed	-0.013	0.000	0.031	-0.066	0.004	-0.058
Dense forest pd	0.098	0.010	0.085	0.097	0.010	0.137
Sparse forest pd	-0.009	0.000	0.014	0.009	0.000	0.021
Grassland pd	0.041	0.002	0.052	-0.015	0.000	-0.010
Unvegetated area pd	0.107	0.011	0.077	-0.175	0.030	-0.114
Anthropogenic area pd	0.010	0.000	0.034	-0.064	0.004	-0.057
Elevation	-0.603	0.364	-0.436	-0.198	0.039	-0.090
Slope	0.130	0.017	0.082	0.068	0.005	0.047
Southness	0.144	0.021	0.043	0.121	0.015	0.106
TPI	0.028	0.001	0.021	-0.041	0.002	-0.030
Roughness	0.167	0.028	0.082	0.037	0.001	0.043
HLI	0.173	0.030	0.078	0.022	0.000	0.029
TRI	0.104	0.011	0.041	-0.076	0.006	-0.035
TWI	-0.112	0.012	-0.068	0.074	0.005	0.043
T_mean	0.596	0.355	0.432	0.211	0.044	0.088
T_range	0.258	0.067	0.165	0.187	0.035	0.093
Tmax_warm	0.594	0.352	0.432	0.214	0.046	0.090
Tmin_cold	0.600	0.361	0.439	0.200	0.040	0.083
Precipitation	-0.426	0.181	-0.327	-0.227	0.052	-0.108
GSL	0.583	0.340	0.414	0.213	0.045	0.084
SCD	-0.581	0.337	-0.413	-0.212	0.045	-0.083

Appendix 14: Other PDPs

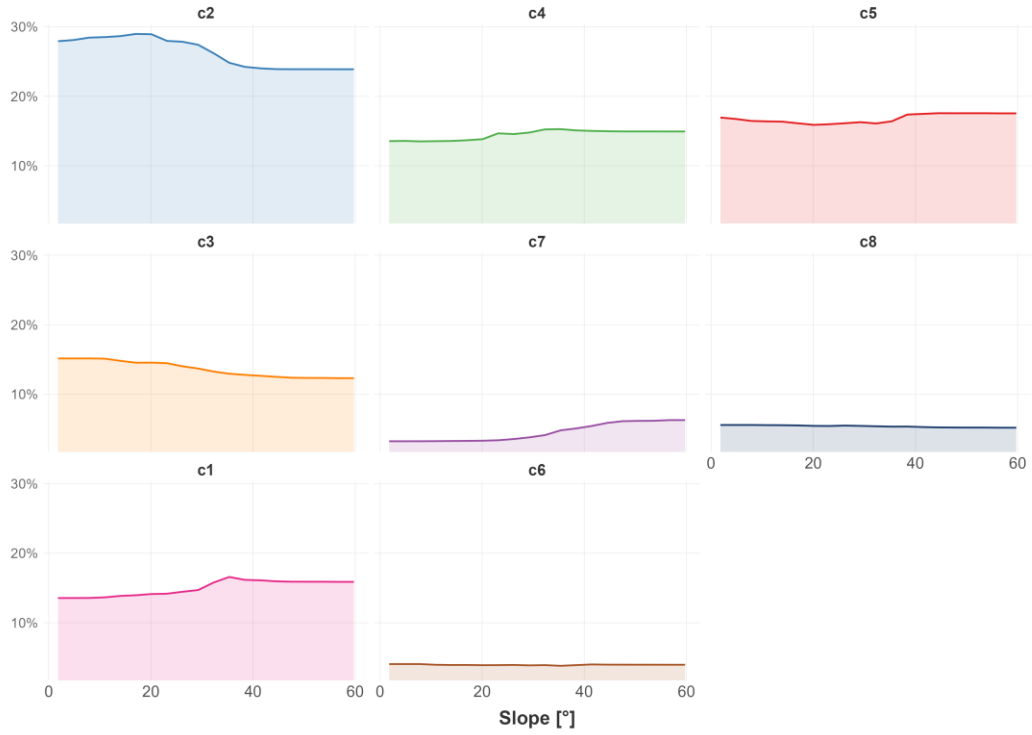

Figure 35: PDPs for the slope.

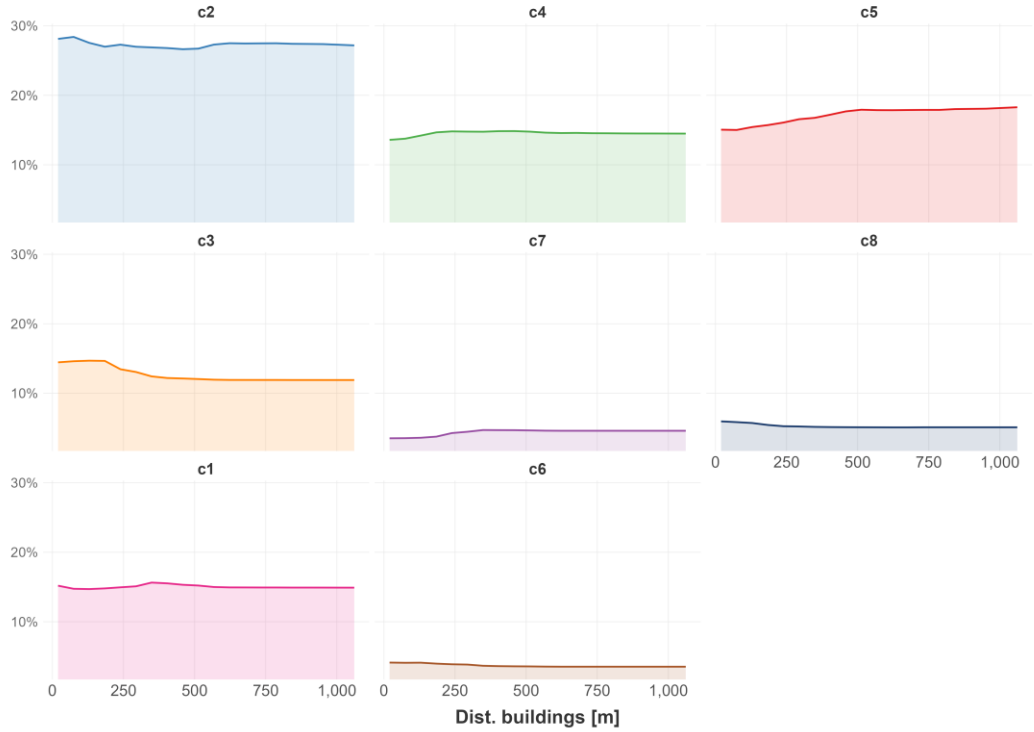

Figure 36: PDPs for the distance to buildings.

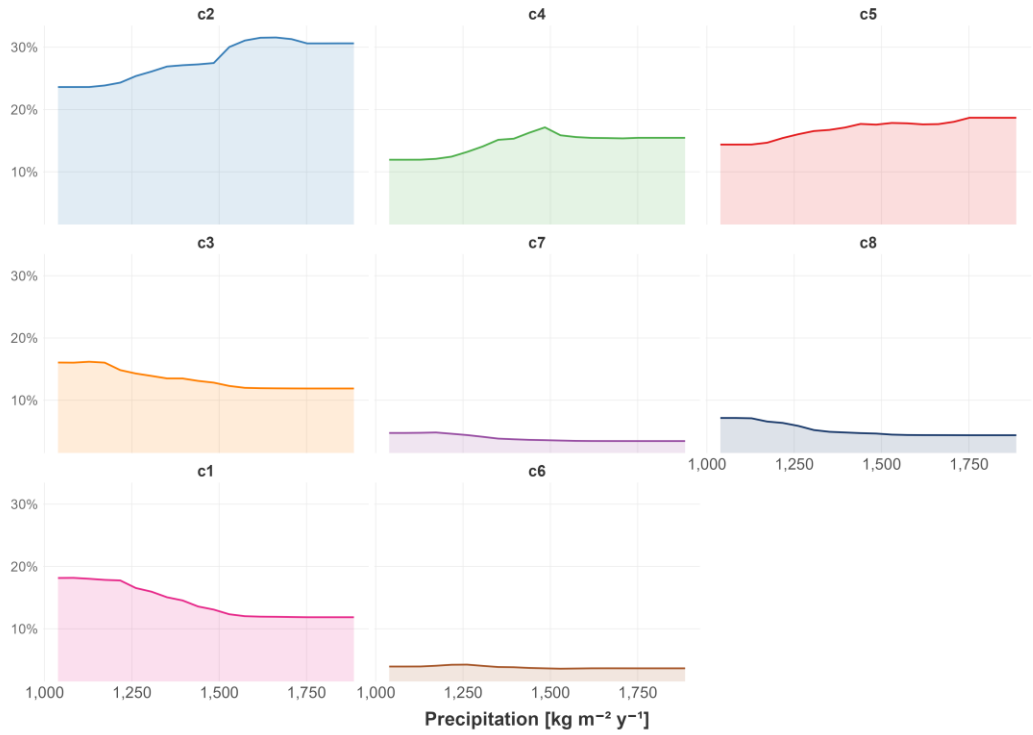

Figure 37: PDPs for the precipitation

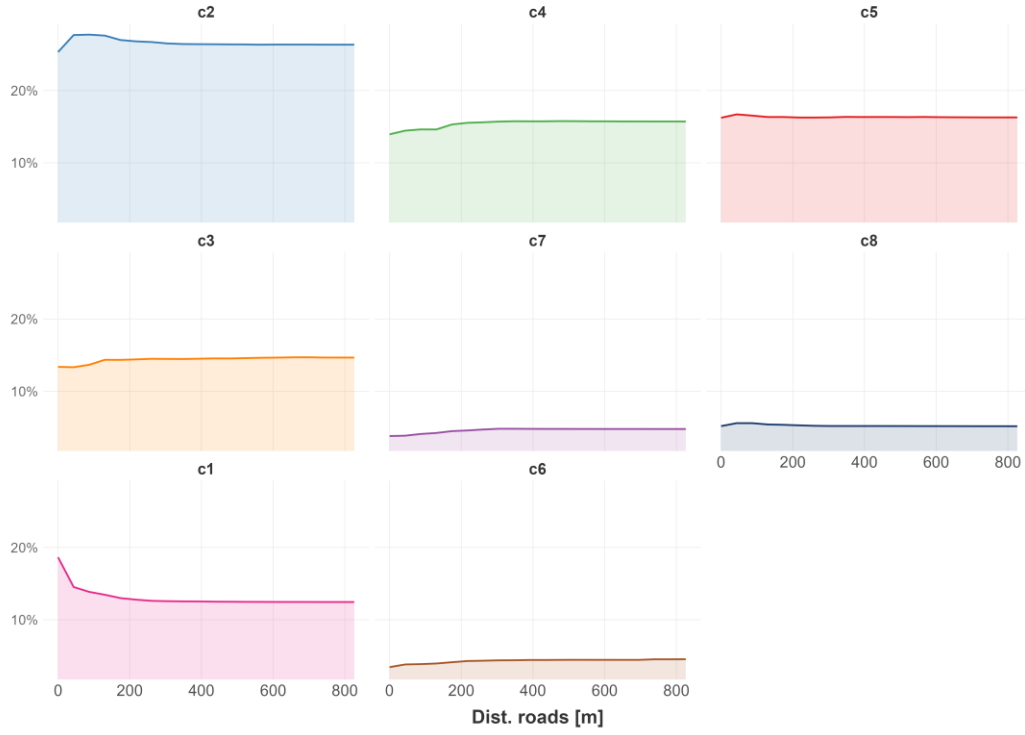

Figure 38: PDPs for the distance to the roads.

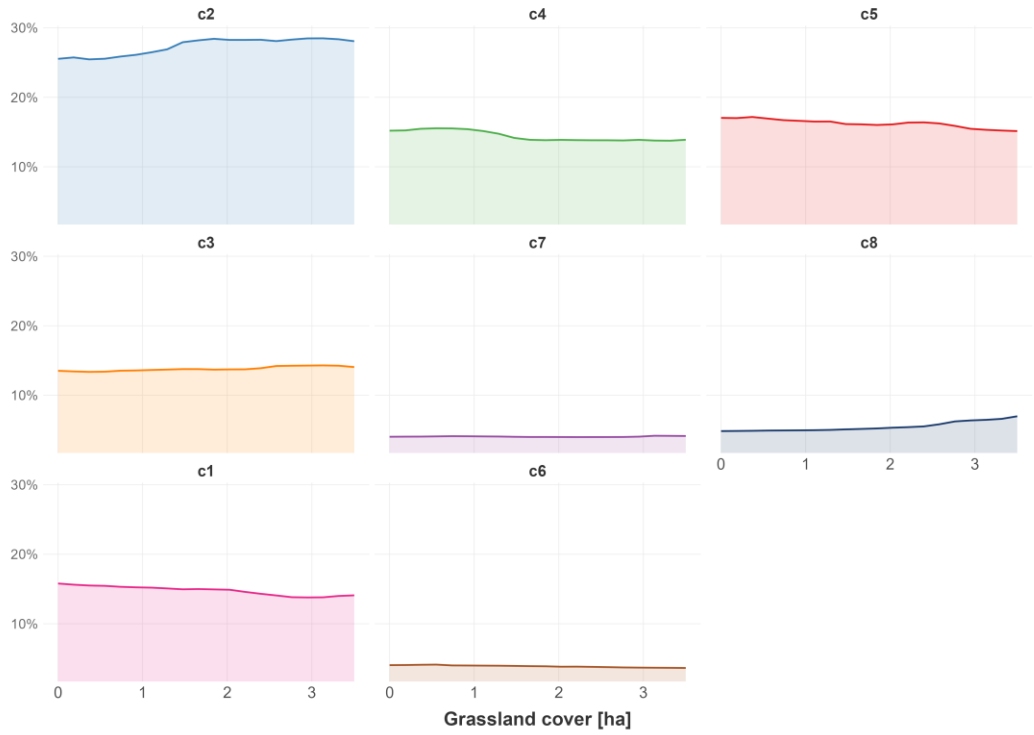

Figure 39: PDPs for the grassland cover.

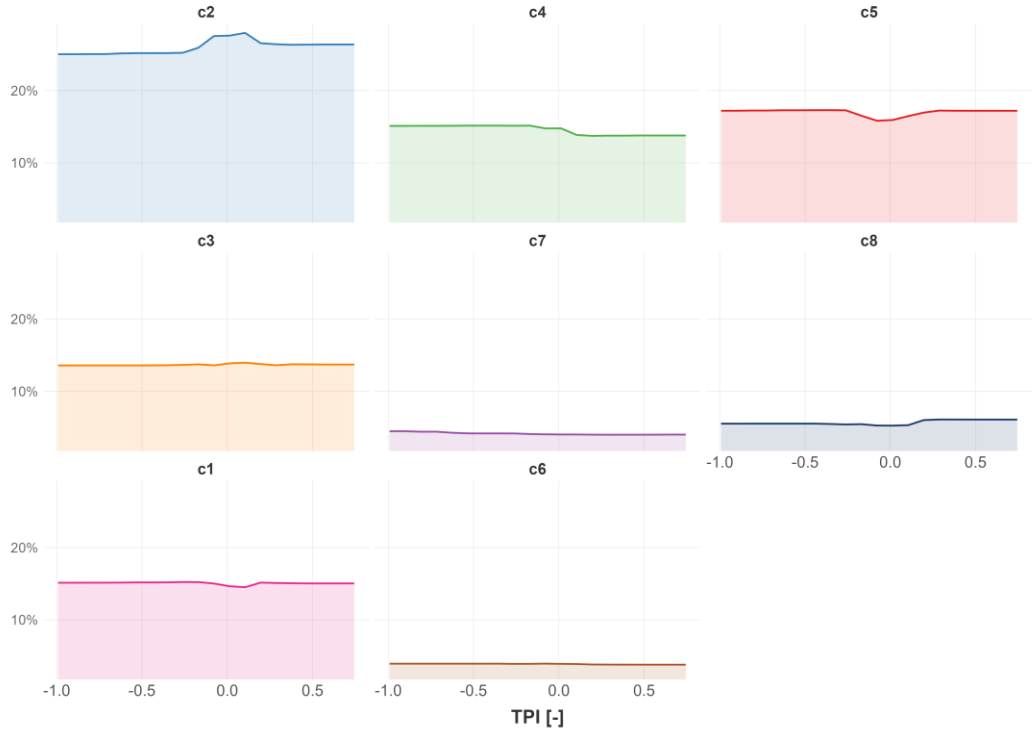

Figure 40: PDPs for the TPI.

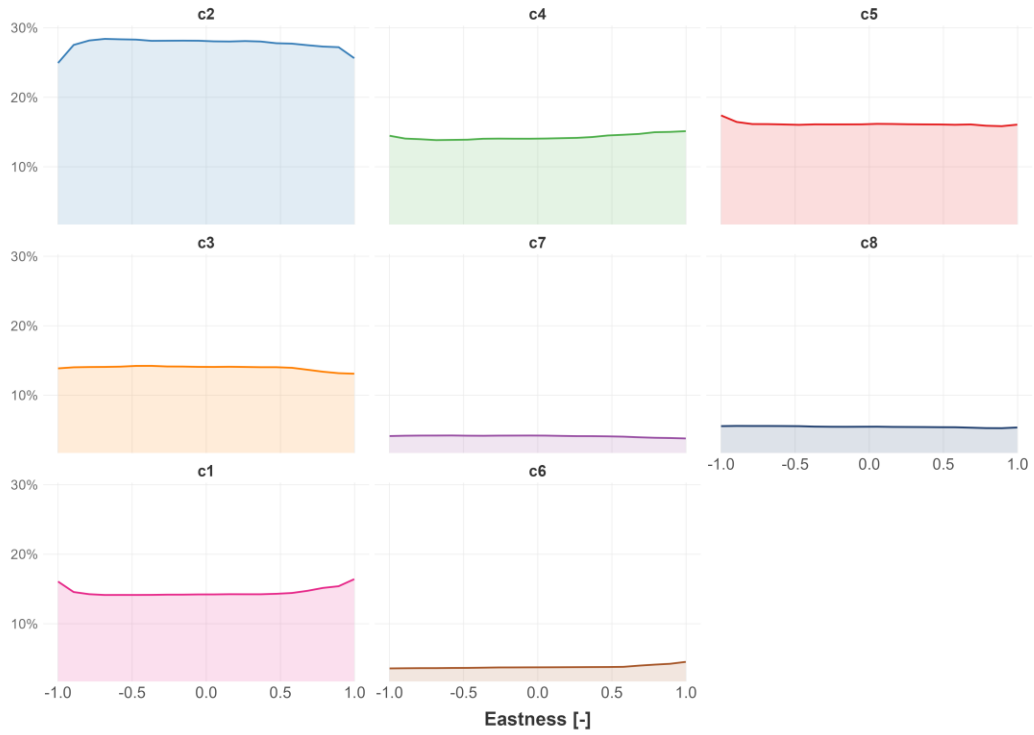

Figure 41: PDPs for the eastness.

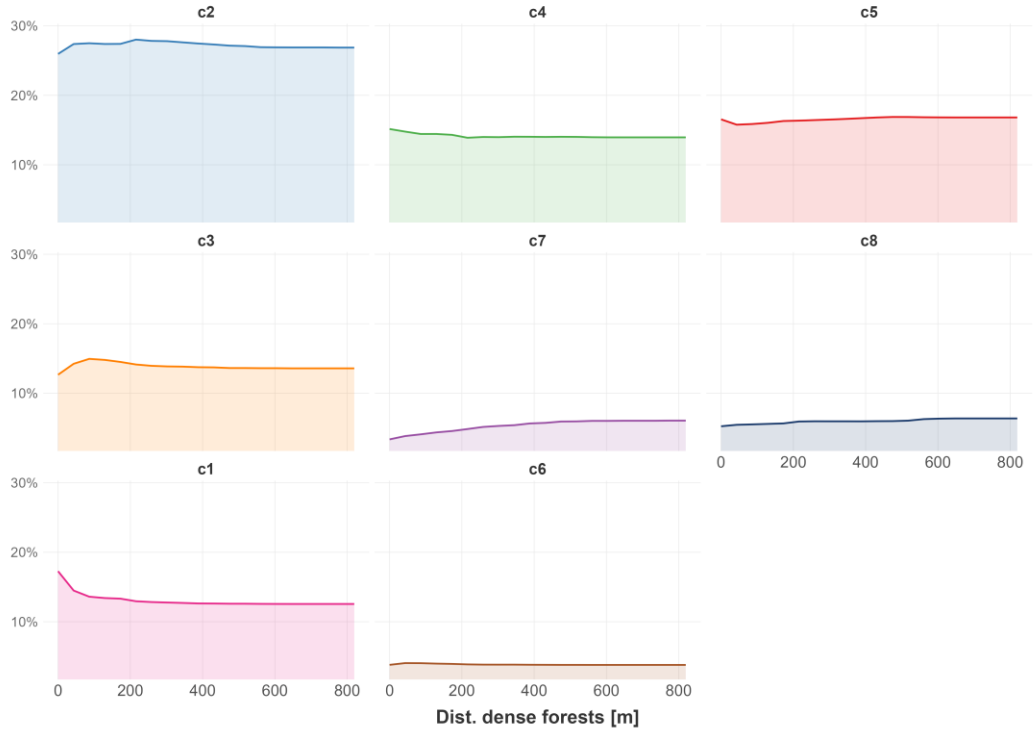

Figure 42: PDPs for the distance to dense forests.

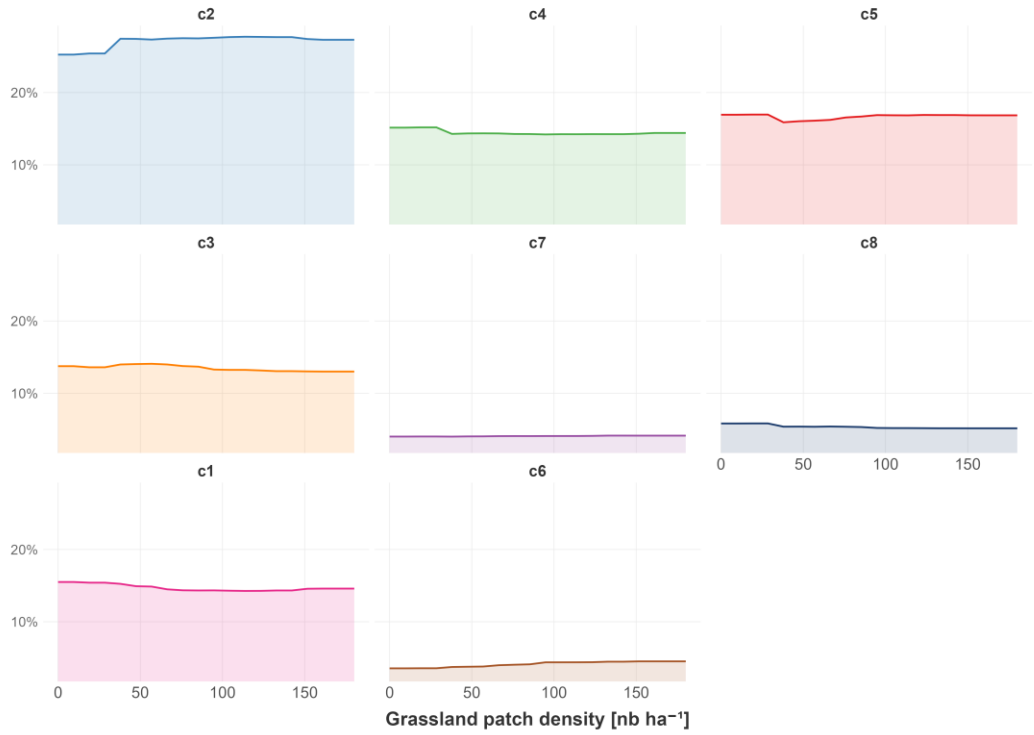

Figure 43: PDPs for the grassland patch density.

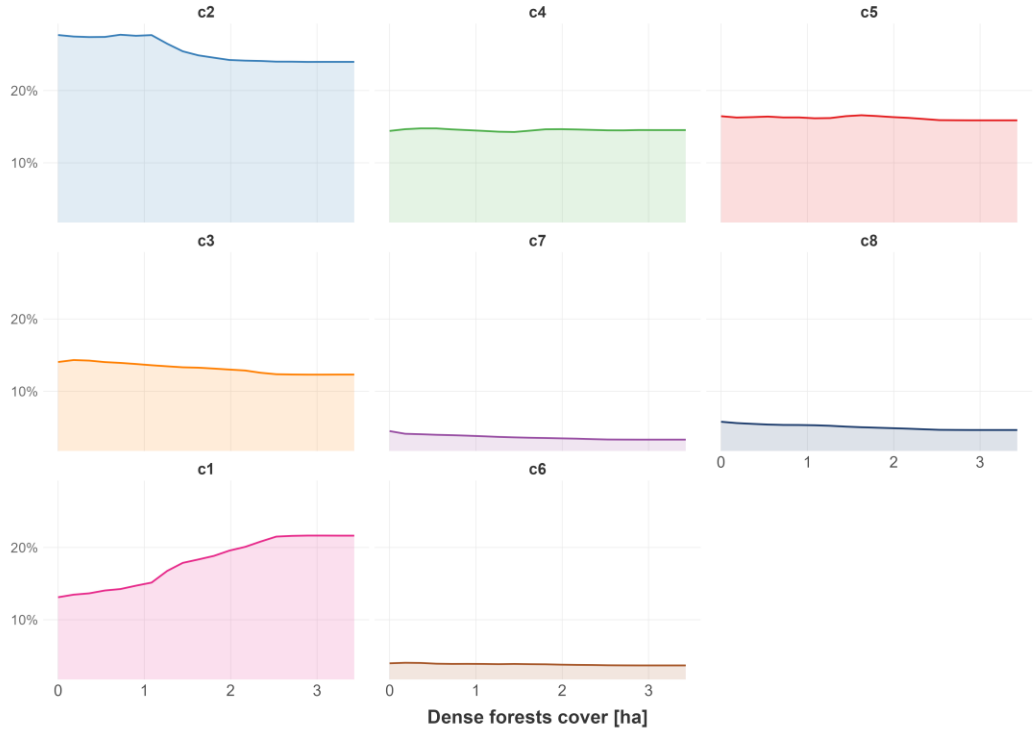

Figure 44: PDPs for the dense forest cover.

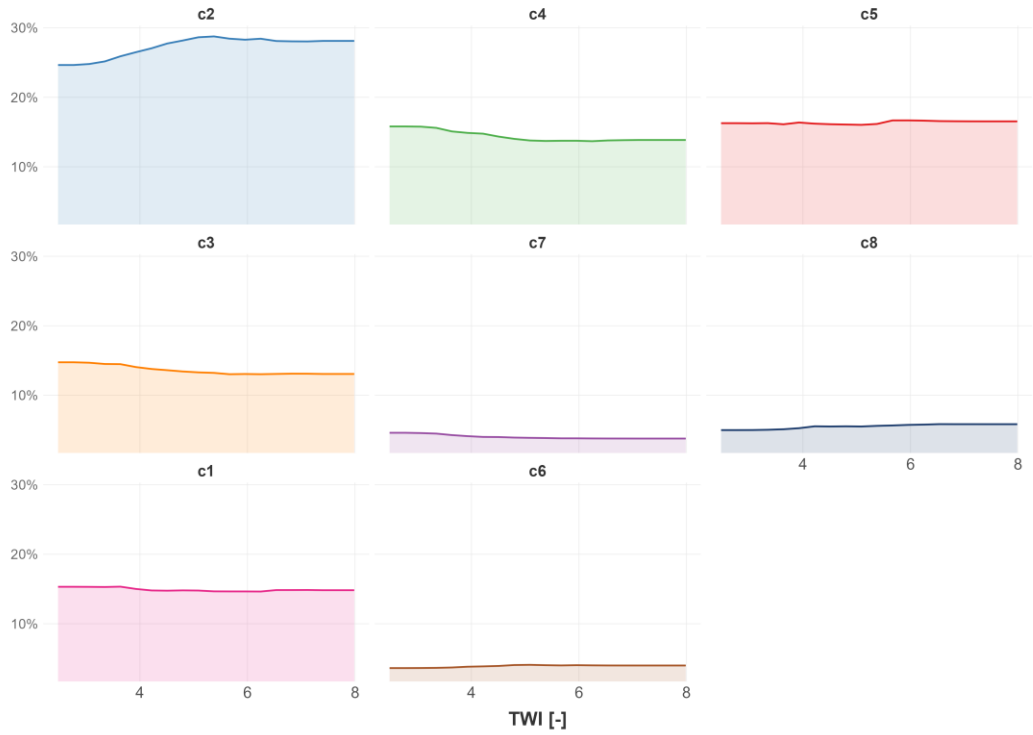

Figure 45: PDPs for the TWI.

What are the environmental factors determining the secondary forest diversity in mountain ecosystems?

Louis Léonard

Land abandonment since the 19th century has driven a widespread expansion of secondary forests across the European Alps, generating heterogeneous mosaics whose composition and structure are still poorly understood. Trajectories of these stands do not converge towards a single natural state but remain shaped by the climatic, topographic and anthropogenic conditions. The factors driving this diversity, however, have received comparatively little attention, limiting our ability to predict which forest type will develop at a given site.

This master's thesis characterises the diversity of secondary forests in the Gran Paradiso National Park (Western Italian Alps). The analysis is based on 283 sampling plots. Forest structure, composition and regeneration were measured in the field and combined with a set of climatic, topographic, landscape and anthropogenic descriptors.

Eight forest types were identified and grouped into two macro-groups: a broadleaved and mixed group, and a larch-dominated group. A principal component analysis revealed two main ecological gradients: a species-composition gradient separating the two macro-groups and a maturity-and-legacy gradient opposing mature, well-established stands to pioneer, newly-established ones. A Random Forest analysis identified elevation as the single dominant driver, accounting for 64.5% of the total variable importance, far ahead of southness and mean diurnal temperature range; anthropogenic and 1954 landscape variables together contributed less than 10%.

These results converge towards a hierarchical interpretation of secondary forest diversity. A primary thermal-accumulation filter, acting through elevation and secondarily through slope aspect and temperatures, determines which successional trajectory is ecologically possible at a given site. A secondary filter, linked to land-use legacies inherited from the 1954 landscape, controls how far a stand has progressed along its trajectory. The type of secondary forest developing at a given location in the Park is therefore primarily determined by where it lies on the thermal-accumulation gradient, and only secondly by its land-use history. This framework provides a synthetic and transferable answer to the question of what drives secondary forest diversity in mountain landscapes.

UNIVERSITÉ CATHOLIQUE DE LOUVAIN
Faculté des bioingénieurs
Croix du Sud, 2 bte L7.05.01, 1348 Louvain-la-Neuve, Belgique | **www.uclouvain.be/agro**